Thesis/
Reports
Bunte, K. I.

Comparison of Phase 2 Sediment Transport Initiation Approaches

Revised report submitted to the

Stream Systems Technology Center

USDA Forest Service
Rocky Mountain Research Station
2150 Centre Avenue
Fort Collins, CO 80523

by

Kristin Bunte

Engineering Research Center
Colorado State University
Fort Collins, CO 80523

July, 2007

Abstract

If water is being diverted from streams, flow may no longer be sufficient to transport gravel supplied from tributaries through the stream, causing channel aggradation. A certain amount of water should therefore be reserved and allowed to pass through the channel during the highflow season as channel maintenance flows. These flows are to maintain the channel shape and the bedmaterial composition and ensure that the normal adjustments and interactions between the bed and bedload transport occur. A variety of different methodologies has been proposed over the past two decades to estimate rates of flow required for channel maintenance. This study evaluates five of the more recent procedures developed for this computation.

There are two parts in this study. Part A is a literature review regarding different phases or stages of bedload transport in gravel-bed streams. Part B describes five channel maintenance procedures, their computation and the results obtained when applying the procedures to three data sets collected in mountain gravel-bed streams using two different bedload samplers at each site. The five procedures are bedload explosion (Emmett 1999), breakpoint analysis (Ryan et al. 2002, 2005), the Idaho collapse-size analysis (Whiting and King 2003), the Klamath Falls site-calibrated approach (Bakke et al. 1999; McNamara et al. 2000), and an approach based on measured flow competence curves.

Channel maintenance flows computed using the different procedures varied widely, encompassing flows as low as 16% and as high as 206% of bankfull flow. Results from this study can only be evaluated comparatively because the true percentage of flow needed is not known. The commonly cited value that channel maintenance flow should be at 80% of bankfull discharge is the result of gross arithmetic averaging over a wide range of channel maintenance flows (40 to 130% Q_{bkf}) reported in several studies that examined up to about 20 different streams.

The collapse-size analysis gave a consistently low result, while the flow competence analysis for the surface D_{50} particle size gave a consistently high result for channel maintenance flows for both samplers. Results differed between the two samplers, but tended to be generally lower for samples collected with a Helley-Smith sampler than for samples collected with bedload traps. The flow competence procedure was an exception.

An evaluation and ranking of the procedures with respect to effort expended for data collection, ease of computation and potential for operator and computational errors placed the flow competence approach first, followed by the visually estimated and statistical computed breakpoint flows.

Abbreviations of frequently used technical terms

D	particle size or particle size class
D_{max}	largest particle size; refers also to very large particles in general
D_{50}	median particle size, 50th percentile
D_i	particle of the i^{th} particle size class
Q	water discharge
Q_B	bedload transport rate
Q_{Bi}	Bedload transport rate of the i^{th} particle size class
Q_{bkf}	discharge at the bankfull stage when the floodplain is about to be inundated
Q_{crit}	flow at the onset of (some specific particle size of) bedload transport
Q_{25}, Q_{100}	flood stage with a 25-year and a 100-year return interval

Table of content

Abstract 2
Abbreviations of frequently used technical terms 4
Glossary 5

Part A. Literature review of Phase 1, 2, and 3 transport

1. Introduction 8

2. Results 9

2.1 Stages of bedload transport without change in Q_B vs. Q relationship 18
2.1.1 Several stages of armor and subarmor mobility 18
2.1.2 Phase 1 and Phase 2 transport 18
2.1.3 Three phases of bedload transport 19
2.1.4 Marginal and general transport 20

2.2 Stages or phases of bedload transport linked to changes in the Q_B vs. Q relationship 21
2.2.1 Phase 1 and 2 transport linked to steepening Q_B *vs.* Q relationships 22
2.2.1.1 Breaks in the Q_B vs. Q relationship 22
2.2.1.2 Abrupt increase in bedload particles sizes 22
2.2.1.3 Breakpoint flows and the shift from Phase 1 to Phase 2 transport 23
2.2.2 Stages or phases of bedload transport with flattening Q_B *vs.* Q relationship 24
2.2.2.1 Gravel bedload transport equations: flattening out at high flow 24
2.2.2.2 Flattening Q_B vs. Q relationships rarely observed in armored, gravel- and cobble-bed streams 24
2.2.2.3 Partial transport and fully mobilized transport 25

2.3 Discussion 26
2.3.1 Effect of plotting scale 26
2.3.2 Role of sediment supply and armoring on steepness of Q_B *vs.* Q relationships 27
2.3.3 Flattening of Q_B *vs.* Q relationship: transition from selective transport to equal mobility? 29
2.3.4 Comparison of transport phases and their flow ranges among studies 31
2.3.4.1 Low intensity or Phase 1 transport 31
2.3.4.2 High intensity or Phase 2 transport 32
2.3.4.3 Highest intensity or Phase 3 transport 33
2.3.4.4 Problems in differentiating between transport phases 33

2.4 Summary and conclusion 34

Part B: Computation and comparison of several channel maintenance procedures 37

1. Introduction 37
1.1 Channel maintenance flows 37
1.2 The channel maintenance procedures: overview 38
1.3 Study aim 39

2. Field methods 39

2.1 Streams sampled 39
2.2 Data collection 40
2.3.1 Bedload sampling 40
2.3.1.1 Helley-Smith sampler 40
2.3.1.2 Bedload traps 40
2.3.1.3 Measured bedload transport rates 42
2.3.2 Bedmaterial sampling 42

3. Computation and comparison of various channel maintenance procedures 44
3.1 "Explosion" diagrams 44
3.1.1 Methods 44
3.1.2 Results 44
3.1.3 Discussion 46
3.2. Breakpoint analysis 48
3.2.1 Rationale 48
3.2.2 Methods 49
3.2.2.1 Piecewise regression analyses (SAS) 49
3.2.2.2 Visual determination of breakpoint flows 52
3.2.4 Results of breakpoint analyses 55
3.2.4.1 Comparison of computed (SAS) and visually estimated breakpoint flows 55
3.2.4.2 Differences between samplers: effects of rating curve steepness 59
3.2.4.3 Effect of measured range of flows: scale dependency 61
Power function rating curve plotted in different linear scales 61
Knick points in power function relationships are general 63
Stepwise truncation of data sets 63
Appearance of breakpoint flows in log-log plots 69
3.2.4.4 Differences in breakpoints between streams 70
3.2.4.5 Predictability of breakpoint flows 70
3.2.4.6 Particle sizes transportable by breakpoint flows 73
3.2.5 Summary and conclusion 73
3.3 Collapse-size analyses 78
3.3.1 Introduction 78
3.3.2 Methods 79
3.3.2.1 Bedmaterial sampling 79
Idaho study (Whiting and King 2003) 79
This study 80
3.3.2.2 Computations of collapse sizes 83
3.3.3 Results 84
3.3.3.1 Different collapse sizes in the two studies 84
3.3.3.2 Different surface- and subsurface-size distributions in the two studies 86
3.3.3.3 Differences between surface and subarmor sizes affect collapse sizes 86
3.3.4 Discussion 88
3.3.4.1 Differences due to basin lithology and valley morphology 89

3.3.4.2 Differences in methods for bedmaterial collection and analysis 91
Pebble counts: Heel-to-toe walks versus sampling frame 91
b-axes measurements with a ruler 92
Subarmor samples: barrel sampler versus plywood shield 93
3.3.4.3 Recomputed collapse sizes with adjusted size distributions 94
Simulating sampling techniques of the Idaho study 94
Post-adjustment collapse sizes 95
3.3.4.4 Predictability of collapse sizes from bedmaterial characteristics 97
3.3.4.5 Critical flow needed for incipient motion of collapse sizes 98
3.3.5 Summary and Conclusion 100
3.4 Klamath Falls site-calibration procedure 102
3.4.1 Introduction 102
3.4.1.1 Overview of the Klamath Falls procedure 102
3.4.1.2 Site-specific calibration procedure 102
3.4.2 Methods 103
3.4.2.1 Bedmaterial sampling 103
3.4.2.2 Computation of framework sediment size 104
3.4.2.3 Data input requirements to run site-calibrated approach in BAGS 105
Cross-section 106
Stream gradient 106
Bedmaterial size distributions 107
Largest particles at the sampling site 107
Bedload samples and their size distributions 107
3.4.2.4 Bedload data selection for the calibration procedure 108
3.4.2.5 Computations of bedload transport relationships and threshold flows 109
3.4.3 Results 110
3.4.3.1 Transport relationships from the uncalibrated Parker equations 110
3.4.3.2 Transport relationships from site-calibrated approach 114
Better fit for bedload trap samples than for Helley-Smith samples 114
Sample selection affects calibration results 114
Unexpected values of exponents and τ^*_{r50} 115
3.4.3.3 Fractional transport rates 117
3.4.3.4 Threshold flows for framework gravel based on 2% criterion 118
3.4.3.5 Attempts to explain the poor success of site-calibrated approach to indicate threshold flows 120
Degree of fit with measured transport rates 120
Values of exponents and τ^*_{50} 120
Different bedload sampling devices 120
Streams in this study too different from the Klamath Falls study 121
Did something go wrong with the computations? 121
3.4.3.6 Site-specific threshold transport rates and resulting threshold flows ... 122
3.4.4 Summary and Conclusion 122
3.4.4.1 Overview of the study outcome 122
3.4.4.2 Why not plot fractional transport and flow competence curves directly from measured bedload samples? 124

3.5 Measured mobility of coarse gravel bedload 126
3.5.1 Introduction 126
3.5.2 Methods 127
3.5.2.1 Flow competence curve 128
3.5.2.2 Bias correction factor 128
3.5.3 Results 129
3.5.3.1 D_{max} vs. Q and fitted flow competence curves 129
3.5.3.2 Effect of bias correction factors 131
3.5.3.4 Mobilizing flows for three coarse gravel sizes in the three study streams 131
3.5.3.5 Difference in mobilizing flows for Helley-Smith and bedload trap samples 131
3.5.3.6 Mobilizing flows for surface and subarmor sizes as well as framework gravel 132
3.5.4 Summary and Conclusion 134

4. Comparison of channel maintenance flows obtained from different procedures 136
4.1 Differences in channel maintenance flows between samplers 137
4.2 Comparison among procedures 139
4.2.1 Variability and ranking 139
4.2.2 Similarity among procedures 140
4.2.3 Channel maintenance flows less variable for bedload traps 141
4.3 Differences in channel maintenance flows between streams 141
4.3.1 Streams with consistently higher or lower channel maintenance flows 141
4.3.2 Prediction of channel maintenance flows? 142
4.4 Evaluation of different channel maintenance procedures 143
4.4.1 Effort involved in the computations 143
4.4.2 Computations of channel maintenance flows: a big task 146

5. References 148

A. Literature review of Phase 1, 2, and 3 transport

1. Introduction

Phase 1, 2, and 3 transports refer to stages of increasing intensities of bedload transport in gravel- and cobble-bed streams. Milhous (1973) was one of the first researchers who thoroughly measured bedload transport rates and its particle sizes over a wide range of flows in a gravel-bed stream and provided a detailed account of different stages of bedload transport intensities. Jackson and Beschta (1982) coined the terminology of Phase 1 and Phase 2 transport to distinguish between the transport of sand over a stable bed with little if any effect on the channel shape and gravel transport off and onto riffles that shape the channel and explain the longitudinal conveyance of bedload through a riffle-pool system. Several authors have since used the Phase 1 – Phase 2 terminology to describe bedload transport of varying intensities in gravel- and cobble-bed streams or in coarse-bedded flumes, while others created their own terminology or added a third phase. The identified transport stages do not necessarily match among studies, nor are the transport processes ascribed to the different stages identical.

A factor contributing to differing descriptions of stages in bedload transport is the natural variability encountered among gravel-bed streams. Streams vary with respect to channel gradient, bed coarseness, bedmaterial sorting (roughly the ratio between the surface D_{84} and D_{16} sediment size), relative roughness (ratio of flow depth to the surface D_{50} or D_{84} particle size), the degree of bed armoring (ratio of the surface to subsurface D_{50} sediment sizes), the amount of entrainable sediment for a given flow, and stream morphology, to name a few. Stream characteristics affect the interaction between bedload transport and the stream bed, and a process that is prominent in one particular stream may not be prominent in another or occur at a different flow. Bedload transport rates and particle sizes measured at a given flow can therefore vary among streams and different phases or intensities of bedload transport can be due to transport of particles entrained from different bedmaterial strata or sources in the bed, or they might be due to one process only that increases in intensity. Interpretation and guesswork are involved when attributing a specific cause to some observed bedload intensity because processes occurring on the stream bed and the interaction between bedload and the bed surface, armor, and subarmor sediment can not be directly observed in streams but can only be deduced from sampling results of bedload transport[1].

Another factor contributing to diverging conclusions regarding transport stages is the use of different bedload sampling devices. Dissimilar sampling devices collect different amounts and particle sizes of bedload at a specified site and flow (e.g., O'Leary and Beschta 1981, Wilcox et al. 1996; Ryan and Porth 1999, Sterling and Church 2002, Bunte and Abt 2005, Bunte et al. 2007 *in press*). The interpretations regarding bedload transport processes are therefore markedly influenced by the sampling device used.

---

[1] *An exception are the few video recordings of gravel transport made in a natural stream (e.g., Dixon and Ryan 2001; Ryan and Dixon 2002).*

All of these factors, the different terminology, the varying prominence of bedload transport processes between streams (or flumes), the dissimilar sampling devices used, as well as differences in preconceived notions of bedload transport, contribute to varying observations of bedload transport intensities. There is no consensus regarding the nature of transport stages and how the stages or phases progress with increasing flows.

The purpose of this literature review is to compile descriptions of different stages of bedload transport and the processes that created them. An attempt is made to explain the variability. An important question to be answered from the literature review is whether the relationship between bedload transport rates (Q_B) and discharge (Q) progresses at a constant rate over phases of bedload transport or whether the Q_B *vs.* Q relationship changes with a shift from one phase or stage to another. If the Q_B *vs.* Q relationship changes with a shift in phases, how does the change look: do transport rates increase more steeply with flow during low flows and less steeply at high flows or is it the other way around? Which views are supported and on which grounds? Clarifying this point is important because an abrupt increase in the steepness of the bedload transport – discharge relationship has been claimed as a basis for one of the channel maintenance flow procedures (breakpoint flows) analyzed in Sections 3.1 and 3.2 of this study.

More than 40 articles were reviewed with respect to transport stages. Because these studies follow an evolution of concepts and terminology, and attempt has been made to describe the sequence of work in this area chronologically. The findings of the literature review are summarized in Table 1a-d. The first column provides general information about the studies while the other three columns describe the different transport stages, including the causing processes (if provided) and effects on the Q_B *vs.* Q or D_{max} *vs.* Q relationships (if provided). The three columns are simply titled low, higher, and highest intensity of bedload transport to provide an overarching terminology that accommodates the different terminologies used in the studies.

2. Results

Most of the articles analyzed were sorted into four groups (Table 1a - d). They describe stages of bedload transport with increasing intensity that occur:

a) without change in the rate of increase of the Q_B *vs.* Q relationship (Table 1a)
b) with steepening of the Q_B *vs.* Q relationship for high flows (Table 1b)
c) with flattening of the Q_B *vs.* Q relationship for high flows (Table 1c)
d) with different steepness of the Q_B *vs.* Q relationship for different streams (Table 1d)

Within each group, studies were sorted more or less chronologically, but a sequence of studies by the same author or group of authors was kept together.

Table 1a: Summary of descriptions of different bedload transport intensities without changes in the Q_B *vs.* Q relationship.

Reference	Low intensity transport	Higher intensity transport	Highest intensity transport
Milhous (1973) Small coarse-bedded pool-riffle stream; Vortex sampler; He proposes a multi-stage conceptual model of Q_B	During low Q only sand scattered among the armoring particles is transported. At 20-40% Q_{bkf},[(1)], small armor layer particles are dislodged and release finer subarmor sediment that is likewise transported over a generally stable armor. Q_B is low.	At a Q_{crit} of ≈ 80% Q_{bkf} [(1)], about 1/3 of the armor layer is mobile. Entrained armor particles expose and entrain sand and small gravel particles from the subarmor. Sand move downstream over the armor while fine gravel becomes entrapped in armor hiding places. [(1)] Milhous (pers. comm. April 2003) revised the Q_{bkf} at Oak Cr. from 280 cfs (Milhous 1973) to 45-53 cfs. The % Q_{bkf} here refers to the new estimate.	At high flows (100-200% Q_{bkf}), a large portion but not all of the armor layer particles are mobile. Armor and subarmor sediment mix. During the falling limb of flow, armor particles become stable again while the sand and fine gravel continue to be entrained from around armor particles.
Jackson and Beschta (1982) Small gravel-bed pool-riffle stream; Helley-Smith sampler; They establish the Phase 1 - Phase 2 concept to explain longitudinally varying bedload transport rates and how bedload is routed through riffle-pool sequences.	**Phase 1:** Fine sediment is entrained from local accumulations in the stream (e.g., pools, channel margins and wake deposits) and transported over a stable bed. Only minor channel adjustment occurs in locations of scour and deposition of fines within the low-flow bed.	**Phase 2:** Armor particles on riffles are entrained and transported through a downstream pool. The sediment is deposited on the next riffle or the one after that, wherever recent scour created local hydraulics susceptible to deposition. In Phase 2 transport that occurs at $Q > Q_{bkf}$, gravel leapfrogs from riffle to riffle.	
Beschta (1987) He describes the Phase 1 and 2 concepts in order to explain longitudinally varying bedload transport rates and the mechanism of bedload routing through riffle-pool sequences.	**Phase 1:** At the beginning of a highflow, sand and finer sediment is entrained from deposits in pools, channel margins and wakes and moves over a coarse, immobile bed. At slightly higher Q (Phase 1b?), sand and fines from the bed in general are entrained.	**Phase 2:** At higher Q, riffle surface particles are entrained as the armor layer is disrupted. The flow velocity in pools is high enough to transfer these particles (velocity reversal) onto the next riffle(s). Entrainment of (large) armor particles release finer subsurface sediment which causes increased Q_B and bed scour. This may change local hydraulics and initiate more scour nearby (positive feedback).	
Bathurst (1987a) Small step-pool, boulder-bed channel; Helley-Smith sampler, tracer; He uses Phase 1 and Phase 2 transport to distinguish between bedload transport in mainly immobile boulder-beds and in fully mobile gravel-bed streams.	**Phase 1:** Sand and fine gravel pass over a coarser and immobile bed. Due to the limited availability of fines on the bed, the resulting Q_B < than Q_B expected in a uni-sized bed of the same D_{50}. In boulder-bed streams, most transport occurs as Phase 1 with size-selective entrainment. Q_B increases to approach rates obtained in uniform sediment of same D_{50}.	**Phase 2:** Q_B comprises all bedmaterial D, thus there is no limit in sediment supply. D of Q_B is similar to D of subsurface, but finer than D of the surface sediment. Transport occurs as equal mobility. Phase 2 transport occurs mainly in streams with relatively well-sorted beds, with gradients < 0.01, in which Q is frequently > Q_{crit} for D_{max}.	

Carling (1987) Two small, gravel-cobble bed British highland streams; Sediment trap collecting the sediment per event. At what Q do channel-forming gravel particles start to move?	**Winnowing flows (Phase 1):** Lower Q (23-36% Q_{bkf}) winnow fine matrix (< 4 mm) sediment from the bed surface, leaving an open framework gravel layer. The fines are transported over a stable coarse bed as throughput load or under-capacity load, much of it in suspension. These fines can enter and exit the coarse matrix.	**Scouring flows (Phase 2):** At higher Q, the framework becomes disrupted (partial mobility) as increasingly larger D are entrained until bedload D_{50} approaches the bed D_{50} and significant changes in bed morphology become possible (bedmaterial load or capacity load). Scouring flows started at 75-94% Q_{bkf}. Most bedload D and bedload D_{50} was > 4 mm.	
Carling (1988) Small, gravel-cobble bed British highland streams; Sediment trap collecting the sediment per each event. 3-Phase model with strong increases of Q_{eff}, D_{max}, and D_{50} apparent at 60-80% and 130% Q_{bkf} in linearly plotted data.	**Phase 1 (Winnowing flows)** During under-capacity flows < 60-80% Q_{bkf}, fines are winnowed from the bed and transported over a stable bed. Stable gravel framework is not disturbed and no channel adjustment occurs.	**Phase 2 (Scouring flows)** Partial mobilization of the bed at Q > 60-80% Q_{bkf} causes abrupt increase in surface D_{50} and D_{max} in linear plots vs. Q. Only a few particles are transported such that Q_B remains small. Bed remains structurally intact and channel change is minor. Q_{eff} is within the range of Phase 2 flows.	**Phase 3 (Overbank flows)** Most of the bed is mobilized and morphological adjustments occur at Q > 130% Q_{bkf} in alluvial streams, but not in immobile beds such as a step-pool streams.
Ashworth and Ferguson (1989) Small proglacial streams with generally high Q_B; Helley-Smith samples; They suggest a 3-phase model.	**Phase 1:** At low Q, only occasional grains overpass a static bed.	**Phase 2:** A higher Q, size-selective entrainment moves individual particles from exposed positions in the surface sediment.	**Phase 3:** At further increasing Q, near equal mobility occurs as coarse surface D move and release finer D from behind and below them.
Warburton (1990; 1992) Small step-pool proglacial stream with fine gravel deposits (D_{50} of 18-35 mm) between steps (D_{50} of 128-430 mm); 6-inch Helley-Smith sampler; 3 phases of Q_B are tied to the mobility of 3 distinct sedimentary features	**Phase 1:** Tongues or sheets of sand and fine gravel move in a mobile carpet over a stable coarse bed (Q< 2 m^3/s). The bedload is finer than the bed and may also be called "throughput load". A few large particles may be intermixed with the otherwise fine bedload.	**Phase 2:** Significant increase in D_{max} at Q>2 m^3/s in linear plot of D_{max} *vs.* Q as the armor layer is disrupted and releases smaller D beneath it. The bedload D_{max} is coarser than the relatively fine gravel deposits between the steps and indicates a restructuring of these deposits. Limited size-selectivity of transport. The logarithmically plotted relationship between Q_B and stream power increases steadily over the entire range of measured Q.	**Phase 3:** At further increasing Q (>10 m^3/s), boulder steps and cobble clusters are broken up and restructured.
Lenzi et al. (2004) Step-pool stream Volume of gravel accumulated in a trap is reported hourly. They follow terminology by Ashworth et al. (1989).	**Phase 1 :** Not measurable with the device.	**Phase 2:**	**Phase 3:** Near equal mobility for pebbles and boulders during an event with high Q and very high Q_B.
Andrews and Smith (1992) Flume experiments and prior observations in small coarse-bedded mountain streams	Sand transport not considered.	**Marginal transport** Marginal transport occurs at τ^* of 0.02 - 0.06 and consists of the occasional entrainment of a gravel	**General transport** General transport occurs at τ^* > 0.06 or 0.07. A substantial fraction of the bed particles is

(Andrews 1983, 1984, Andrews and Erman 1986); Helley-Smith sampler;		particle out of shallow pockets and results in low Q_B. The particle rolls over the bed surface until coming to rest at some place. Marginal transport occurs at the majority of all Q, except for the very highest flood and produce steep increase of Q_B with Q.	in vivid motion saltating over the bed surface. General transport occurs at the highest floods, perhaps the Q_{100}.
Andrews (1994) Small coarse gravel-bed stream; 6-inch Helley-Smith sampler;		**Marginal transport** Marginal transport with low Q_B occurs at τ^* of 0.02 - 0.06 (50-350 % Q_{bkf}).	**General transport** General transport occurs at τ^* > 0.06 or 0.07 which happens very rarely.

Table 1b: Summary of descriptions of different bedload transport intensities with steepening of the Q_B *vs.* Q or D_{max} *vs.* Q relationships.

Carling (1988) Small, gravel-cobble bed British highland streams; Sediment trap collecting the sediment per each event. 3-Phase model with significant increases Q_{eff}, D_{max}, and D_{50} apparent at 60-80% and 130% Q_{bkf} in linearly plotted data.	**Phase 1 (Winnowing flows)** During under-capacity flows < 60-80% Q_{bkf}, fines are winnowed from the bed and transported over a stable bed. Stable gravel framework is not disturbed and no channel adjustment occurs.	**Phase 2 (Scouring flows)** Partial mobilization of the bed at Q > 60-80% Q_{bkf} causes abrupt increase in surface D_{50} and D_{max} in linear plots *vs.* Q. Only a few particles are transported such that Q_B remains small. Bed remains structurally intact and channel change is minor. Q_{eff} is within the range of Phase 2 flows.	**Phase 3 (Overbank flows)** Most of the bed is mobilized and morphological adjustments occur at Q > 130% Q_{bkf} in alluvial streams, but not in immobile beds such as a step-pool streams.
Warburton (1990; 1992) Small step-pool proglacial stream with fine gravel deposits (D_{50} of 18-35 mm) between steps (D_{50} of 128-430 mm); 152 mm opening Helley-Smith sampler; 3 phases of Q_B are tied to the mobility of 3 distinct sedimentary features: 1) sand and fine gravel overlying coarser gravel, 2) armored gravel bed, and 3) boulder steps.	**Phase 1: fines move over mobile bed** Tongues or sheets of sand and fine gravel move in a mobile carpet over a stable coarse bed (Q< 2 m^3/s). The bedload is finer than the bed and may also be called "throughput load". A few large particles may be intermixed with the otherwise fine bedload.	**Phase 2:** Significant increase in D_{max} at Q>2 m^3/s in linear plot of D_{max} *vs.* Q as the armor layer is disrupted and releases smaller D beneath it. The bedload D_{max} is coarser than the relatively fine gravel deposits between the steps and indicates a restructuring of these deposits. Limited size-selectivity of transport. The logarithmically plotted relationship between Q_B and stream power increases steadily over entire range of Q.	**Phase 3:** At further increasing Q (>10 m^3/s), boulder steps and cobble clusters are broken up and restructured.
Emmett (1999) Moderately sized coarse-bedded mountain stream (Little Granite Creek); 3-inch Helley-Smith sampler	**Supply-limited transport:** At lower Q prior to the disruption of the bed surface, rel. fine Q_B moves over a non-moving, coarse bed. Q_B is less (and finer) than predicted from a definable relationship (such as Bagnold's).	**Hydraulically limited transport:** With increasing Q, armor particles are entrained and release smaller D below. Q_B abruptly increases (in a linear plot of Q_B *vs.* Q) from a suppressed or supply-limited value to a value close to the definable relationship. This shift (or bedload "explosion") may be the transition between Phase 1 and Phase 2 transport. For streams in the Snake River Basin, the initiation Q occurred at 60-130% Q_{bkf}.	

Emmett and Wolman (2001) Moderately sized coarse gravel-bed rivers, Helley-Smith samples The steepness of the Q_B *vs.* Q relationship is determined by the degree of supply limitation and increases with the surf. D_{50} and D_{90} sizes	**Supply-limitation:** The immobility of large armor particles limits Q_B at moderate flows.	**End of supply limitation: Phase 2** When larger particles of the armor layer become entrained, subsurface particles are released and Q_B rapidly rise as seen in the abrupt increase in Q_B in <u>linear</u> plots of Q_B *vs.* Q and marks the beginning of Phase 2 transport.	.
Ryan et al. (2002) Moderately sized coarse gravel-bed rivers, Helley-Smith samples	**Phase 1** Bedload transport consists primarily of sand and fine gravel that is entrained from in pools and tranquil areas of the bed and moves over a stable bed. Phase I transport is associated with a low rate of increase (low slope) in the Q_B *vs.* Q relationship.	**Phase 2** Entrainment and transport of the larger surface D release smaller D from the subsurface. Together, the transport of surface gravels and subsurface material **produce a rapid increase in Q_B** in a <u>linear</u> plot of Q_B *vs.* Q that is significantly steeper than the Q_B *vs.* Q relationship in Phase 1. The beginning of Phase 2 transport defines the Q_{crit} for (coarse) gravel Q_B and is often assumed to start at Q_{bkf}, but may vary among streams due to rel. roughness, particle clusters, shape and packing (**avg. of** 91% Q_{bkf}). The piecewise regression analysis is used to define the breakpoint as the transition between the flat and steep increase in the Q_B *vs.* Q relationship.	
Ryan et al. (2005) Moderately sized coarse bedded mountain gravel-bed rivers, **Various Helley-Smith samplers**	**Phase 1** Sand and fine gravel, supplied from patches of fines or pools, move at low rates over a stable channel surface.	**Phase 2** As Q_B is supplied from the armor as well as the subarmor layer, Q_B and D increase abruptly in <u>linear</u> plot of Q_B *vs.* Q, becoming irregular and vigorous. The Q **at** the breakpoint (computed using piecewise regression) marks the transition between Phase 1 and 2 and occurs near 80% Q_{bkf} for 19 streams. Phase 2 transport entrains bed surface D_{16} to D_{25} sizes.	

Table 1c: **Summary of descriptions of different bedload transport intensities with flattening of Q_B *vs.* Q or D_{max} *vs.* Q relationships at high flows.**

Bagnold (1973) Theoretical consideration based on physics of particle motion. Based on his findings, **Leopold and Emmett (1975)** produce a generalized relationship of bedload transport and stream power for different D.	At low flows bedload transport increases steeply with stream power (with an exponent of approximately 3).	At high flows, transport becomes a linear function of stream power.	
Emmett (1976) Relative large, bimodal gravel-sand bed streams; Helley-Smith samples; He attributes shielding and releasing functions to the armor layer that cause two different Q_B *vs.* Q relationships, one for stable and one for mobile armor.	During the falling limb of Q, coarse D cease to move, deposit on the bed and armor it, covering potentially mobile finer sediment and shielding it from flow. Measured Q_B drops below the transport capacity and is less than the generalized transport relationship from Bagnold (1973) and Leopold and Emmett (1976). The Q_B *vs.* Q relationship is different from the one at high Q_B.	Q is sufficiently high to move almost all bedmaterial D. The Q_B *vs.* Q relationship is different from the one at low Q_B.	
Klingeman and Emmett (1982) Several streams, some of them with bimodal bedmaterial distribution; Several samplers (vortex, conveyor belt, 3-inch Helley-Smith sampler. They emphasize the effects of bimodal size distributions.	**Sand transport** At low flow, Q_B consists only of sand.	**Gravel transport** At higher flows, Q_B is mostly gravel. As Q decreases, Q_B shifts abruptly from gravel to sand and has low Q_B. Bimodality makes this shift particularly prominent due to the changing availability of bedmaterial for transport with changing Q.	
Parker et al. (1982) Oak Creek , small pool-riffle stream; Vortex sampler; Only the 22 data with highest Q_B and D_{max} from Milhous (1973) for $Q > Q_{crit}$ (40 cfs ≈ 80%Q_{bkf}?) were used for the analyses. They introduce the idea of equal mobility.	Not considered At $Q < Q_{crit}$, sandy bedload moves on top of an immobile pavement. Q_B are generally low and governed by availability. This transport is not considered in the equal mobility analyses.	At $Q>Q_{crit}$, more of the pavement particles are transported, releasing the finer sediment beneath which is likewise transported. Over a short range of Q, all D become entrained in proportion to their availability on the bed (equal mobility transport). Q_B becomes governed by hydraulic conditions rather than sediment availability.	
Andrews (1983) Large rivers with bimodal bedmaterial distribution; 3-inch Helley-Smith sampler; East Fork River that transports mainly sand; conveyor belt sampler.	Washload or throughput load consisting of sand.	D_{max} increased from 25 to 100 mm within a small range of Q (74-87% Q_{bkf}), suggesting a relative sudden increase of D (but in small numbers) as well as near equal mobility of most gravel sizes on the bed.	
Andrews and Erman (1986) Coarse gravel-bed stream; 6-inch Helley-Smith sampler; very high Q (150-350% Q_{bkf})	Sand transport not considered.	All bed D are entrained during Q of 150-350 % Q_{bkf} but at low numbers (marginal Q_B). With increasing Q, the frequency of particle entrainment increases, but without much	

		coarsening of the bedload D distribution (equal mobility) (sampling artifact of the HS?). Despite D being mobile at very low rates, some small gravel (tracer) particles never moved, suggesting that the armor did not break up.	
Kuhnle (1992) Small stream with sand/gravel bed; HS	**Transport more size selective** at lower Q when D of Q_B is finer than the bed.	**Equal mobility at highest flows** when D of Q_B approaches the D of the bed.	
Kuhnle (1993) Small stream with sand/gravel bed; modified Helley-Smith and pit traps	**Size selective entrainment** may be caused by large portion of sand in the bed.	**Equal mobility** may be caused by **absence of sand in** the bed.	
Komar and Shih (1992) Oak Creek data, Vortex sampler	**Transitional Phase** Bedload D_{max} and other percentiles strongly increase with increasing Q and transport is size selective. The range of Q with size selective Q_B (transitional phase) likely varies with stream characteristics and may extend over all commonly occurring highflows or be quickly exceeded and turn into equal mobility transport (**Thorne 1992**).	**Equal mobility at high flows** At high Q, the size distribution of Q_B approaches that of the bedmaterial because all sizes are entrained. This condition constitutes equal mobility transport.	
Bunte (1992a and b; 1996); Moderately-sized coarse gravel-bed stream; Net-frame sampler **collects** particles > 10 mm	**Selective transport until D_{max} sizes are entrained**: Strong increase of measured bedload D_{max} with Q shows that increasingly larger particle sizes are included in Q_B and transport is size-selective.	**Equal mobility after D_{max} sizes have been entrained**: Postulates that once the bed D_{max} has been entrained, any further increase in Q leads to only small increases in the bedload D_{max} and equal mobility of all D is reached. In poorly sorted and coarse-bedded mountain gravel-bed streams, equal mobility might be reached at $Q >> Q_{bkf}$. Streams with finer gravels and better sorted bedmaterial may reach equal mobility near Q_{bkf}.	
Bunte et al. (2007) *(in press)* Small to moderately sized, armored mountain gravel-bed streams; Bedload **traps with 4 mm mesh** width	**Selective transport** Strong increase of measured bedload gravel D_{max} over entire range of measured Q is shown for 8 streams. The increasingly larger D_{max} in Q_B indicates size-selective transport.		
Whitaker (1997) Moderately-sized coarse gravel-bed river, poorly armored Net-frame sampler collects particles > 32 mm	**Phase 1 transport** Q_B of sand and fine gravels not measured using a 32 mm mesh width at relatively high Q: Meas'd range of Q: 65-147% Q_{bkf}.	**Phase 2** D_{50} and D_{max} increase with Q, indicating size-selective transport. Q_B *vs.* Q and D_{max} *vs.* Q relationships flatten at about 110% Q_{bkf} and might indicate equal mobility. He did not measure Phase 1 transport but postulates that the onset of Phase 2 is characterized by a quick increase of Q_B and D_{max} with Q, i.e., a wide	

		range D are entrained over a narrow range of Q. As Phase 2 continues, further increase in Q is required to entrain larger D.	
Wilcock and McArdell (1993) Recirculating flume with poorly sorted trimodal bedmaterial ranging from sand to coarse gravel ("bed of multiple colors") with peaks at the size classes > 0.25, 4, and 16-32 mm. Dunes and bedload sheets makes Q_B spatially and temporally variable in almost all runs. Bedload was collected in a sediment trap at the flume end. Q_B is expressed per size fraction Q_{Bi} and scaled by the % of D_i on the bed surface (F_i) to yield Q_{Bi}/F_i.		**Partial transport:** Only a portion of the particles in a size fraction (typically the larger D) on the bed are entrained which results in substantially smaller Q_{Bi}/F_i of coarser particles than Q_{Bi}/F_i of finer particles. In partial transport, Q_{Bi}/F_i depends not only on the proportion of D_i on the bed, but the proportion of D_i that is mobile. Conditions of W^*=0.002 are well within partial transport. Partial transport is not to be equated with Phase 1 transport in which particles not derived from the bed move over a static bed.	**Fully mobilized transport:** Fully mobilized transport begins when the percentage of D_i in Q_B exceeds that percentage in the bed. All D (typically the smaller ones) on the bed are regularly entrained (at least once per event). This happens at τ 2.1-2.6 times > τ_{rci} (= ref. shear stress for incipient motion at W^*=0.002). The τ^* for fully mobile Q_B is 0.02 for gravel of 22 mm and 0.05 for 2 mm. Equal mobility of all mobile D prevails. Q_{Bi}/F_i depends on the proportion of D_i on the bed surface (F_i) and on the total transport rate. The D from which on all particles are entrained increases with increasing Q and Q_B.
Wilcock (1997); Wilcock and McArdell (1997) Flume with poorly sorted bedmaterial ranging from sand to coarse gravel ("bed of multiple colors") Q_B is expressed per size fraction Q_{Bi} and scaled by the % of D_i on the bed surface (f_i) to yield Q_{Bi}/f_i.		**Partial transport:** Partial transport is common in many gravel-bed rivers and is associated with a rapid decrease in Q_B for larger D. It produces non-negligible Q_B and much of the annual load, particularly in steep streams with poorly sorted coarse beds and snowmelt regimes.	**Complete mobilization of the bed** is associated with equal mobility transport Displacement frequency decreases with D_i, while displacement length increases with D_i.
Haschenburger and Wilcock (2003) Moderately sized coarse gravel-bed stream with large bar areas. Tracer experiments		**Partial transport:** The active proportion of particles declines with D. With increasing Q, partial transport shifts from finer to coarser D and the % streambed area with partial transport increases. Partial transport can cause large Q_B, and entrainment of D_{max} does not qualify for a fully mobile bed. At 50-70% Q_{bkf}, about 60% of the bed area was partially, and 30% fully mobile.	**Full mobility** All particles within a specified streambed area are mobile, and this area increases with increasing Q. Most of the channel area was fully mobile during a 7-year recurrence interval flood that reached bankfull.
Hassan and Church (2001) Moderately sized coarse gravel-bed stream with alternate bars; Pit traps installed at different locations on a bar were emptied hourly or daily.	**Phase 1: steeply increasing Q_B due to overpassing sand** In the bar center, Q_B comprised mostly of sand increased steeply and especially dropped steeply during relatively low Q.	**Phase 2: gradual increase of Q_B during gravel transport** At higher flows, when significant amounts of gravel started to move, Q_B increased slowly with increasing Q.	
	At the bar head and tail, Q_B simply increased with increasing Q without change in the Q_B *vs.* Q relationship.		

Table 1d: **Summary of descriptions of different bedload transport intensities with changing Q_B *vs.* Q or D_{max} *vs.* Q relationships in different streams.**

Laronne and Reid (1993); Reid and Laronne (1995) Several streams, several samplers	**Armored streams** Streams in humid environments have low Q_B and steep Q_B *vs.* Q relationships.	**Unarmored streams** Stream in desert environments have high Q_B and flat Q_B *vs.* Q relationships.	
Lisle (1995)	**Armored streams** Q_B finer than bed, selective transport.	**Unarmored streams** Q_B same size as bed, equal mobility transport.	
Lisle and Church (2002); Lisle (submitted) Various sets of flume and field data Want to explore the reservoir transport – storage relationship; They use the terminology of Phase I and II transport but not in the sense of Jackson and Beschta (1982).	**Supply-limited transport (Phase II)** Size selective transport with generally low Q_B and significant change in Q_B *vs.* Q relationships (=steep rating curves) in well-armored beds. Less fluctuating Q_B and bed structures (e.g., stone rings) Q_B responds to decreasing supply by progressive armoring that may become static.	**Transport-limited transport (Phase I)** Non-size selective transport with generally high Q_B and little change in Q_B *vs.* Q relationships (=flat rating curves) in weakly-armored beds, potentially highly fluctuating Q_B and bed forms (dunes, bedload sheets). Q_B does not respond to decreasing supply.	
Barry et al. (2004) Gravel- and sand-bedded streams in the granitic Idaho Batholith; Helley-Smith samples; The degree of bed armoring determines the degree of increase in Q_B	**Phase 1** The supply of fine material on the bed determines, in part, the magnitude of Phase 1 transport (i.e., Q_B of fines over an immobile bed). The coarse armor layer limits gravel Q_B. A well-armored stream delays the onset of Q_B and causes a steeper increase in Q_B with Q than in less-armored streams. (i.e., higher rating curve exponent).	**Phase 2** Once larger armor particles are mobilized, finer subsurface particles are exposed to flow and entrained.	
Bunte et al. (2006b) Coarse-bedded, armored, mountain streams; Bedload traps	**Armored streams** Among armored streams, those that are least armored had the steepest Q_B *vs.* Q and D_{max} *vs.* Q relationships, while well-armored streams (due to high amount of subarmor fines) had flatter Q_B *vs.* Q and D_{max} *vs.* Q relationships.		

2.1 Stages of bedload transport without change in Q_B vs. Q relationship

The majority of articles found for this literature review describe phases of bedload transport without associating the transition between phases with a steepening or flattening of the relationship between bedload transport rates and discharge. These findings are explained below. Unless otherwise noted, a Helley-Smith sampler or similar device was used for collecting bedload in the field studies.

2.1.1 Several stages of armor and subarmor mobility

Milhous (1973) was one of the first researchers who made detailed measurements and analyses of bedload transport rates and particle sizes that were sampled over multiple highflow events using a vortex sampler in a small gravel-bed stream. Interpreting his results, he provided a detailed description of bedload transport processes during increasing and decreasing flows. Without explicitly calling them such, Milhous (1973) defined several transport stages. During low flows, only sand scattered among the armoring particles is transported over a stable armor layer. At 20-40% Q_{bkf}[2] small armor layer particles are dislodged and release finer subarmor sediment that is, likewise, transported over a generally stable armor, but transport rates remain low. At about 80% Q_{bkf}, one third of the armor layer is mobile. Entrained armor particles expose sand and small gravel particles from the subarmor which allows then to be entrained as well. Sand continues to move downstream over the armor while fine gravel becomes entrapped in armor hiding places. At high flows (100-200% Q_{bkf}), a large portion but not all of the armor layer particles are mobile and are transported together with the released subarmor sediment. During the falling limb of flow, armor particles become stable again while the sand and fine gravel continue to be entrained from around armor particles.

2.1.2 Phase 1 and Phase 2 transport

Jackson and Beschta (1982) coined the Phase 1 and Phase 2 terminology in order to describe longitudinally varying transport rates and the conveyance of bedload through riffle-pool sequences. During Phase 1 transport at relatively low flows, sand is mobilized from deposits of fines and, later, from the armor as well and travels over a stable bed. Only minor channel changes occur. At higher flows during Phase 2 transport, riffle particles are entrained as the armor layer is disrupted. The flow velocity in pools is high enough (due to velocity reversal) to transfer these particles onto one of the next riffle(s) downstream where conditions are favorable for deposition. Entrainment of large armor particles release finer subsurface sediment which causes increased transport rates and bed scour. This may change local hydraulics and initiate more scour nearby (positive feedback) (Beschta 1987). Phase 2 transport occurs at flows larger than bankfull. It enables gravel to leapfrog from riffle to riffle and allows the streambed to adjust to flows.

---

[2] *Milhous (pers. comm. April 2003) revised his estimate of bankfull flow at Oak Cr. from 280 cfs (Milhous 1973) to 45-53 cfs. The % Q_{bkf} here refers to the new estimate.*

The Phase 1 – Phase 2 terminology was soon adopted by other researchers and is still in use today, although its meaning changed slightly, referring not to the transport state that enables riffle-to-riffle transport but distinguishing, more generally, between lower and higher transport intensities.

Sampling in a small step-pool, boulder-bed channel, Bathurst (1987a) concluded that most transport occurs as Phase 1 during which sand and fine gravel pass over a coarser and immobile bed. The limited availability of fines on the bed keeps measured transport rates smaller than those expected from a bed comprising sand and fine gravel only. With increasing flow, transport rates approach those expected in sand/fine gravel streams. The increase of the D_{max} particle size with flow suggests size-selective particle entrainment. In Phase 2 transport, all bedmaterial particle sizes are mobilized, there is no limit in sediment supply, and bedload particle sizes approach that of the subsurface but remain finer than the surface sediment. Phase 2 transport occurs rarely in boulder-bed streams, but is common in streams with relatively well-sorted beds, with gradients less than 1%, and in which the largest bedmaterial particle sizes can be frequently entrained. Bathurst's description of Phase 1 and Phase 2 transport aims in the direction of a distinction between selective transport and equal mobility.

Based on bedload particles accumulated in pit traps during storm events in small gravel-bed streams, Carling (1987) distinguished between winnowing (Phase 1) and scouring flows (Phase 2). Low flows winnow fine matrix (< 4 mm) sediment from the bed surface, leaving an open framework gravel layer. The fines are transported over a stable coarse bed as throughput or under-capacity load, much of it in suspension. These fines can enter and exit the coarse framework. At higher flows, the framework becomes disrupted (partial mobility) as increasingly larger particles are entrained until the bedload D_{50} size approaches the bed material D_{50} sizes, and significant changes in channel bed morphology become possible (Phase 2). Other terms that Carling (1987) used for this transport stage were bedmaterial load or capacity load. In the two streams analyzed, scouring flows or Phase 2 transport started at 75-94% Q_{bkf}.

2.1.3 Three phases of bedload transport

Several authors proposed a three-phase model to describe increasing bedload transport intensity. Reanalyzing data from two small gravel-bed streams, Carling (1988) describes Phase 1 as winnowing or under-capacity flows during which fines are winnowed from the bed and transported over a stable bed at flows below 60-80% Q_{bkf}. The stable gravel framework is not disturbed and no channel adjustment occurs. Scouring flows (Phase 2) partially mobilize the bed at flows larger than 60-80% Q_{bkf} and cause an abrupt increase in surface D_{50} and D_{max} in linear plots versus flow. Only a few particles are transported such that bedload transport rates were small. The bed remains structurally intact and channel change is minor. During overbank flows at $Q > 130\%\ Q_{bkf}$ (Phase 3), most of the bed is mobilized and morphological adjustments occur in alluvial streams, but not in immobile beds such as a step-pool streams.

Measuring in proglacial streams, Ashworth and Ferguson (1989) found that at low flow, only occasional grains overpass a static bed (Phase 1). At higher flow, size-selective entrainment moves individual particles from exposed positions in the surface sediment (Phase 2). At still higher flow, near equal mobility occurs as coarse surface particles move and release finer particles from behind and below them (Phase 3). The transport phases are conceptually tied to selective transport and equal mobility.

Sampling bedload in a small step-pool proglacial stream with fine gravel deposits between steps, Warburton (1990; 1992) also defined three phases of bedload transport and tied them to the mobility of three distinct sedimentary features. At low flows (Phase 1), tongues or sheets of sand and fine gravel move in a mobile carpet over a stable coarse bed. The bedload is finer than the bed and may also be called "throughput load". A few large particles may be intermixed with the otherwise fine bedload (a sampling artifact of the Helley-Smith sampler?). At some higher flow, a linear plot of D_{max} *vs.* Q suggests an abrupt increase in the largest entrained particle size which is interpreted to indicate disruption of the armor layer and the release of smaller particles beneath it (Phase 2). The bedload D_{max} is coarser than the relatively fine gravel deposits between the steps and indicates a restructuring of these deposits. Transport is considered somewhat size-selective. At further increasing flow, boulder steps and cobble clusters are broken up and restructured (Phase 3). In contrast to the abrupt increase in the largest bedload particle size in a linear plot of D_{max} versus Q, the logarithmically plotted relationship between bedload transport rates and stream power increases steadily and steeply over the entire range of flow.

Working in an alpine step-pool stream, Lenzi et al. (2004) measured the volume of gravel accumulated in a debris basin in hourly intervals. They also delineated three transport phases, although Phase 1 transport (sand and fine gravel) is not measurable with their device. While most of the observed events classify as Phase 2, they observed Phase 3 transport with near equal mobility for pebbles and boulders during an extreme event with very high transport rates.

2.1.4 Marginal and general transport

Based on flume experiments and prior observations in small coarse-bedded mountain streams (Andrews 1983, 1984; Andrews and Erman 1986), Andrews and Smith (1992) and Andrews (1994) distinguished between marginal and general transport. Sand transport (that would likely be classified as Phase 1 transport) is not considered in these studies. During marginal transport of gravel (which consequently falls into the category of Phase 2 transport), a few gravel particles are entrained out of shallow pockets on the bed surface, roll over the bed surface and come to rest. The resulting transport rates are low. Marginal transport occurs over a wide range of flows and produces steeply increasing relationships between transport rates and flow. During general transport, a substantial fraction of the bed particles is in vivid motion saltating over the bed surface. General transport in mountain gravel-bed streams occurs only at the highest floods, perhaps the 100-year flood.

All of the studies described in Section 2.1 portray different stages of bedload transport intensity but none describes a concomitant link of phase shifts to changes in the relationship between bedload transport and discharge. This means, the different phases or stages are seen as characteristic points along the continuous and steady increase of transport rates with flow. By contrast, studies discussed in the following section link (in one way or another) stages of bedload intensity to changes in the Q_B *vs.* Q relationship.

2.2 Stages or phases of bedload transport linked to changes in the Q_B vs. Q relationship

A bedload transport – discharge relationship can basically take three shapes: 1) it can increase at a steady rate over the entire measured range of flow or the rate of increase can change at some flow. 2) The change can take the form of steeply increasing transport rates at lower flows and a less steep increase at higher flows (concave function; Figure 1a). 3) The other possibility is that transport rates increase slowly during low flows and much more strongly at some higher flows (convex function; Figure 1b). Examples for both were found in the literature and are presented below.

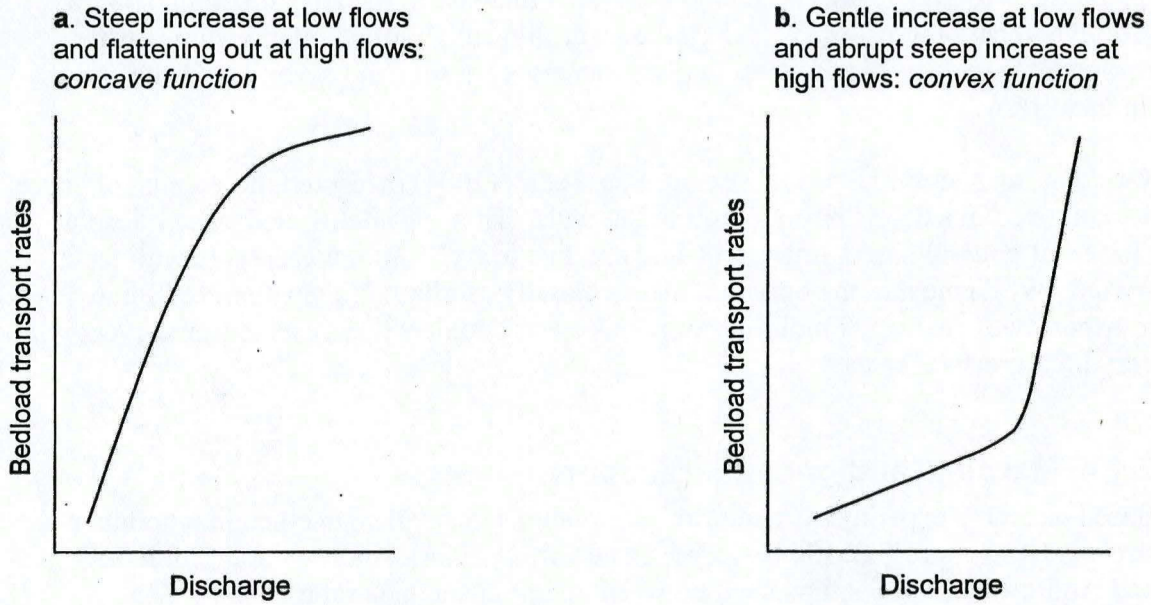

Figure 1: Different shapes of the bedload transport – discharge relationship: Steep increase at low flows followed by a flattening at high flows (a); gentle increase at low flows followed by an abrupt steep increase at high flows (b).

2.2.1 Phase 1 and 2 transport linked to steepening Q_B *vs.* Q relationships

Section 2.2.1 describes the studies that link Phase 1 and 2 transport to a steepening in the Q_B *vs.* Q relationship.

2.2.1.1 Breaks in the Q_B *vs.* Q relationship

Based on bedload transport rates sampled in two large gravel-bed streams with bimodal bedmaterial size distributions, Emmett (1976) and Klingeman and Emmett (1982) suggest that two functions separated by a "break" are needed to describe the Q_B *vs.* Q relationship, one for sand transport at low flows, a stable armor and low sediment supply and one for high flows with a mobile armor. The idea of a "break" in the transport relationship is born.

2.2.1.2 Abrupt increase in bedload particles sizes

Carling (1988) observed an abrupt increase in the D_{50} and D_{max} particle sizes in linear plots versus flow at about 60-80% Q_{bkf} and interpreted this as the onset of scouring flows in Phase 2 transport. Warburton (1990, 1992) also noted an abrupt increase in the bedload D_{max} size with flow in a linear plotting scale, and he used this observation to support the idea of a shift from Phase 1 to Phase 2 transport, although the logarithmically plotted relationship between bedload transport rates and stream power showed no concomitant change in steepness.

Emmett (1999) developed the idea of a breakpoint further and tied it to the shift from Phase 1 to Phase 2 transport. Based on a large data set of bedload samples from a mountain gravel-bed stream, he concluded that at low flows, fine bedload moves over a non-moving, coarse bed (Phase 1). Transport rates are supply-limited and smaller as well as finer than predicted from a definable relationship (such as Bagnold's). With increasing flow, armor particles are entrained and smaller particles below the armor are released. This opens up a large bedload supply and makes transport rates hydraulically limited, i.e., determined by flow and not sediment availability.

Based on a plot of fractional transport rates versus flow in a linear plotting scale in which transport rates appeared to increase abruptly with flow ("bedload explosion"), Emmett (1999) suggested that transport rates abruptly increase from a suppressed (or supply-limited) value to a value close to the definable relationship and suggested that the "explosion" marks the transition between Phase 1 and Phase 2 transport.

In a subsequent step, Emmett (1999) then linked the onset of Phase 2 transport to channel maintenance flows. He found that for several streams in the Idaho Snake River Basin, the onset of Phase 2 transport occurred at 60-130% Q_{bkf}.

2.2.1.3 Breakpoint flows and the shift from Phase 1 to Phase 2 transport

Adding four more (relatively large) streams to the analyses, Emmett and Wolman (2001) again ascribed the onset of Phase 2 to the armor break-up and the end of supply-limitation and linked the steepness of the Q_B *vs.* Q relationship to whether transport is supply- or transport limited. They proposed that at moderate flows, large armor particles remain immobile and limit transport rates. During Phase 1 transport with supply limitation, transport rates increase slowly with flow. Once larger armor particles are entrained, they release subarmor particles. This causes rapidly rising transport rates and a faster increase of transport rates with flow. The abrupt increase marks the beginning of Phase 2 transport that can be visually identified in linearly scaled plots of the fractional bedload transport rates versus discharge. Andrews (1983) at one of the streams examined by Emmett and Wolman (2001) found that the size of the largest transported particle sizes increased swiftly from 25 to 100 mm within a small range of flow (74-87% Q_{bkf}). This was seen as supporting the notion of rapidly increasing transport rates at some point in flow. Ryan and Emmett (2002) also showed the abrupt increase in linearly plotted transport rates for Little Granite Creek. They visually defined the flow at which transport rates start to increase at a steep rate, called it "breakpoint flow" and declared it useful for defining phases of transport.

Ryan et al. (2002) took up the concept that the shift from Phase 1 to Phase 2 transport is associated with rapidly increasing transport rates after the armor break up. They further developed the idea that the Q_B *vs.* Q relationship changes at the onset of Phase 2 transport and that the flow at which the shift from Phase 1 to Phase 2 transport occurs can be quantified. Their analyses are based on bedload samples collected at several sites along one mountain gravel-bed stream and its tributaries. During Phase 1 transport, sand and fines are entrained from pools and tranquil areas with patches of fines moving at low rates over a stable bed. When plotted in a linear scale, transport rates during Phase 1 transport increase at a low rate with flow. During Phase 2 transport, entrainment and transport of larger surface particles releases smaller particles from the subsurface. The combined transport of surface and subsurface material produces a rapid increase in bedload transport rates in a linear plot of Q_B *vs.* Q that is significantly steeper than the Q_B *vs.* Q relationship in Phase 1. The beginning of Phase 2 transport defines the critical flow for the transport of medium and coarse gravels. The "break" in slope of the relationship between bedload transport and discharge is called the breakpoint flow and can be determined consistently from a statistical procedure called piecewise regression[3]. Applying the piecewise regression procedure to five sites along a mountain cobble-bed stream and two of its tributaries, the breakpoint flow was found to occur on average at 91% Q_{bkf}.

Ryan et al. (2005) added data from more mountain gravel- and cobble-bed streams in which transport rates were collected using a Helley-Smith sampler (or similar handheld devices) to the analyses of breakpoint flows with the piecewise regression. Breakpoint flows at the 19 sampling sites were believed to mark the transition between Phase 1 and 2 and occurred between 40 and 110% of bankfull flow with an average of 81% Q_{bkf} while

[3] *The Piecewise regression procedure is described in Section 3.2.*

the range of one standard deviation encompassed 65 to 95% Q_{bkf}. At the onset of Phase 2 transport, particles of the bed surface D_{16} to D_{25}[4] sizes were mobile. In these streams this constituted medium (D_{16} = 11 to 36 mm) and coarser gravel.

2.2.2 Stages or phases of bedload transport with flattening Q_B *vs.* Q relationship

Section 2.2.2 describes the studies that link phases or stages of transport to a flattening of the Q_B *vs.* Q relationship.

2.2.2.1 Gravel bedload transport equations: flattening out at high flow

A variety of bedload transport equations commonly used for gravel-bed streams predict a steeply increasing and then flattening (i.e., a concave) function between bedload transport rates and flow. The plotting scale is always logarithmic on both axes. The bedload transport equations by Einstein (1950) and Paintal (1971) that are based on the probability of particle entrainment, transport, and deposition take concave shapes. Based on the physics of particle motion, Bagnold's (1973, 1980) bedload equation also shows a steep increase during low flows. At high flows, when all particles of the bed surface are involved in bedload transport, the transport relationship flattens and becomes a linear function (exponent of 1) of stream power. Leopold and Emmett (1976) replot Bagnold's relationship for different bedload efficiencies and particle sizes and arrive at bedload trends that are steeper during low flows and flatter, linearly, related to stream power at high flow. The bedload equations formulated by Parker and Klingeman (1982), Parker et al. (1982), as well as a number of related equations (Parker 1990; Bakke et al. 1999; Wilcock and Crowe 2003) also show a steep increase for lower flows and a flattening out at higher flows. The reason why bedload transport equations predict the steep trend at low flows and become flatter at high flows is typically not well explained[5]. The question arises whether the transition between steeper and flatter portions of the predicted transport equations can be associated with a transition from selective transport to equal mobility.

2.2.2.2 Flattening Q_B *vs.* Q relationships rarely observed in armored, gravel- and cobble-bed streams

While a flattening of the bedload transport relationship seems to be the typical case for bedload transport equations, a flattening of a bedload transport relationship is rarely observed in coarse-bedded, armored mountain gravel-bed streams, irrespective of the sampling device used. The bedload rating and flow competence curves measured by Milhous (1973) with a vortex sampler in flows up to 200% Q_{bkf} show no flattening. Ten of the 12 data sets that were collected in Idaho mountain streams during the Snake River Adjudication (King et al. 2004) using Helley-Smith sampler show a continuously

---

[4] *Particle sizes for the D_{25} were not indicated but are typically about twice as large as the D_{16} sizes.*

[5] *In measured Q_B vs. Q relationships, a flattening of the relationship might be caused by overbank flooding when increasing flow volume leads to small increases in shear stress exerted to the channel bottom.*

increasing trend of transport rates with flow in log-log scaled power function relationships (Whiting et al. 1999; Emmett and Wolman 2001; King et al. 2004; Barry et al. 2004). Similarly, of the 19 data sets collected in mountain gravel-bed streams using a Helley-Smith sampler during snowmelt highflows in flows up to 170 and 190% Q_{bkf} by Ryan et al. (2005), perhaps three suggest a flattening trend for the highest flows. Also, all of the nine bedload transport relationships and flow competence curves measured in coarse-bedded mountain gravel-bed streams in flows up to 130 and 150% Q_{bkf} using bedload traps show a continuous steep increase with flow (Bunte et al. 2007, *in press*). This discrepancy between predicted and measured bedload transport relationships is not well understood.

2.2.2.3 Partial transport and fully mobilized transport

Wilcock and McArdell (1993) distinguished between partial and fully mobilized transport based their observations and analyses of experiments in a recirculating flume with poorly sorted trimodal bedmaterial ranging from sand to coarse gravel[6]. Bedload was collected in a sediment trap at the flume end. These studies did not involve Phase 1 transport that the authors considered as movement of particles that are not derived from the bed over a static bed surface. During partial transport (lower flows), only some of the particles in each size fraction on the bed are entrained. Compared to their presence on the bed, the percentage of the small particles entrained is greater than the percentage of larger particles. Partial transport is common in many gravel-bed rivers and can be identified by a rapid decrease in the percentage of mobilized particles of the largest sizes. Partial transport can produce high transport rates and accounts for much of the annual load, particularly in steep streams with poorly sorted coarse beds and snowmelt regimes (Wilcock 1997; Wilcock and McArdell 1997). Fully mobilized transport begins at higher flows when the percentage of bedload particles per size class in motion equals or exceeds the percentage of that size fraction in the stream bed. Attaining fully mobilized transport requires large flows that exceed the critical flow for incipient motion (defined as W^*=0.002 by Parker et al. 1982) by 2.1-2.6 times[7]. During complete mobilization of the bed, all particle sizes on the bed are involved in bedload transport and equal mobility prevails. The measured relationship between transport rates and shear stress increases steeply during low flows and flattens out during high flows.

Haschenburger and Wilcock (2003) observed the shift from partial to full mobility via extensive tracer experiments in a mountain gravel-bed stream. As flow increases, the percent streambed area with partial transport expands, while the percentage of streambed area that is immobile shrinks. At further increasing flows, some of the streambed area becomes fully mobile, and this area grows with increasing flow. At the study stream, about 60% of the bed area was partially, and 30% fully mobile at moderate flows (50-70% Q_{bkf}), while most of the channel area was fully mobile during a 7-year recurrence interval flood that reached bankfull.

---

[6] *Each particle size-class was colored differently, resulting in a "bed of multiple colors".*

[7] *Mueller et al. (2005) showed for 45 gravel-bed streams that the flow at which W^* = 0.002 occurs on averaged at 67% Q_{bkf}. Fully mobilized transport would thus set in at flows exceeding about 140% Q_{bkf}.*

2.3 Discussion

Findings from the literature review of different phases or stages of bedload transport raise several questions:

- The steepening of the relationships between bedload transport rates and flow that was taken as the transition between Phase 1 and Phase 2 transport (Section 2.2.1) appears to be limited to studies that use a linear plotting scale for the Q_B *vs.* Q relationship. What effect does plotting scale have on the Q_B *vs.* Q relationship?

- Studies described in Section 2.2.1 link the break-up of the armor layer to an increase in sediment supply that consequently results in an abrupt increase in bedload transport rates, a steepening of the Q_B *vs.* Q relationship, and the onset of Phase 2 transport (Section 2.2.1). In other studies, however, high sediment supply seems to be related to equal mobility transport and a flattening of the Q_B *vs.* Q relationship. In which way does a change in sediment supply relate to a change in the Q_B *vs.* Q relationship?

- While bedload transport equations for gravel-bed streams typically predict a Q_B *vs.* Q relationship that steeply increases at low flows and flattens out at high flows, the same phenomenon is rarely observed in bedload transport rates measured in armored coarse gravel- and cobble-bed streams (Section 2.2.2). Does the flattening reflect the transition from selective transport to equal mobility, and is that shift limited to streams with finer, better sorted, or unarmored gravel beds?

- The studies introduced in Sections 2.1 and 2.2 reported either 2 or 3 transport phases, and used different terminologies. Flows assigned to the transport stages varied widely. Is it possible to match Phases 1, 2 and, if provided 3, among the different studies and unite all 2 or 3 phases into a common system? What are the flows for the onset of each phase?

The following section discusses these questions.

2.3.1 Effect of plotting scale

Several studies on transport phases link the onset of Phase 2 transport to the abrupt steepening of the Q_B *vs.* Q relationship (Section 2.2.1). These studies have a commonality:

They plot and analyze Q_B *vs.* Q relationships in a linear scale. Use of a linear plotting scale for Q_B *vs.* Q relationships is relatively new and largely confined to one group of researchers (Emmett 1999, Troendle et al. 2001, Emmett and Wolman 2001, Ryan and Emmett 2002, Ryan et al. 2002, 2005, Rosgen 2006).

Bedload transport rates collected over a wide range of flows extend over at least three and typically five or six orders of magnitude, depending on the sampling device used (Bunte et al. 2007, *in press*). The Q_B *vs.* Q relationship also describes a power function (Bagnold 1973; Milhous 1973; Klingeman and Emmett 1982; Whiting et al. 1999; King et al. 2004;

Barry et al. 2004, Bunte et al. 2007, *in press*), to name a few[8]. It is therefore customary to plot a Q_B *vs.* Q relationship in logarithmically scaled plots such that the smallest transport rates are as visible as the large rates.

While a logarithmical plotting scale makes even the smallest measured value visible on the plot, a linear plotting scale squeezes transport rates smaller than about 10-20% of the highest measured transport rates against the lower edge of the plot. Data points for these transport rates are then barely distinguishable from each other and appear to increase at a low rate with flow. By contrast, transport rates between about 10-20 and 100% of the maximum measured transport rate visually dominate the plot and visually increase at a faster rate with flow than low transport rates squeezed against the x-axis. Transport rates between about 10 and 100% of the highest measured transport rates represent the upper one order of magnitude of the data range, but they occupy most of the plot. Transport rates less than 10% of the highest measured value encompass a wide range of transport rates that span 2 to 5 orders of magnitude, but these data points are barely visible in the linear plot.

Linear regression functions fitted to the data mimic the visual impression. The function fitted to the lower portion of the data that crowd along the x-axis is almost flat, while the function fitted to the upper portion of the data starting at the abrupt increase in transport rate is steep, and both fitted functions are statistically different from each other. The intersection between the upper and lower linear regression functions is the breakpoint between Phase 1 and Phase 2 transport. This breakpoint is only visible in a linearly scaled plot of the data; it is not visible when the same data are plotted in logarithmical scale on both axes.

Use of a linear plotting scale for Q_B *vs.* Q relationships might be related to using a Helley-Smith sampler for collecting bedload samples. The Helley-Smith sampler is prone to involuntary particle pick up at low flows (Bunte et al. 2005), and unlikely to sample the largest particles mobile in a coarse-bedded stream at the highest flows due its small opening size and short sampling time (Bunte and Abt 2005). Transport rates obtained for a Helley-Smith sampler thus span a smaller range, typically 2-4 orders of magnitude, than transport rates sampled in the same streams with other samplers (4-6 orders of magnitude) (Bunte et al. 2004; Bunte et al. 2007, *in press*). The comparatively small range of transport rates obtained from Helley-Smith samplers may be the reason why a linear plotting scale is selected by some researchers.

2.3.2 Role of sediment supply and armoring on steepness of Q_B *vs.* Q relationships

Several authors link transport stages and changes in the steepness of the Q_B *vs.* Q relationship to changes in sediment supply and the degree of bed armoring. However, findings vary widely between studies.

---

[8] Note however, that a Q_B *vs.* Q relationship plotted in logarithmic scales on both axes becomes flatter in its upper end when the difference of $Q - Q_{crit}$ is plotted on the x-axis.

One group of researchers (Emmett 1999; Emmett and Wolman 2001; Ryan and Emmett 2002; Ryan et al. 2002, 2005) relate low transport rates that slowly increase with flow during Phase 1 transport to supply-limited conditions on the bed when the armor is intact and shields the finer sediment beneath from the force of flow. Consequently, the flat part of the bedload rating curve is attributed to low sediment supply from the bed. High transport rates that steeply increase with flow during Phase 2 transport are linked to transport-limited conditions. This means that the steep part of the bedload rating curve is attributed to unlimited sediment supply after the armor breakup (situation depicted in Figure 1b).

Other researchers have found the opposite general trend between rating curve steepness and sediment supply. Dietrich et al. (1989) and Lisle (1995) found that strongly armored streams—resulting from low sediment supply to the stream—have steeper bedload transport relationships than streams that are not at all or poorly armored. Reid and Laronne (1993) and Laronne and Reid (1995), e.g., point out that Q_B *vs.* Q relationships are much steeper in armored streams in humid environments than in unarmored beds typical of desert streams. Lisle and Church (2002), and Lisle (submitted) also associate well-armored beds with generally low transport rates, with bedload particle sizes that are finer than the bedmaterial, with size-selective transport, and with a significant increase of transport rates with flow (=steep rating curves). By comparison, high sediment supply (i.e., a transport-limited condition) is understood to cause weakly-armored beds, generally high transport rates, and bedload particles sizes that are similar to the bedmaterial size. These characteristics result in a poorly defined increase of bedload particle sizes with flow, in transport rates that start out high, and in relatively flat bedload transport relationships.

Although these connections seem intuitively plausible, positive relationships between the degree of bed armoring and rating curve steepness have not been observed for bedload rating curves measured in armored mountain gravel-bed streams. Barry et al. (2004) found no relationship between measured bed armoring and rating curve steepness in the large data sets of Helley-Smith samples collected in streams in the Idaho Batholith during the Snake River Adjudication (King et al. 2004). Instead, they showed that the steepness of the Q_B *vs.* Q relationships decreased with the parameter q^* (Dietrich et al. 1989) that indicates sediment supply and, among other variables, includes an indirect ratio of the surface and subsurface D_{50} sizes. They argued that a delayed onset of transport in the coarser beds (i.e., transport starts at high flow) causes steeper rating curves.

Bunte et al. (2006b) found a negative relationship between rating curve steepness and the degree of bed armoring for armored mountain gravel- and cobble-bed streams sampled with bedload traps. Bedload rating curves were less steep in heavily armored streams than in less armored streams. The effect is partially attributable to a high proportion of coarse surface particles that limits the availability of entrainable particles and consequently requires a large increase in flow to entrain more sediment. Another part of the effect is attributed to a high amount of sand and fine gravel in the bed. Some of the fines are stored in the subsurface (where they cause a low subarmor D_{50} size and thus a

high degree of armoring), while some of the fine sediment is stored in deposits of fines. Fine particles, particularly those entrained from easily erodible fine-grained deposits cause relatively large transport rates at low flows. This makes a rating curve start at a relatively high transport rate and limits its overall steepness.

This discussion shows that the effects of sediment supply and the degree of bed armoring on the rating curve steepness are not yet understood in sufficient detail.

2.3.3 Flattening of Q_B *vs.* Q relationship: transition from selective transport to equal mobility?

A bedload transport relationship with a steep lower and a flatter upper part can easily be brought into connection with the transition from selective transport to equal mobility. In poorly sorted gravel- and cobble-bed streams, rising flows entrain increasingly larger particles from the bed (selective transport) which typically provides a well defined relationship between the bedload D_{max} (or D_{50}) particle size with flow. Because the addition of progressively larger particles quickly adds a lot of mass to the transported amount of bedload, transport rates increase steeply with flow. Under equal mobility transport, all particle sizes in the bed are mobile and all size fractions move in proportion to their percentages in the bedmaterial; the size distribution of bedload approaches that of the bed. When bedload particle sizes cease to increase with flow (once all particle sizes in the bed have become mobile), bedload transport rates probably increase less steeply with flow.

While several researchers postulated that gravel bedload transport virtually functions with equal mobility at all but the lowest flows (e.g., Parker and Klingeman 1982; Parker et al. 1982; Andrews 1983, 1984; Andrews and Parker 1987), others proposed that selective transport and equal mobility are sequential processes that occur one after the other during increasing flow (e.g., Ashworth and Ferguson 1989; Komar and Shih 1992; Komar 1996; Bunte 1992, 1996). However, data collected in coarse gravel-bed streams did not show the transition. While there was significant coarsening in bedload particle sizes as flows increased, flows measured in these coarse-bedded streams were not high enough to entrain the largest bedmaterial particle sizes in proportion to their occurrence in the bed (Komar and Shih 1992; Bunte 1992, 1996). Kuhnle (1992), however, working in a stream with a finer bed (sand/gravel) demonstrated the transition from selective transport to equal mobility and a concurrent flattening of the Q_B *vs.* Q relationship at high flows. Selective transport prevailed when transport rates were increasing during lower flows while equal mobility transport occurred during the highest flows. Coarse gravel transport rates collected by Whitaker (1997) in an unarmored, coarse gravel-bed stream indicated the same phenomenon: increasing particle sizes and transport rates with increasing flow, while both ceased to increase when the flow became still higher.

Selective transport and equal mobility synonymous with transport phases?

The next question is whether the shift from selective transport to equal mobility is likewise related to a shift in transport phases, which means that selective transport and

equal mobility each represent a transport phase. Measuring bedload transport in a gravel bed flume over a wide range of flows, Wilcock and McArdell (1993, 1997) and Wilcock (1997) distinguished between partial and full transport (Section 2.2.2.3) and linked the transition from partial to full transport to the transition from selective transport to equal mobility. At low flows, only a few particles are in motion and those are mostly small, although occasionally a larger particle might move as well. As flow increases, the proportion of mobile small particles approaches that of the bed while the proportion of mobile larger particles is less than on the bed. At the same time, the bedload size distribution coarsens with increasing flow, and transport rates increase steeply. Once all particle sizes are entrained in proportion to their availability on the bed at higher flows, equal mobility is reached. The bedload size distribution no longer coarsens and transport rates increase less steeply with flow.

Given that the studies by Wilcock (1997) and Wilcock and McArdell (1997) did not consider the transport of sand over a stable bed (Phase 1 transport), and given that the authors believed partial transport to be the dominant phase in gravel-bed streams, partial and full transport, and thus selective transport and equal mobility, should fall into the categories of Phase 2 and Phase 3 transport, as described by Ashworth and Ferguson (1989).

Equal mobility (Phase 3 transport) in better sorted or finer grained gravel-bed streams
Thorne (1992) raised the question of whether streams might be differentiated into those that experience equal mobility on a fairly regular basis and those that do not. Similarly, Komar and Shih (1992) speculated that larger valley streams are more prone to experience equal mobility transport than steeper, more poorly sorted mountain streams. Findings by Lisle (1995) support these suggestions. Comparing the bankfull bedload grain-size distribution with the bed material grain-size distribution, Lisle (1995) found that the ratio of the D_{50} particle size of bedmaterial to the bankfull bedload (D^*) approached unity for streams with larger drainage areas, higher bankfull flow and higher dimensionless stream power, all of which increase in a downstream direction and are associated with larger, flatter, better sorted and less armored streams. He concluded that ratios of D^* close to 1 suggest equal mobility while larger values would indicate selective transport. It thus appears that a transition from selective transport to equal mobility only occurs in streams that have the competence to mobilize their entire bed.

Flattening of Q_B vs. Q relationship not always indicative of equal mobility
A caveat needs to be made regarding the connection between a flattened bedload transport rating curve and equal mobility. The mere observation of a flattening Q_B *vs.* Q relationship does not indicate the transition between selective transport and equal mobility. Hassan and Church (2001) attributed the flattening of an otherwise steep transport relationship at high flows measured on a submerged gravel bar to a change in the bedload path that limited sediment supply to the sampling location. Another example of flattening Q_B *vs.* Q relationships that are not related to a shift from selective transport to equal mobility is a counterclockwise hysteresis relationship. During short highflow events, transport rates can lag behind, remain high, or show a second rise during the

falling limb of flow (e.g., Reid et al. 1985; Lisle 1989; Rickenmann 1994). Likewise, once a large proportion of the flow has become overbank flow, bedload transport rates likely flatten because the relatively slow flow velocity on the inundated (and likely vegetated) floodplain do not contribute much sediment to the stream. These examples make it clear that a shift from selective transport to equal mobility cannot simply be inferred from a flattening of the Q_B *vs.* Q relationship. An analysis of the collected particle sizes and their relation to the bedmaterial-size distribution with increasing flow is required to identify selective transport and equal mobility and the flow at which a transition occurs (Wilcock and McArdell 1993, 1997; Wilcock 1997).

2.3.4 Comparison of transport phases and their flow ranges among studies

Sections 2.1 and 2.2 described a variety of different transport stages or phases that are reported in different studies. Unfortunately, the described phases cannot easily be matched among the studies. One problem is the inconsistent terminology used to describe different transport stages. For example, some authors use the Phase 1 – Phase 2 terminology, while others describe an increase in transport intensity in terms of marginal versus general transport or partial versus full mobility of the bed. Another problem is that some studies describe two, others three phases of transport. Finally, the reported phases differ strongly in the range of flows covered. In order to shed some light into this jumble, this study tried to place all transport phases into one of three groups and provided a graphic comparison of the range of flows reported for Phase 1, Phase 2, and Phase 3 transport. For studies that expressed flows for the observed phases or stages in percent of bankfull flow, the phases are displayed in Figure 2.

2.3.4.1 Low intensity or Phase 1 transport

At the lowest intensity transport, which some call Phase 1, sand and fine gravel is mobilized from deposits of fines (Jackson and Beschta 1982), or winnowed from the armor (Carling 1987, Beschta 1987) and there is general agreement that these fines move over a stable gravel or cobble bed (Milhous 1973; Emmett 1999, Ryan and Emmett 2002, Ryan et al, 2002, 2005), sometimes in tongues, sheet or mobile carpets (Warburton 1992). Some call this throughput load (Carling 1987), under-capacity flows (Carling 1988) or washload (Andrews 1983). Some authors do not consider Phase 1 transport (Andrews and Smith 1992; Andrews 1994; Wilcock 1997; Wilcock and McArdell 1993, 1997) at all, while others place most transport in boulder bed streams into the Phase 1 category Bathurst (1987a).

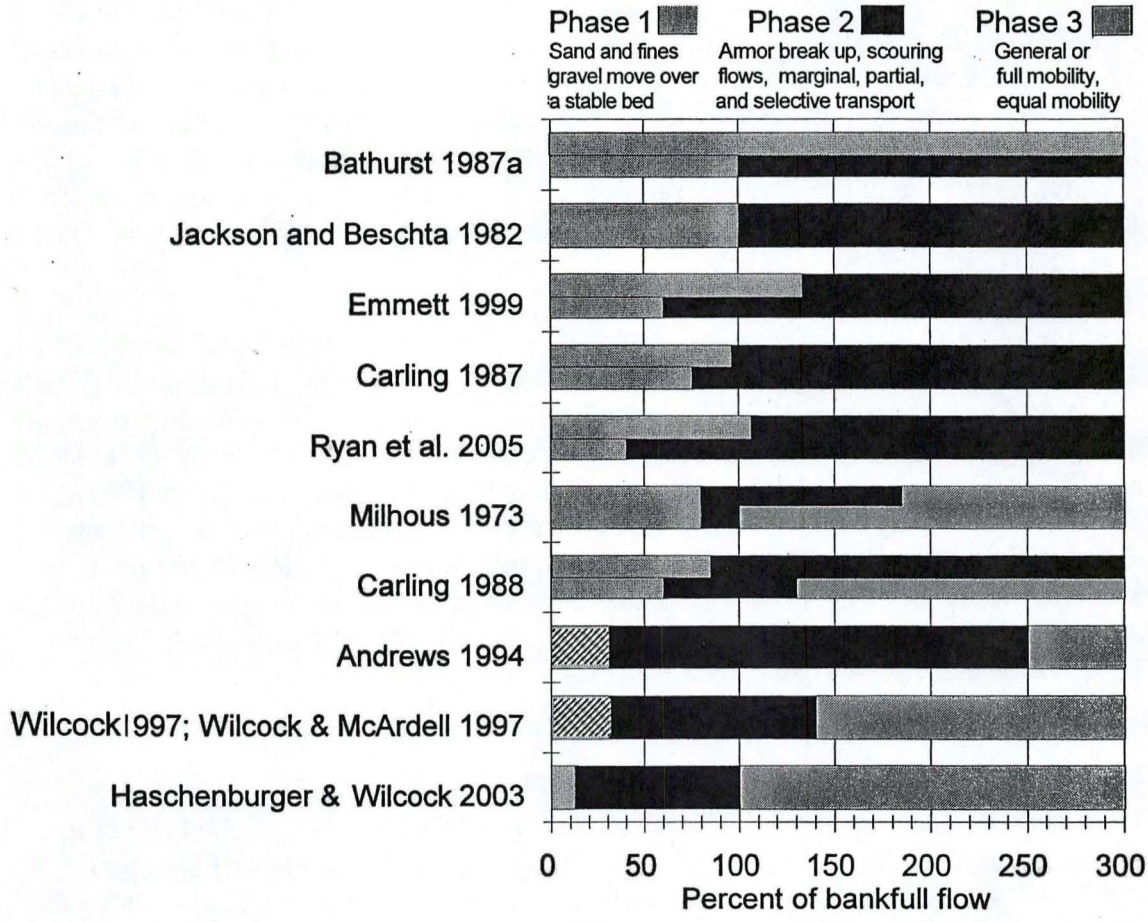

Figure 2: Range of flows covered by Phase 1, 2 and 3 transport. The split horizontal bars mark the lowest and highest observed flow for the shift in transport stages in a study. The studies by Andrews and by Wilcock did not measure Phase 1 flows. The dense hatching indicates estimates.

2.3.4.2 High intensity or Phase 2 transport

With increasing intensity of bedload transport, more and more particles from the armor layer become mobilized (Milhous 1973). Jackson and Beschta (1982) see this as the phase when particles from the armor of riffles are entrained, transported through pools, and deposited at some riffle below, enabling riffle-to-riffle transport and riffle shaping. Marginal transport identified by Andrews and Smith (1992) and Andrews (1994), as well as partial transport identified Wilcock and McArdell (1993, 1997) and (Wilcock 1997) fall into the group of Phase 2 transport because these authors do not consider sand transport. Phase 2 transport has been reported for a wide range of flow, starting at the earliest onset of movement for small gravel particles. Ryan et al. (2005) show that Phase 2 transport can start anywhere between 40 and 110 % Q_{bkf}, Emmett (1999) sets the onset at 60 - 130 % Q_{bkf}, while Bathurst (1987a) postulates that transport in boulder bed streams almost never even reaches Phase 2 transport. The upper limit of flows of Phase 2 transport is likewise quite variable. Some authors place it at highflows of 100-140 % Q_{bkf} (Milhous 1973, Carling 1988; Wilcock and McArdell 1993, 1997; Wilcock 1997;

Haschenburger and Wilcock 2003), others extend it to flows 200% Q_{bkf} (Milhous 1973) or even the 100-year flood (Andrews 1994). Thus, the transport that is declared to be Phase 2 spans the entire range of flow that is commonly sampled in gravel-and cobble-bed streams. The wide variability not only reflects the wide range of stream conditions (from step-pool streams to gravel-bed flumes) but also the different criteria that researchers used to define Phase 2 transport. Encompassing all commonly encountered flows in gravel- and cobble-bed streams, the classification of transport simply as Phase 2 is not a very precise characteristic.

Some researchers consider transport during Phase 2 to occur as equal mobility (Parker et al. 1982, Andrews 1983, Andrews and Erman 1986, Bathurst 1987a; Andrews and Parker 1987; Andrews and Smith 1992, Andrews 1994). By contrast, others consider transport in Phase 2 to be size selective (Ashworth and Ferguson 1989; Bunte 1992a, 1996; Komar and Shih 1992; Whitaker 1997; Wilcock 1997; Wilcock and McArdell 1993, 1997). Several authors suggest that Phase 2 transport is limited to streams with relatively well sorted beds, relatively gentle stream gradients, and where critical flow to entrain all bed particles are frequently exceeded. Boulder beds, by contrast, experience Phase 2 transport rarely (Bathurst 1987a; Bunte 1992a, 1996; Komar and Shih 1992; Thorne 1992; Lenzi et al. 2004.).

2.3.4.3 Highest intensity or Phase 3 transport

There seems to be agreement that with increasing bedload intensity, almost all particle sizes present in the bed are entrained. Some researchers call this Phase 3 transport (Carling 1988; Ashworth and Ferguson 1989, Warburton 1992, Lenzi et al. 2004), others call this stage fully mobilized transport (Wilcock and McArdell 1993, 1997, Wilcock 1997, Hassan and Church 2001). Full mobility that may occur locally in the streambed at lower flows expands over much of the streambed area at high flows (Haschenburger and Wilcock 2003). General transport identified by Andrews and Smith (1992) and Andrews (1994) for the very highest, rarely occurring flows can also be classified as Phase 3 transport. Most authors agree that this stage occurs rather infrequently at flows larger than bankfull and has the competence to move large bedmaterial particles and the capacity to shape the channel (but not necessarily in boulder bed streams (Bathurst 1987a, Carling 1988)).

Most authors also agree that this stage is connected with equal mobility transport (Ashworth and Ferguson 1989; Warburton 1992; Bunte 1992a, 1996; Komar and Shih 1992; (Wilcock and McArdell 1993, 1997, Wilcock 1997; Lenzi et al. 2004). In step-pool streams, boulder steps may be moved and the bed may be restructured (Warburton 1990, 1992; Lenzi et al. 2004) which is referred to as stage or Phase 3 transport and associated with equal mobility of all particle sizes.

2.3.4.4 Problems in differentiating between transport phases

Several factors make the distinction between transport stages, particularly Phase 2 and 3 transport, problematic. One is that observers are rarely present during large floods that

might produce a Phase 3 event and sampling bedload under those conditions is typically not possible. Even if measurements are possible, it may not clearly be known when Phase 3 sets in (Lenzi et al. 2004, Lenzi 2005). The collection of an occasional particle of the bedmaterial D_{90} or larger size does not certify complete bed mobility (Haschenburger and Wilcock 2003). Some streams, particularly those with relatively well-sorted bedmaterial, might not have a Phase 3 that differs from Phase 2 because there are no other strata or sediment sources than those already involved in transport from which bedload could be entrained. The transition between Phase 2 and 3 transport can also not be expected to occur abruptly. It is a true transition in which the streambed area that experiences Phase 3 transport expands with increasing flow until much or most of the total area is involved (Haschenburger and Wilcock 2003). Several authors do not even consider Phase 3 transport. As a result of these problems, flows and transport processes that some studies call Phase 2 transport, other studies call Phase 3 transport.

Even if the Phase 2 – Phase 3 transition could be analyzed based on entrained particle sizes that are scaled to bedmaterial particle sizes, it may be necessary or useful to differentiate between streams with different bedmaterial characteristics and establish different criteria for the transition between transport phases. Using inferred streambed processes rather than quantifiable bedload characteristics to differentiate between processes, such as an assumed breakup of the armor layer or the burial of fines under the armor at falling flow, leaves room for much speculation.

2.4 Summary and conclusion

A variety of different transport phases are reported in the literature. Some studies relate different intensities of bedload transport to the entrainment of bedload sediment from different bed strata (such as surface or subsurface) or different sources (deposits of fines, riffles), while others refer to just one bedload process that happens with increasing intensity. Of the over 40 articles compiled in this literature review, most studies do not associate the shift of transport stages with a change in the Q_B *vs.* Q relationship while others relate a shift in transport phases to changes in the Q_B *vs.* Q relationship. The studies also differ in the use of terminology, and while some studies identify two phases of transport, other identify three. All of these factors make is problematic to compare and match transport phases between studies.

Breakpoints and the Phase 1- Phase 2 shift tied to linear plotting scale

The studies that report a steepening of the Q_B *vs.* Q relationship see the flow at which the steepening occurs as the onset of Phase 2 transport which means the beginning of medium to coarse gravel transport and steeply increasing transport rates. However, the steepening of the bedload transport relationship is only visible and statistically detectable in a linear plotting scale that all of these studies use. The same data plotted in a logarithmic scale do not show a change in the rate of increase in transport rates with flow. The authors attribute the low rate with which bedload transport increases during Phase 1 transport to limited sediment supply. The steep increase is attributed to unlimited

sediment supply once the armor is disrupted, and armor particles, together with the released finer particles beneath, are transported.

Effect of sediment supply and bed armoring on rating curve steepness still debated

The way in which sediment supply influences the steepness of a Q_B *vs.* Q relationship is still debated. The proponents of a breakpoint between Phase 1 and Phase 2 transport relate low sediment supply and an intact armor to low and barely increasing bedload transport relationships, whereas high sediment supply and a disrupted armor is connected to high and steeply increasing bedload transport relationships. However, other studies report different relationships between sediment supply, armoring, and the rating curve steepness. One group of studies connected high sediment supply with poorly armored streams and generally high transport rates that increase slowly with flow, whereas streams with low sediment supply and high armoring produce steep rating curves that start at low transport rates and reach high transport at high flows. Another group of studies working in fairly well armored mountain gravel-bed streams found that there was either no relationship between measured armoring and rating curve steepness or that the rating curve steepness decreased for more heavily armored streams. The different findings suggest that the interrelationships between sediment supply, degree or armoring and the rating curve steepness are not clearly understood. Thus, using an inferred condition of armor condition and sediment supply and does not appear well suited for supporting the onset of Phase 2 transport.

Flattening only for predicted but not for measured bedload transport relationship

While flattening Q_B *vs.* Q relationships are commonly predicted from bedload transport equations, they are rarely measured in coarse-bedded gravel-bed streams. However, flattening Q_B *vs.* Q relationships are shown for fine-grained as well as for unarmored gravel-bed streams. Several researchers proposed that flattening is associated with the transition from selective transport to equal mobility. Flume studies by Wilcock (1997) and Wilcock and McArdell (1993, 1997) showed that selective transport and equal mobility can be equated with partial (Phase 2) and fully mobilized transport (Phase 3). The state of equal mobility may be frequently reached in fine-grained or well-sorted gravel-beds, whereas equal mobility with complete mobilization of all bedmaterial particle sizes occurs in mountain gravel-bed streams only during very high and infrequently occurring extreme events. This explains why flattened Q_B *vs.* Q relationships are rarely, if at all, measured in mountain gravel-bed streams.

Reported transport phases can be organized into 3 groups but flows (in % Q_{bkf}) vary widely

It was possible to fit all reported transport stages and the flows (in % of Q_{bkf}) at which these occurred into a 3-group scheme. However, the range of bankfull flow associated with each phase varied widely between studies. The onset of Phase 2 transport was reported for flows between 40 and 110% Q_{bkf} for armored gravel-bed streams, while the onset of Phase 3 ranged between 100 and 200% Q_{bkf} and even higher. Part of the wide

range in bankfull flow at the onset of Phase 2 is due to differences between streams; another part is due to different concepts and computational methods used to define the various transport stages, as well as to difficulties associated with the correct identification of bankfull flow. Nevertheless, with the current wide lack of specificity, simply defining a transport intensity as Phase 2 or 3 does not seem to be very useful.

Part B: Computation and comparison of several channel maintenance procedures

1. Introduction

1.1 Channel maintenance flows

When water is diverted from a stream, the amount and size of bedload sediment that can be transported by the remaining flow may be decreased. This may cause channel aggradation and a reduction in cross-sectional area if not all of the bedload delivered to the stream by tributaries can be conveyed through the stream system. Even relatively small floods could then cause overbank flooding and instability of the channel bed. To prevent these detrimental effects, it has been proposed to let some of the high flows that have the competence of moving channel-forming particles (e.g., perhaps the surface bedmaterial D_{50} size) pass through the stream to maintain the channel bed. Such flows are called channel maintenance flows, i.e., flows that maintain the channel size and the bedmaterial characteristics. The magnitude of channel maintenance flows needs to be large enough to transport all of the bedload mass and sizes supplied to the channel in the long run such that neither aggradation nor degradation occurs (Emmett and Wolman 2001). While the idea and necessity of channel maintenance flows is easily understood, researchers have not reached a conclusion about the exact rate of flow, its durations, frequency and timing, nor has agreement been reached on how to determine the parameters of channel maintenance flows based on measurements of channel geometry, bedmaterial size, bedload transport rates and particle sizes. A variety of different methods for quantifying channel maintenance flows have been proposed (e.g., Rosgen et al. 1986; Hill et al. 1991; Troendle 1993; Troendle and Olson 1994; Ligon et al. 1995; McBain and Trush 1997; Leaf 1998; Andrews and Nankervis 1995; Wilcock 1998; Emmett 1999; Bakke et al. 1999; McNamara et al. 2000; Trush et al. 2000; Emmett and Wolman 2001; Schmidt and Potyondy 2001, 2004; Ryan et al. 2002, 2005; Whiting and King 2003; Mueller et al. 2005).

This study compares five selected approaches that define channel maintenance as those flows associated with the onset of Phase 2 transport. Each of the selected methods uses a different computational or analysis approach to make this determination. The onset of Phase 2 transport is assumed to be necessary for channel maintenance. Each of the five procedures are applied to three coarse-bedded mountain gravel-bed streams in which bedload transport was measured using the Helley-Smith samplers and bedload traps and for which detailed data on surface, armor, and subsurface bedmaterial, channel morphology, bedload transport rates and particle sizes as well as flow discharge was gathered during intensive field data collection programs.

1.2 The channel maintenance procedures: overview

The channel maintenance procedures applied in this study are listed in Table 2. Procedures 1-4 were devised as channel maintenance procedures, while the flow competence analysis was suggested as a potential; alternative tool.

Table 2: Channel maintenance approaches investigated in this study.

No.	Phase 2 Approaches	Reference
1	"Explosion" diagram	Emmett, W.W., 1999. Quantification of channel maintenance flows for gravel-bed rivers. In: *Wildland Hydrology*. D.S. Olsen and J.P. Potyondy (eds.), American Water Resources Association, Herndon VA, TPS-99-3, p. 77-84.
2	Piecewise regression	Ryan, S.E., L.S. Porth and C.A. Troendle, 2002. Defining phases of bedload transport using piecewise regression. *Earth Surface Processes and Landforms*, 27(9): 971-990. Ryan S.E., Porth, L.S. and Troendle, C.A., 2005. Coarse sediment transport in mountain streams in Colorado and Wyoming, USA. *Earth Surface Processes and Landforms* 30: 269-288. DOI: 10.1002/esp.1128.
3	Surface/subsurface collapsed-size approach	Whiting, P.J. and J.G. King, 2003. Surface particle sizes on armoured gravel stream-beds: effects of supply and hydraulics. *Earth Surface Processes and Landforms* **28,** 1459-1471, DOI: 10.1002/esp.1049.
4	Klamath Fall procedure: Modeled incipient motion of framework gravels	Bakke, P.D., P.O. Basdekas, D.R. Dawdy, and P.C. Klingeman, 1999. Calibrated Parker-Klingeman model for gravel transport. *Journal of Hydraulic Engineering* 125 (6): 657-660. McNamara, M.L., P.C. Klingeman, P.D. Bakke and R.J. Sullivan, 2000. Channel Maintenance flows in the upper Klamath Basin, Oregon. In: *Riparian Ecology and Management in Multi-Land Use Watersheds*. P.J. Wigington and R.L. Beschta (eds.), American Water Resources Association, Middleburg, Virginia, TPS-00-2, 616 pp.
5	Flow competence analysis	General technique for analyzing the largest bedload particle sizes transportable by a specific flow.

The visual "explosion" diagram (1) and the piecewise regression (2) link the concept of channel maintenance flows to the Phase 2 concept (see Part A or this report), i.e., the flow associated with the sudden increase in gravel transport rates and particle sizes that is attributed to the break up of the armor layer. Both methods attempt to define the flow at which bedload transport rates increase abruptly (i.e., the onset of Phase 2 transport) compared to those at lower flows. The first method does so by visual examination and interpretation of plotted fractional transport rates over flows. The piecewise regression approach is a statistical refinement over the visual method. It fits linear regression functions to the portions of data with relatively low and steep increases of transport rates and defines the intersection point as the onset of Phase 2 flows.

While the first two methods focused on a change in transport rates, the other methods attempt to determine a critical particle size that needs to be transported for channel maintenance. The collapse-size analysis (3) compares the surface and subsurface particle-size distributions and, starting from the largest size, finds the size at which both distributions start to deviate. This is the collapse size, and the flow required for transport

of the collapse size is considered to be the channel maintenance flow. The Klamath Falls procedure (4) compares armor and subarmor particle size distributions to determine the size of framework gravels. The procedure then applies a bedload transport equation and models the flow at which framework gravels start to move, the assumed channel maintenance flow. The flow competence approach (5) uses a measured relationship between the largest transported bedload particle sizes and flow to determine flows at which framework gravels, or characteristic bedmaterial particle sizes such as the median sizes of the surface, armor or subarmor sediment begin to move. Agreement on which bedmaterial particle size needs to be moved is tentative at best. A detailed description of each procedure is provided in each of the sections that apply these procedures.

1.3 Study aim

The aim of this study is twofold: one is to compute the different channel maintenance procedures for the three study streams, compare the results, and evaluate the variability among the proposed methods. A secondary aim is to investigate whether channel maintenance procedures that depend on measured bedload transport rates as an input variable will yield different results depending on the sampling device used for collecting bedload transport. More specifically, the question is whether channel maintenance flows computed from bedload samples collected with bedload traps are different from channel maintenance flows computed from Helley-Smith samples.

2. Field methods

2.1 Streams sampled

Data from three Rocky Mountain Gravel-bed streams (Little Granite Creek, Halfmoon Creek and Hayden Creek) were used for the comparative analyses of channel maintenance procedures. Summary information of the stream morphometrics for the three streams is provided in Table 3 (see also Table 14). These streams did not appear to

Table 3: Characteristics of the streams near the study sites (see Table 14 for bedmaterial characteristics at the study sites).

Parameter / Stream and year sampled	Location	Basin area (km^2)	Bank-full flow (m^3/s)	Bank-full width (m)	Water surface slope (m/m)	Reach-averaged surface D_{16}, D_{50}, D_{84} (mm)	Subsurface near sampling site D_{16}, D_{50}, D_{84} (mm)	Predominant stream type (Montgomery & Buffington 1997)
Little Granite Cr., 1999	W. Central WY	55	5.66	14.3	0.017	23, 59, 133	6, 45,140	plane-bed
Halfmoon Cr., 2004	Central CO	61	6.23	8.6	0.014	14, 49, 119	3, 29, 130	plane-bed, w/ pool-riffle
Hayden Cr., 2005	S. Central CO	39	1.92	6.5	0.038	18, 63, 169	5, 50, 119	step-pool, plane-bed, mixed

be disturbed or otherwise unusual. There were no major recent watershed effects (such as from logging, roading, forest fires, mining, debris flows), although each stream has their own small-scale sedimentary effects such as build-up and decay of upstream beaver dams, log jams, low grade-control structures, a fish barrier at Hayden Creek, local bank collapse as well as roads close to streams and off-road vehicle traffic; these disturbances are common in many mountain gravel-bed streams.

2.2 Data collection

The first two channel maintenance procedures analyzed in this study require as input a relationship of bedload transport rates versus discharge measured during one or several highflow seasons (Table 4). The other three procedures require detailed information on bedmaterial characteristics that is measured during low flows when the bed is covered by only a little water, as well as bedload transport measurements. Bedload sampling techniques, discharge measurements, and bedmaterial collection for two of these streams are described in detail in Bunte (1999a) and Bunte and Swingle (2005). A brief description is provided below.

2.3.1 Bedload sampling

2.3.1.1 Helley-Smith sampler

The most commonly used device for bedload sampling in wadeable coarse-bedded mountain streams is a handheld Helley-Smith sampler with a 3-inch opening (e.g., Whiting et al. 1999; Ryan et al., 2002, 2005, King et al. 2004). Portability and ease of use (particularly in connection with a footbridge) and inclusion of sand-sizes bedload in the sample are the main advantages of this device. The Helley-Smith sampler used for sampling in this study was a thin-walled model with a 3.22 opening ratio and a 0.25 mm mesh width sampling bag[9]. Ryan et al. (2002, 2005) used a thick-walled Helley-Smith sampler that yields slightly lower transport rates (Ryan and Porth 1999).

2.3.1.2 Bedload traps

Bedload traps were constructed in 1998 as an alternative sampling device for gravel and cobble bedload. The large opening size allows cobbles to enter. Mounting the sampler frame onto ground plates avoids unwanted particle pick up and allows long sampling times. The large sampler capacity permits samples of large volumes to be collected. A larger sampler opening, long sampling times, large sample volumes and the prevention of unwanted particle pick-up are required for accurate samples of coarse gravel bedload transport. Sampler construction and data collection are described in Bunte (1999a), Bunte and Swingle (2005), and Bunte et al. (2006c).

Up to 8 or 9 bedload samples were collected using bedload traps on most days during the snowmelt highflow season. This resulted in 163 and 192 samples at Halfmoon and

[9] Fabricated by the company GBC in Lakewood, CO.

Table 4: Field techniques used by the channel maintenance approaches applied in this study for determining bedload transport rates as well as surface and subsurface particle-size distributions.

No.	Phase 2 Approaches	Field methods used to obtain the necessary data for each Phase II Approach		
		Bedload transport rates and particle sizes	Surface or armor layer	Subsurface or subarmor sediment
1	"Explosion" diagram	Bedload samples from incipient motion to above bankfull flow	N/A	N/A
2	Piecewise regression	Bedload samples from incipient motion to above bankfull flow	N/A	N/A
3	Surface/-subsurface collapsed size	(Bedload samples from incipient motion to above bankfull flow)	100+ particle pebble count, 4-5 transects near subsurface sampling location, b-axis particle sizes measured with ruler[10].	Barrel samples at 3 locations. Armor layer removed to depth of the surface D_{90}. Subsurface sed. sampled to depth of 2 particle diameters and until $vol_{Dmax} < 5\%\ vol_{tot}$.
			This study collected 400+ particles and measured particle sizes using a 0.5 phi template.	This study sampled the subarmor to a depth slightly deeper than the armor layer using the plywood shield.
4	Klamath Falls site calibrated approach with determination of framework gravels	A few bedload samples for site-calibration of the Parker-Klingeman (1982) bedload transport equation	Armor layer sampled to embedded depth of D_{max} particle size[11] using a barrel sampler at 5 locations.	Subarmor layer sampled to a depth equal to armor layer sample using barrel sampler[12].
			This study used the plywood shield instead of a barrel sampler.	This study used the plywood shield at 5 locations and sampled the subarmor to a depth slightly deeper than the armor layer depth.
5	Measured flow competence curves	Bedload samples from incipient motion to above bankfull flow	400+ particle pebble count, reach spanning, particle sizes measured with template	Surface (or armor*) particles within sampling area removed (but sampled and analyzed) before sampling the subsurface (or subarmor*).

*Term in parentheses indicates different strata, NOT alternative terms for same strata.

Hayden Creek, respectively. Only 3-4 samples per day were collected using bedload traps at Little Granite Creek, yielding 58 samples. One or 2 samples a day were collected using the Helley-Smith sampler at each site, yielding about 30-50 samples per data set.

[10] Ruler-measurements differ from template measurements – a conversion is required for comparison.

[11] The embedded depth of the local D_{max} particle size may vary between sites and differ in depth as well as sample mass of armor layer samples.

[12] Results in relative small sample mass that may not meet the 5% criterion by Church et al. (1987).

2.3.1.3 Measured bedload transport rates

Relationships between bedload transport rates and flow obtained for bedload traps and the Helley-Smith sample are shown in log-log plots for all three sites in Figure 3 in units of g/s, while transport relationships in units of kg/min are shown in Section 3.4.3.1. Transport rates sampled in bedload traps cover gravel only and range from 4 to 64 mm, on rare occasions to 90 mm. Samples from the Helley-Smith sampler include sand and range from 0.25 to 45 mm, on rare occasion to 64 mm. Note that transport rates collected with the two samplers during the same highflow season differ considerably. Transport rates collected with bedload traps extend over 5 to 6 orders of magnitude, while transport rates from the Helley-Smith samples extend over about half this range. Consequently, power function regressions fitted to the data are much steeper for bedload traps than for Helley-Smith samples. The power function exponents range between 7 and 16 for bedload trap samples and between 1.6 and 3 for Helley-Smith samples. Similar differences between transport rates collected with bedload traps and the Helley-Smith sampler have been observed at all (eight) sites at which the two samplers were used concurrently (Bunte et al. 2007, *in press*). Relationships between the largest bedload particle sizes and flow are shown in Figure 3.5.3.1.

2.3.2 Bedmaterial sampling

Several of the channel maintenance procedures require information on bedmaterial size-distributions as input. Surface, armor and subarmor bedmaterial was sampled at each of the three stream sites. Sampling methods used in this study were generally similar to those used in the channel-maintenance studies, but varied in some details. Comprehensive descriptions of bedmaterial sampling procedures used in this study are therefore discussed together with the channel maintenance methods in which they were applied, in Sections 3.3.2.1 and 3.4.2.1, respectively.

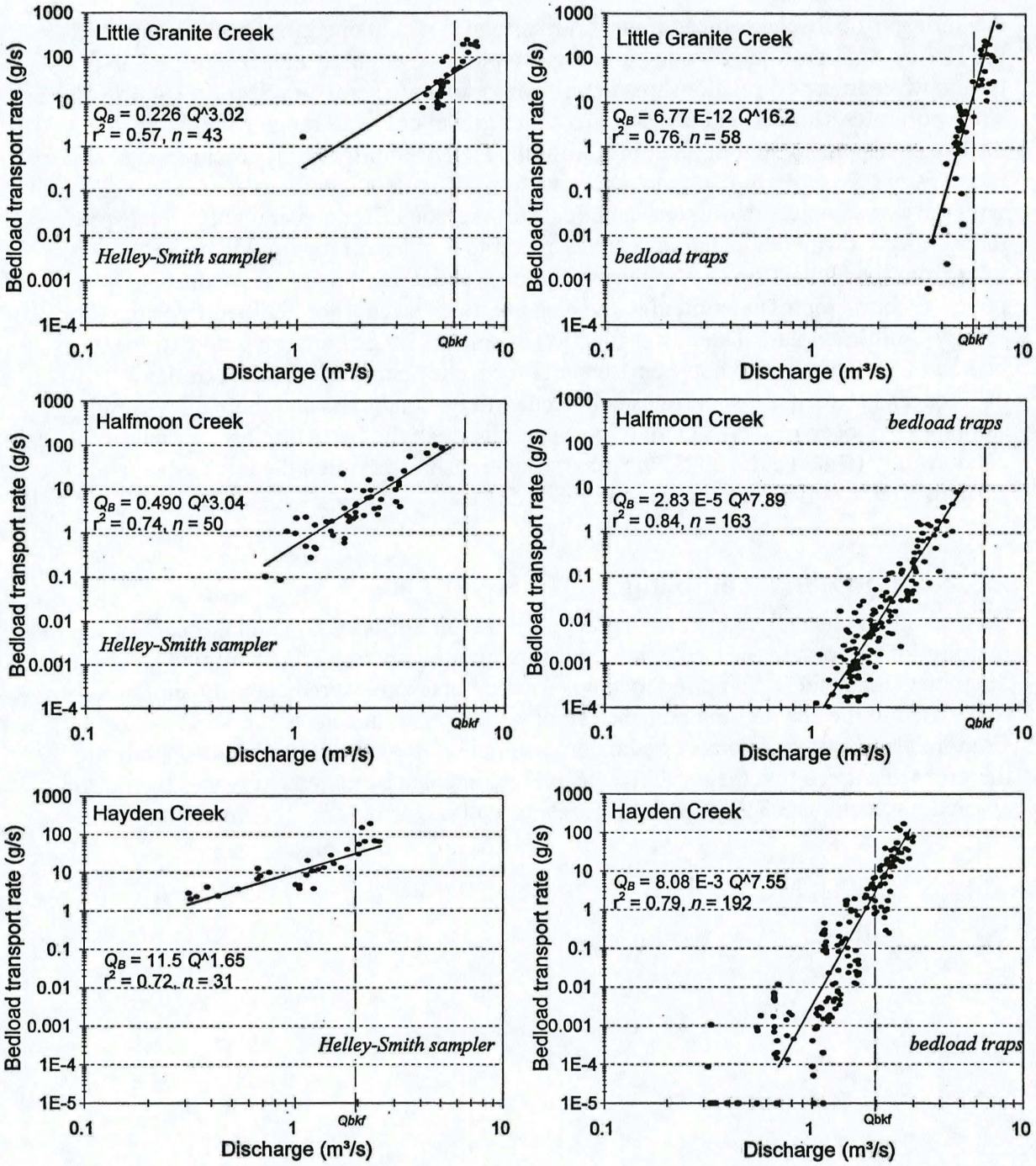

Figure 3: Measured bedload transport rates collected with bedload traps (left column) and a Helley-Smith sampler (right column). Bedload trap samples typically contain particles between 4 and 64 mm, Helley-Smith samples include sand and typically have particle sizes between 0.25 and 45 mm.

3. Computation and comparison of various channel maintenance procedures

3.1 "Explosion" diagrams

Several researchers support the idea that bedload transport occurs in 2 or 3 phases (see Part A of this study). At Phase 1 transport, sand and fine gravel entrained from pools and low flow deposits travel over a stable gravel or cobble bed. As transport increases to Phase 2, particles from the armor layer are entrained. This exposes particles from the subsurface and subarmor that are then released as well. However, while most studies make no inferences about whether transport rates at the onset of Phase 2 transport continue to increase at the same rate with flow as they did during Phase 1 transport, Emmett (1999) and Ryan et al. (2002, 2005) concluded that the transition from Phase 1 to Phase 2 transport is associated with a pronounced increase in transport rates and that the flow at which transport rates switch from a low increase to a steep increase is often visible in linear plotting scale. Emmett (1999) called this increase in flow "explosion point" and links the onset of Phase 2 transport to channel maintenance flows.

3.1.1 Methods

In order to compute explosion flows for the three study streams, fractional bedload transport rates for particles collected with the Helley-Smith sampler and bedload traps were plotted versus flow in linear scale on both axes (Figure 4). Emmett (1999) plotted fractional transport rates in 1.0 phi size classes, starting at the 2-4 mm class. This study had sieve results in 0.5 phi sizes that facilitated plotting fractional transport rates in a finer size resolution. For the Helley-Smith sampler, the smallest plotted size class was 2-2.8 mm, for bedload traps 4-5.6 mm. The *y*-axis (fractional bedload transport rates) was scaled such that the largest measured transport rates plotted towards the upper right-hand corner of the diagrams, thus *y*-axis scales vary among individual plots of Figure 4.

The plots were then visually evaluated to estimate the explosion flow. At low flows, fractional transport rates are clustered along the *x*-axis (discharge). As flows increase, transport rates increase as well. At some flow, fractional transport rates appear to increase somewhat abruptly, and this flow was taken as the bedload "explosion".

3.1.2 Results

Visually estimated bedload "explosion" flows occurred at 109% bankfull flows for samples from the Helley-Smith sampler at Hayden Creek, at 87% bankfull flow for Little Granite Creek, and at approximately half bankfull flow at Halfmoon Creek (Table 5). Explosion flows for samples collected with bedload traps at Hayden and Little Granite Creek occurred at 130 and 107% Q_{bkf} and were thus about 20% higher than those estimated for Helley-Smith samples, whereas the explosion flow for both samplers remained at half bankfull flow for Halfmoon Creek.

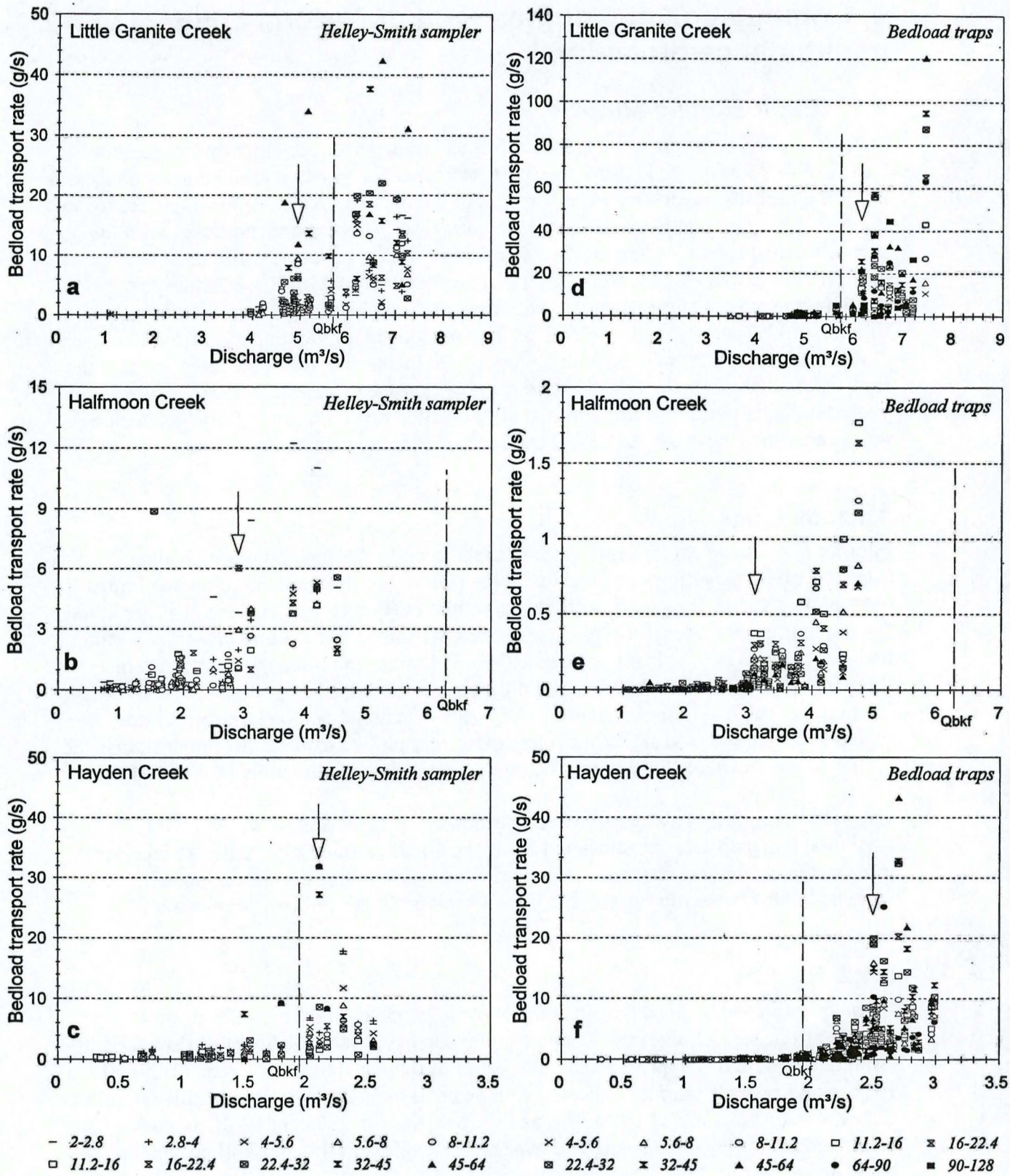

Figure 4: "Explosion" diagrams: Fractional bedload transport rates plotted versus flow in linear scale on both axes for samples collected with the Helley-Smith sampler (a, b, c) and bedload traps (d, e, f) in the three study streams. Arrows mark the estimated onset of Phase 2 transport.

Table 5: Explosion flows estimated visually from "Explosion" diagrams.

	"Explosion" flow (m^3/s)		"Explosion" flow (% Q_{bkf})	
Stream	HS	Traps	HS	Traps
Hayden	2.1	2.5	109	130
Little Granite	4.95 (6.05)	6.05	87	107
Halfmoon	2.87	3.1 (4.0	46	50

The low explosion point at half bankfull flow indicated by both samplers at Halfmoon Creek deserves some discussion. Flows at Halfmoon Creek reached only about 80% Q_{bkf}. This small range of flows does not meet the requirement of samples to be collected up to or beyond bankfull flow. Thus, one could argue that the absence of higher transport rates during which an "explosion" might occur could be responsible for the low explosion flow. However, Ryan et al. (2005) likewise observed an abrupt increase in transport rates around 40% of bankfull flow for linearly plotted transport rates collected with a Helley-Smith sampler at Halfmoon Creek in flows up to 171% of bankfull. It might thus be the case that Halfmoon Creek has a genuinely low explosion point, independently of the range of sampled flows.

3.1.3 Discussion

The visual estimation of "explosion" flows is faced with several problems:

- Visual overemphasis of the first large bedload sample exceeding its neighbors
- Subjectivity in the selection of explosion points (operator variability)
- Effect of bedload sampler used
- Variability in the flow at which the "explosion" occurs for a given year, and
- Chance whether or not samples are collected during the "explosion" flow

These points are discussed below.

Visual overemphasis of the first sample exceeding its neighbors

Using fractional transport rates as opposed to total transport rates visually overemphasizes the effect of a single, relatively large sample in the explosion diagrams. A small sample does not comprise many size fractions, and the few and relatively low fractional transport rates mostly plot on top of each other such that individual symbols in the plot have little visual "weight". A larger sample has not only more size fractions but also higher fractional transport rates, thus the plotted sample visually sticks out with numerous and distinct symbols. Using fractional instead of total transport rates makes the "explosion" effect particularly eye-catching. While catchiness is desirable in a visual technique, it may cause an operator to select the first, but anomalous, occurrence of a sample with a transport rate visibly higher than its neighbors.

Subjectivity in the selection of explosion points (operator variability)
Another concern is that identifying the particular sample that determines the "explosion" flow is not obvious. For example, in Figure 4a that shows Helley-Smith samples collected at Little Granite Creek, any of the bedload samples at flow of 4.6, 4.7, or 4.9 m^3/s could have been identified as the explosion flow. This study selected the flow of 4.7 m^3/s as a midpoint. Similarly, possible candidates for the explosion flow for Helley-Smith samples at Hayden Creek in Figure 4c were 1.5, 1.8, and 2.1 m^3/s. This study selected the data point at a flow of 2.1 m^3/s as most indicative of the bedload explosion. A different operator might have made different selections.

Effect of bedload sampler used
Transport rates differ depending on the sampler used (Figure 3), and this difference affects estimated explosion flows as well. Compared to samples collected with a Helley-Smith sampler, explosion points appear to be more easily identifiable from bedload trap samples. For bedload traps, sampled low-flow transport rates are typically very small and plot closely along the *x*-axis. This produces a less "cluttered" plot in the range of flows at which transport rates start to increase visibly above those hugging the *x*-axis. However, even for bedload trap samples the only clear-cut case for identifying the explosion point in Figure 4 was Little Granite Creek—the stream used by Emmett (1999) for developing the technique. Sampler choice affects not only the relative ease with which an explosion point can be identified, but also the explosion flow itself. For samples collected with bedload traps, explosion flows were about 20% higher than those identified from samples collected with the Helley-Smith sampler.

Variability in the "explosion" flow and odd chance of sampling it
Depending only on the presence of transport rates that exceed those measured at smaller flows, the explosion method is subject to variability, randomness, and chance. For one thing, the first higher than average transport rate is unlikely to occur at the same flow each year, thus explosion flows are likely to vary between years. Besides, short-term transport rates and particle sizes fluctuate considerably over time, and samples collected an hour earlier or later likely differ in mass and particle-size composition, particularly when sampling time is short. These fluctuations introduce randomness into the analysis. Chance comes into play because it is uncertain whether an operator actually collects a sample at the time and flow at which the first high transport rate occurs. In order to improve the chance and not miss the event, one would have to sample very intensively.

In summary, defining explosion flows from linearly plotted fractional transport rates is problematic. There is ambivalence and subjectivity in the selection of explosion points, and that causes operator variability. There is randomness in the occurrence of a transport rate that exceeds its neighbors and there is chance in whether that occurrence is sampled. Thus, data from different sampling crews likely produce different explosion points, and results likely vary between years. Explosion flows also appear to be significantly affected by the sampler used and were 20% higher for samples from bedload traps compared to samples from the Helley-Smith sampler.

3.2. Breakpoint analysis

3.2.1 Rationale

The rationale behind the analysis of breakpoint flows is the concept that bedload transport shifts from Phase 1 to Phase 2 transport with increasing flow (Ryan et al. 2002, 2005). During Phase 1 transport, sand and fines are entrained from pools and tranquil areas with patches of fines, and they move at low rates over a stable bed. During Phase 2 transport, entrainment and transport of larger surface particles releases smaller particles from the subsurface. Comprising surface gravel particles as well as subsurface fines, transport rates at Phase 2 are considerably larger than those at Phase 1.

When plotted in a linear scale, transport rates (Q_B) during Phase 1 transport increase at a low rate with flow (Q), whereas the combined transport of surface and subsurface material produces a rapid increase in bedload transport rates that is significantly steeper than the Q_B *vs.* Q relationship during Phase 1 transport. Concomitantly with the increase in transport rates that is visually observable in linear plots, particle sizes start to increase during Phase 2 transport as well, typically comprising particles of the surface D_{16} to D_{25} size. The beginning of Phase 2 transport defines the critical flow for the transport of medium and coarse gravels, i.e., a flow considered necessary for channel maintenance. The change or "break" in slope of the relationship between bedload transport and discharge that is observable at the transition between Phase 1 and Phase 2 transport is called the breakpoint flow and can be determined consistently from a statistical procedure called piecewise regression (Ryan et al. 2002, 2005).

Piecewise regression is a statistical tool that can be used for identifying thresholds. Piecewise regression models can be described as "broken-stick" models that fit sections of linear functions joined at breakpoints to a data set (Toms and Lesperance 2003). The analysis computes the steepness of the linear functions as well as the x-axis value(s) at which the knickpoint(s) or breakpoint(s) are placed. An analysis of breakpoints can thus be used to estimate thresholds. Compared to a visual analysis of the bedload explosion (Section 3.1), a piecewise regression provides a qualitative but less subjective statistical analysis of the onset of Phase 2 transport.

The reason why Ryan et al. (2002) chose piecewise regression analysis over other models to describe relationships between transport rates and discharge was not that this model provides a superior fit to the data. In fact, when applied to entire data sets of measured relationships between bedload transport and discharge, piecewise linear regressions, three-parameter power functions, and polynomial functions obtained similar model standard errors. However, the piecewise regression provides thresholds, and determining thresholds was a major aim for Ryan et al. (2002). Being a statistical analysis that takes into account the entire data set, piecewise regression eliminates operator subjectivity and the focus on a particular, significant sample, thus piecewise regression eliminates several of the problems plaguing the visual analysis of bedload explosion flows (Emmett 1999).

Studies by Ryan et al. (2002, 2005)

Ryan et al. (2002) applied the piecewise regression analysis to data sets of total (not fractional) bedload transport rates versus discharge in order to identify the threshold or breakpoint flow at which transport rates abruptly increase, i.e., the shift from Phase 1 to Phase 2 transport. Bedload samples were collected using a Helley-Smith sampler (or similar handheld devices) at five sites along a mountain cobble-bed stream and two of its tributaries. Breakpoint flows on average occurred at 91% Q_{bkf}. Ryan et al. (2005) added data from several other mountain gravel- and cobble-bed streams to the analyses of breakpoint flows using piecewise regression. All data sets were large and, except for one, extended to flow up to 107 and 193% Q_{bkf}. For the analyzed 19 streams, breakpoint flows occurred between 40 and 110% of bankfull flow with an average of 81% Q_{bkf}. One standard deviation encompassed the range of 65 to 95% Q_{bkf}. At the onset of Phase 2 transport, particles of the bed surface D_{16} to D_{25}[13] sizes were mobile. In these streams this constituted medium (D_{16} = 11 to 36 mm) and coarser gravel.

3.2.2 Methods

This study applied two methods to identify breakpoint flows in measured data sets of transport rates and flow:

- Piecewise Regression analysis, and
- Visual estimates of data sets plotted in a linear scale.

Both methods are described below.

3.2.2.1 Piecewise regression analyses (SAS)

Porth (2004) used a combination of different procedures (including piecewise regression) available within the SAS[14] application to compose a routine called 1_BRKPTREG.SAS that computes breakpoints. The 5-step routine is rather involved and described in detail in Ryan and Porth (2007). An overview as well as a narrative description of the 5 steps is provided below.

1. Apply a smoothing function (LOESS fit) to the data of bedload transport and discharge plotted in linear scale to help with a visual approximation of the range of flows within which the breakpoint could occur;
2. Fit a linear regression to the entire data set.
3. Apply the piecewise linear regression procedure that fits two linear but continuous regression functions to the upper and lower portions of the data to compute the flow at which the breakpoint occurs. Obtain the parameters of the best-fit regression functions below and above the breakpoint.
4. Fit a three-parameter power function regression to the data of bedload transport *vs.* discharge.
5. Merge results and plot together with the data to compare the outcome of different curve fitting models.

---

[13] *Particle sizes for the D_{25} were not indicated but are typically about twice as large as the D_{16} sizes.*

[14] *SAS (Statistical Analysis System), software package for statistical analyses*

1. Plot the data and apply a smoothing function

The data of bedload transport (Q_B) versus discharge (Q) are plotted in a linear scale together with a nonparametric smoothing function (LOESS fit). This function fits two (or more) line segments to the data that intersect in the flow range of the approximate breakpoint, i.e., the plot provides the user with a range of flows within which the breakpoint might occur. From within this range, the user visually estimates three breakpoint flows: a low, a medium and a high one. These breakpoint estimates are then used as starting values for the piecewise regression analysis.

2) Fit a linear regression

A linear regression is fitted to the entire data set to determine whether a linear fit adequately describes the data in which case a breakpoint is not expected, and further analyses are not necessary. If the fit is poor (most likely), it is assumed that the two segments of the piecewise regression, one for the lower and one for the upper portion of the data might characterize the Q_B *vs.* Q relationship better than a linear fit.

3) Apply the piecewise regression procedure to compute the breakpoint discharge

The input data of Q_B *vs.* Q are divided into two portions, one below and one above the visually estimated breakpoint from the LOESS fit. Two separate linear regressions functions are fitted to the data, one to the lower portion (low transport rates and small increase with flow) and one to the higher portion (high transport rates and steep increase with flow). The SAS routine then uses the parameters of the two regressions (intercept and slope) as well as their intersection point as input for the piecewise regression analysis. The piecewise regression procedure then iteratively determines the best-fit combination of an upper and lower segment for an unsteady but continuous linear regression function with

$$Q_B = a_1 + b_1 Q \quad \text{for the lower segment } (Q < c) \text{ and} \qquad \text{(Eq. 1)}$$

$$Q_B = a_2 + b_2 Q \quad \text{for the upper segment } (Q > c). \qquad \text{(Eq. 2)}$$

The intercept of the upper segment a_2 is computed from

$$a_2 = a_1 + c\,(b_1 - b_2) \qquad \text{(Eq. 3)}$$

where c is the breakpoint flow at the intersection point of the two segments. The iterative piecewise regression procedure is repeated for the other two visual breakpoint estimates.

The SAS program provides a list with the results for each of the three trial runs (i.e., for the low, medium and high initial visual breakpoint estimates from the LOESS fit). Results include the parameters slope (b) for the two segments of the regression functions below and above the breakpoint flow, the intercept (a) for the segment below the breakpoint flow, the breakpoint flow c and the ±95% confidence intervals around it, t-values and probabilities for the model parameters, as well as the model standard error.

The three trial runs often arrive at the same computed breakpoint flow. If different breakpoint results are obtained, the one with the lowest standard error is selected as representative. The user might also investigate whether some of the data points should be classified as outliers and be removed from the analyses. Breakpoint can then be computed with outliers removed to determine whether this measure provides a more representative result.

4) Fit a power function to the Q_B vs. Q relationship

A three-parameter power function in the form $Q_B = b_0 + b_1 Q^{b2}$ is fitted to the entire data set. Its degree of fit is expressed in terms of *t*-values of the model parameters as well as a mean model standard error.

5) Merge results and plot together with the data to compare the outcome of different curve fitting models

A plot of bedload transport rates versus discharge in linear scale is overlain with plotted functions of the best-fit linear regression (2), the piecewise regression function with its portions below and above the breakpoint (3), as well as the fitted power function (4). Plotting the fitted functions together with the measured transport rates provides an opportunity to catch gross computing errors. It also allows the user to visually evaluate the most appropriate model for a specified data set. The fit (i.e., the model standard error, MSE) for a single linear regression is typically much poorer than the fit obtained by piecewise linear regression and a three-parameter power function, both of which typically yield similar values for MSE. Given similar MSE, the piecewise regression is selected because it determines thresholds or breakpoint flows, which is the aim of breakpoint analyses.

Application of the canned "Piecewise regression" SAS routine in this study

This study used Porth's (2004) SAS routine to compute breakpoint flows. Although the routine was designed to be run by inexperienced SAS users, running the program still requires rudimentary knowledge of SAS because the user must perform several SAS commands[15]. The input data (i.e., the discharge and bedload transport values) are supplied from an Excel spreadsheet and require a specific format (such as column headings, sheet naming, etc.).

The Piecewise Regression routine was run in this study to determine the breakpoint flows for six data sets: data obtained for Little Granite Creek in 1999, Halfmoon Creek in 2004

---

[15] *This program comprises 3 steps: 1) The user specifies in the SAS routine the location of the SAS folder on the PC. The Excel input files are stored in this folder. 2) The user lets SAS make a printed list of the data and a list of summary statistics, such as minimum, mean and maximum values. 3) The user enters appropriate files names and other instructions such as the range of x and y values to run two macros. The first macro conducts a loess-fit that provides information on the range of x and y data which is used as input in the second macro that computes the remainder of the analyses. The SAS program provides output graphs and a list of computed parameters.*

and Hayden Creek in 2005 using the Helley-Smith sampler as well as bedload traps. The fitted piecewise regression functions for the lower and upper segments as well as their intersection point are shown for all data sets in Figure 5. The piecewise regression procedure typically provides one breakpoint per data set. An exception were bedload trap samples collected at Halfmoon Creek for which the SAS procedure indicated a secondary breakpoint flows (although with a higher standard deviation) at a lower flow.

3.2.2.2 Visual determination of breakpoint flows

The increase in transport rates beyond a breakpoint flow is visually notable in linear plots of transport rates versus discharge and can be estimated from plotted data. The SAS application is not freely available and running the SAS routine for piecewise regression analysis, even with the tutorial provided by Ryan and Porth (2007), requires some knowledge about how a SAS application operates. Not having to run the breakpoint procedure in SAS but getting results from viewing plotted data has an appeal, even if the result is at the expense of some uncertainty. This study therefore examines how visual estimates of breakpoint flows for all six data sets compare to those computed with the SAS procedure.

In a linear plot of bedload transport rates versus flow, transport rates cluster along the x-axis at lower flows and increases more steeply at higher flows. The human eye does not have too much trouble fitting linear regression functions to the upper and lower segments of the data and estimating the intersection point (see step 1 in Section 3.2.2.1). It must be noted though, that the presence of individual high data points influences the estimate, such that the visual estimate of breakpoint flows is derived from the combination of two factors: the intersection point of the two visually or hand-fitted lines and the first occurrence of high transport rates. The hand-fitted lines and the visually estimated breakpoint flows are shown for samples from the Helley-Smith sampler and bedload traps collected in the three study streams in Figure 6.

Breakpoint flows were also visually estimated for the 19 streams for which Ryan et al. (2005) had determined breakpoint flows using the SAS procedure.

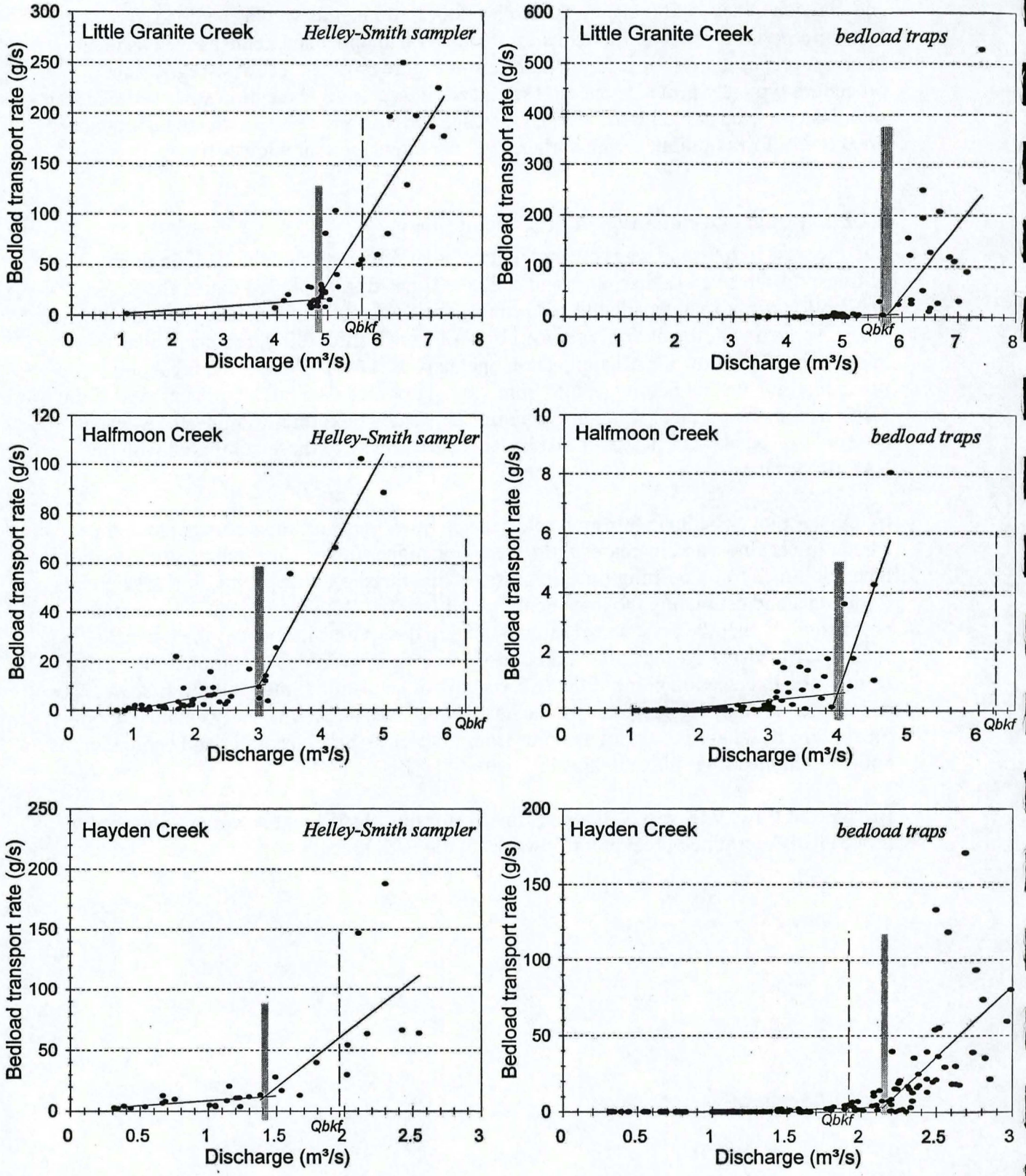

Figure 5: The upper and lower segments of the piecewise regression functions and the breakpoint flows at the intersection for samples collected with a Helley-Smith sampler (left column) and bedload traps (right column). The light gray bars indicate the breakpoint flow at the intersection point.

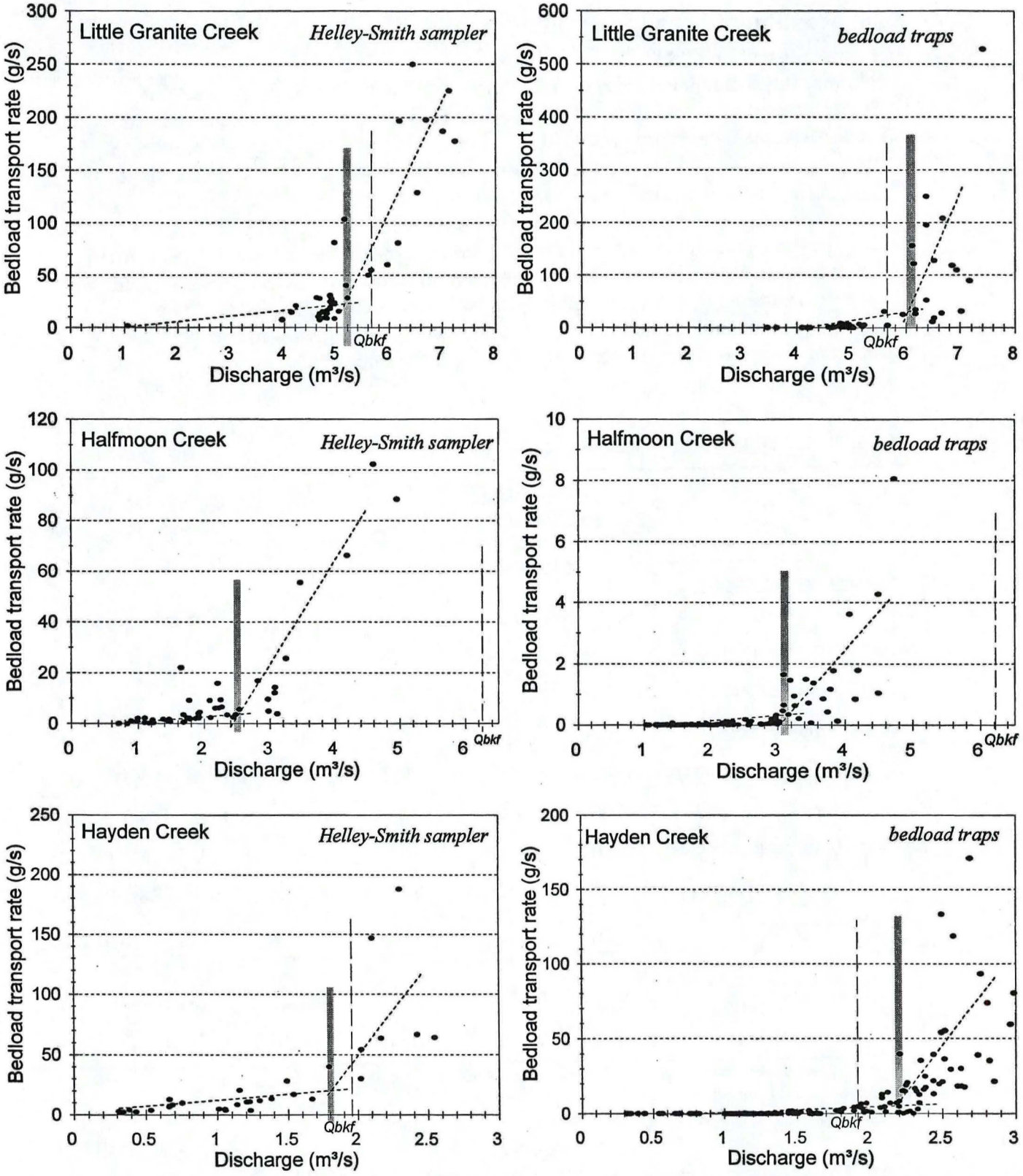

Figure 6: Visually estimated breakpoint flows (indicated by light gray bars) based on hand-fitted upper and lower regression functions (stippled lines) as well as a perceived abrupt increase of transport rates for bedload samples collected with a Helley-Smith sampler (left column) and bedload traps (right column).

3.2.4 Results of breakpoint analyses

Piecewise regression (SAS)

Breakpoint flows computed from the piecewise regression method for data sets of bedload transport rates and flow collected with a Helley-Smith sampler and bedload traps in the three study streams are presented in Table 6. Outputs from the breakpoint SAS routine (Porth 2004) include breakpoint flows (c), their 95% confidence limits, slopes (b_1 and b_2) of the upper and lower segments of the fitted regression function (see Eqs. 1 and 2), the intercept (a_1) of the lower segment (a_2 is computed subsequently from Eq. 3), as well as the three parameters (b_0, b_1 and b_2) of the three-parameter power functions fitted to the entire data sets. The output also includes information on t-values, the probability of t for each parameter, as well as model standard errors (Table 7). Note that the probability of t, the model standard errors for the piecewise regression, and the three-parameter power functions are generally similar for the three study streams.

Table 6: Results of the SAS breakpoint analyses.

Parameter	Helley-Smith data			Bedload trap data		
	Litl. Granite Cr., 1999	Halfmoon Cr., 2004	Hayden Cr., 2005	Litl. Granite Cr., 1999	Halfmoon Cr., 2004	Hayden Cr., 2005
Piecewise linear regression:						
Breakpoint flow c (m^3/s)	**4.80**	**2.97**	**1.41**	**5.75**	**3.97 (3.06)***	**2.15**
Lower 95% conf. limit of c	4.50	2.79	0.87	5.21	3.86 (2.89)	2.05
Upper 95% conf. limit of c	5.10	3.15	1.94	6.29	4.07 (3.23)	2.25
Breakpoint flow c (% Q_{bkf})	**84.8**	**47.7**	**73.2**	**102**	**63.7 (49.1)**	**112**
Intercept a_1 (lower segment regr.)	-1.87	-4.17	0.895	-4.86	-0.358 (-0.065)	-2.33
Slope b_1 (lower segment regr.)	3.67	4.82	7.81	1.77	0.240 (0.049)	2.63
Intercept a_2# (upper segment regr.)	-378	-131	-112	-805	-26.7 (-6.90)	-196
Slope b_2 (upper segment regr.)	82.1	47.5	87.7	141	6.87 (2.28)	92.9
Power function:						
Power fit b_0	-27.2	0.135	-0.719	12.0	0.0508	-1.32
Power fit b_1	0.119	0.389	9.73	3.48E-12	2.90E-6	0.205
Power fit b_2	3.88	3.50	2.63	16.2	9.41	5.54

*Values in parentheses show a secondary breakpoint for bedload trap data from Halfmoon Creek.
Values computed from Eq. 3.

3.2.4.1 Comparison of computed (SAS) and visually estimated breakpoint flows

The piecewise regression method and visual estimates are conceptually closely related. It is therefore useful to know how well quickly estimated visual breakpoint flows match

Table 7: Probability of t and model standard errors for results of the SAS Piecewise Regression analyses.

Parameter	Helley-Smith data			Bedload trap data		
	Litl. Granite Cr., 1999	Halfmoon Cr., 2004	Hayden Cr., 2005	Litl. Granite Cr., 1999	Halfmoon Cr., 2004	Hayden Cr., 2005
Piecewise linear regression:						
Breakpoint flow (m^3/s) c	<0.0001	<0.0001	<0.0001	<0.0001	<0.0001	<0.0001
Intercept a_1 (lower segment regr.)	0.96	0.21	0.96	0.91	<0.0001	0.49
Slope b_1 (lower segment regr.)	0.66	0.01	0.65	0.85	<0.0001	0.31
Intercept a_2 (upper segment regr.)	-	-	-	-	-	-
Slope b_2 (upper segment regr.)	<0.0001	<0.0001	0.0017	0.0005	<0.0001	<0.0001
Model standard error	845	40	779	3970	0.184	225
Power function:						
Power fit b_0	0.24	0.94	0.95	0.19	0.11	0.40
Power fit b_1	0.29	0.087	0.26	0.87	0.35	0.15
Power fit b_2	0.0001	<0.0001	0.014	<0.0001	<0.0001	<0.0001
Model standard error	940	58	805	3234	0.153	239

with those laboriously computed from the piecewise regression procedure (SAS) and whether visual estimates could be used as reliable estimates. For easier comparison, breakpoint flows computed from the piecewise regression procedure (denoted as "SAS") and estimated visually ("visual") are combined in Table 8. To enlarge the data set for comparison of SAS computed and visually estimated breakpoint flows, breakpoint flows computed by Ryan et al. (2005) from Helley-Smith samples for Little Granite, Halfmoon, and Hayden Creek as well as the breakpoint flows that this study visually estimated from the data plotted by Ryan et al. (2005) are also included in Table 8 and denoted as "HS Ryan". All computed breakpoint flows are presented in units of m^3/s and as percentages of bankfull flow (% Q_{bkf}).

Breakpoint flows computed from the SAS procedure and visual estimates (Figure 7) are similar but not identical. The ratios of breakpoint flows between the two methods vary between streams and between data sets (Table 9). Breakpoint flows from visual estimates may be as small as 78% and as large as 128% of the values obtained from the SAS procedure, although in 4 out of the 9 data sets, visual estimates were within ±5% of those from the SAS procedure. There does not seem to be a trend for a better match between SAS and visual breakpoints for a particular sampler or data set. A similar result was found when comparing visual breakpoint estimates fitted to the data by Ryan et al. (2005) to those computed from the SAS procedure: in 13 out of 19 data sets, the visual estimate matched the SAS value to within ±5%. In the remaining 6 cases, breakpoint flows from both methods differed by as much as ±30%.

Table 8: Breakpoint flows computed from the piecewise regression procedure and visual estimates for bedload trap and Helley-Smith samples collected in the three study streams.

Stream	Sampler	Method	Measured Q_{max} ($\%Q_{bkf}$)	Breakpoint flows (m^3/s)	Breakpoint flows ($\%\ Q_{bkf}$)	Mean ($\%\ Q_{bkf}$)
Little Granite Creek	Bedload traps	SAS	131	5.75	102	105
		Visual		6.05	107	
	HS	SAS	128	4.8	85	85
		Visual		5.0	85	
	HS Ryan[#]	SAS	193	4.83	81	91
		Visual		6.0	101	
Halfmoon Creek	Bedload traps	SAS	80	3.97 (3.06)*	64 (49)	57 (44.5)
		Visual		2.5	40	
	HS	SAS	80	2.97	48	44
		Visual		2.5	40	
	HS Ryan	SAS	175	2.51	40	39.5
		Visual		2.4	39	
Hayden Creek	Bedload traps	SAS	156	2.15	112	113.5
		Visual		2.2	115	
	HS	SAS	133	1.41	73	83.5
		Visual		1.8	94	
	HS Ryan	SAS	109	1.68	88	83
		Visual		1.5	78	

* Values in parentheses refer to a secondary breakpoint determined by the SAS procedure at Halfmoon Creek. [#] HS Ryan refers to results for streams included in this study by Ryan et al. (2005).

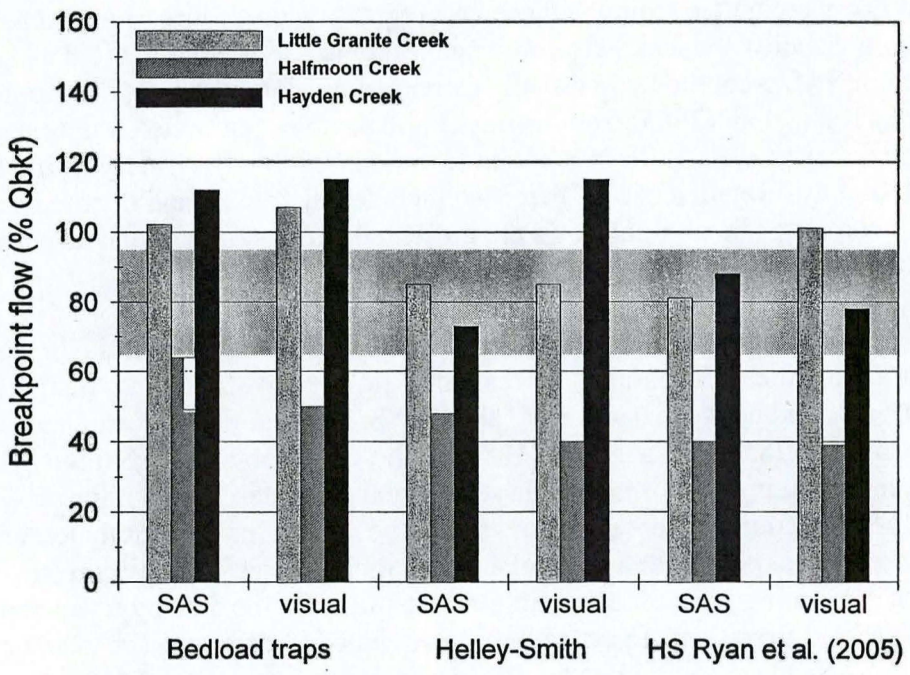

Figure 7: Comparison of breakpoint flows computed for data sets from bedload traps and the Helley-Smith sampler at the three study streams using the SAS procedure and visual estimates.

Table 9: Ratio of breakpoint flows computed from the piecewise regression analysis (SAS) to those obtained from visual estimates for the three study streams.

Data set	Little Granite Cr. 1999	Halfmoon Cr. 2004	Hayden Cr. 2005
Bedload trap	0.95	1.28 (0.99)*	0.98
Helley-Smith	1.00	1.20	0.78
HS (Ryan et al. 2005)	0.81	1.05	1.12
Mean ratios	0.92	1.17 (1.08)	0.96

*Values in parentheses refer to a secondary breakpoint determined in the SAS procedure.

Precision of SAS breakpoints versus visual estimates

The piecewise regression analysis eliminates operator judgment on which visual estimates are based. As the piecewise regression analysis encompasses all data of a data set, a computed breakpoint is also less influenced by the presence or absence of high data points than a visual estimate. With less influence from specific data points and no operator discretionary decision, the piecewise regression is likely to produce breakpoint flows with higher precision than visual estimates.

Being a statistical procedure, the piecewise regression analysis provides confidence limits. In this study, the ±95% confidence interval[16] of breakpoint flows from the piecewise regression analysis (Table 6) typically encompassed a range of ±3 to ±9% around the computed breakpoint flow. This range is somewhat narrower than the difference between SAS computed and visually estimated breakpoint flows that typically remains within ±5%, but may be as large as ±30%.

Glimpse into variability between studies

For the three streams analyzed in this study, independent analyses of breakpoint flows from the SAS procedure are available from Ryan et al. (2005). Their data sets were collected with a Helley-Smith or similar sampler over two or more years several years prior to this study. The data sets are larger (100-200 samples) than the Helley-Smith data used for this study (30-50 samples). Breakpoint flows from Ryan et al. (2005) are listed as "HS Ryan" in Table 8 together with breakpoint flows computed for this study. A comparison of breakpoint flows from the two studies provides an opportunity to assess the variability in breakpoint flows computed for different data sets collected at the same stream with the same or similar sampler but at different sites (up to about 0.5 miles apart) by different crews in different years. For the three study streams, breakpoint flows

[16] *Confidence limits are only valid if the data set's residuals are normally distributed and without a temporal trend – a prerequisite that most measured data of bedload transport and discharge do not fulfill. In this case, confidence limits can be computed from a bootstrap procedure. Bootstrap confidence limits are considerably wider than those computed from the SAS routine for piecewise regression. For example, the bootstrap 95% confidence limits for the Helley-Smith data sets collected by Ryan et al. (2005) span flows of 42-120% Q_{bkf} for Little Granite Creek, 0-97% Q_{bkf} for Halfmoon Creek, and 67-108% Q_{bkf} for Hayden Creek.*

obtained by Ryan et al. (2005) are 0.83 - 1.20 times those computed for the same streams with a Helley-Smith sampler in this study (Table 10). The observed differences are due to the combined effects of interannual variability of the Q_B *vs.* Q relationship, differences in sample size and the range of the measured data, as well as slightly different versions of the Helley-Smith sampler. Based on results from these three streams, breakpoint flows computed in different studies for the same stream may vary by as much as ±20%, although averaged over all three streams, both studies arrived at similar results.

Table 10: Ratios of breakpoint flows between Helley-Smith samples collected by Ryan et al. (2005) and in this study for computations from the SAS procedure as well as visual estimates.

Method of breakpoint computation	Little Granite Cr., 1999	Halfmoon Cr., 2004	Hayden Cr., 2005	Mean for all sites combined
Piecewise regression (SAS)	1.01	0.85	1.19	1.02
Visual estimates	1.20	0.96	0.83	1.00
Average	1.11	0.91	1.01	1.01

3.2.4.2 Differences between samplers: effects of rating curve steepness

A major question of this study was to assess the difference in breakpoint flows computed from Helley-Smith samples (HS) and bedload traps collected at the same stream during the same highflow season. Ideally, data sets used for this comparison should have the same number of data points and the same range of sampled flow. In this study, though, HS-samples were collected only once or twice a day. The data sets are therefore smaller (n = 31 to 50) than those from bedload traps (n = 58 to 192; 4-9 samples a day) and may not include samples from the highest flows. However, the "once-a-day" HS data sets are more typical of data sets obtained when a stream is monitored in a non-research setting.

A comparison of breakpoint flows between Helley-Smith samples and bedload traps shows that bedload trap samples generally yield higher breakpoint flows than Helley-Smith samples. Bedload traps have breakpoint flows 120 to 153% (mean 136%) of those computed for Helley-Smith samples (Table 11) when computed from the piecewise regression analysis. The difference between samplers is slightly less for visual estimates that yield breakpoint flows for bedload trap samples that are 122% to those from Helley-Smith samples. These results suggest that bedload traps produce breakpoint flows 20-30% larger than Helley-Smith samples.

Table 11: Ratios of breakpoint flows between Helley-Smith and bedload trap samples computed from the piecewise regression procedure and visual estimates for the three study streams.

Method of breakpoint computation	Little Granite Cr. 1999	Halfmoon Cr. 2004	Hayden Cr. 2005	Mean for all sites combined
Piecewise regression (SAS)	1.20	1.34	1.53	1.36
Visual estimates	1.21	1.24	1.22	1.22
Average	1.20	1.29	1.37	1.29

The persistent difference in breakpoint flows between the two samplers is striking but not unexpected and may be attributed to the difference in steepness of the Q_B *vs.* Q relationship. To ensure that the lower Helley-Smith breakpoint flows relative to those from bedload traps are not caused by a few odd data points in the samples from the study streams, this study compared breakpoint flows for bedload transport rating curves fitted to data collected with both samplers at eight different field sites in mountain gravel-bed streams. Helley-Smith rating curves are relatively flat and typically have power function exponents b ($Q_B = a\,Q^b$) between 2.4 and 4.4, while the steeper bedload trap rating curves have exponents between 7.6 and 16.7 (Bunte et al. 2007, *in press*). To compare rating curves among streams and between samplers, flow is expressed as a percentage of bankfull flow and transport as a percentage of the bankfull bedload transport rate. Breakpoints are visually estimated for the fitted power functions that are plotted up to 110% of bankfull flow in a linear scale. Figure 8 shows that breakpoint flows generally increase with the steepness of the bedload rating curve, i.e., for higher rating curve exponents. One could quantify the relationship between breakpoints and rating curve exponents either by computing breakpoint flows for a large number of measured data sets or through an analytical analysis (e.g., relating the point of maximum curvature—an indication of the breakpoint flow—to the power function exponent). For the present

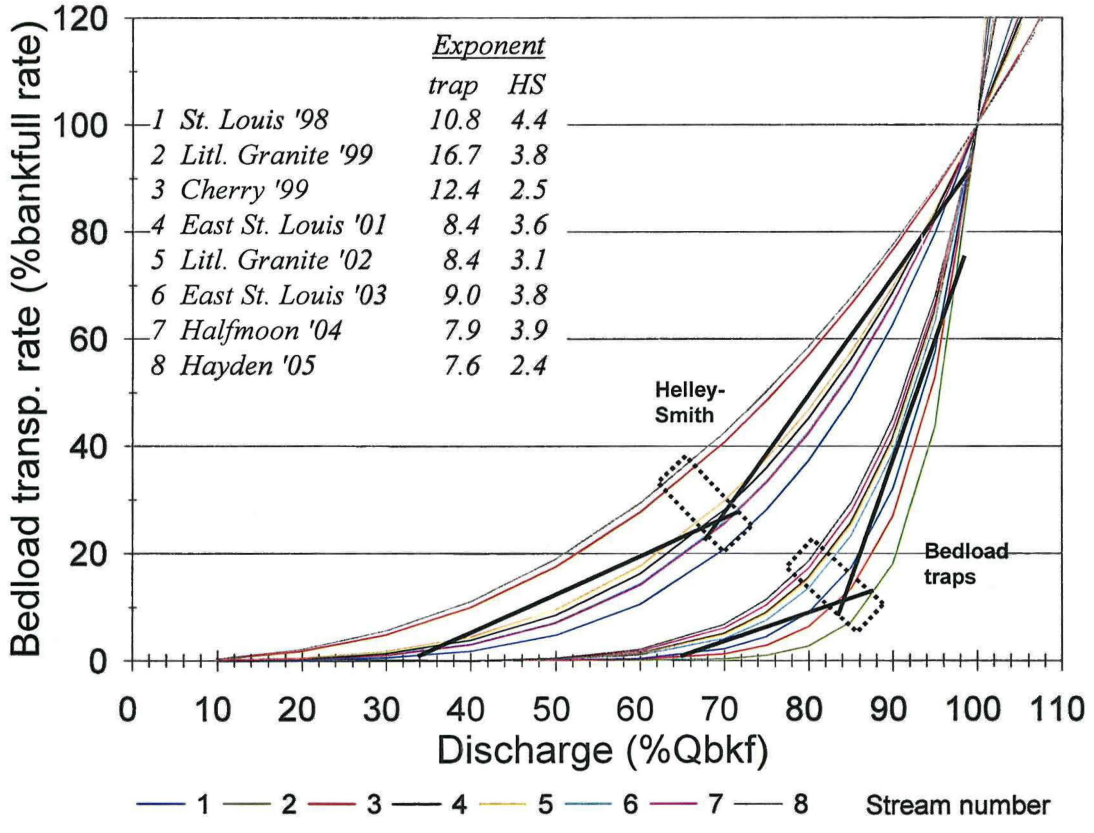

Figure 8: Bedload transport rating curves obtained at 8 field sites using a Helley-Smith sampler and bedload traps plotted in non-dimensional form (i.e., normalized by the bankfull flow and bankfull transport rate). The pairs of upper and lower linear regressions functions (thick black lines) were fitted by eye to a regression function in the center of the data for each sampler. The two stippled rectangles indicate the potential range of breakpoint flows for Helley-Smith and bedload trap samples at the 8 field sites.

study, it suffices to point out that for Helley-Smith rating curves with exponents between about 2 and 4, visually estimated breakpoints occur at approximately 70% Q_{bkf}, while for bedload traps, they occur at about 85% Q_{bkf}. Breakpoint flows for bedload traps are thus on average about 15% higher than of those computed for Helley-Smith samples. These results show that sampling devices and (the resulting) rating curve steepness greatly affect computed breakpoint flows. Samplers that produce steeper bedload transport curves yield higher breakpoint flows.

3.2.4.3 Effect of measured range of flows: scale dependency

Breakpoint flows are not only dependent on the rating curve steepness, but also on the range of measured flows (Bunte 1999b). Two approaches are pursued in this study to examine the effects of the measured range of flow on breakpoint flows. One uses a power function bedload transport rating curve that is typical of bedload trap samples. The other approach uses measured data sets of bedload *vs.* discharge and truncates these stepwise from the highest measured flow to bankfull flow.

Power function rating curve plotted in different linear scales

Bunte (1999b) had attributed the dependency of breakpoints on the range of measured flows to the self-similarity of a power function that is plotted over different scales. A power function $Q_B = 1E\text{-}17 \cdot Q^8$ that is typical of a bedload transport rating curve fitted to bedload trap samples collected in a mountain gravel-bed stream is selected for the analyses[17]. The graph of this power function is plotted in a linear scale with axes scaled such that the graph passes through the lower left- and the upper right-hand corner of the plot. The function is plotted over three ranges of flow, extending to a unit flow of 100 (e.g., % Q_{bkf}) in the first plot, and to unit flows of 150 and 200 (e.g., % Q_{bkf}) in the other two plots (Figure 9 a-c).

When the highest measured flow (Q_{max}) extends to 100% Q_{bkf}, a breakpoint can be visually estimated near a flow of 75-80% Q_{bkf} (Figure 9 a). When the measured range of flows extends to 150 and 200% Q_{bkf}, breakpoints can be visually estimated at about 115-120 and 150-160% Q_{bkf}, respectively (Figure 9 b-c). In each case, the general shape of the power function graph looks identical, and breakpoints consistently occur at the same relative position in each plot which is approximately at 75-80% of the highest measured flow (Q_{max}). Similarly, breakpoints also occur consistently at about 20% of the highest measured transport rate. In absolute terms, breakpoints shift to progressively higher flows and transport rates with an increasing range of measured flows and transport rates. Consequently, differences in the range of measured flows contribute significantly to a variability of breakpoint flows computed for different streams. Thus, bedload data collected at a specified stream can produce radically different breakpoints simply based on differences in the highest flows sampled.

---

[17] *The scale dependency is not affected by the power function coefficient (i.e., 1E-17 in this case). The exponent, though, influences the result, causing breakpoints to be at higher flows for higher exponents (Section 3.2.4.2).*

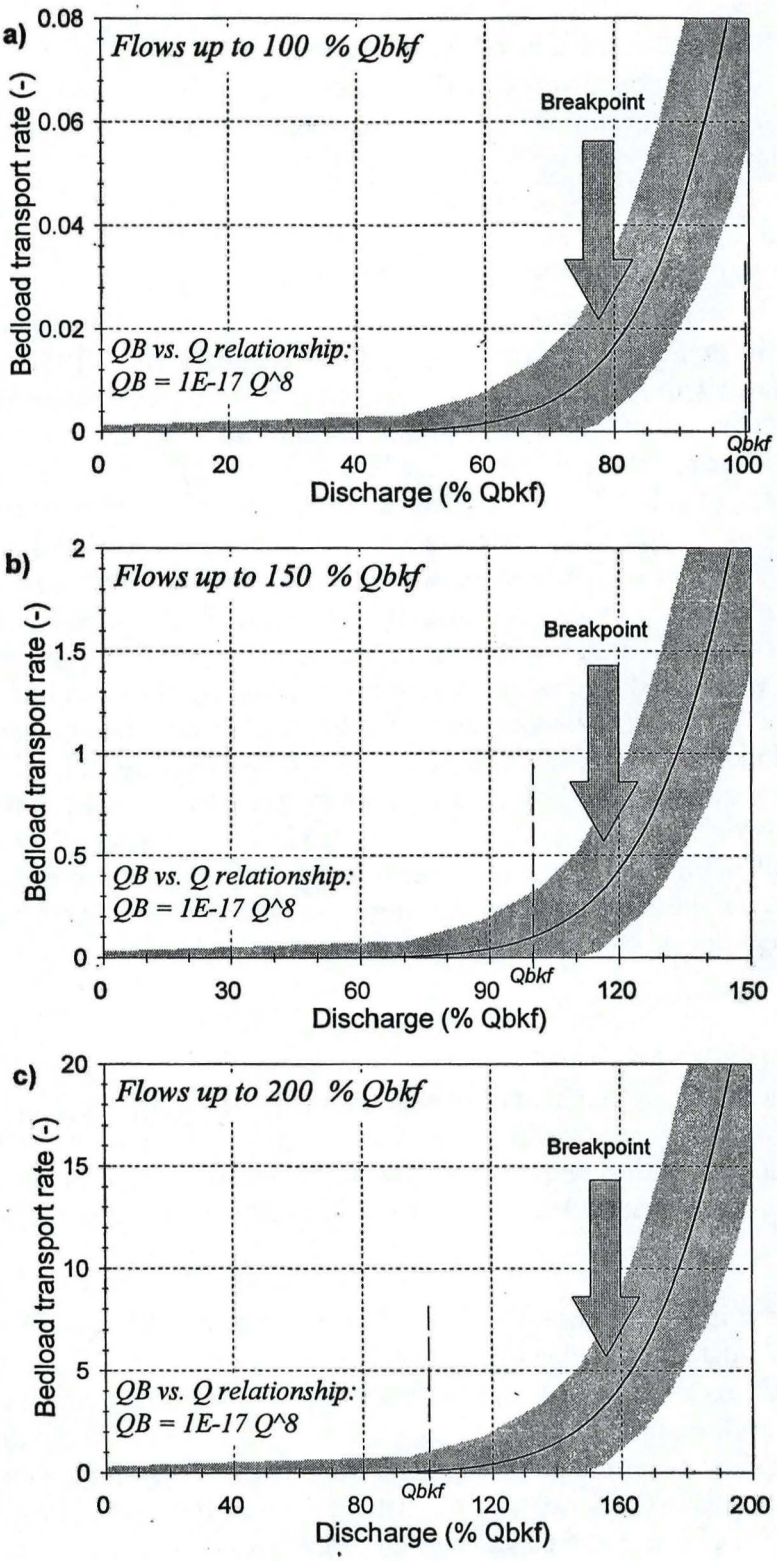

Figure 9: Self-similarity of a power function (e.g., Q_B = 1E-17·Q^8, typical of bedload trap samples) plotted over three increasingly larger ranges of flow and bedload transport rates: 0-100% Q_{bkf} (a), 0-150% Q_{bkf} (b), and 0-200% Q_{bkf} (c). The gray area denotes the range of x- and y-values in which most of the data points are expected. In all three cases, breakpoints occur at about 75-80% of the highest measured flow.

Breakpoint flows of 75-80% of Q_{max} are obtained from a Q_B *vs.* Q relationship with an exponent of 8. Based on results in Figure 8 (Section 3.2.4.2), a flatter relationship of Q_B *vs.* Q with a lower exponent would yield a value smaller than 75-80% Q_{max}, whereas a steeper Q_B *vs.* Q relationship with a larger exponent would yield a higher value for the breakpoint flow.

Knick points in power function relationships are general

The analysis of scale-dependency (above) used a specific power function to demonstrate the effect of the range of measured flows on the breakpoint flow. The increase of breakpoint flows with increasing Q_{max}, however, is general. The power function coefficient does not affect the outcome, and a similar increase in knick points with an increasing x-value range would be obtained for any power function with an exponent b within the range of about 2 to 16. If a knick point at which the curvature visibly steepens can be identified for *any* power function with $b > 2$ that is plotted in a linear scale—regardless of the described process—, then the occurrence of a breakpoint is not necessarily linked to a specific process in the interaction between bedload transport and flow. Based on this finding, breakpoints in bedload transport data sets simply constitute knick points, visible and statistically determinable in linear plots and linear analyses of power function relationships. Although the concept of breakpoints that occur around 80% Q_{bkf} and indicate the onset of Phase 2 transport has some appeal, knick points always occur at about 55-90% of the maximum measured value when a power function relationship (with an exponent of 2 - 16) is plotted in a linear scale. Knick points are neither dependent on nor necessarily caused by an abrupt increase in transport rates and the onset of Phase 2 transport. They are simply an artifact of plotting a power function relationship in a linear scale.

Stepwise truncation of data sets

Having shown a constant position of breakpoint flows near 75-80% Q_{max} for the case of a plotted power function graph (with an exponent of about 8 (Figure 9)), this study wanted to confirm that the position of the breakpoint flow also occurs at a fixed percentage of Q_{max} when measured data sets of bedload transport rates are truncated step by step at the upper end.

Data sets most suitable for truncation in several steps between Q_{max} and bankfull flow are the bedload trap data for Hayden Creek that extend to flows up to 155% Q_{bkf}. Bedload trap data for Little Granite Creek and Helley-Smith data from Hayden and Little Granite Creek extend to flows of around 130% Q_{bkf} and are also suitable. Bedload data measured with both samplers at Halfmoon Creek extend to only 80% Q_{bkf} and are not suited for this analysis. For the analysis of stepwise truncated data sets, breakpoint flows are visually estimated instead of computed using the SAS procedure. Visual estimates are not only much faster and easier to do than running the SAS routine, but also provide results that in most cases are within about ±5% of the breakpoint flow determined from the SAS analysis (Section 3.2.4.1).

It is important for the accuracy of visual estimates of breakpoint flows that the linear plots are scaled to place the highest measured flow and transport rate in the upper right-hand corner of the plot. Thus, for each stepwise truncation of the data, the x and y-axes are rescaled to achieve this aim. Bedload data from Hayden Creek cover the largest range and can be truncated in three equal steps between 3.0 and 1.92 m^3/s, such that the considered Q_{max}-values are 3.0, 2.64, 2.28, and 1.92 m^3/s. For the entire data set (Q_{max} = 3 m^3/s and Q_{Bmax} = 170 g/s), a breakpoint can be visually estimated at a flow of about 2.2 m^3/s. This equals 115% Q_{bkf} and 74% of Q_{max} (Figure 10a).

The first truncation to Q_{max} = 2.64 m^3/s (139 % Q_{bkf}) in Figure 10b has no effect on the absolute breakpoint that remains at 2.2 m^3/s and 115 % Q_{bkf}, but in terms of Q_{max}, the breakpoint increases to 83% Q_{max}. The second truncation to Q_{max} = 2.28 m^3/s (121% Q_{bkf}) yields a breakpoint at a flow of 2.0 m^3/s. This equals 104% Q_{bkf} and 88% Q_{max} (Figure 10c). In the final truncation to Q_{max} = 1.92 m^3/s or 100 % Q_{bkf}, a breakpoint is visible at 1.4 m^3/s which equals 73% Q_{bkf} and 73% Q_{max} (Figure 10d).

Similar analyses were conducted using data measured with bedload traps at Little Granite Creek (Figure 11 a-c) as well as with the Helley-Smith data collected at Hayden and Little Granite Creek (Figure 12 a-c). Due to the smaller range of flows sampled in these data sets, truncation was limited to two steps, one to the midpoint flow between Q_{max} and Q_{bkf} and one to 100% Q_{bkf}. Breakpoint flows estimated for the stepwise truncations of data sets from both streams and both samplers are summarized in Table 12.

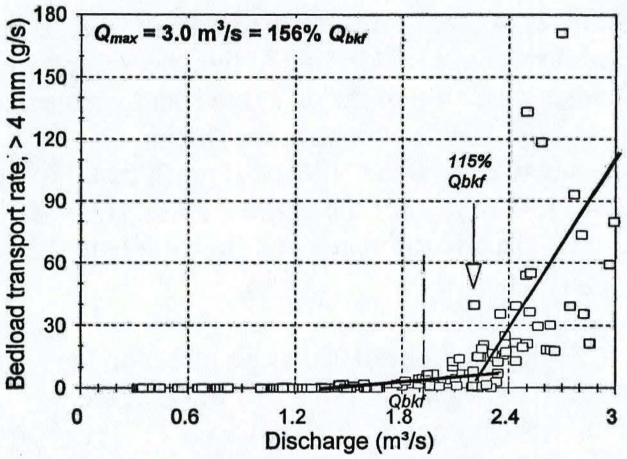

Figure 10 a: Bedload and discharge data measured with bedload traps at Hayden Creek plotted in a linear scale. For Q_{max} = 3.0 m^3/s (= 156% Q_{bkf}), a breakpoint occurs at a flow near 2.2 m^3/s (= 115% Q_{bkf} = 74% Q_{max}). The regression lines are hand-fitted. The arrow indicates the breakpoint flow.

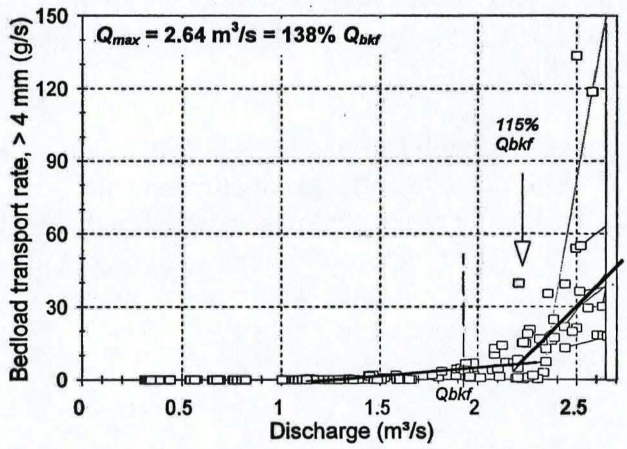

Figure 10 b: For Q_{max} = 2.64 m^3/s (= 138% Q_{bkf}), the breakpoint remains at a flow near 2.2 m^3/s (= 115 % Q_{bkf} = 83% Q_{max}).

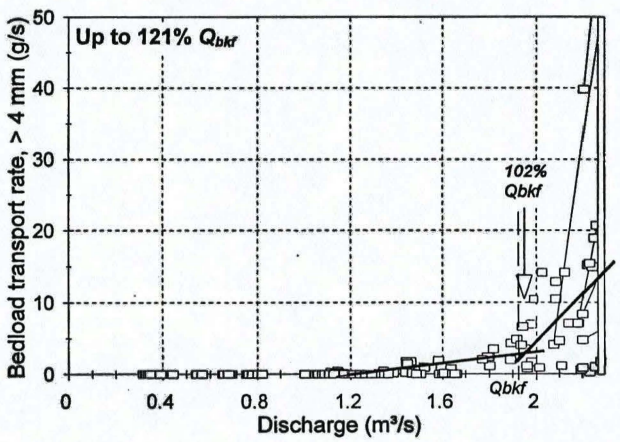

Figure 10 c: For Q_{max} = 2.28 m^3/s (= 119% Q_{bkf}), a breakpoint occurs at a flow near 1.95 m^3/s (= 102% Q_{bkf} = 86% Q_{max}).

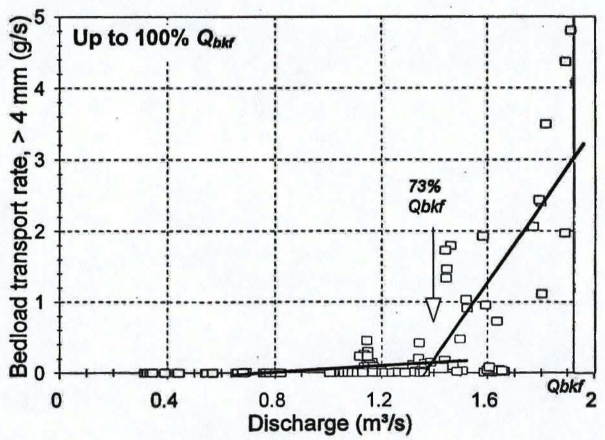

Figure 10 d: For Q_{max} = 1.92 m^3/s (=100% Q_{bkf}), a breakpoint occurs at a flow near 1.4 m^3/s (= 73% Q_{bkf} = 73% Q_{max}).

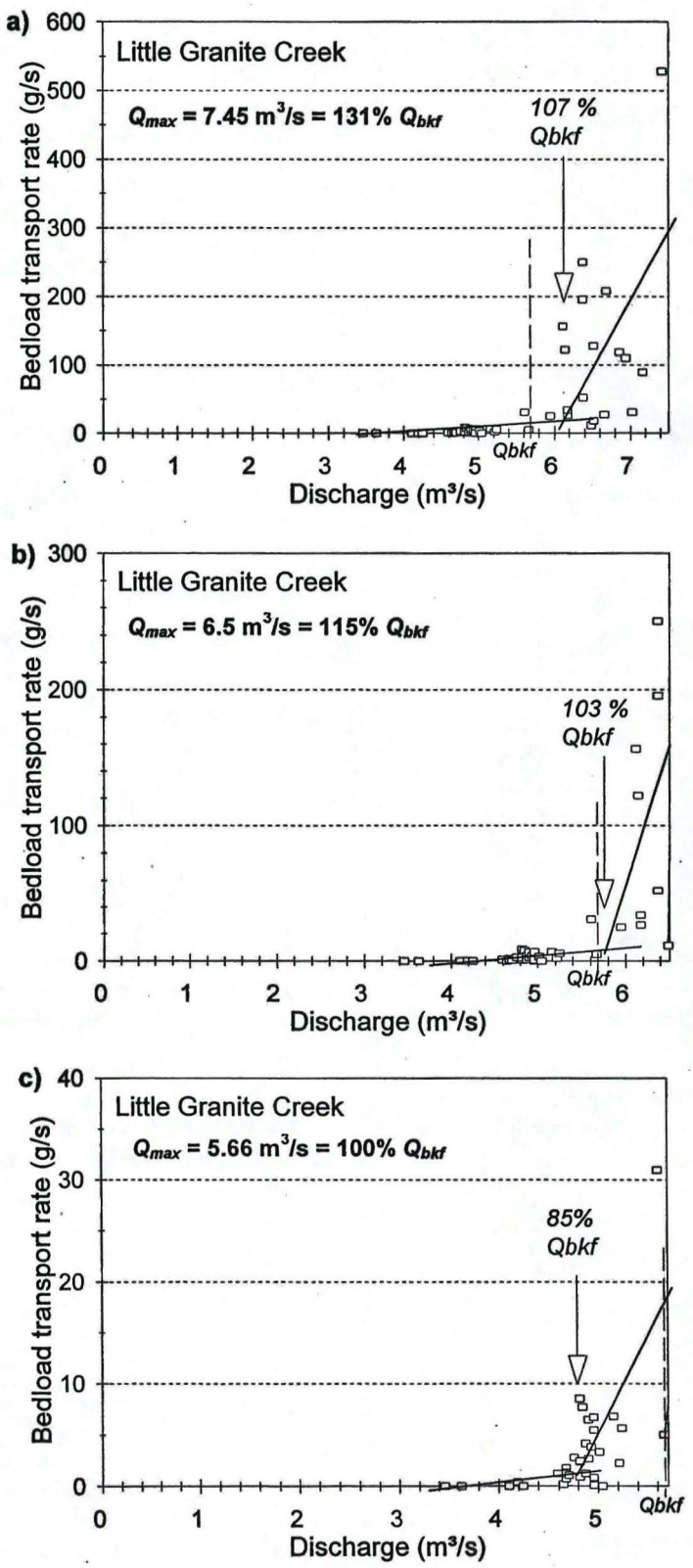

Figure 11: Visually estimated breakpoint flows from bedload trap samples collected at Little Granite Creek, 1999 for: a) All data measured up to 131% Q_{bkf}; b) Data truncated at 115% Q_{bkf}; c) Data truncated at 100% Q_{bkf}.

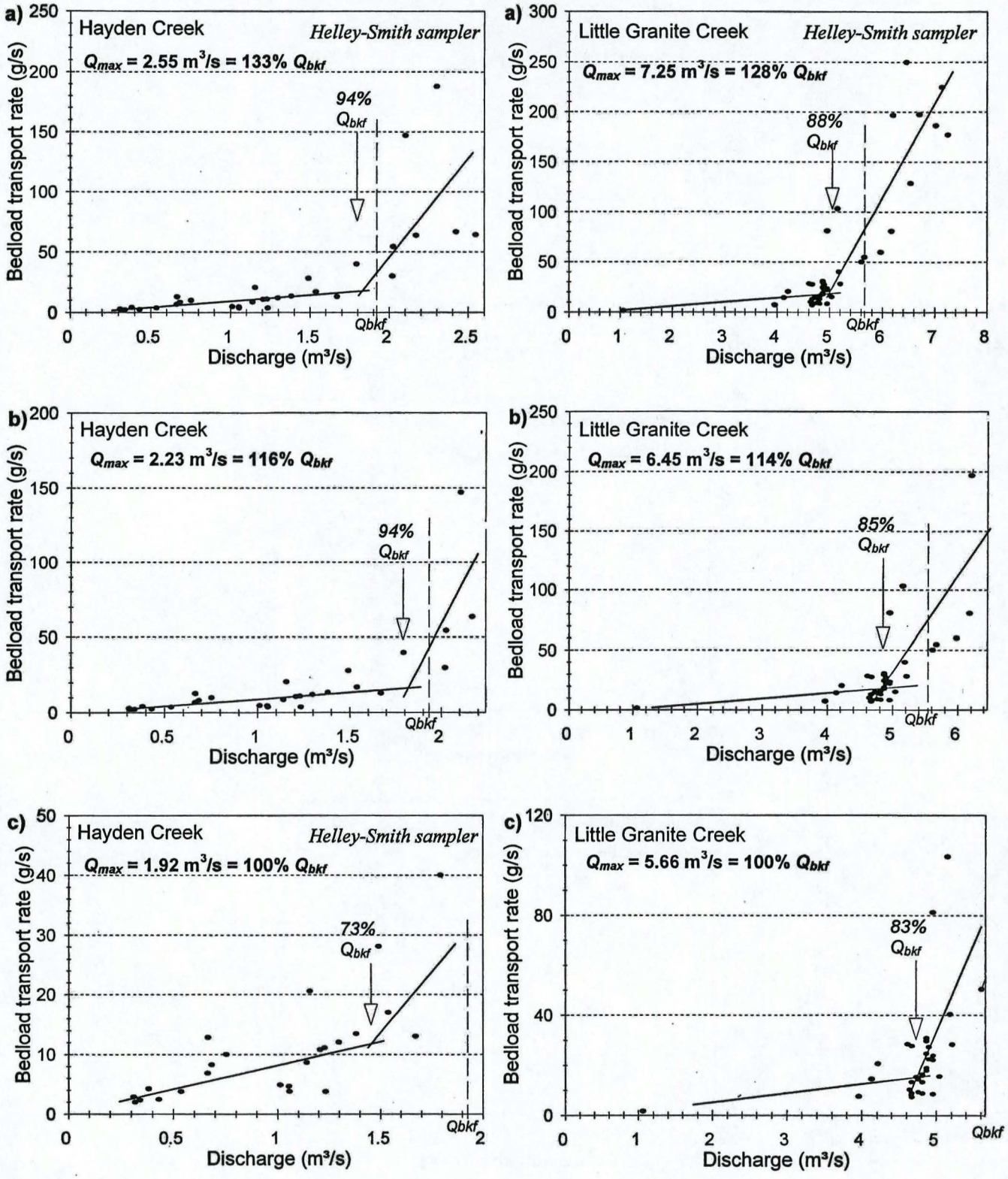

Figure 12: Visually estimated breakpoint flows from Helley-Smith samples collected at Hayden Creek, 2005 (left column) and Little Granite Creek, 1999 (right column) for: a) All data measured; b) Data truncated at the midpoint between Q_{max} and Q_{bkf}; c) Data truncated at 100% Q_{bkf}.

Table 12: Visually estimated breakpoint flows for different ranges of analyzed flows (Q_{max}) and transport rates ($Q_{B\,max}$) for bedload trap and Helley-Smith data collected in two of the study streams.

Stream	$Q_{B\,max}$ (g/s)	Q_{max}		Number of truncated data points	Breakpoint flow (visual estimate)			
		(m^3/s)	(% Q_{bkf})		(m^3/s)	(% Q_{bkf})	(% Q_{max})	Avg. % Q_{max}
Bedload traps:								
Hayden Creek, 2005	170	3.0	156	0	2.2	115	73	79
	135	2.64	138	9	2.2	115	83	
	40	2.28	119	23	1.95	102	86	
	5	1.92	100	31	1.4	73	73	
Little Granite Creek, 1999	525	7.4	131	0	6.05	107	82	85
	250	6.5	115	9	5.8	102	89	
	8.6	5.66	100	9	4.8	85	85	
Helley-Smith sampler:								
Hayden Creek, 2005	190	2.55	133	0	1.8	94	71	75
	150	2.23	116	6	1.8	94	81	
	55	1.92	100	3	1.4	73	73	
Little Granite Creek, 1999	250	7.25	128	0	5	88	69	75
	200	6.45	114	4	4.8	85	74	
	105	5.66	100	3	4.7	83	83	

The truncation results clearly show that computed breakpoint flows decrease when the range of measured flows and transport rates (or those included in the analyses) is decreased. This suggests that breakpoint flows do not occur at a fixed percentage of bankfull flow, but rather at a fixed percentage of the highest flow measured. For the two streams used for these analyses, breakpoints occurred on average at 79 and 85% Q_{max} for bedload trap samples and at 75% Q_{bkf} for Helley-Smith samples (Table 12). These values are similar to those obtained from the analysis in which a power function fitted to measured data was plotted for progressively larger ranges of flow and transport rates (Figure 8).

Effects of scale dependency

Results from these analyses not only suggest that breakpoint flows increase with the range of measured flows, but also that this increase follows a logarithmic relationship for both streams (Figure 13) and both samplers. For bedload trap samples, increasing the measured range of flows from 100% to 120% Q_{bkf} increases the breakpoint flow by 20-30% Q_{bkf}, whereas further increases in flow cause less drastic changes in the breakpoint flow. For Helley-Smith samples, the effect of the sampled data range on breakpoint flows is less pronounced (Figure 13) and may become quite small for flows exceeding 120% Q_{bkf}. Data sets from more streams would have to be analyzed to see whether the trend suggested by data from Little Granite and Hayden Creek holds for other streams as well. However, knowing the effect of the measured data range on breakpoint flows

would be very useful because it could be used to eliminate the effects of scale dependency on breakpoint flows.

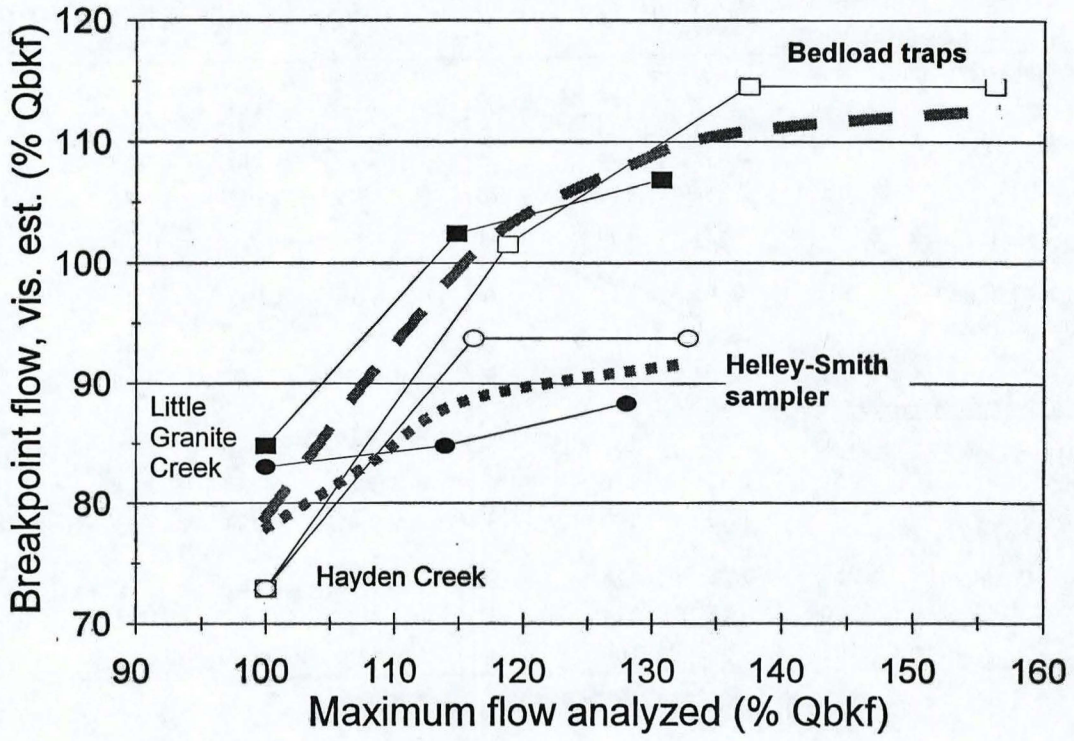

Figure 13: Increase in breakpoint flows with analyzed range of flow for samples from Little Granite (black symbols) and Hayden Creek (white symbols) collected with a Helley-Smith sampler (circles) as well as bedload traps (squares). Also shown are suggested hand-fitted logarithmic functions (gray dotted line for Helley-Smith sampler and dashed line for bedload traps).

Implications for sampling requirements

Scale dependency, i.e., the finding that breakpoint flows become larger when higher flows and transport rates are included in the analyses, has implications on the sampling requirements for breakpoint analyses. It means that if breakpoint flows are to be compared among streams, all streams need to be sampled to about the same percentage of bankfull flow. Based on results from Figure 13, this flow should be approximately 115 to 120% Q_{bkf} for Helley-Smith samplers and 120 or 130% Q_{bkf} for bedload traps. Below those values, breakpoint flows are highly, and above those flows less affected by the range of measured flows.

Appearance of breakpoint flows in log-log plots

Previous sections of this study suggested that breakpoints are visually detectable as notable increases in transport rates only in a linear plotting scale. To see if breakpoint flows would be recognizable in logarithmically plotted data, breakpoints flows computed

from various analyses are marked with arrows in a logarithmically scaled plot of bedload transport rates from bedload trap samples at Little Granite and Hayden Creek (Figure 14 a and b). Neither the breakpoint flow determined from the piecewise regression analysis in SAS at 2.15 m^3/s (black arrow), nor the visually estimated breakpoint flows identified for the entire as well as the successively truncated data (2.2, 1.95 and 1.4 m^3/s; see Table 12 and Figure 10 a-d) (white arrows) stand out as significant increases in transport rates. This suggests that breakpoint flows are not notable as significant increases in transport rates in logarithmically scaled plots of bedload transport rates versus flow.

3.2.4.4 Differences in breakpoints between streams

Breakpoint flows obtained from various methods are listed for the three streams in Table 8 and graphically presented in Figure 7. Halfmoon Creek clearly has the lowest breakpoint flows among the three streams for all analyses, including the Helley-Smith data analyzed by Ryan et al. 2005 (39 - 64 % Q_{bkf}). This consistency suggests that a particular bedload transport process is predominant at Halfmoon Creek but less so at the other streams. A possibility is the relatively high availability and entrainment of fine gravel at relatively low flows at Halfmoon Creek. Breakpoint flows computed for Hayden and Little Granite Creek are generally higher (73 – 115% and 81 – 107% Q_{bkf}), but the mean breakpoint flow averaged over all procedures, samplers and data sets is 93.3 and 93.5% Q_{bkf} for the two streams.

3.2.4.5 Predictability of breakpoint flows

Combining the observation that breakpoint flows increase with the rating curve steepness (Section 3.2.4.2) and the finding that the rating curve steepness is negatively related to the degree of bed armoring (Bunte et al. 2006b), it is likely that breakpoint flows are predictable from the degree of bed armoring as well.

The hypothesis seems to hold for the three study streams, of which Little Granite and Hayden Creek are much less armored ($D_{50\ surf}/D_{50\ sub}$ = 1.31 and 1.26, respectively) than Halfmoon Creek ($D_{50\ surf}/D_{50\ sub}$ = 1.69), while breakpoint flows are smallest for Halfmoon and much larger for Little Granite and Hayden Creek. The high degree of armoring for Halfmoon Creek is attributable to a high percentage of subsurface fines that is produced by the weathering of granite. It is thus possible that breakpoint flows set in at relatively low flows when easily entrainable fine gravel is available. The notion that sediment supply might have an effect on breakpoint flows is supported by data from Ryan et al. (2005) that show a decreasing trend between breakpoint flows and the bankfull bedload transport rate, meaning that streams with high bankfull transport rates are likely to have lower breakpoint flows (Figure 15), although the trend (r^2 = 0.24) is relatively week.

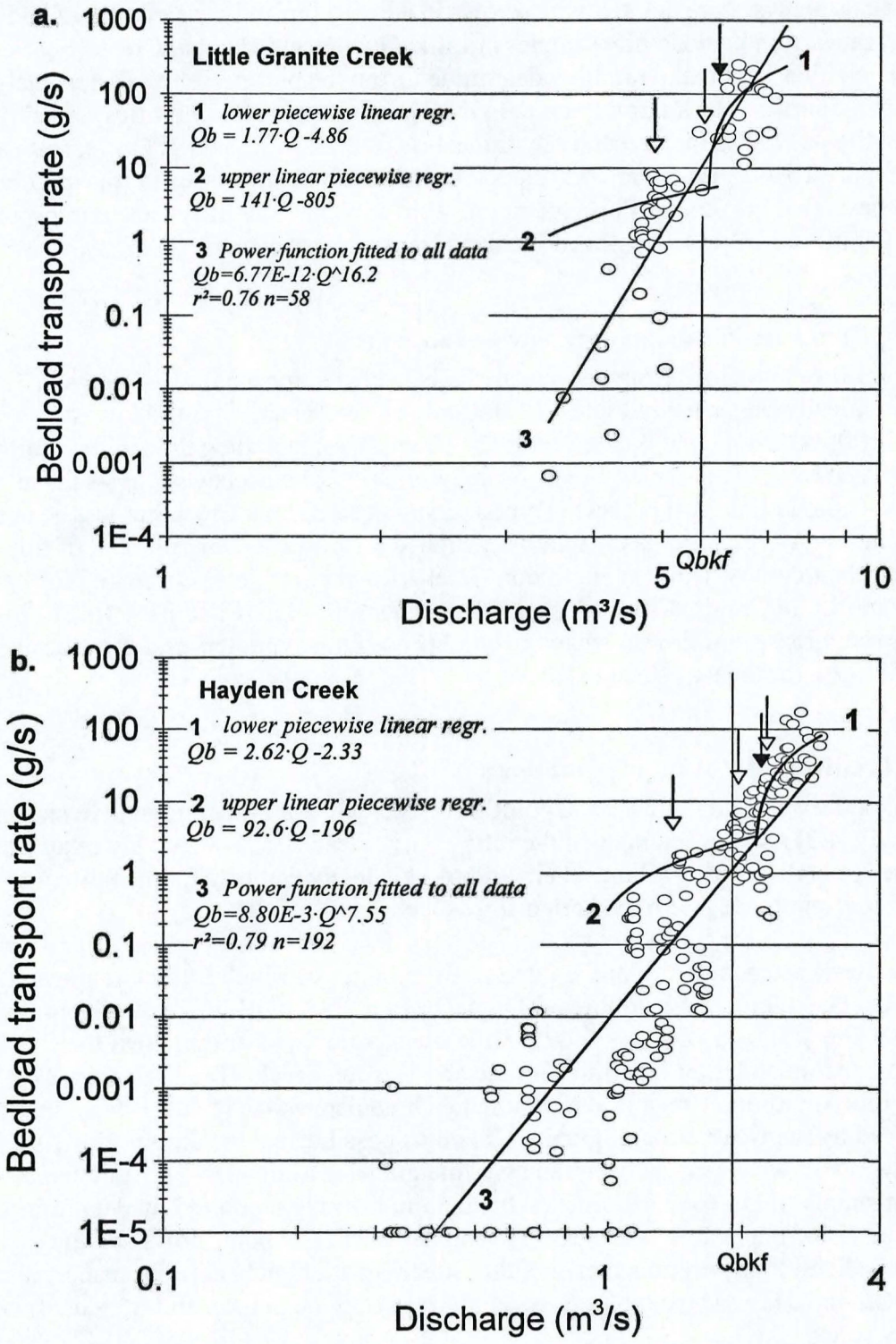

Figure 14: Log-log plot of the bedload transport data collected with bedload traps at (a) Little Granite and (b) Hayden Creek showing the upper and lower segments of the piecewise regression function as well as a power function ($Q_B = aQ^b$) fitted to the entire data set. Black arrows indicate breakpoint flows from the piecewise regression (SAS) procedure. White arrows indicate breakpoint flows from visual estimates of data truncated at various flows. Due to strong clockwise hysteresis and the wide range of transport rates at lower flows, the power function fitted to the entire Hayden Creek data does not describe the data very well. Stratifying the data into rising and falling limb would have obtained better fits.

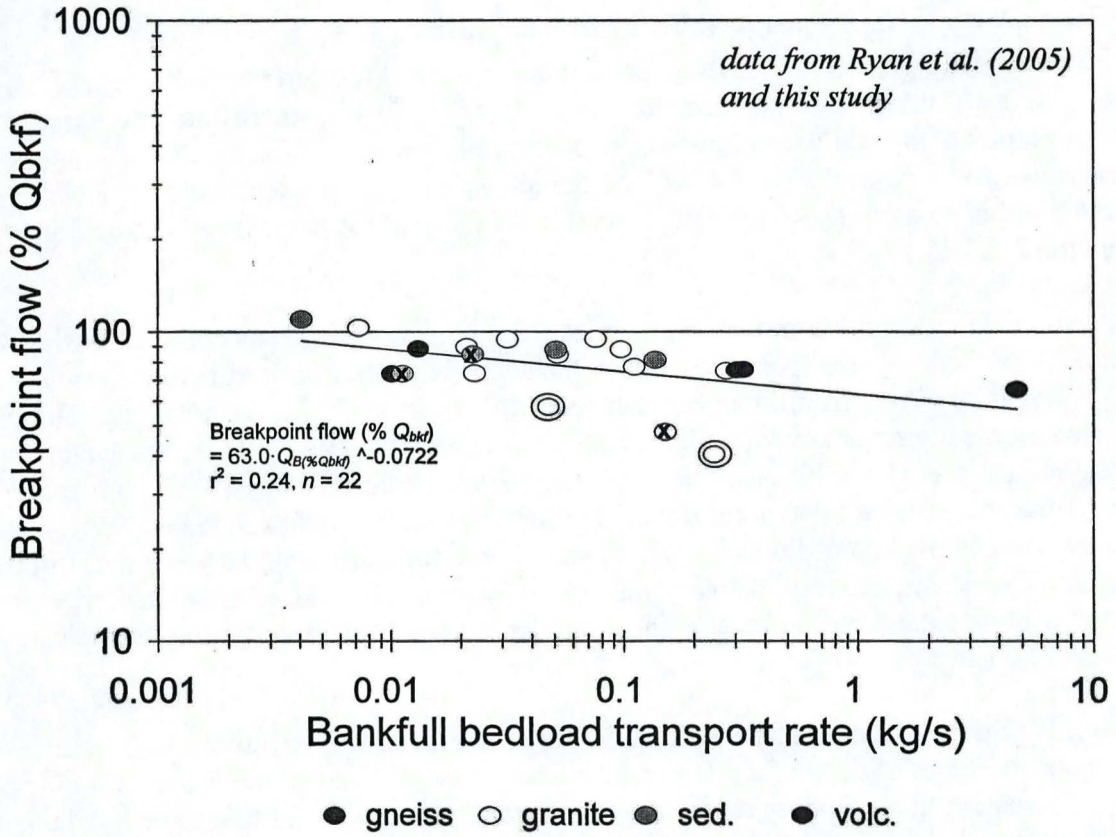

Figure 15: Breakpoint flows computed for Helley-Smith samples from the piecewise regression procedure by Ryan et al. (2005) and this study (data points marked **x**) show a decreasing trend with the bankfull transport rate. Data points circled with a stippled line indicate that the piecewise regression either did not yield a breakpoint or that it deviated considerably from the visual estimate.

The variability of breakpoint flows in the 19 streams by Ryan et al. (2005) could not be explained by variations in channel parameters (e.g., stream gradient, drainage area, bedmaterial sorting, surface D_{50}, the ratios of D_{50}/stream width and D_{84}/bankfull flow depth), or by streams types (such as step-pool, plane-bed or pool-riffle) (Ryan et al. 2002, 2005). However, the correlation coefficient r^2 in Figure 15 can be improved slightly (from 0.24 to 0.27) when the bankfull transport rate is divided by the ratio D_{84}/D_{16} (an indication of bedmaterial sorting) and by stream gradient.

These results suggest that breakpoint flows are related to bedload availability, bedmaterial characteristics, and stream gradient to some degree. However, more streams need to be analyzed to tease out predictive parameters for breakpoint flows.

3.2.4.6 Particle sizes transportable by breakpoint flows

The study by Ryan et al. (2005) suggested that particles of the surface bedmaterial D_{16} - D_{25} size are transported at the onset of Phase 2 transport[18]. It is interesting to compare those results with results from this study. Measured flow competence curves, i.e., relationships between the largest bedload particle size (D_{max}) and discharge for Helley-Smith and bedload traps samples are available for the study streams (see Figure 33 in Section 3.5.3.1).

Based on Helley-Smith samples and the piecewise regression analysis computed using the SAS procedure, breakpoint flows have the competence to transport bedload sizes of 23, 19, and 20 mm at Halfmoon, Hayden, and Little Granite Creek, respectively. Theses bedload sizes are remarkably similar for the three streams. Bedload traps, that have breakpoint flows about 20% higher than Helley-Smith samples, consequently transport larger particle sizes at breakpoint flows. For the three study streams, bedload D_{max} sizes transported at breakpoint flows are 27, 38 and 52 mm for Halfmoon, Hayden, and Little Granite Creek, respectively, with a mean size of 39 mm. These sizes are about twice as large as those transported at breakpoint flows determined from Helley-Smith samples (mean of 21 mm).

In terms of the bedmaterial size, breakpoint flows computed from Helley-Smith samples transport particles of the surface D_{25} and the subsurface D_{40} size which is similar or slightly coarser than the sizes reported by Ryan et al. (2005). According to bedload trap samples, breakpoint flows transport the surface D_{40} and the subsurface D_{50} sizes (Table 13).

Table 13: Particle sizes transportable by breakpoint flows for bedload trap and Helley-Smith samples.

Stream	Helley-Smith				Bedload traps			
	Breakpoint flow (% Q_{bkf})	Transportable particle size			Breakpoint flow (% Q_{bkf})	Transportable particle size		
		mm	Surface Percentile	Subarmor percentile		mm	Surface Percentile	Subarmor percentile
Little Granite	85	20	D_{25}	D_{31}	102	52	D_{47}	D_{52}
Halfmoon	48	23	D_{25}	D_{49}	64	27	D_{30}	D_{53}
Hayden	73	19	D_{26}	D_{35}	112	38	D_{42}	D_{50}
Average		21	D_{25}	D_{38}		39	D_{40}	D_{52}

3.2.5 Summary and conclusion

Breakpoint flows were computed for bedload samples collected with a Helley-Smith sampler and bedload traps in the three study streams, using the SAS routine for piecewise

[18] *The breakpoint grain size to which Ryan et al. (2005) refer is the smallest particle size that exceeds the largest sizes found in bedload samples below the breakpoint flow.*

regression as well as visual estimates. The SAS procedure eliminates operator variability and provides statistical information on error ranges, but requires access to and familiarity with the SAS software. Without at least some proficiency in SAS, the procedure is cumbersome. Visual estimates of breakpoint flows were introduced in this study as a more convenient and faster alternative. The main findings of this study are summarized below.

Variability of breakpoint flows between streams and between studies
Breakpoint flows computed with the SAS routine for Helley-Smith samples collected the three study streams were 85, 48, 73% Q_{bkf} for Little, Granite, Halfmoon, and Hayden Creek, respectively. These results are generally within the range of breakpoint flows computed independently for the same streams in a study by Ryan et al. (2005), but for a given stream, breakpoint flows may deviate by as much as 20% between studies due to interannual variability of the Q_B *vs.* Q relationship as well as differences in sample size, range of measured flows, and perhaps the sampling scheme. Halfmoon Creek has an uncommonly low breakpoint flow in both studies, suggesting that the high availability of fine gravel (granite grus) causes ample particle entrainment at relatively low flows and thus a low breakpoint flow.

Breakpoint flows mostly similar between SAS procedure and visual estimates
Breakpoint flows obtained from the SAS procedure and visual estimates generally match each other within a few percent, and their ratio is unbiased. However, in about one third of the cases, visual estimates can deviate by as much ±30% from the SAS result.

Differences between samplers— dependency on rating curve exponent
Based on results from the SAS procedure, breakpoint flows obtained from bedload trap samples are on average 136% of the breakpoint flows obtained from Helley-Smith samples. When the comparison was based in visual estimates, the difference decreased to 122%. Thus, this study suggests that bedload traps produce breakpoint flows about 20-30% higher than those from Helley-Smith samples.

The difference in breakpoint flows between the two samplers is mainly attributable to the difference in the steepness of the Q_B *vs.* Q relationships measured with the two samplers. This effect was shown using power functions fitted to the Q_B *vs.* Q relationships measured at eight mountain gravel-bed streams. When measured with a Helley-Smith sampler, the Q_B *vs.* Q relationships typically have exponents of 2 to 4, while bedload traps yield Q_B *vs.* Q relationships with exponents of 7 to 16. Breakpoint flows were visually estimated for those bedload transport power functions plotted in a linear scale. For the relatively flat Helley-Smith Q_B *vs.* Q relationships, breakpoint flows typically occurred around 70% Q_{bkf}, whereas for the relatively steep Q_B *vs.* Q relationships for bedload traps, breakpoint flows typically occurred around 85% Q_{bkf}. Based on the data from eight study streams, breakpoint flows for bedload trap samples occur at flows 20% higher than those for Helley-Smith samples. Breakpoint flows are therefore greatly

affected by the sampler used. Bedload samplers with large openings and long sampling times tend to produce steeper rating curves and thus higher breakpoint flows than samplers with small openings and short sampling times that are repeatedly placed onto a bed.

Effects of measured range of flow and scale dependency

Two separate analyses in this study showed that breakpoint flows are scale dependent and vary with the range of data included in the computation. One analysis used a power function plotted in linear scales over 100, 150, and 200% of bankfull flow. The other analysis was a stepwise truncation of data sets from the highest measure flow (Q_{max}) to bankfull flow. Both analyses showed that as higher flows and transport rates were included (or excluded) in the analyses, breakpoint flows increased (decreased) with respect to the percentage of bankfull flow, but remained constant in terms of Q_{max}, at about 75% Q_{max} for Helley-Smith samples and at 79-85% Q_{max} for bedload trap samples. The reason for an increase in absolute breakpoint flows with increasing Q_{max} is the self-similarity of power function relationships that are plotted in linear scale over different data ranges.

Results from the stepwise truncation of data sets suggested that the relationship between breakpoint flows and the largest analyzed flow is logarithmic, indicating that breakpoint flows increase more when the range of measured flows is increased from 100 to 120% Q_{bkf} than from 120 to 140% Q_{bkf}. There are again sampler-specific differences. For Helley-Smith samples, breakpoint flows increase by 10-15% when the range of measured flows is extended from 100 to 120% Q_{bkf}. For bedload trap samples, the effect of the measured range of flow is much larger, and an extension of measured flows from 100 to 120% Q_{bkf} increases breakpoint flows by 20-30%. Extending the sampled range from 120 to 140% Q_{bkf} elevated breakpoint flows negligibly for Helley-Smith samples and by about 5-10% for bedload traps. Based on results from this study, samples for breakpoint analyses should be collected to at least 120% Q_{bkf}.

Breakpoint flows can only be seen when a linear scale used for plotting and analyses.

Breakpoints are visibly and statistically discernible only when the Q_B *vs.* Q relationship is plotted and analyzed in a linear scale. The same Q_B *vs.* Q relationship plotted in a log-log scale forms a straight line power function. Breakpoint flows are not recognizable in data plotted in a logarithmic scale.

Linear analysis is problematic for data ranges that span several orders of magnitude

The range of measured bedload transport rates (Q_B) over a highflow season spans 2 to 3 orders of magnitude when collected with a Helley-Smith sampler and 5 to 6 orders of magnitude when samples are collected with bedload traps. When the relationship between Q_B and Q is plotted in linear scale with the highest flows and transport rates in the upper right hand corner of the plot, data points of transport rates smaller than 5 or 10% of $Q_{B\,max}$ are bunched together hugging the x-axis, and individual data points

become visually indistinguishable. A linear plotting scale for the Q_B *vs.* Q relationship may not cause problems for Helley-Smith samples that typically span only 2-3 orders of magnitude over a highflow season. In this case, the data up to 5 or 10% Q_{Bmax} that plot along the x-axis span only 1-2 orders of magnitude, and most of the data points are still visible and thus assessable for visual analysis.

However, for bedload trap samples, transport rates below 10% of $Q_{B\,max}$ span 4 to 5 orders of magnitude, while the range between 10 and 100% $Q_{B\,max}$ spans only one order of magnitude. If data are sampled evenly over the entire range of flow, only the highest 20% of transport rates are visible and distinguishable in a linear plotting scale, while individual data points are indistinguishable within lowest 80% of the data and are subsequently poorly represented in analyses of the entire data set. It seems that a process that spans several orders of magnitude in its independent value should be graphically displayed and analyzed over its entire range.

Knick points are a general feature of power functions plotted in linear scale

Any power function—regardless of the described process—that has an exponent larger 2 appears to have a knick point or breakpoint close to the point of maximum curvature when plotted in a linear scale. If knick points are a general feature of power functions plotted in linear scale, then there is no necessity that breakpoint flows are caused by a prominent increase in transport rates.

Elimination of effects of scale dependency: Mandatory data and adjustment function

The measured range of flow greatly affects computed breakpoint flows. In order to eliminate much of the scale effects in breakpoint flows, a computation procedure needs to specify a mandatory data range (and sample size) for the analyses. Based on the limited data sets analyzed in this study, it appears that the range of measured flows should extend to at least 120% of bankfull flow. To adjust for differences in measured ranges in a finer scale, a relationship could be built between breakpoint flows and Q_{max} from a variety of different streams.

Predictability of breakpoint flows

The variability of breakpoint flows can be attributed to differences in the steepness of the transport-discharge relationship among streams, and the bankfull bedload transport rate, although currently, the trends are not well enough defined to allow a prediction. Given that breakpoint flows were found to increase with rating curve steepness, and that rating curve steepness was found to decrease with the degree of bed armoring (Bunte et al. 2006b), it is likely that the measured degree of bed armoring could be used to estimate breakpoint flows. Using data from the study by Ryan et al. (2005) showed a trend for breakpoint flows to decrease with decreasing bankfull bedload transport rates, suggesting that streams with high bed mobility have lower breakpoint flows.

Largest particle sizes transportable by breakpoint flows

The largest particles transported by breakpoint flows computed for Helley-Smith samples inn this study range between 19 and 23 mm. These sizes correspond on average to the surface D_{25} and the subarmor D_{38} sediment size. By comparison, the largest bedload particle sizes transportable by breakpoint flows computed with the SAS procedure for bedload trap samples is twice as large and range between 38 and 52 mm. On average, these sizes correspond to the surface D_{40} and the subarmor D_{50} size. The range of D_{max} particle sizes transportable at breakpoint flows is quite narrow for Helley-Smith samples. This might be accidental or confirm a trend observed by Ryan et al. (2005) who reported that breakpoint flows transport particle sizes in the surface D_{16} to D_{25} range

In summary

Variability of breakpoint flows:

- Among operators: none when using the SAS procedure, some when using visual estimates
- Among streams: two streams had similar breakpoint flows of 81 and 73% Q_{bkf} while one had a breakpoint notably smaller (48% Q_{bkf})
- Between studies: differences by up to 20% due to interannual variability of bedload transport and slight differences in sampling.
- Between methods: visual estimates are mainly within ±5% of SAS procedure, but can differ by up to ±30%.
- Between samplers: Breakpoint flows from bedload trap samples exceed those from Helley-Smith samples by 15 to more than 30% depending on the analysis.
- With the range of measured flow: Two analyses showed that breakpoint flows in terms of Q_{bkf} increase with an increased range of measure flow but in terms of the highest measured flow remain constant at 75 – 85% of Q_{max}. The effects of measured range of flow:
  - Are most pronounced for flows below 120% Q_{bkf} and become less for higher flows. Samples from bedload traps are more affected by scale dependency than Helley-Smith samples.
  - Can be diminished by sampling up to 120% Q_{bkf} and applying an adjustment function.

Breakpoint flows are only visible and determinable in a linear plotting scale. Breakpoint flows are not discernable in log-log plots. Any power function—regardless of the process described—shows a knick point near the point of maximum curvature when plotted in a linear scale. A shift in process that causes a pronounced increase in transport rates does not seem to be necessary to create a knick point or breakpoint.

3.3 Collapse-size analyses

3.3.1 Introduction

It is commonly accepted that the surface of a streambed adjusts to the relationship between sediment supply and transport capacity of the stream. A decrease in transportable sediment supply leads to a coarsening of the surface sediment and thus to a stronger degree of armoring ($D_{50\ surf}/D_{50sub}$). Conversely, an increase in the supply of transportable sediment leads to a decrease in armoring and a higher similarity between surface and subsurface sediment to the extent that streams with no limitation of sediment supply develop little if any armoring (Dietrich et al. 1989). Whiting and King (2003) refined this concept. Based on the idea that a limitation of sediment supply may not extend over all particle sizes on the bed, Whiting and King (2003) attempt to differentiate between particle sizes that are supply-limited and those that are not. They postulate that fine gravel particles supplied to the stream in quantities less than the transport capacity are winnowed from the bed surface which causes a deficiency of fines on the surface sediment compared to the subsurface. The transport of fine gravel occurs in accordance to its supply on the bed and is thus supply-limited, meaning that increasing flows do not substantially increase the transport rate of this size class. By contrast, particle sizes for which the supply is larger than the transport capacity of the current flow regime are abundant on the bed, and their transport rate increases as a direct function of increasing flow. These particle sizes are transport-limited. If supply-limited finer gravel is added to a stream, the bed will not show a fining response until the supply meets the transport capacity. However, an increase in the supply of coarser particle sizes that are transport-limited could cause bed coarsening and aggradation.

Whiting and King (2003) propose a methodology called collapse-size analysis that allows a user to determine the threshold size between supply-limited finer gravel and transport-limited larger gravel via a comparison of the surface and the subarmor particle-size distributions. Once this threshold size is known, a measured flow competence curve ($D_{max,\ QB} = f(Q_{bkf})$ can be used to determine the percentage of bankfull flow needed to move this threshold size. Flows capable of moving transport-limited large gravels are needed to prevent aggradation, particularly if large gravels were added to a stream. Making such flows available is also necessary to counteract aggradation of coarse particles that might occur if flow diversions limit highflows. Whiting and King's (2003) collapse-size analysis that determines the threshold size between supply-limited and transport-limited particle sizes might thus be useable as a channel maintenance tool, with the additional assumption that flows needed to move the threshold size are necessary for channel maintenance.

Whiting and King (2003) computed collapse sizes for 12 streams in central Idaho and found that the smallest transport-limited particle sizes (as indicated from the collapse sizes) ranged between 32 and 108 mm. On average, these particle sizes were transported at flows 88% (53-115) of bankfull flow. The study presented here computes the collapse sizes for three coarse gravel-bed mountain streams and evaluates how the percentages of

bankfull flow required for transport of the smallest transport-limited particles agree with threshold flows identified by other channel maintenance procedures.

3.3.2 Methods

3.3.2.1 Bedmaterial sampling

The methods used for bedmaterial sampling in this study are not identical but similar to those applied by Whiting and King (2003). In order to detect differences in bedmaterial particle-size distributions that would be due to differences in sampling methods, methods used by Whiting and King (2003) and in this study are described and compared.

Idaho study (Whiting and King 2003)

Whiting and King (2003) performed their study in 12 rivers and streams in central Idaho. Basin area sizes range from 99 to 4,947 km^2 and stream gradients from 0.0005 to 0.0268. Eight of the streams have cobble beds, three have coarse gravel beds and one stream is considerably finer. Ten of the streams have basins with predominantly granitic lithology, the other two sites have metamorphic rocks (King et al. 2004). The study sites are located at USGS or USFS operated gauging stations.

Whiting and King (2003) collected 3-4 subarmor samples per site using a 55-gal drum[19]. The morphological units of the sampling sites were not specified. After removing a layer with the thickness of the D_{90} particle size[20], the subarmor layer was sampled to the thickness of two particle diameters (the size of which was not specified). Particle sizes smaller than 64 mm were sieved in 1-phi increments, while the size of larger particles was determined from ruler measurements of the particle *b*-axes[21]. The *b*-axis length of the largest particle in the sample was taken as the sample D_{max} size instead of the sieve-size class as is standard procedure. The size distributions for the Idaho streams are available from the Boise Adjudication Team (BAT) website (with summary information in King et al. (2004)) and were plotted in this study. In order to avoid "kinks" near the D_{max} particle size, the largest 1 or 2 particles were not included in the plot of cumulative particle-size distributions (Figure 16). The similarity of the subarmor sediment samples for the 12 different Idaho streams is remarkable.

The bed surface in the Idaho study was sampled along 4-5 transects using Wolman (1954) pebble counts. Transects were spaced a few m upstream and downstream of the subsurface sampling site and extended across the bankfull channel width. Particles were picked up blindly from approximately equal-spaced intervals along transects. Particle *b*-

---

[19] *According to King et al. (2004), 33-gal drums were used. The commonness of 55-gal drums and the uncommonness of 33-gal drums suggest that mention of 33-gal drums is a typo.*

[20] *King et al. (2004) specify the thickness of the removed layer as similar to the larger particles near the sampling location.*

[21] *This switch in measurement technique causes a "kink" in the upper portion of the cumulative distribution curve which is not visible in the tight x-axis scale used in the plots by Whiting and King (2003), Fig. 2, or in King et al. (2004).*

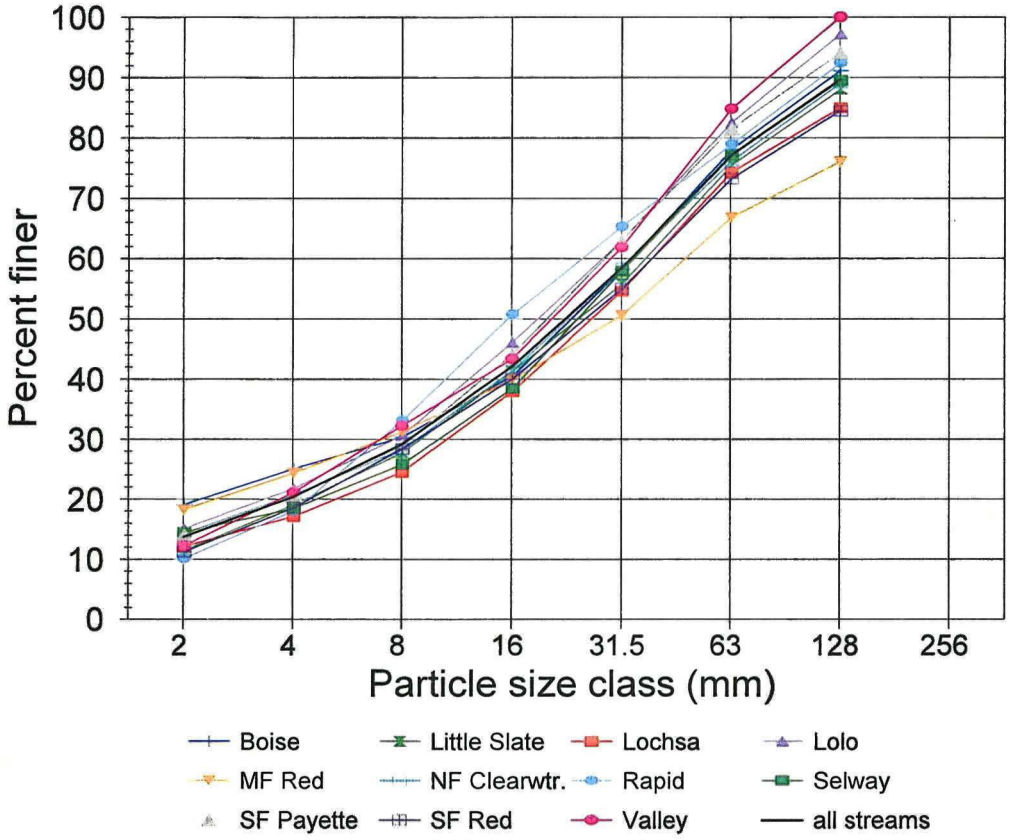

Figure 16: Subarmor particle-size distributions of the streams analyzed by Whiting and King (2003). Data were downloaded from the BAT website. The sandy subsurface sediment of the SF Salmon River (D_{50} and D_{90} sizes of 0.2 and 0.5 mm) is not plotted. Due to the unbinned upper end of the reported distributions, distributions are plotted to the size of the second or third largest particle.

axes were measured to the nearest mm using a ruler. The pebble count data are available from the Boise Adjudication Team web site[22]. The pebble count particle-size distributions are quite different between streams and span a wide range of sizes with D_{50} sizes ranging from 40 to 180 mm (Figure 17). An exception is the SF Salmon River that is considerably finer than the others.

This study

For this study, bedmaterial was sampled in three coarse gravel-bed mountain streams: Little Granite Creek, Halfmoon Creek, and Hayden Creek. Basin area sizes were smaller than for the Idaho streams, while most of the Idaho streams had less steep gradients

[22] *Several pebble count data sets are available from the BAT website for most of the sites. It was unknown which of the data sets had been used by Whiting and King (2003). Due to likely differences in the selection of the data to be plotted, and because the originally untallied data were tallied into 0.5 phi size classes for plotting, D_{50} sizes shown here are not identical to those reported by Whiting and King (2003). Most D_{50} sizes vary by less than ±10% but two vary by ±30%. The surface D_{50} size of 31 mm reported for the SF Salmon River by Whiting and King (2003) should be about 3.1 mm based on data by King et al. (2004).*

(Table 3). Little Granite and Hayden Creek have predominantly sedimentary lithologies, while Halfmoon Creek has mostly granitic rocks. Study site $_{\text{Surface}}$ wide riffles at which bedload traps had been deployed in previous years.

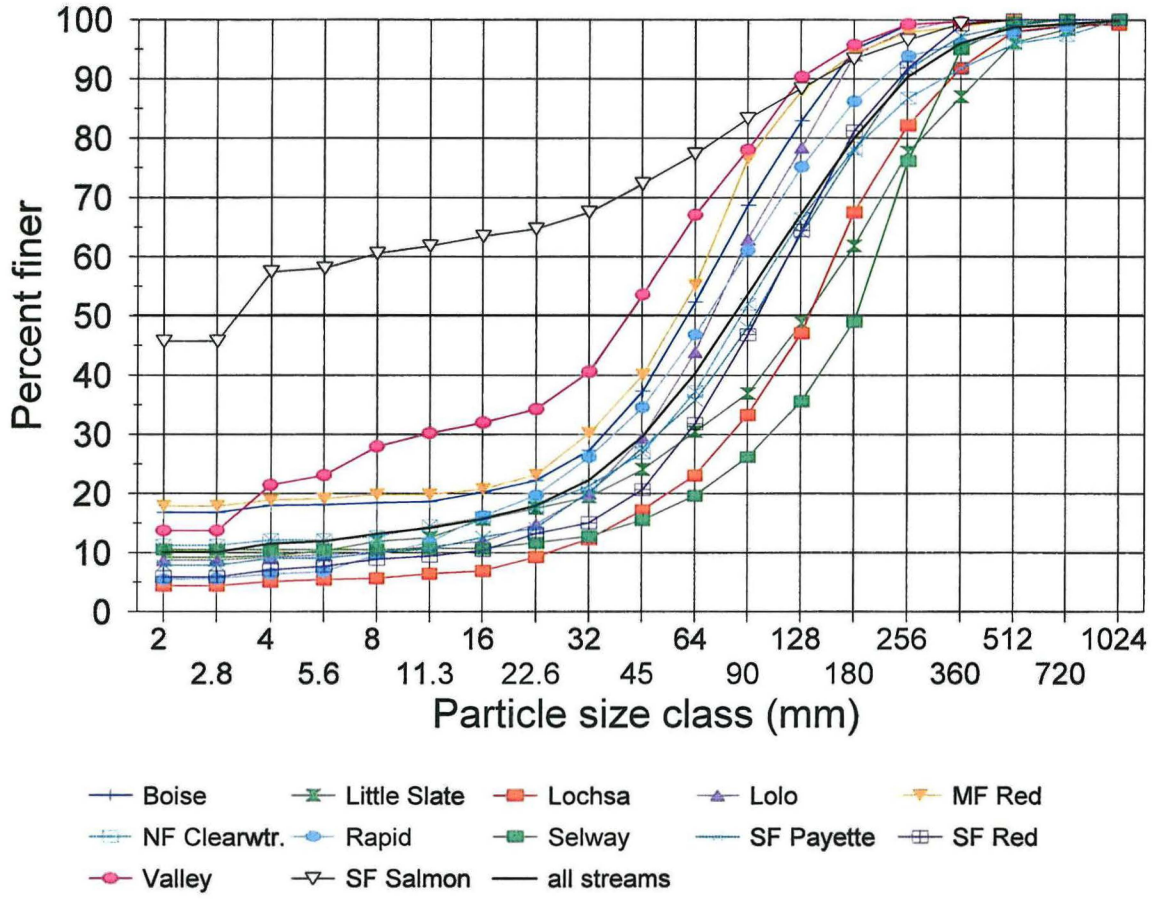

Figure 17: **Surface pebble count particle-size distributions of the streams analyzed by Whiting and King (2003).**

Subarmor samples were collected using a 0.6 by 0.6 m plywood shield (Bunte and Abt 2001a). The enclosed sample area of 0.36 m^2 is larger than the 0.16 m^2 area inside a 55-gal drum. Following Bakke et al. (1999) and McNamara et al. (2000) (see Klamath Falls site calibrated approach in Section 3.4), the armor layer thickness was taken as the depth of the deepest embedded particle and averaged 65, 90 and 75 mm for the three sites (Table 14). The subarmor layer was sampled to a depth of 100 mm in all three streams to ensure a large sample mass. Five samples were collected in the vicinity of the bedload transport measuring cross-section at each site, with the exception of Hayden Creek where only three subarmor samples were collected near the bedload trap cross-section[23]. The

[23] *Another two subarmor samples were collected in a steeper reach a few meters upstream. These samples were similar to those close to the bedload trap cross-section in the gravel portion but contained more cobbles. These two samples were not used to characterize the subarmor sediment near the bedload traps.*

subarmor samples from two of the three sites (Hayden and Little Granite Creek) are notably coarser than those from the Idaho study (Figure 18).

Table 14: Bedmaterial characteristics near bedload and bedmaterial sampling site of the three streams sampled in this study. See Table 2 for reach-averaged values.

Stream	Surface D_{16}, D_{50}, D_{84} (mm)	Subarmor D_{16}, D_{50}, D_{84} (mm)	$D_{50\ surf}$/ $D_{50\ subarm}$	Depth of armor layer removed (mm)	Thickness of subarmor sample (mm)
Hayden	11, 46, 114	3, 36, 114	1.3	70-80	100
Little Granite	20, 53, 124	5, 47, 146	1.1	50-80	100
Halfmoon	14, 49, 115	2, 23, 92	2.1	80-100	100
average	49	35	1.5		

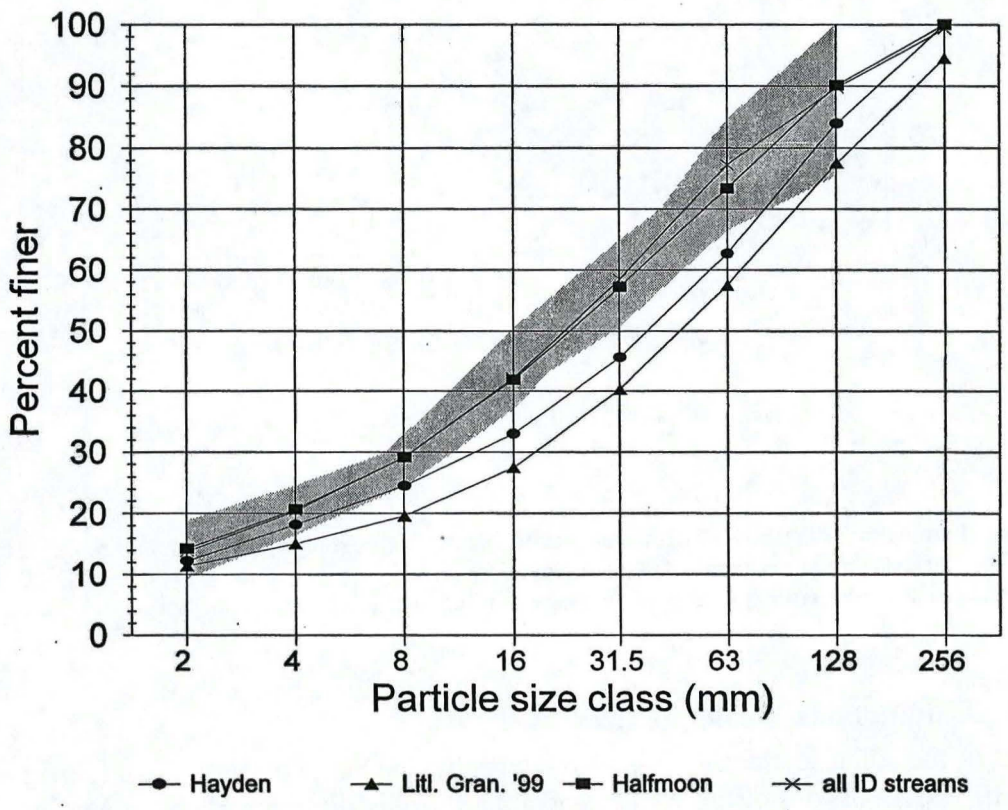

Figure 18: Particle-size distributions of subarmor samples in this study. The mean and range of the Idaho subarmor distributions (except the SF Salmon River) are indicated by the line with cross symbols and the gray-shaded field.

Similar to the Idaho study, pebble counts at the study sites were also collected from 4-6 transects in the vicinity of the subarmor sampling locations, and transects extended over the bankfull channel width. However, particles selected for pick up were identified by

the cross-points of four elastic bands that spanned a 0.3 by 0.3 m grid within a 0.6 by 0.6 m sampling frame (Bunte and Abt 2001a, b), and particle sizes were measured with a square-hole template in 0.5 phi increments. Particle sizes computed from pebble counts in this study are generally finer on the coarse end and coarser on the fine end than those in the Idaho study (Figure 19).

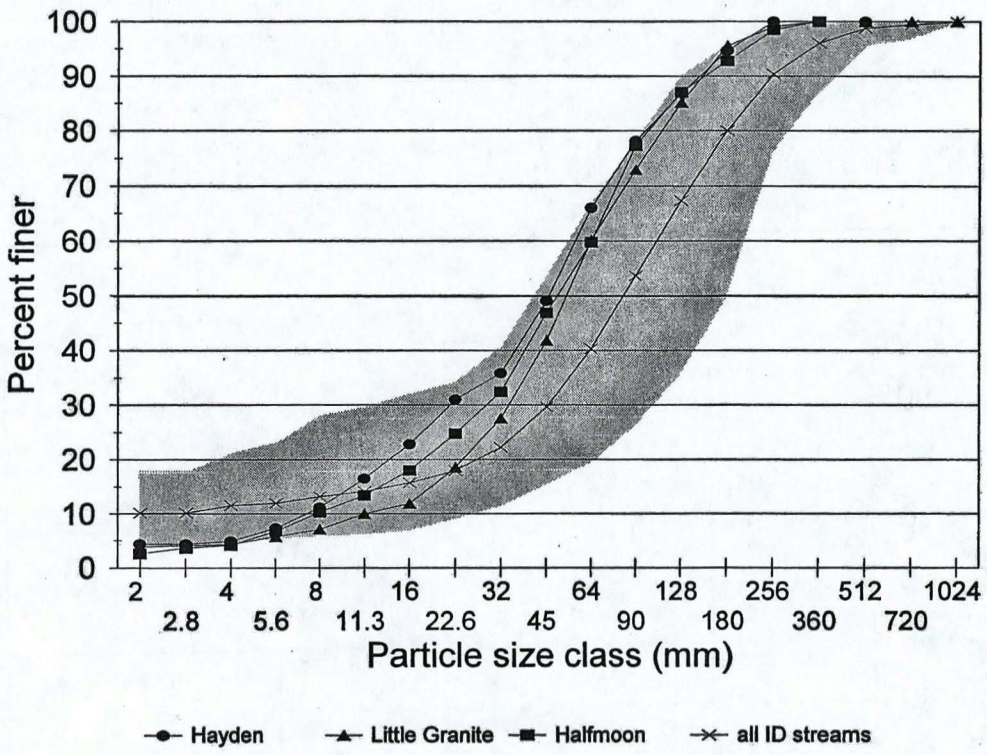

Figure 19: Particle-size distributions of surface pebble counts in this study. The mean and range of the Idaho subarmor distributions are indicated by the line with cross symbols and the gray-shaded field. The sand-bedded SF Salmon River is neither plotted here nor included in the mean distribution.

3.3.2.2 Computations of collapse sizes

The aim of the collapse-size analysis is to determine the range of particle sizes over which the upper portions of the surface and subarmor distributions are most similar. The particle size below which the distributions become markedly dissimilar indicates the threshold between supply-limited and transport-limited sizes.

To compute collapse sizes, the upper ends of the surface and the subarmor cumulative particle-size distributions are truncated at the largest common particle size, while the lower ends are truncated initially at 2 mm, and cumulative particle-size distributions are re-computed. The degree of similarity between the truncated surface and subarmor distributions is determined from what Whiting and King (2003) call normalized residuals and normalized squared residuals (residuals^2). Normalized residuals are calculated from

the difference in the cumulative percent frequency that the surface and the subarmor distributions have for each particle-size class. The differences are computed over all size classes, summed, and divided by the number of size classes used in the comparison. To obtain residuals^2, the differences are squared before summing. The truncation at the lower end of the particle-size distributions then proceeds to the next larger particle-size class, and the residuals are re-computed. The procedure is repeated over all but the largest size class. In a plot of residuals versus the particle size at the lower truncation, residuals tend to increase from negative to positive values and decrease sharply after a maximum. By contrast, residuals^2 first decrease towards a minimum and them display a maximum. The truncation diameter for which residuals are 0 and residuals^2 attain a minimum[24] is the collapse size D_{col}, i.e., the truncated size class for which the pebble count and the subarmor particle-size distributions have the closest similarity. Following this procedure, collapse sizes were computed for the surface and subarmor distributions of the three streams in this study.

3.3.3 Results

3.3.3.1 Different collapse sizes in the two studies

The collapse sizes that Whiting and King (2003) obtained for the 12 Idaho streams range from 32 to 108 mm and correspond, on average, to the D_{36} particle size of the surface and the D_{73} of the subarmor sediment (see Table II in Whiting and King (2003)). The collapse sizes computed for the three study streams are considerably smaller (Figure 20), reaching pea gravel sizes for Little Granite and Hayden Creek that correspond to the D_{15} of the surface and the D_4 of the subarmor sediment (Table 15). At Halfmoon Creek, the collapse size is somewhat closer to the Idaho results (16 mm) and corresponds to the D_{42} and D_{18} of the surface and subarmor layer.

Table 15: Collapse size D_{col} (mm) for three mountain gravel-bed streams in this study and the corresponding % finer of the surface and subarmor distributions.

Stream	At residuals = 0	At residuals^2 = min.	Corresponding % finer of surface size	Corresponding % finer of subarmor size
Hayden Creek	2.8	2.6	4	15
Little Granite Creek	4	3	4	15
Halfmoon Creek	16	16	18	42

[24] *Whiting and King (2003) do not state these requirements. In their example data set, the residuals and the residuals^2 "...drop to small values at 45 mm (the collapse size in their example) and remains small for larger sizes...". This statement is incorrect because only residuals^2 have an initially falling trend while residuals increase from negative to positive values. Unfortunately, Whiting and King (2003) do not explain whether the condition of residuals = 0 identifies the collapse size or whether the relative constancy of successive values in the residuals is the defining condition. Whiting and King (2003) also do not explain whether residuals and residuals^2 necessarily indicate the same collapse size (in which case one of the procedures is redundant) or whether both procedures could indicate different values.*

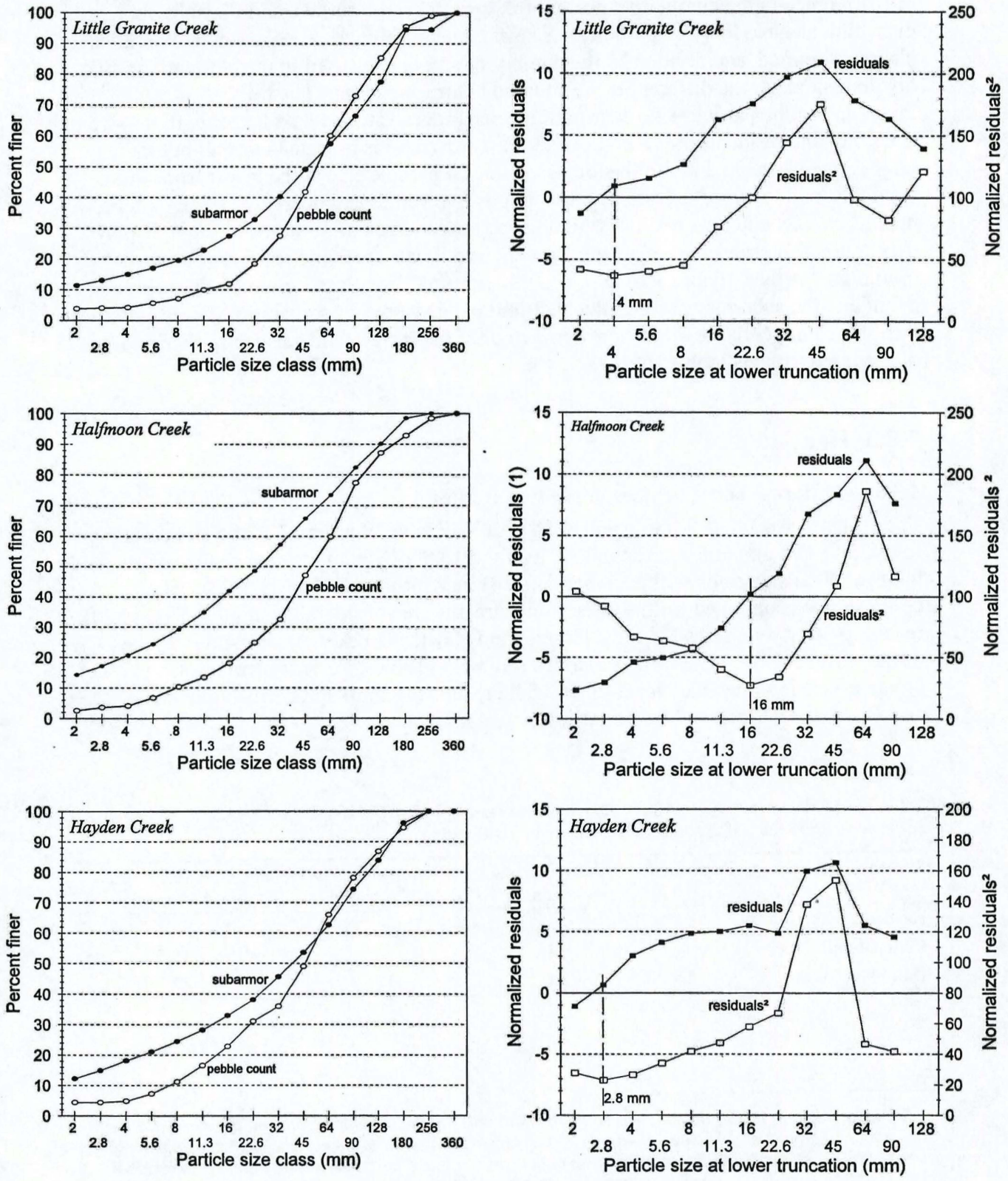

Figure 20: Particle-size distributions of the surface and subarmor sediment for the three streams analyzed in this study (left column of plot) as well as the computed residuals and residuals^2 (right column of plots). The collapse size is indicated by the vertical dashed line in the residual plots.

3.3.3.2 Different surface- and subsurface-size distributions in the two studies

The question arises why the two studies yield such different results. The reason is likely due to differences in the surface and subarmor bedmaterial sizes between the Idaho and this study. Streams in this study have coarse gravel beds with average surface D_{50} and D_{90} particle sizes of 49 and 160 mm, respectively (Figure 19). By contrast, seven of the 12 Idaho streams have cobble beds with D_{50} surface particle sizes of 80-180 mm, and D_{90} sizes of 200-400 mm (Figure 17; Whiting and King 2003, Table I; King et al. 2004). The subarmor sizes of the study streams have average D_{50} and D_{90} particle sizes of 35 and 160 mm (Figure 18), while the Idaho streams have average subarmor D_{50} and D_{90} particle sizes of 21 and 123 mm (Figure 16). Thus, the Idaho streams have coarser surface but finer subarmor sizes than the streams in this study.

The relationships between surface and subarmor size-distributions are consequently different in the two studies as well. In the streams of this study, surface and subarmor distributions are similar in their coarse part (both have D_{90} sizes of about 160 mm), while they differ moderately in their D_{50} sizes (49 *vs.* 35 mm) (Figure 20). The degree of armoring is on average 1.5 and thus relatively low. In the Idaho streams, the surface bedmaterial is much coarser than the subarmor sediment. The surface D_{90} sizes are about twice as coarse (or 1 phi-unit coarser), while the surface D_{50} sizes are about 4 times (or 2 phi units) coarser than the subarmor.

3.3.3.3 Differences between surface and subarmor sizes affect collapse sizes

The magnitude of the difference between the surface and subarmor distributions determines the outcome of the collapse-size analysis. When the upper ends of the cumulative surface and subarmor distributions are far apart, such as in the Idaho study, cumulative distributions that are re-computed after truncation at the lower (fine) end of both data sets continue to run parallel to each other for all truncation sizes. The graphs move closer to each other with increasing truncation diameters until an optimum or no further improvement in the similarity between the two graphs is reached. This typically occurred at some coarse gravel or cobble size (See Fig. 2 in Whiting and King 2003). When the surface and subarmor distributions approach each other steadily with increasing truncation size, differences in the cumulative percent frequencies between the surface and subarmor distributions remain positive, which causes residuals to increase, while residuals^2 decrease. If, by contrast, the upper (coarser) ends of the cumulative surface and subarmor distributions are similar, such as at Little Granite and Hayden Creek in this study (Figure 20), the re-computed cumulative distributions cross each other, and they continue to cross each other for all truncation sizes, as is shown for the example of Hayden Creek in Figure 21. The crossing causes the differences in the cumulative percent frequencies of the surface and subarmor distributions to be positive for some size classes and negative for others. The summed residuals and the residuals^2 then do not steadily increase or decrease, but cross 0 or obtain a minimum at some arbitrary small gravel particle size.

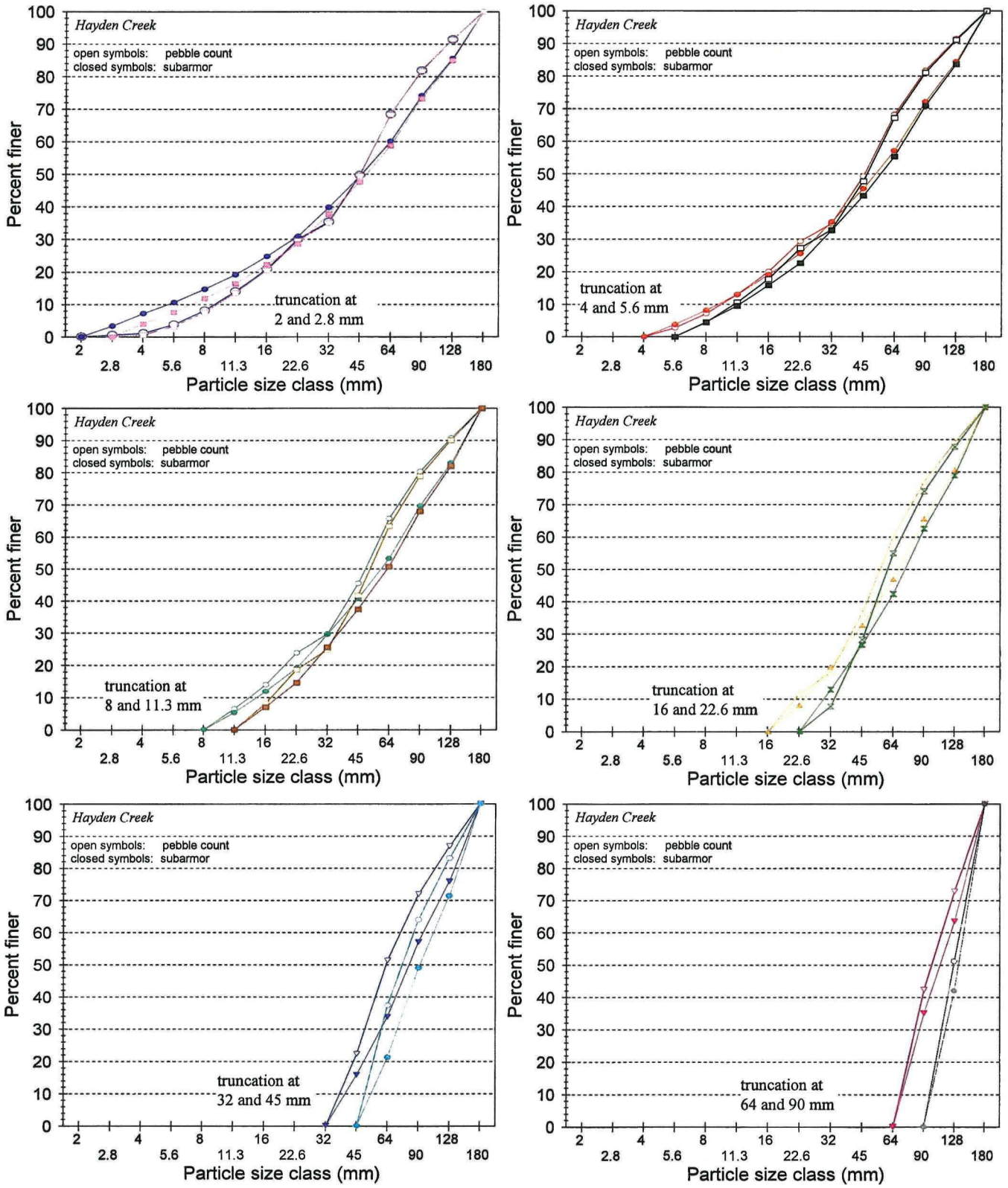

Figure 21: Crossing of surface- and subarmor-size distributions collected at Hayden Creek when truncated at various particle sizes.

Results from this study show that the collapse-size analysis requires a wide gap between the upper (coarse) ends of the surface and subarmor cumulative distributions in order to yield a "reasonable" result, meaning that the threshold between supply- and transport-limited particle sizes occurs somewhere in the coarse gravel or small cobble range as it does for the Idaho streams. If the cumulative distributions of surface and subarmor are similar at their upper ends such as in this study, the collapse-size analysis fails to produce "reasonable" results, and places the threshold between supply- and transport-limited particle sizes into the pea-gravel range.

Visual inspection of the cumulative distribution plots in Figure 20 shows that surface- and subarmor are quite similar to each other in the range between about 64 mm and the D_{max} size. If the crossing of the two distribution curves had not caused a decrease in the degree of similarity, and the two curves had simply approached each other, the collapse size might have occurred in the coarse gravel or small cobble range. Unfortunately, the degree of similarity indicated by the residuals and residuals^2 starts to lose its validity for large particles because only 2-3 size classes remain involved in the collapse-size analysis.

3.3.4 Discussion

It appears that the collapse-size analysis is applicable only if the distribution of the surface size is much coarser than that of the subarmor size. Two factors might cause the wide gap between the two strata. One possibility is that the drainage basin lithology and valley morphology of the Idaho streams, and thus natural conditions, are responsible for the large difference in the bedmaterial sizes between the two studies. The decomposition of granitic rocks in the Idaho streams produces coarse sand and fine-gravelly sediment (grus) that would be expected to accumulate in the subarmor sediment. In contrast to subsurface grus, rockfall from steep hillslopes flanking the banks or downcutting of the channels into glacial deposits provides large cobbles and boulders to the stream bed which act particularly to coarsen the surface size distribution[25]. If thus basin lithology and valley morphology are the main determinants of the streambed substrate, the application of the collapse-size analysis is limited to granitic streams flanked by steep valley walls. Section 3.3.4.1 explores this option.

Another possibility is that methodological differences in sampling and analyzing surface and subsurface sediment in the two studies causes the wide gap between the surface and the subsurface sediment size. To find out if the failure of the collapse size analysis is due to differences in sampling methods between the two studies, effects of the methodological differences can be quantified, and adjustment factors can be applied to the surface and subarmor size-distributions to account for methodological differences This approach is pursued in Section 3.3.4.2. Once collapse sizes computed for the modified data are free of methodological differences (Section 3.3.4.3), they can be compared between studies.

---

[25] *Streams with boulders at the surface (that are included in pebble counts) usually have boulders in the subsurface sediment as well, but boulders are typically not included in a subsurface sample.*

3.3.4.1 Differences due to basin lithology and valley morphology

A large difference in the coarse parts of the surface and subarmor distributions can be due to a relatively fine subarmor distribution. An abundance of grus is produced by weathering granite. All streams in the Idaho study had surprisingly similar subarmor particle-size distributions (Figure 16), suggesting that the subarmor sediment in all streams was affected by weathering granite.

In order to evaluate whether basin lithology significantly affects the subarmor sediment-size, subarmor particle-size distributions available from several streams with granitic and sedimentary lithology and sampled using the plywood shield were compared to the grouped subarmor particle-size distributions for the granitic Idaho streams. Sedimentary streams (Hayden and Little Granite Creek at the '99 and '02 sites) have considerably coarser subarmor-size distributions than those from granitic streams (Halfmoon Creek and SF Cache la Poudre) (Figure 22). An exception is Little Granite Creek at the confluence with Granite Creek. Despite its predominantly sedimentary lithology (and its name), this site has relative fine subarmor sediment possibly due to the proximity to the confluence[26]. Subarmor samples collected in granitic streams using the plywood shield are similar to those collected with the barrel sampler in the granitic streams in Idaho.

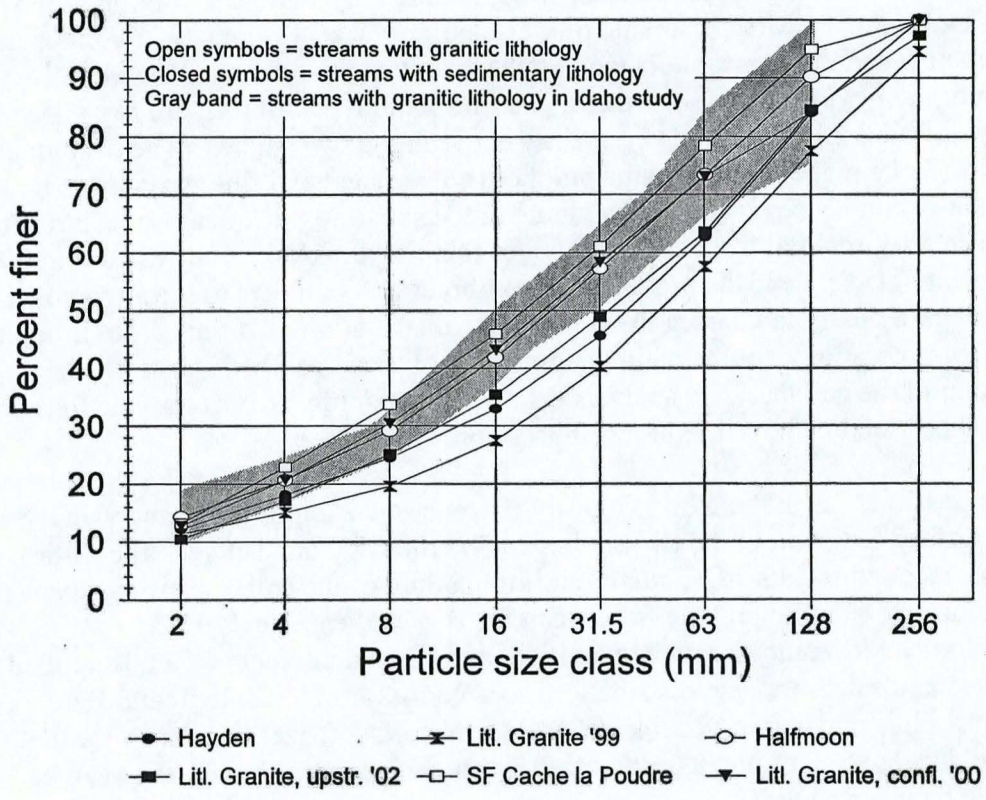

Figure 22: Subarmor size distributions of granitic streams from the Idaho study, as well as streams with granitic and sedimentary lithology sampled using the plywood shield.

---

[26] *Granite Creek has some granitic lithology within its catchment, and Little Granite Creek is incised into a floodplain at the confluence with Granite Creek.*

The mean subarmor distributions for the granitic and the sedimentary streams show that granitic streams have a higher percentage of sand and gravel, while sedimentary streams have a higher percentage of subarmor cobbles (Figure 23a). The average cumulative frequency distribution of the subarmor sediment is considerably coarser in streams with sedimentary lithology than in granitic streams (Figure 23b). The differences in the D_{25}, D_{50}, D_{75} and D_{84} particle sizes amount to about 0.6, 0.75, 0.6 and 0.5 phi units, respectively.

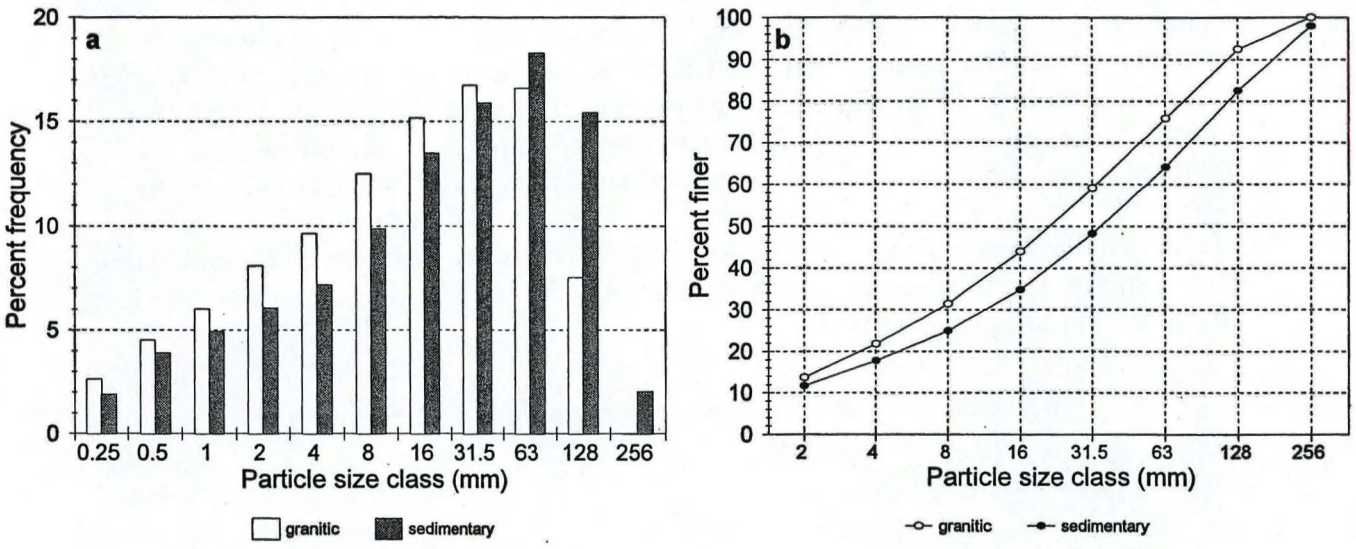

Figure 23: Average percent frequency distribution (a, left) and cumulative particle-size distributions (b, right) of subarmor samples collected in 2 granitic streams and four sedimentary streams using the plywood shield (data from this study and unpublished data by Bunte and Swingle 2000).

Differences in non-transportable large clasts

A large difference in the coarse parts of the surface and subarmor distributions can also be due to an abundance of boulders in the surface distribution which hints at a local input of untransportably large clasts from non-fluvially derived sources, such as rockfall or exhumed boulders. Eight of the Idaho streams are cobble-bed streams with ample boulders in the study reach, four are gravel-bed streams with a few boulders and one is a sand-bedded stream with boulders. Photos and maps of the Idaho study sites (BAT website) confirm that several streams have steep mountain slopes directly adjacent to the stream. By comparison, the streams in this study are gravel-bed streams in which boulders contribute only a few percent to the total distribution. Although truncating the upper end of the surface and subarmor distribution at the largest common particle size eliminates much of the effect of surface boulders on collapse sizes, the average collapse sizes in the Idaho study are nevertheless larger for cobble-bed streams (62 mm) than for gravel-bed streams (45 mm).

3.3.4.2 Differences in methods for bedmaterial collection and analysis

Pebble counts: Heel-to-toe walks versus sampling frame

Differences in pebble count techniques affect the particle-size distribution. Whiting and King (2003) picked up particles blindly from the bed and likely used a heel-to-toe walk to identify the location from which the particles were to be collected. In a comparison of particle-size distributions from heel-to-toe pebble counts in which particles were picked blindly at the tip of the boot with those where the sampling location was determined from the cross points of elastic bands spanned within a sampling frame at Little Granite Creek, Bunte and Abt (2001a, b) found that heel-to-toe walks with blind particle pick-up consistently collected more "handy" mid-sized and coarse gravels but fewer cobbles than using the sampling frame. Similar results were obtained at the South Fork Cache la Poudre River (Bunte and Swingle 2000, unpublished data). Ratios in the percent frequency of particle sizes between heel-to toe walks and the sampling frame become positive for mid-sized and coarse gravel but negative for cobbles (Figure 24). For size classes smaller than 5.6 mm, ratios varied too much between the two sites for computing a meaningful mean, but for the size range 8 to 180 mm, ratios had a similar trend for both operators and both sites (Table 16).

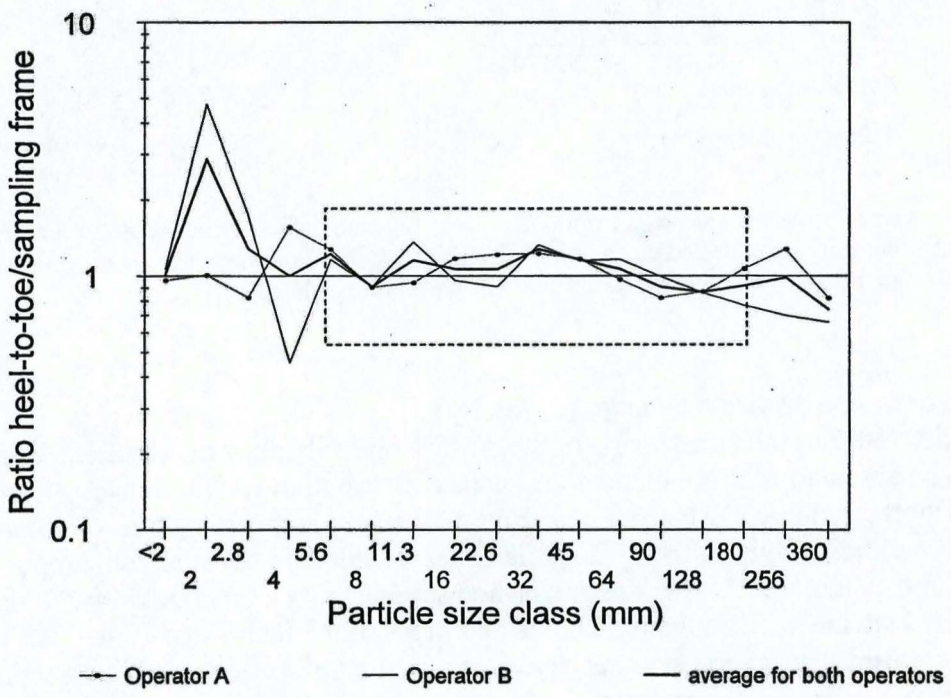

Figure 24: Ratios of the percent frequency per size class between heel-to-toe walks and a sampling frame for two operators in two mountain coarse gravel-bed streams and the mean ratio for both operators and streams (thick line).

The size distribution that pebble counts in the study streams might have obtained had a heel-to-toe walk been used instead of the sampling frame can be mimicked if the percent frequencies for size classes between 5.6 and 180 mm are multiplied by the mean ratios of

the percent frequencies per size class between heel-to-toe samples and samples obtained from the sampling frame (Table 16).

Table 16: Mean ratio of the percent frequency per size class from heel-to toe walks versus sampling frame.

Retained particle-size class (mm)	5.6	8	11.3	16	22.6	32	45	64	90	128	180
Mean ratio for two streams	1.16	0.90	1.15	1.06	1.06	1.27	1.16	1.06	0.90	0.86	0.91

b-axes measurements with a ruler

Whiting and King (2003) measured the *b*-axes of particles picked up in the pebble counts with rulers to the nearest mm. The size distribution obtained from ruler measurements (that are analogous to those from round-hole sieves) is typically *coarser* than the size distribution obtained from template measurements (that are identical to square-hole sieves). Ruler and template measurements are only identical for spheres, and the difference between ruler and template measurements increases with particle flatness. For known particle flatness, ruler and template measurements are convertible. The conversion factor increases from 0.7 for flat particles (ratio of *c*- to *b*-axis <0.1) to 1 for spheres. For fluvially transported particles that commonly have ellipsoidal shapes (ratio of *c*- to *b*-axis between 0.5 and 0.8), Church et al. (1987) proposed a conversion factor of 0.8 to 0.9 (Bunte and Abt 2001a). A factor of 0.85 renders a distribution 0.24 phi units coarser (Figure 25). The pebble count surface particle-size distributions in the studies by Whiting

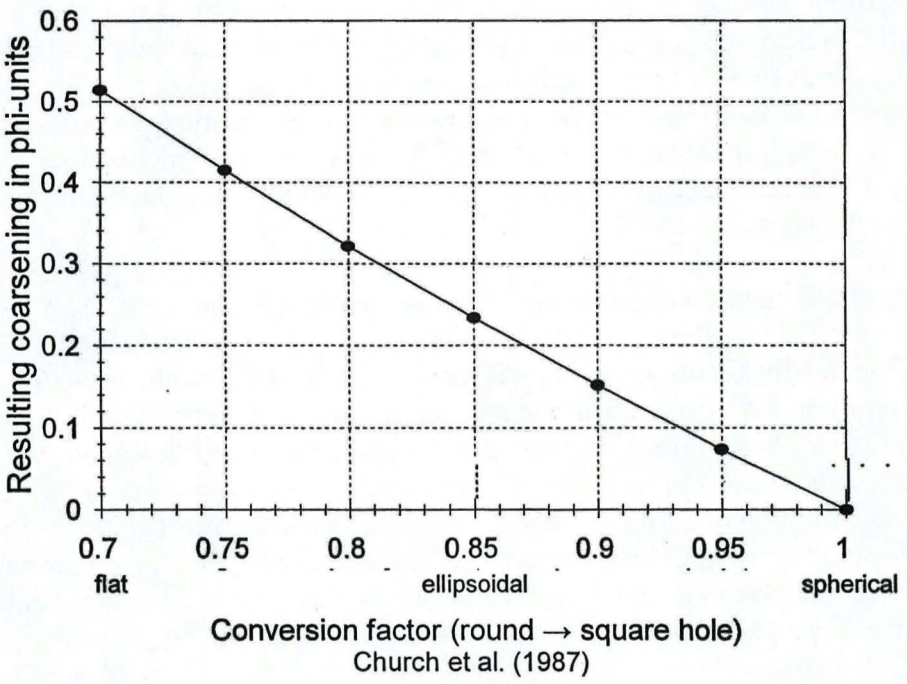

Figure 25: Conversion factors for particle sizes measured with rulers or round-hole sieves to particle sizes obtained from using templates or square-hole sieves.

and King (2003) are thus almost a quarter phi-unit coarser than they would have been had a 0.5 phi template been used for measuring particle size. The effects of heel-to-toe walks and blindly picking particles from the bed further coarsen the lower portion of the cumulative distribution. The pebble count distribution that might have been obtained in this study (had particle *b*-axes been measured with a ruler) can be mimicked by coarsening the pebble count distribution from this study by 0.24 phi units for each size class.

Subarmor samples: barrel sampler versus plywood shield

Riffles that are formed by relatively frequently occurring highflows should typically have similar distributions in the coarse part of the surface and subarmor sediment. The size of the coarsest surface particles should also be present in the subarmor, albeit in lower concentrations per sample mass than on the surface.

A dearth of coarse particles in subarmor samples can be caused by an insufficient sample mass which needs to be quite large considering the relatively rare occurrence of large cobbles and small boulders in subarmor sediment. Given that the average mass of 180 and 256 mm particles is 17 and 50 kg, respectively, sample masses ought to be 340 to 1000 kg following the 5% criterion by Church et al. (1987). However, individual samples larger than 100 kg are difficult to collect, particularly when using a barrel sampler, and more than three samples are typically not collected per site.

Whiting and King (2003) used a 55-gal drum to collect subarmor samples. The sampling area within the barrel is small (about 0.16 m^2) and can only be seen from above. This makes it difficult to excavate large particles that are partially buried under the barrel rim and to determine whether 50% of the particle volume is inside the sample area or not is problematic. It also makes it difficult to maintain a cylindrical excavation hole—the sample hole tends to become conically shaped such that particles deeper in the bed are less represented in the sample. Using a three-sided 0.6 by 0.6 m plywood shield not only increases the sampling area (to 0.36 m^2), but also makes it much more accessible to the operator who kneels at the open downstream side. Both effects reduce sampling errors when using the plywood shield.

Subarmor samples collected in granitic Idaho streams using a barrel sampler were compared to samples collected in granitic streams using the plywood shield (using data from Halfmoon Creek in this study as well as the SF Cache la Poudre River (unpublished data by Bunte and Swingle 2000)). Figure 26a shows that barrel samples contain less pea gravels, more mid-sized gravel, and fewer coarse gravels and cobbles than subarmor samples collected using a plywood shield. Figure 26b compares the cumulative frequency distribution of barrel and plywood shield samples collected in granitic streams. The barrel samples are finer by about 0.25 phi-units in the cobble range than samples collected with the plywood shield, and 0.2 phi-units coarser in the medium and fine gravel range. The D_{65} particle size is least affected by using the different sampling devices. Thus, compared to the effects of basin lithology, the effects of sampling method (barrel *vs.* plywood shield) are relatively small, and much of the difference in the

subarmor distributions between the two studies is attributable to different basin lithologies.

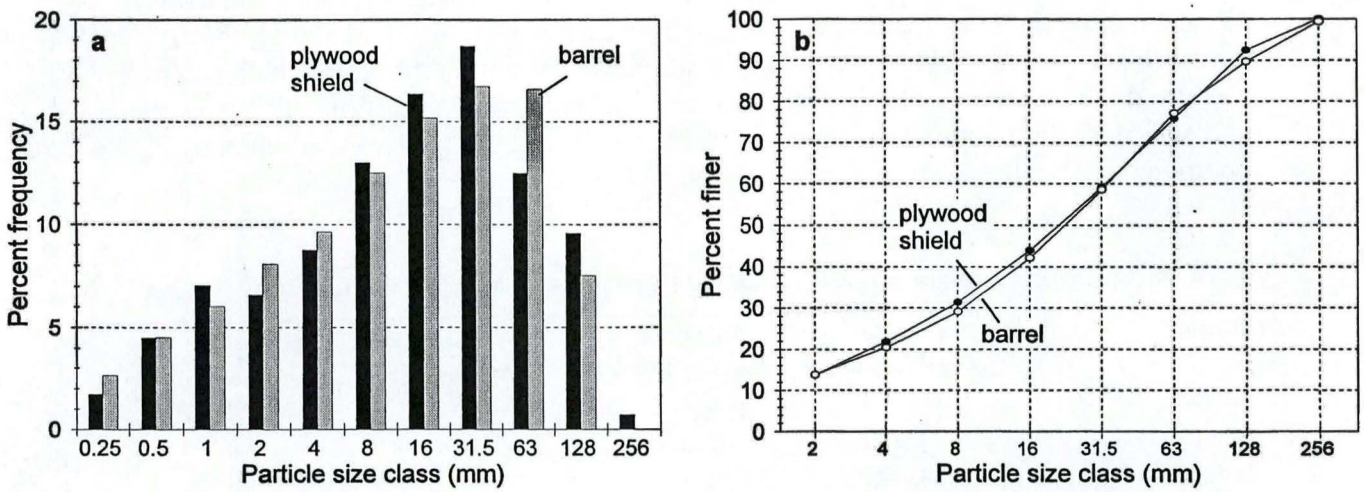

Figure 26 a and b: Average percent frequency distributions (a) and cumulative particle-size distributions (b) of subarmor samples collected in 11 granitic Idaho streams using a barrel sampler (data from King et al. 2004) and two subarmor samples collected in granitic streams using the plywood shield (data from this study and unpublished data by Bunte and Swingle 2000).

Once the difference between samples collected with a barrel and a plywood shield are known, ratios can be computed of the percent frequency per size class for both sampling methods (Table 17). The percent frequencies of the subarmor distribution can then be multiplied with these ratios to mimic the subarmor distribution that might have been obtained had a barrel sampler been used to collect the samples in this study instead of the plywood shield.

Table 17: Ratios of the % frequency per size class of subarmor samples collected using a barrel versus a plywood shield.

Size class (mm)	2	2.8	4	5.6	8	11.3	16	22.6	32	45	64	90	128	180
Ratio	0.85	0.90	0.95	1.00	1.05	1.07	1.09	1.13	1.16	0.99	0.82	0.88	0.95	0.98

3.3.4.3 Recomputed collapse sizes with adjusted size distributions

Simulating sampling techniques of the Idaho study

To determine and eliminate the effects that differences in sampling techniques have on the outcome of the collapse-size analysis, the particle-size distributions of the streams in this study were adjusted in several ways to be made comparable to those in the Idaho study. (1) To mimic heel-to-toe walks with blind particle pick up, the adjustment factors

in Table 16 were applied to the surface-size distributions in this study. This measure slightly increased the percentage of surface gravel particles, while decreasing the percentage of cobbles. (2) To imitate particle measurements with a ruler, the surface distributions of the three study streams were also coarsened by 0.25 phi units. Finally, (3) to simulate the effects of using a 55-gal drum instead of a plywood shield, the adjustment factors in Table 17 were applied to the subarmor distribution which slightly increased the percentage of mid-sized gravels. The characteristics of the adjusted surface and subarmor distributions are shown in Table 18. The collapse sizes were then re-computed for the three streams in this study.

Table 18: Characteristics of the adjusted surface and subarmor particle sizes of the three study streams.

Stream	Surface D_{50}, D_{90} (mm)	Subarmor D_{50}, D_{90} (mm)	$D_{50\ surface}/D_{50\ subarmor}$	$D_{90\ surface}/D_{90\ subarmor}$
Hayden	50, 180	34, 152	1.5	1.2
Little Granite	57, 180	41, 180	1.4	1.0
Halfmoon	56, 185	23, 119	2.4	1.6
Idaho streams:			2.7	1.7
Mean and range			1.9-3.4	1.4-1.9

Post-adjustment collapse sizes

As expected from the post-adjustment coarsened surface and fined subarmor sizes, the collapse sizes become 1 to 1.5 phi-units coarser (Figure 27) than the collapse sizes computed without adjustments (Figure 20) and come closer to those obtained by Whiting and King (2003) for Idaho granitic gravel-bed streams (Table 19). Halfmoon Creek which its granitic lithology has an adjusted collapse size of 32 mm that is within the range of collapse sizes (32-54 mm) that Whiting and King (2003) obtained for the *gravel*-bed streams in the Idaho study (not the seven cobble-bed that have an average collapse size of 62 mm). However, the streams with sedimentary basin lithology, Little Granite and Hayden Creek, retain low collapse sizes of 11.3 and 5.6 mm, respectively, that are

Table 19: Collapse size D_{col} (mm) for the three study streams **after adjustments** of the surface and subarmor size distribution as well as the percentiles of the surface and subarmor distribution corresponding to the collapse size.

Stream	Collapse size (mm)	Percentile of surface distribution	Percentile of subarmor distribution
Hayden Creek	5.6	6	21
Little Granite Creek	11.3	8	23
Halfmoon Creek	32	28	59
Mean and range for Idaho	45	44	71
gravel-bed streams	32 – 54	34 - 64	62 - 80
Mean and range for Idaho	62	29	75
cobble-bed streams	38 – 108	19 - 41	60 – 86

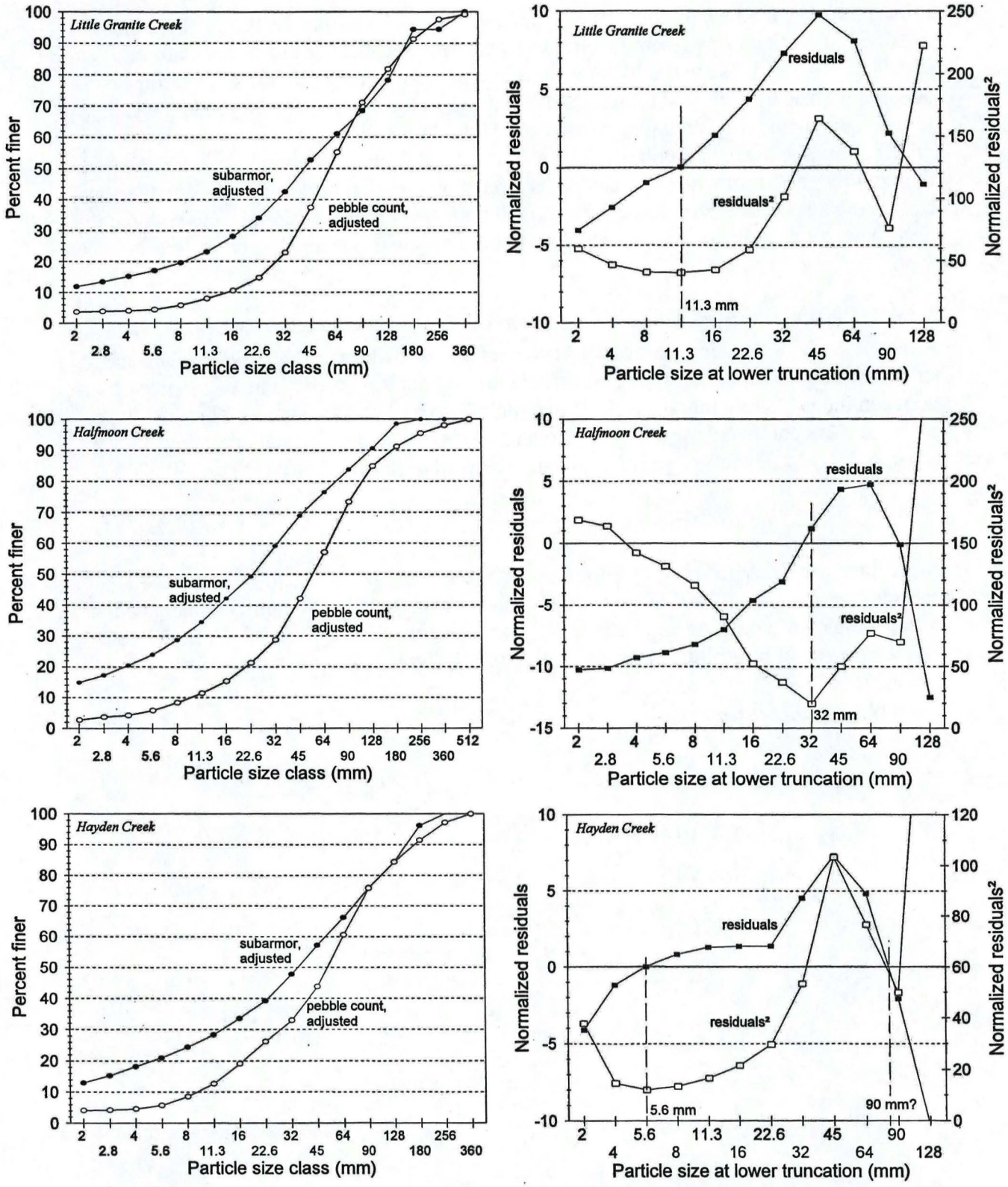

Figure 27: Particle-size distributions of the **adjusted** surface and subarmor sediment for the three streams analyzed in this study (left column) as well as the computed residuals and residuals^2 (right column). The collapse size is indicated by the vertical dashed line in the residual plot.

much smaller than the collapse sizes of the Idaho streams. Similarly, the collapse sizes obtained in this study represent much lower percentiles of the surface and subarmor distributions than those in the Idaho study. The persistent low collapse sizes of the streams with sedimentary lithologies are explainable: the adjustment for differences in sampling and analysis is relatively small compared to the differences in the subarmor distribution due to basin lithology. The residual graphs have a second x-axis intercept in the vicinity of 90 mm while the residual^2 graph shows a relative minimum. Whether this truly indicates collapse sizes near 90 mm is doubtful, given that residuals and residuals^2 become zero when the truncation size has reached the distribution D_{max} size.

3.3.4.4 Predictability of collapse sizes from bedmaterial characteristics

A dependency of the computed collapse size on a large difference between surface and subarmor size distributions appeared evident throughout this study. The difference between the two strata manifests itself in a high degree of bed armoring. Plotting collapse sizes computed for the Idaho streams versus the degree of bed armoring ($D_{50surf}/D_{50\ subarmor}$) shows a positive, linear relationship (Figure 28a)

$$D_{col} = 12.8\ D_{50surf}/D_{50sub} + 1.65, \qquad r^2 = 0.79 \qquad \text{(Eq. 4a)}$$

A similarly well-defined relationships exists between collapse sizes and the surface D_{50} particles size in units of mm (Figure 28b) which is likely due to the tightly established codependency of armoring and surface D_{50} size (r^2-value of 0.88) and which indicates that the degree of armoring is effectively determined by the surface coarseness.

$$D_{col} = 0.48\ D_{50surf} + 10.5, \qquad r^2 = 0.79 \qquad \text{(Eq. 4b)}$$

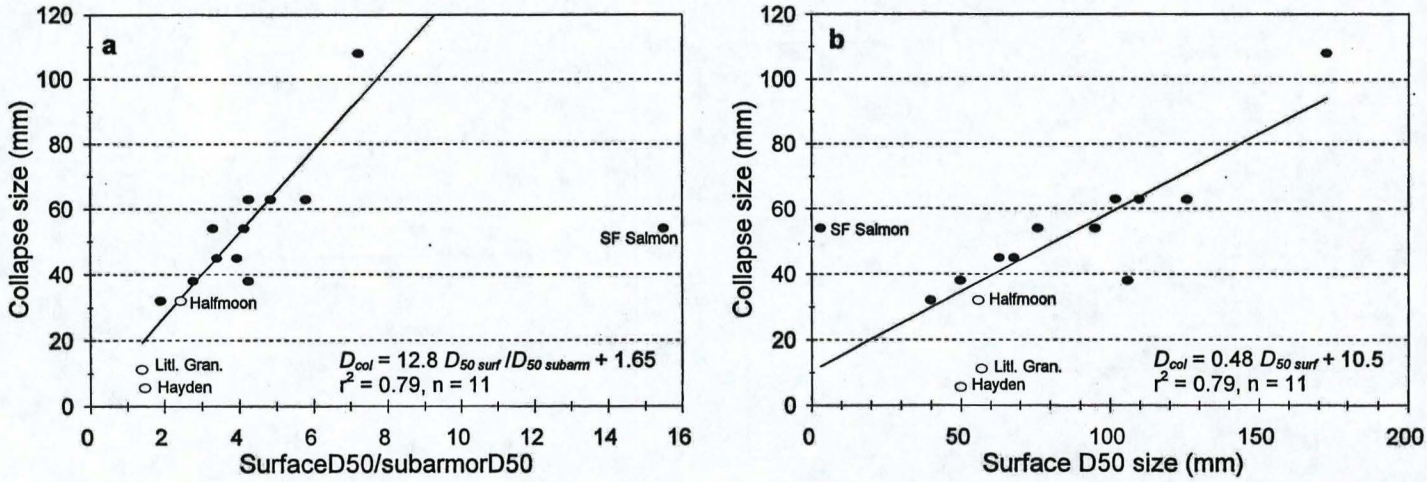

Figure 28: Relationship between collapse sizes and the degree of bed armoring (a) as well as the surface D_{50} sizes (b). The SF Salmon River is a sand-bedded stream that includes a few cobbles and boulders. Its data were not used for the fitted regressions.

The relationships with armoring and the surface D_{50} size are so well defined that they could be used to predict collapse sizes (D_{col}). Particularly the simplified equation

$$D_{col} \approx 0.5\, D_{50surf} + 12 \qquad \text{(Eq. 4c)}$$

could serve as a quick field estimate of the threshold particle size between supply- and transport-limited particles from the surface D_{50} size, a parameter that is relatively easy to measure.

The granitic Halfmoon Creek fits the relationship of collapse size with armoring perfectly if the surface D_{50} size and the degree of armoring are computed from the surface and subarmor-size distributions adjusted for differences in bedmaterial sampling techniques (Figure 28a). The two streams with sedimentary basin lithologies, Little Granite and Hayden Creek, fit the general trend of the relationship but fall outside the data range established for the granitic Idaho streams. If results for these two streams are considered valid, one has to conclude that the collapse-size analysis indicates a low threshold between supply- and transport-limited particles for streams in which surface- and subarmor-size distributions are similar (i.e., relatively low degree of armoring), and that such streams would require channel-maintenance flows to set in at a small percentage of bankfull flow. Extrapolated to unarmored streams, the collapse size would become very small, meaning that no flows could be diverted but that all flows are needed to prevent aggradation and maintain the channel.

Although the idea that channel maintenance flows ought to start at lower flows in less armored streams to prevent channel aggradation sounds plausible, several caveats remain in classifying the results for the three study streams as accurate: (1) The main point of concern is that the crossing of the cumulative size distributions of the surface and subarmor sediment when being iteratively truncated from the lower side renders the computed collapse size somewhat arbitrary (Section 3.3.3.3, Figure 21). (2) Furthermore, the relationship between armoring and collapse sizes for Little Granite and Hayden Creek is not within the range of the Idaho study (Figure 28a), and (3) these two streams do not fit the relationship with the surface D_{50} size (Figure 28b). These three facts should lead one to conclude that the collapse-size analysis is not suitable for streams with relatively similar surface and subarmor distributions, but is tailored (or restricted) to granitic Idaho streams with a particularly large difference between surface- and subarmor-size distributions.

3.3.4.5 Critical flow needed for incipient motion of collapse sizes

The critical flow needed for mobilizing the collapse sizes is determined from flow competence relationships. Whiting and King (2003) used the average result obtained from three variants of flow competence[27]. At the three streams investigated in this study

[27] *The three variants are: 1)a relationship between the upper limit of the size class of the largest particle collected in each bedload sample and the corresponding flow; 2) a relationship between the size of the larges particle and the dimensionless shear stress computed from the depth-slope product converted back*

critical flow was computed from well-defined flow competence curves established from bedload samples collected with a 3-inch Helley-Smith sampler as well as bedload traps at the three study streams (Table 20). Although Whiting and King (2003) do not explicitly state so, the flow distinguishing between supply- and hydraulic-limited transport is the channel maintenance flow. Based on flow competence curves established from Helley-Smith samples, all flows larger than 16 and 46% of bankfull flow are required for channel maintenance at Hayden and Little Granite Creek, respectively, while the granitic Halfmoon Creek requires flows larger than 67% Q_{bkf}. Compared to channel maintenance flows derived from the collapse size analyses for the granitic Idaho streams that ranged from 53-115% Q_{bkf} with an average of 90% Q_{bkf} (Whiting and King 2003), the computed lower boundary of channel maintenance flows for the study streams is quite low, particularly for the two non-granitic streams.

Table 20: **Collapse sizes and resulting channel maintenance flows (in percent of bankfull flow).**

Stream	Collapse size (mm)	Channel maintenance flows (from collapse-size analyses)	
		Helley-Smith	Bedload traps
Hayden Creek	5.6	16	38
Little Granite Creek	11.3	46	70
Halfmoon Creek	32	67	72
Mean and range for streams in this study	13 5.6 - 32	43 16 - 67	60 38 - 72
Mean and range in Idaho gravel-bed streams	44 32 - 54	90 53 - 115	-
Mean and range in Idaho cobble-bed streams	60 38 - 108	86 65 - 111	-

The relationship between D_{max} and discharge, i.e., the flow competence curve, varies with the sampler used to collect bedload transport. Flow competence curves obtained from bedload traps are considerably steeper than those obtained from samples collected with a 3-inch Helley-Smith sampler, and curves from both samplers cross in the range of medium to coarse gravel (Bunte et al. 2007) (see also Figure 33 in Section 3.5.3.1). Consequently, critical flows computed from competence curves derived from the two samplers vary as well. When flow competence curves from bedload traps samples are used to determine the critical flow for hydraulically limited transport, channel maintenance flows for the three streams in this study start at higher flows (38 -72% Q_{bkf}) than for Helley-Smith samplers, particularly for the two non-granitic streams.

to discharge; 3) a relationship between the size of coarsest particle in bedload samples that was adjusted to instantaneous peak discharge and the largest particle size moved (not quite clear to me).

3.3.5 Summary and Conclusion

The collapse-size analysis applied by Whiting and King (2003) to 12 streams in Idaho indicated that the threshold between supply- and transport-limited particle sizes ranged from 32 to 108 mm. The collapse sizes computed for three mountain gravel-bed streams in this study were considerably smaller than those for the Idaho streams, ranging from 2.8 to 16 mm. Some part of the difference could be attributed to differences in sampling techniques between the two studies. When sampled surface and subarmor particle-size distributions were adjusted to eliminate the effects in sampling technique between the two studies, collapse sizes computed for this study doubled in size, ranging from 5.6 to 32 mm.

Critical flows (=channel maintenance flows) necessary to transport particle sizes from the collapse size analysis averaged 90% of bankfull flow (53 – 115% Q_{bkf}) in the Idaho streams (Whiting and King 2003). Based on flow competences curves derived from Helley-Smith bedload samples, average channel maintenance flows of 43% of bankfull (16 – 67% Q_{bkf}) are needed for in the three study streams. If the analyses are based on bedload traps, channel maintenance flows need to exceed on average 60% of bankfull (38 – 72% Q_{bkf}). Results obtained from the collapse size analysis in this study thus indicate a much lower onset of channel maintenance flows than the commonly held assumption that channel maintenance flows should start in the neighborhood of 80 (Ryan et al. 2005) to 90% of bankfull flow (Ryan et al. 2002; Whiting and King 2003).

The main factors causing the difference between collapse sizes in this study and the Idaho streams are basin lithology as well as the presence of steep hillsides directly adjacent to the stream. Differences in sampling methods have smaller effects, and those effects can be factored out. The Idaho streams have coarse surface sediment because rockfall from steep hillslopes contributes coarse particles to the stream while downcutting and exhuming boulders also provide large clasts. By contrast, the weathering products of the granitic Idaho watersheds provide a lot of fine (granule and grus) sediment that accumulates in the subarmor sediment. Thus, surface-size distributions in the Idaho streams are comparatively coarse, while subarmor-size distributions are relatively fine. This results in heavy armoring ($D_{50\ surf}/D_{50\ subsurf}$) for the Idaho streams.

A large difference between surface and subarmor distributions is instrumental in providing collapse sizes that are in the coarse gravel and cobble range. Simply due to the mathematics of the collapse-size computations, collapse sizes become large when the surface is considerably finer than the subarmor-size distribution, and become small when the surface and subarmor distributions approach each other. This is demonstrated in the well-defined relationships of collapse sizes with the degree of bed armoring (Figure 28 a).

The question arises whether the small collapse sizes of 5.6, 11.3, and 32 mm computed for the three study streams are true and, consequently, whether channel maintenance flows starting as low as 16, 46, and 67% Q_{bkf} (based on Helley-Smith samples) are a true requirement for the streams in this study. The alternative possibility is that the low collapse sizes for the streams in this study are an artifact of the collapse-size

methodology that is tailored to the characteristics of the granitic Idaho study streams and that therefore the collapse-size analysis is not a suitable tool for streams with non-granitic lithologies.

Validity of the computed results, i.e., that the collapse sizes for streams with small differences in surface and subarmor distributions are small, and that consequently channel maintenance flows need to set in at a low percentage of bankfull flow, is supported by the fact that the three study streams generally fit the relationship between the degree of bed armoring and collapse sizes (Figure 28 a). By contrast, a limitation of the collapse-size analysis to streams with large differences between the surface and the subarmor distributions is expressed by the fact that the two streams with a small difference in the surface and subarmor size distributions fall outside the range of the relationship between the surface D_{50} size and the collapse size (Figure 28b). Besides, channel maintenance flow requirements starting at 16 and 46% Q_{bkf} have so far not been reported in the literature and would need to be confirmed by field studies.

The close relationship of collapse sizes with the surface D_{50} size is of concern. The increase of collapse-sizes with the surface D_{50} size appears to be a computational artifact. It suggests that coarse-bedded streams require only the largest flows for channel maintenance while finer grained streams require lower flows, too.

A general concern of the collapse-size methodology, which may also decrease the validity of the collapse sizes computed for the study streams, is that reading collapse size from plotted normalized residuals and residuals^2 can be subjective in cases when the truncated surface- and subarmor-size distributions cross. Another point that adds confusion is that the residuals for the streams in this study have a second x-axis intercept near 90 mm. This could indicate that collapse sizes for the study streams might be near 90 mm and thus be similar to those in the Idaho streams. However, residuals also decrease for large particle sizes because the number of size classes involved in the analysis has dropped to 2 or 3, which renders the indicated collapse size much less valid. The situation of collapse size falling within the largest 2 or 3 size classes of the armor and subarmor sediment did not occur in the example given by Whiting and King (2003), and the interpretation of their plot of residuals was unambiguous. Finally, the computation of collapse sizes is already a relatively time-consuming procedure, particularly for streams in which a similarity of the surface and subarmor distributions requires multiple reanalysis of the computations. On top of this effort, the second step of the Whiting and King (2003) analyses requires the user to perform a flow competence analysis to compute flows required to transport the collapse sizes, i.e., the channel maintenance flows.

3.4 Klamath Falls site-calibration procedure

3.4.1 Introduction

The site-calibration approach was developed by the Winema National Forest in Klamath Falls, OR, as a tool for identifying channel maintenance flows. The procedure was applied to make claims for channel maintenance flows in several streams in the Winema National Forest.

3.4.1.1 Overview of the Klamath Falls procedure

The Klamath Falls procedure is based on the assumption that channel maintenance flows need to mobilize the smallest bedmaterial particle size that acts as a stabilizer for the channel bed (Bakke et al. 1999; McNamara et al. 2000). Gravel particle sizes that stabilize the channel bed are called framework gravel. Conceptually, framework gravels are those that would touch each other if finer particle sizes were removed. The finer particles filling the spaces between framework gravels are called matrix. Framework and matrix gravel sizes are determined from volumetric bedmaterial samples. The flow at which framework gravels start to move is taken as the channel maintenance flow.

In the Klamath Falls study, bedload transport was measured using a 3-inch Helley-Smith sampler. However, the samples were not used directly to determine the mobility of framework gravel, but served to calibrate the Parker-Klingeman bedload transport equation (Parker and Klingeman 1982) to each site. Fractional transport rates predicted from the site-calibrated Parker-Klingeman equation were then used to determine the flow at which framework gravels comprise 2% or more of the total transport rate. This is considered to be the channel maintenance flow.

3.4.1.2 Site-specific calibration procedure

Theoretically, incipient motion of framework gravels could be determined from detailed field measurements of bedload transport rates from which either the fractional rating curve for the framework gravel size or the flow competence curve could be derived. However, collection of a sufficient number of samples that span a large range of flows including high flows is not only time-consuming but might take more than one field season because flows competent to move framework gravels may not occur every year or may not happen to be sampled. To avoid a complete dependency on measured bedload transport data, the Klamath Falls channel-maintenance procedure computes a transport relationship based on the Parker and Klingeman (P-K) bedload equation. However, to improve the match between measured and modeled transport rates, the Klamath Falls procedure uses measured bedload samples to calibrate two parameters of the P-K equation, that are otherwise used as constants, to a specific stream site. One parameter is the reference shear stress τ^*_{r50} which is the dimensionless Shields value associated with the D_{50} particle size. It is computed from

$$\tau^*_{r50} = \frac{\rho \cdot g \cdot d \cdot S}{(\rho_s - \rho_f) \cdot g \cdot D_{50}} \qquad \text{(Eq. 5)}$$

where ρ and ρ_f are the sediment and fluid density, g is acceleration due to gravity, d is water depth, S is stream gradient, and D_{50} can denote either the armor or the subarmor sediment size. For silicate-rich sediment ($\rho_s \cong 2{,}650$ kg/m^3) and moderate suspended sediment concentrations that do not significantly change the clear water density ($\rho_f \cong$ 1,000 kg/m^3), this equation can be simplified to $\tau^*_{r50} = 0.61\, d \cdot S/D_{50}$. If D_{50} refers to the armor layer, the P-K equation assumes a constant value of 0.0872 for τ^*_{r50}, and a value of value 0.0375 when referring to the subarmor layer (based on Oak Creek bedmaterial samples collected by Milhous (1973)).

The other parameter is the hiding factor which is the exponent (*exp*) of the equation

$$\frac{\tau^*_{ri}}{\tau^*_{r50}} = \left(\frac{D_i}{D_{50}}\right)^{-exp} \qquad \text{(Eq. 6)}$$

where τ^*_{ri} is the dimensionless Shields value associated with the i^{th} particle size class. Parker and Klingeman (1982) determined an exponent of -0.982 for the Oak Creek samples collected by Milhous (1973). A value of -1 indicates equal mobility for all particle sizes[28] meaning that a relatively wide range of particle sizes is entrained over a relatively narrow range of flows. An exponent that tends towards zero indicates the absence of a hiding factor. In this case, the critical dimensionless shears stress is only a function of particle size (Ashworth and Ferguson 1989), and transport occurs as size selective (selective transport), meaning that a flow needs to increase significantly to mobilize larger particles.

3.4.2 Methods

3.4.2.1 Bedmaterial sampling

The Klamath Falls procedure (Bakke et al. 1999; McNamara et al. 2000) computed the size of framework gravels from the particle-size distributions of the armor and subarmor layers. The armor layer thickness is assumed to be equal to the embedded depth of the largest exposed particle within the sample area. The armor layer is sampled volumetrically by collecting sediment from the bed surface down to the depth of the deepest embedded particle. The subarmor layer beneath the armor is assumed to be equally thick and is also sampled volumetrically. Like the Idaho study (Whiting and King 2003), the Klamath Falls study used a 55-gal drum (barrel sample) to collect the volumetric armor and subarmor samples. To obtain a large sample volume and focus on the average bedmaterial in the reach, five sampling locations are selected in the vicinity of the bedload sampling cross-section. These five locations are expected to be representative of the bedmaterial in the vicinity of the bedload sampling site. The samples should therefore not cover the extremes in bedmaterial size but represent the middle range.

---

[28] *Andrews (1983, 1994, Andrews and Nankervis 1995) determined values close to -0.9 for mountain gravel-bed streams, while other researchers computed values of -0.4 to -0.8 for their field data (e.g., Komar and Shih 1992; Ashworth and Ferguson 1989, Petit 1994; Whitaker and Potts 1996).*

Our study used the plywood shield for collecting the armor and subarmor samples instead of the barrel sampler. The plywood shield provides a larger sampling area (0.36 m^2 compared to 0.16 m^2 inside the barrel sampler), reduces the influence of sloping sidewalls on the subarmor-size distribution and allows the operator to collect the sample in a more comfortable position. All of these factors improve sampling accuracy. Otherwise, bedmaterial samples in this study were collected following the procedure used in the Klamath Falls study, with the exception that the subarmor layer was sampled to a depth of 10 cm (instead of the armor layer thickness) in order to increase sample volumes.

3.4.2.2 Computation of framework sediment size

The size of the framework gravels is calculated by subtracting the percent weight frequency of the subarmor layer from the percent weight frequency of the armor layer for each size class (Figure 29). The smallest size class for which the difference is positive is

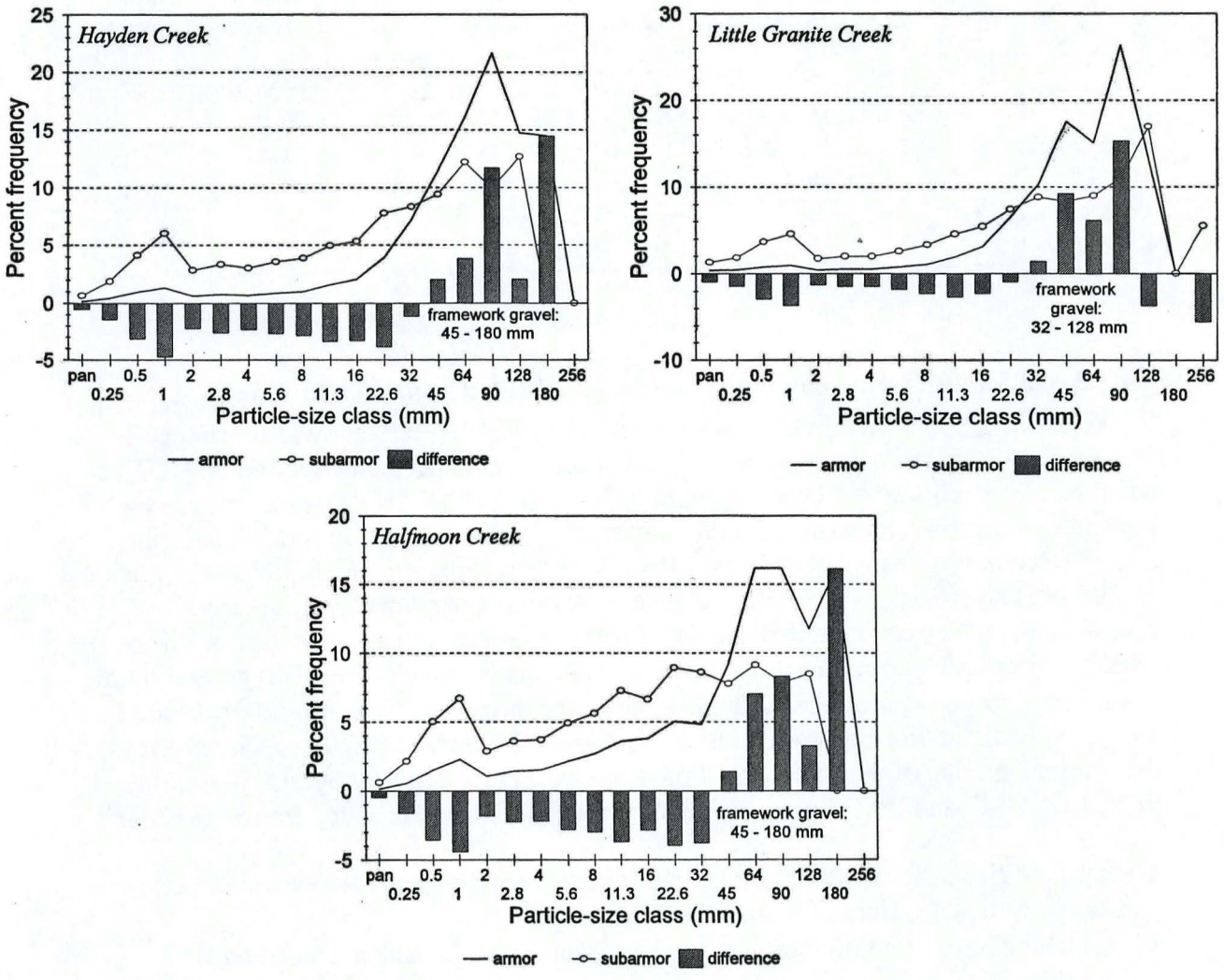

Figure 29: Percent weight frequency of armor- and subarmor-size distributions and their differences computed for the three streams in this study.

the smallest framework size. In the three streams examined in this study, framework gravels started at the size classes of 32-45 and 45-64 mm (Table 21). For Hayden and Halfmoon Creek, the framework gravel size was close to the surface D_{50} size obtained from a pebble count in the vicinity of the bedload sampling site. At Little Granite Creek, the framework size was smaller than the surface D_{50}. Note that the framework gravel sizes at Hayden and Little Granite Creek were considerably larger than the threshold sizes between supply- and transport-limited particles of 5.6 - 32 mm that were computed from the collapse size analysis (Whiting and King (2003). For Halfmoon Creek with its granitic watershed lithology, the difference was less.

Table 21: Bedmaterial and framework gravel sizes (mm) in the vicinity of the bedload sampling locations in the three study streams, as well as the threshold gravel size obtained from the collapse-size analysis (Whiting and King 2003). See Table 2 for reach-averaged bedmaterial characteristics.

Stream	Surface D_{16}, D_{25}, D_{50}, D_{84} (mm)	Armor D_{16}, D_{50}, D_{84} (mm)	Subarmor D_{16}, D_{50}, D_{84} (mm)	Armoring $D_{50\,surf}/D_{50subarmor}$	Smallest framework gravel size class (mm)	Threshold gravel size (Whiting and King 2003)
Hayden	11, 18, 46, 114	35, 92, 175	3, 36, 114	1.3	45-64	5.6
Little Granite	20, 29, 53, 124	30, 71, 124	5, 47, 146	1.1	32-45	11.3
Halfmoon	14, 23, 49, 115	15, 80, 182	2, 26, 92	2.1	45-46	32
Mean and range for Klamath Falls study		77 32-154	18 9.5-30			

3.4.2.3 Data input requirements to run site-calibrated approach in BAGS

Bakke et al. (1999) used a FORTRAN model called SEDCOMP that was developed by Dawdy (1995) for the calibration of the Parker-Klingeman bedload equation (P-K equation) to specific sites. Due to unfamiliarity with FORTRAN programs, and in the interest of time, this study used the implementation of the calibration procedure in the BAGS (Bedload Assessment in Gravel-Bedded Streams) program (BAGS 2006, Pitlick et al. 2006). The BAGS program runs as a Microsoft Excel application and provides a relatively user-friendly computation of bedload transport rates using six versions of Parker bedload equations and its derivatives. Like the Fortran SEDCOMP program, the BAGS program computes site-calibrated values for the parameters *exp* and τ^*_{r50} based on measured bedload transport rates and particle sizes. Because P. Bakke was involved in the implementation of the SEDCOMP program within the BAGS program, it is assumed that SEDCOMP and BAGS provide identical results for site-calibrated transport rates.[29]

To compute site-calibrated bedload transport rates over a range of flows, the BAGS program requires a variety of input data:

- A channel cross-section (column A with distance from a bank and column B with depth)

[29] *It turned out that the BAGS program I used was not the final one and improvements were made later.*

- A subarmor-particle size distribution (column A with size classes and column B with the cumulative percent finer starting at 0 and ending at 100%)
- Several measured bedload transport rates and their cumulative percent finer bedload particle-size distributions
- A stream gradient (either the reach-averaged water surface slope, reach-averaged channel bed slope, or the friction or energy slope)
- The range of flows over which transport rates are to be modeled

Cross-section

Entering cross-section data into the BAGS user-interface is generally a straightforward affair. However, a problem arose at the Halfmoon Creek sampling site where flow was stagnant near the left bank of the cross-section due to a bay in the bank line. No gravel bedload was transported here—the bed was covered with mud. To ensure that the BAGS program would not allot flow or transport into this zone, the deadwater zone was truncated from the cross-section before it was entered into the program.

Stream gradient

Dawdy (1995) and Bakke et al. (1999) specify that the SEDCOMP program requires the sampling site to be located in a reach with a relatively uniform water surface slope. The **local** water surface slope that is measured between an upstream and downstream control should be used for the site-specific calibration of the P-K equation. A uniform water surface slope within the reach was not a selection criterion for our bedload sampling sites that needed to be wider than the average stream width. Local stream widening is often associated with a corresponding decrease in stream gradient compared to the reach-averaged value. Thus, reach-averaged water surface slopes are steeper than local water surface slopes within a few meters upstream and downstream of the sampling sites.

The survey resolution in the immediate vicinity of our sampling sites was not high enough to accurately compute a local water surface gradient from the data. Local water surface slopes were therefore estimated from longitudinal water surface profiles plotted over 70 to 120 m long reaches. These plots suggested that local stream gradients in close proximity to the sampling sites were approximately half of the reach-averaged water surface gradients (Table 22).

Table 22: Measured reach-averaged and estimated local water surface gradients.

Stream	Reach-averaged water surface gradient	Estimated local water surface gradient
Hayden Creek	0.0380	0.021
Little Granite Creek	0.0168	0.008
Halfmoon Creek	0.0142	0.007
Mean and range for Klamath Falls study	-	0.0034 0.0010 - 0.0067

Contrary to the requests by Dawdy (1995) and Bakke et al. (1999), the BAGS program explicitly specifies that the **reach-averaged** water surface slope or the reach-averaged channel-bed slope be entered as input for stream gradient when computing the site-calibrated P-K equation. It is unknown whether this inconsistency is a simple wording error or whether the BAGS program has some algorithm that compensates for the difference between reach-averaged and local slopes[30]. To address this issue in this study, site-calibrated transport rates were computed for both, the measured reach-averaged and the estimated local water surface slopes.

Bedmaterial size distributions

The BAGS program accepts entry of bedmaterial particle-size classes in any interval as long as they are sorted from smallest to largest and the percent finer starts at 0 and finishes at 100%. Bakke et al. (1999) specify that the *subarmor* sediment be used to characterize the bed and provide guidance in how the subarmor grain-size distribution is obtained from volumetric samples of the sediment below the armor layer. The BAGS program (BAGS 2006) and the BAGS user's manual (Pitlick et al. 2006) request that the grain-size distribution to be entered for the site-calibration procedure is the "substrate" (which Pitlick et al. (2006) specify to be "below the surface layer"). The term "substrate" is unspecific because in the context of BAGS it could refer either to the subsurface or the subarmor sediment, both of which have different size distributions[31]. This study used the subarmor grain-size distribution. For sand (<2 mm), the size distribution was entered in units of 1 phi, for gravel (>2 mm) in 0.5 phi.

Largest particles at the sampling site

The BAGS program and its manual also deviate from the manual for the SEDCOMP program regarding the coarseness of streambed to which the site-calibrated approach is applicable. Dawdy (1995) specifies that the bedmaterial at the measuring site should not contain particles larger than those moved at bankfull flows, and a site at which some bed particles are larger than half the bankfull flow depth should be avoided[32]. The surface and subarmor sediment at all of our study sites contained particles in the size class 180-256 mm and up to 360 mm at one site, whereas the largest particle sizes mobile at bankfull flows were 32 to 50 mm (as computed from flow competence curves obtained for bedload trap samples). Thus, none of our sites fit the bedmaterial requirements specified in the SEDCOMP program manual.

Bedload samples and their size distributions

The BAGS implementation of the site-calibrated procedure requires that bedload data be entered for the site-calibration. Each bedload entry consists of a measured flow, a measured bedload transport rate, and the cumulative percent finer bedload particle-size

---

[30] *This contradiction between the two sources should be addressed in future versions of the BAGS program.*

[31] *Better choice of terms is "subarmor" or "subpavement" which identifies the bedmaterial strata to be sampled more clearly.*

[32] *The BAGS program and its manual should caution the user that the site-calibration procedure is not applicable to streams with extremely rough beds.*

distribution of that sample. The BAGS program requires that the size classes for the cumulative percent finer information for bedload size data are the same as those used for the subarmor-size distribution. This causes a problem for bedload traps samples. Because bedload traps do not collect particles smaller than 4 mm, the percent finer of bedload in the size class of 4 mm is 0. Consequently, to make the program work, the subarmor-size distributions need to be truncated at 4 mm as well, which pretends that sediment finer than 4 mm does not exist in the bed. This problem did not occur for Helley-Smith bedload samples because their size distributions extended to 0.25 mm, the same smallest size to which the bedmaterial samples were analyzed.

Entering the bedload data one record at a time—first pasting transport rates and discharge, then pasting the particle-size distribution—is cumbersome and provides opportunities for errors. Changing the data sets used for the calibration procedure is time-consuming as well[33]. To reduce the number of trial runs (each of which takes about half an hour when new data are to be gathered and entered), guidance specifying the kind of bedload samples best suited for the site-calibration process would be useful.

3.4.2.4 Bedload data selection for the calibration procedure

Between 10 and 27 samples collected with a Helley-Smith sampler were available per site in the Klamath Falls study, and that number provided a satisfactory fit from the site-calibrated approach. However, Bakke et al. (1999) do not specify whether one should collect at least 10 data sets that are then used for the optimization procedure or whether a larger number of samples should be collected, from which the user selects data until a desired degree of fit of the predicted transport relationship with measured transport rates is reached. Should the user select calibration samples that emphasize high flows or represent the range of measured flows? Recommendations are also not provided regarding the sample particle-size distribution and it remains unclear whether calibration samples should focus on a full size-distribution without empty size classes or on samples with large D_{max} sizes?[34]

As the site-calibration would typically be applied to study streams for which only a few bedload samples are available, this study did not use all of the 55 to 177 bedload samples available per site, but selected between 9 and 16 samples for the site-specific calibration procedure for each study stream (Table 23). The initial selection criterion was to cover the range of measured flows evenly, thus calibration samples were selected systematically from each data set, taking every 3rd, 5th, 10th or 12th sequentially measured bedload sample depending on the number of samples collected per site. Slight deviations from this selection scheme were tolerated in order to substitute a "poor" sample by a neighboring sample that had a fuller size distribution with no or maximally one empty size class. If the original selection of bedload samples did not lead to a satisfactory match between measured and predicted transport rates—which typically meant that the

---

[33] *A pre-labeled spreadsheet table into which all calibration bedload data can be pasted would be useful.*

[34] *Guidance on the number and kind of samples to be selected for an optimal outcome of the calibration procedure in the BAGS manual would be useful.*

predicted transport relationship crossed the measured data at low flows—some of the low flow samples used for calibration were either omitted or substituted by bedload samples collected at high flows (final selection). In some cases, several highflow or low flow samples were added to the original sample selection.

Table 23: Bedload samples used for calibration procedure.

Stream	Number of bedload samples, $Q_B > 0$		Approx. every x^{th} sample used for calibration		Number of bedload samples used for calibration and description		Sample selection	
	HS	traps	HS	traps	HS	traps	HS	traps
Hayden Creek	31	177	3	12	10, evenly spaced	16, evenly spaced	Original selection	Original selection
					11, 3 at low Q replaced by 4 at high Q	13, 3 at low Q omitted	Final Selection	Final Selection
Little Granite Creek	43	55	5	5	10, evenly spaced	11, evenly spaced	Original selection	Original selection
					9, lowest Q omitted	17, 3 at low Q and 3 at high Q added	Final Selection	Final Selection
Halfmoon Creek	50	151	5	10	10, evenly spaced, unrepresentative sample included	15, evenly spaced	Original and final selection	Original selection
					15-20, 5 and 9 from high Q added, unrepresentative one added to 19	15, 2 at low Q substituted by 2 at high Q	Dismissed selections	Final selection

3.4.2.5 Computations of bedload transport relationships and threshold flows

Bedload transport relationships for the three study streams were not only computed from the site-calibration procedure but also by the uncalibrated equations by Parker and Klingeman (1982) and Parker et al. (1982) in order to evaluate the effectiveness of the site-calibration approach. Transport predictions were computed using calibration samples collected with the Helley-Smith sampler as well as bedload traps, for the originally selected (evenly-spaced) set of bedload samples and a few other selections. Transport relationships were computed using two different slopes, the reach-averaged and the local water surface slope. All predicted transport relationships were compared to bedload transport rates measured with a Helley-Smith sampler and with bedload traps. Together with the 12 transport predictions from the two Parker-Klingeman equations, this resulted in 36 cases for which modeled transport relationships were compared with measured ones. Fractional transport rates computed for the size class closest to the smallest framework gravel were compared to 2% of the total transport rate (the threshold

transport rate specified by Bakke et al. (1999)) as well as to other percentages of total transport.

3.4.3 Results

The main questions answered by this study were:

- Does the site-calibrated approach significantly improve the fit of predicted transport relationships with measured ones? Which parameters affect the degree of fit?
- To which percent of bankfull flow do threshold flows correspond (i.e., flows at which transport in the size class of the framework gravel comprises more than 2% of the total transport)?
- Do transport relationships predicted from the site-calibrated approach fit better with transport rates measured from the Helley-Smith sampler or bedload traps?
- Would higher threshold transport rates for framework gravel (e.g., 4, 6, 8 or 10% of the total transport rate) be more suitable?

3.4.3.1 Transport relationships from the uncalibrated Parker equations

The uncalibrated equations by Parker and Klingeman (1982) and Parker et al. (1982) always predicted very similar transport relationships (Figure 30 and Figure 31) for the three study streams. The two equations are therefore lumped in further discussions and are referred to as the "P-K equations".

The transport relationship of the P-K bedload equations are designed to increase steeply during low flows and flatten out at high flows. The resulting graphs are therefore curved in a log-log plot. This means, if power functions in the form $Q_B = a \cdot Q^b$ were fitted to consecutive segments of the transport relationship for increasing flow, the exponent b would decrease from low to high flows. For the study streams, the predicted b was >18 at the lowest flows and decreased to < 1 at the highest flows. By contrast, transport relationships measured in mountain gravel-bed streams over a wide range of flows are typically straight in log-log plots, meaning that the exponent of a power function $Q_B = a \cdot Q^b$ remains constant over the entire range of flows (e.g., Whiting et al. 1999; Barry et al. 2004; Bunte et al. 2007, *in press*). Fitting a curved relationship to straight data (in log-log plots) is generally problematic.

Transport relationships predicted from the uncalibrated P-K equations approached a fit with measured transport rates only in 2 out of 12 cases (Table 24). The value selected for water surface slope had a large effect on the predicted transport relationships that were orders of magnitude larger when computed from the reach-averaged water surface slope compared to computations using the local water surface slope. For Helley-Smith samples, transport predictions from the reach-averaged slope tended to match measured

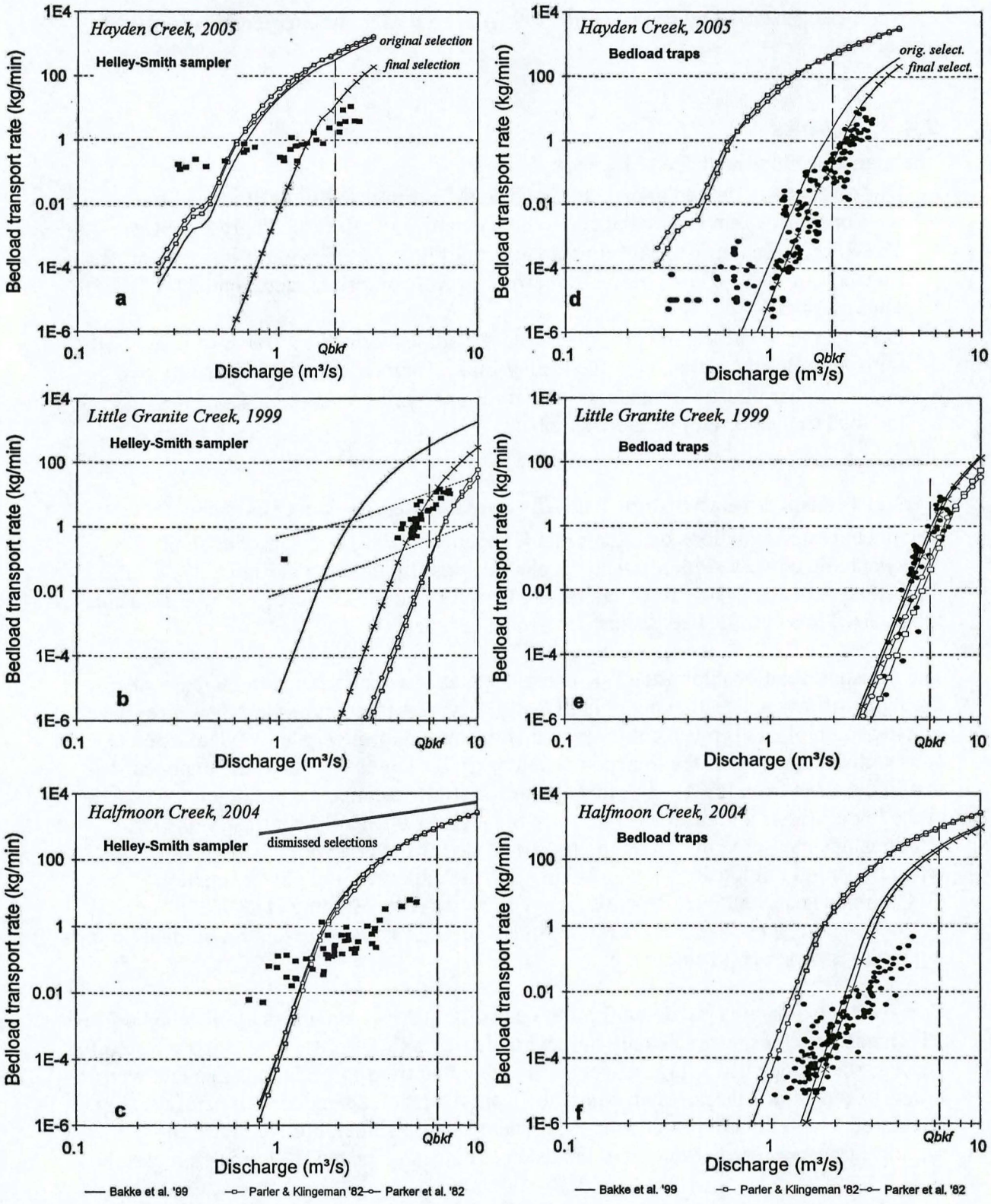

Figure 30: Bedload transport rates collected at the three study sites with a Helley-Smith sampler (a-c) and bedload traps (d-f) as well as rating curves predicted from the two P-K equations and the site-calibrated approach computed from the **reach-averaged** stream gradient. The line with cross symbols shows the prediction from the final selection of calibration samples. The stippled lines in plot b show the range of bedload data measured by Ryan and Emmett (2002). See Sect. 3.4.3.2 for "dismissed selection" in plot **c**.

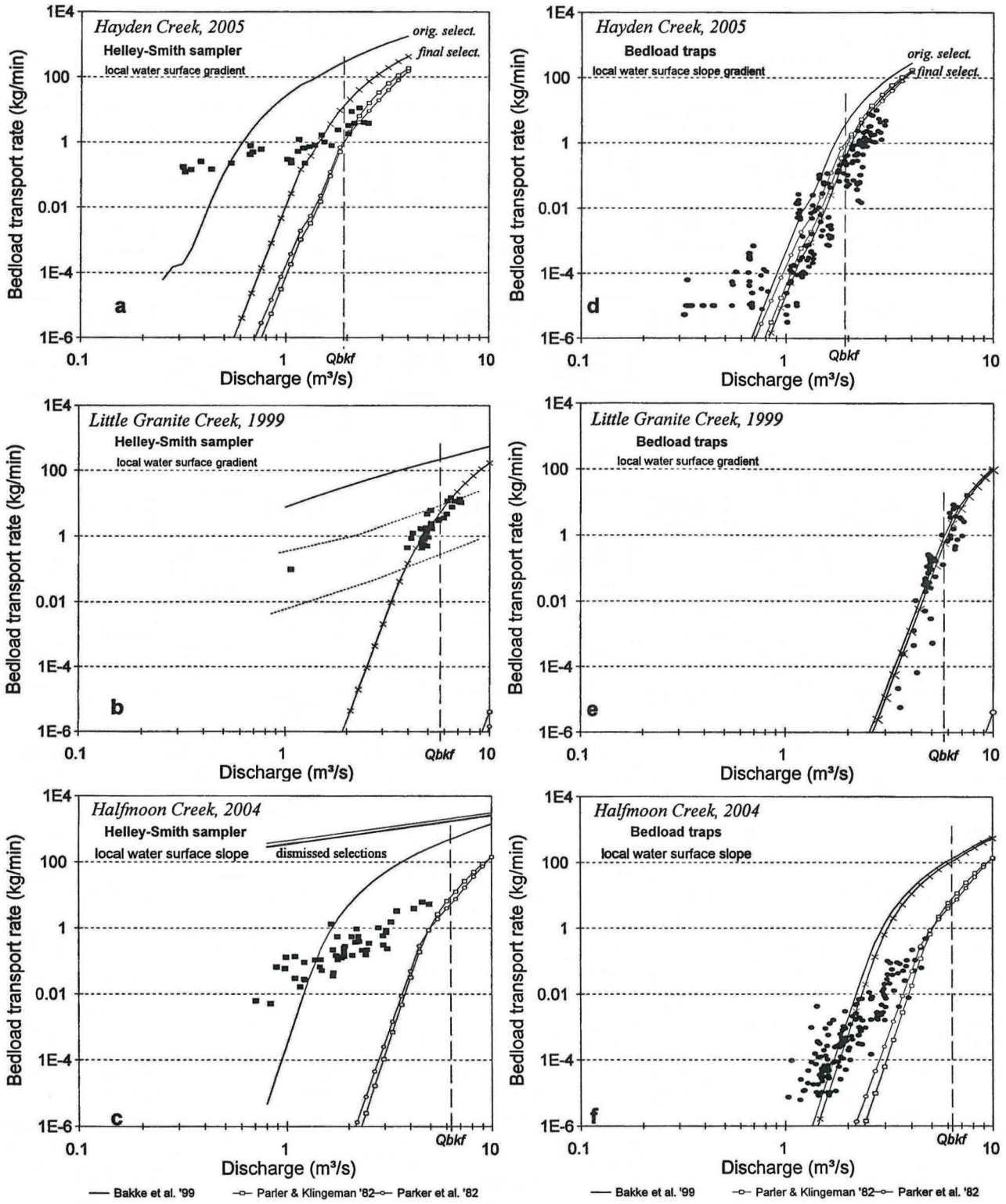

Figure 31: Bedload transport rates collected at the three study sites with a Helley-Smith sampler (a-c) and bedload traps (d-e) as well as rating curves predicted from the two P-K equations and the site-calibrated approach computed from the **local** stream gradient. The line with cross symbols shows prediction from the final selection of calibration samples. The predictions for the two P-K equations are barely visible in the lower right corners of plots b and e. The stippled lines in plot c show the range of bedload samples sampled by Ryan and Emmett (2002). See Sect. 3.4.3.2 for "dismissed selection" in plot c.

Table 24: Comparison of transport rates predicted from the P-K equations and the site-calibrated approach with measured bedload transport rates. Reach-averaged and local water surface slopes were used for the computations. Results are reported for the original selection of samples that cover flows evenly (upper boxes for each stream) and the final selection that includes more high flow samples (lower boxes). Note the color coding: high overprediction, overprediction, fit to slight misfit, underprediction, high underprediction.

Stream	Reach-averaged water surface slope				Local water surface slope			
	P-K equations		Site-calibrated procedure		P-K equations		Site-calibrated procedure	
	Traps	HS	Traps	HS	Traps	HS	Traps	HS
Hayden Creek	Highly overpre-dict	Cross data at low Q; overpre-dicts high Q	Slightly overpre-dicts	Crosses data at low Q; overpredicts at high Q	Slightly overpre-dict	Underpre-dict but fit data at high Q	Slightly overpre-dicts	Crosses data at low Q; overpredicts at high Q
			Fits data	Crosses data at high Q; underpre-dicts low Q			Fits data	Crosses data at high Q; underpre-dicts low Q
Little Granite Cr.	Slightly underpre-dict	Underpre-dict	Fits data	Crosses data near lower Q and overpre-dicts high Q	Highly underpre-dict	Highly underpre-dict	Fits data	Highly over-predicts
			Fits data	Fits at high Q, underpre-dicts at low Q			Fits data	Fits at high Q, underpre-dicts at low Q
Halfmoon Creek	Overpre-dict	Cross data at low Q; overpre-dict at high Q	Overpre-dicts high Q but fits low Q data	Crosses data at low Q; overpredicts at high Q	Underpre-dict but fit data at highest Q	Underpre-dict but fit data at highest Q	Overpre-dicts high Q but fits low Q data	Crosses data at low Q; overpredicts at high Q
			Overpre-dicts high Q but fits low Q data	Highly over-predicts			Overpre-dicts high Q but fits low Q data	Highly over-predicts

Note that the structure of Table 24 is repeated in Table 25 and Table 26.

transport better, while for bedload trap samples, transport predictions from a local slope gradient fared slightly better[35].

[35] *When computed from a reach-averaged slope, the P-K equations crossed measured Helley-Smith data from Halfmoon and Hayden Creek at low flows and overpredicted them at high flow, while transport rates measured with bedload traps were highly overpredicted (Figure 30). At Little Granite Creek, the P-K equations underpredicted Helley-Smith transport rates but predicted bedload trap measurements at Little Granite Creek quite well (Figure 30 c and d). When computed from the local water surface slope, transport predictions from the P-K equations decreased by orders of magnitude. At Little Granite Creek, this lead to a severe underprediction of transport rates measured with both bedload traps and the Helley-Smith sampler (Figure 31 a and d). For Halfmoon Creek, it caused an underprediction of low transport rates, but the trend for unmeasured samples at higher flows was predicted quite well, both for bedload trap and Helley-Smith samples (Figure 31 e and f). At Hayden Creek, the P-K equations also extended the trend of the unmeasured Helley-Smith samples at very high flow (Figure 31 a), while bedload trap samples are predicted acceptably well (Figure 31 b).*

3.4.3.2 Transport relationships from site-calibrated approach

Compared to the P-K equations, transport relationships from the site-calibration procedure are shifted sideways and vertically. However, they remain as curved as the P-K equations (Section 3.4.3.1) and therefore cannot correspond perfectly with measured, straight transport relationships. Nevertheless, the transport relationship predicted from the site-calibration yielded a better fit with measured bedload data than the P-K equations for all three streams in this study (Figure 30, Figure 31). Whether the local or reach-averaged water surface slope does not matter much for the transport relationships computed from the site-calibrated approach, and almost identical predictions were predicted for both slopes.

Better fit for bedload trap samples than for Helley-Smith samples

Transport relationships predicted from the site-calibrated approach generally fit better with transport rates measured by bedload traps than the Helley-Smith sampler (Figure 30, Figure 31). Transport rates from a Helley-Smith sampler increase at a slower rate with discharge than those from bedload traps. In the three study streams, exponents of bedload transport rating curves are 2.4 and 3.9 for Helley-Smith samples (typical of mountain gravel-bed streams) while bedload trap transport relationships have exponents of 7.6 to 16.7. The relatively flat increase of Helley-Smith measured transport rates can generally not be well described by a Parker-type bedload equation. The site-calibrated approach, with a similar shape as the P-K equation, also predicts a steeply increasing transport relationship that typically passes through the lower portion of measured Helley-Smith transport rates. Transport rates at flows below the intersection point are much underpredicted, while those above the intersection point are highly overpredicted. If the intersection point lies near the upper portion of measured flows, the site-calibrated approach predicts the trend of (unmeasured) transport rates for very high flows reasonably well, while highly underpredicting transport rates at low and moderate flows.

The steeper transport relationships obtained from bedload traps can generally be better matched by the site-calibrated approach, and a good fit is obtained with transport rates measured at Hayden Creek and Little Granite Creek. At Halfmoon Creek, the site-calibration approach overpredicts bedload trap transport rates measured at the highest flows.

Sample selection affects calibration results

The site-calibration procedure is sensitive to the specific bedload samples used for calibration, thus guidance on the selection of calibration samples in the BAGS manual would be useful. The original sets of calibration samples were evenly distributed over the range of measured flows, while the final sets emphasized samples collected at higher flows. Using highflow samples for site-calibration resulted in a right-shift of the site-calibrated transport relationship and a better fit with measured data, particularly to transport rates measured by bedload traps.

Unexpected results for Halfmoon Creek

For the Helley-Smith data, the calibration procedure at Halfmoon Creek yielded unexpected results. By oversight, one of the original 10 calibration samples was unrepresentative. It was collected at low flow but contained one 32-mm particle, while the second largest particle size was 4 mm with no particles in between these two sizes. The 32-mm particle raised the D_{50} particle size of the sample to 27 mm, while all other samples had D_{50} sizes in the sand range. Including this odd sample, the 10 original calibration samples produced a transport relationship for the site-calibrated approach that passed through the lower portion of the measured Helley-Smith bedload data. To correct the oversight, the unrepresentative sample was exchanged by a neighboring sample that had no gaps in the size distribution. The resulting transport relationship overpredicted measured Helley-Smith transport rates by several orders of magnitude. Trying to improve the fit, 5 and then 9 samples collected at the highest flows (i.e., below 80% Q_{bkf}) were added to the 10 calibration samples (that included the exchanged sample). The overprediction could not be revoked. Even adding the unrepresentative sample back to 19 samples did not change the result. The one unrepresentative bedload sample with the lone 32 mm particle as part of 10 calibration samples caused the predicted transport relationship to pass through the measured data, while omission of the unrepresentative sample produced absurdly high transport rates.

Effect of bedload particle-size distribution

To investigate the reason for these peculiar results, a closer look was taken at the particle-size distributions of the calibration samples. Bedload samples collected with a Helley-Smith sampler at Halfmoon Creek contained large amounts of sand and fines such that the sample D_{50} size did not exceed 4 mm, even at the highest sampled flows of 80% Q_{bkf}. The reason for the fine bedload is the granitic lithology of the Halfmoon Creek watershed, as well as the relatively low flows that remained below 80% Q_{bkf}. The one 32-mm particle in the unrepresentative sample contributed 96% of the sample weight and caused a large sample D_{50} size of 27 mm. When the 10 original samples contained the unrepresentative sample, it provided at least one sample with a D_{50} size significantly larger than 4 mm. Apparently, one sample with a large D_{50} size was necessary to produce a "reasonable" result, i.e., one that made the predicted transport rates at least pass through the measured data. However, when the unrepresentative sample was added to 19 samples, its influence was not effective, and the prediction remained overly high.

These results suggest that the site-calibrated approach is not suited to streams that transport a large amount of fines, generated from either a granitic lithology or a disturbed watershed. In the Klamath Falls study—where the methodology was developed—most streams had a volcanic lithology that probably did not produce large amounts of fines.

Unexpected values of exponents and τ^*_{r50}

The site-calibration approach computes site-specific values for the exponent of the P-K equation and for τ^*_{r50} (Table 25) that improve the predicted transport relationship compared to the uncalibrated P-K equations. To evaluate whether the computed values of the exponent and τ^*_{r50} were related to the degree of fit obtained between predicted and

measured transport rates, computed values are compared against the constants used in the P-K equation, as well as between sampling devices, stream gradients, sample selections and among streams.

Table 25: Values for the negative P-K exponent and the dimensionless reference shear stress obtained from computations based on **reach-averaged** and the **local** water surface stream gradients.

Stream	Sample selection	Reach-averaged water surface slope				Local water surface slope			
		P-K neg. exponent		Dimensionless shear stress τ^*_{r50}		P-K neg. exponent		Dimensionless shear stress τ^*_{r50}	
		HS	Traps	HS	Traps	HS	Traps	HS	Traps
Hayden Creek	Orig. selection	0.0316	0.0135	0.0941	0.136	0.0301	0.0141	*0.0540*	*0.0815*
	Final selection	0.0244	0.0111	0.128	0.146	0.0216	0.0116	0.0770	*0.0888*
Little Granite Creek	Orig. selection	0.0354	0.0112	0.0547	0.0799	0.442#	0.0115	*0.0955*	*0.0438*
	Final selection	0.0239	0.0114	0.0755	0.0811	*0.0349*	0.0119	*0.0423*	*0.0445*
Halfmoon Creek	Orig. selection	0.0245	0.0150	0.0871	0.114	0.0213	0.0158	*0.0487*	*0.0648*
	Final or dismissed select.	3.7 - 4.4#	0.0137	3.5 - 3.7#	0.118	2 - 2.5#	0.0143	4.2 - 4.5#	0.0669
Mean for all three streams	Final selection	0.0243*	0.0121	0.0969*	0.115	0.0259*	0.0126	*0.0560**	*0.0667*

In the last four columns, values printed in *italics* indicate moderate change, while standard print is used for small or insignificant change.
unreasonable values
* excluding unreasonable values

According to Parker and Klingeman (1982), the value of the exponent (Eq. 5) is (-)0.982, and similar values were obtained in the Klamath Falls study[36]. Several field studies have reported values between -0.4 and -0.8 (see footnote 28). None of the values obtained for exponents in this study was close to (-)0.982, but yielded on average 0.024 for the Helley-Smith sampler and 0.012 for bedload traps. As a value of (-)1 indicates perfect equal mobility, values close to 0 in this study indicate the absence of equal mobility and strong size-selective transport. Exponents larger than (-)1 such as those produced from the highly overpredicted transport rates at Halfmoon Creek are not defined.

Values of the dimensionless reference shear stress τ^*_{r50} (Eq. 4) obtained in this study averaged 0.097 for the Helley-Smith sampler and 0.115 for bedload traps when computations were based on the reach-averaged water surface slope. These values are

[36] *The range of values for the Klamath Falls study was -0.907 to -0.974 with a mean of -0.941(Bakke et al. 1999). The exponent is generally negative, however, some publications report the value without the negative sign and the BAGS program is one of them.*

higher than the value of 0.0375 derived by Parker and Klingeman (1982) for subarmor sediment collected at Oak Creek and indicate poorly erodible beds for the streams in this study. When the local slope was used for the computations, the values dropped to 0.056 for Helley-Smith samples and to 0.067 for bedload traps, indicating a somewhat higher erodibility. The site-calibration responded to the decreased slope with lower values for τ^*_{r50} (i.e., suggesting higher bed erodibility), but oddly, the supposedly less stable bed did not then result in an increase in predicted transport rates. Exponents of the P-K equation were less affected by the difference between a reach-averaged and a local slope. Exponents for the bedload traps samples were just slightly higher compared to those from a reach-averaged water surface slope, while most of the exponents for the Helley-Smith sampler decreased.

Exponents of the P-K equation for bedload traps were always slightly lower than for Helley-Smith samples, while values for τ^*_{r50} were slightly higher. Transport rates from bedload traps thus suggest a higher tendency for selective transport than Helley-Smith transport rates, and slightly higher bed stability.

Compared to the original selection of calibration samples, the final selection generally shifted the transport relationships towards the right and down, such that lower transport rates were predicted for a given flow. This increased the values for τ^*_{r50} (suggesting higher bed stability), while the exponent tended to decrease (suggesting higher size selectivity).

3.4.3.3 Fractional transport rates

The number of size classes for which the BAGS program computed fractional transport rates varied between samplers and between streams for reasons unknown. For Helley-Smith samples, the BAGS program provided fractional transport rates in 16 size classes of 1-phi increments, starting at the 0.25-0.5 mm size class and ending with 6 unnamed size classes beyond the 126-256 mm class for Hayden and Halfmoon Creeks. Assuming a regular progression in 1-phi increments, this would mean the BAGS program predicted transport for particles larger than 16 m! At Halfmoon Creek, transport assigned to the 6 unnamed size classes is miniscule, but at Hayden Creek, transport rates in the 6 highest size classes are similar to those in the other size classes, meaning that the predicted boulder transport up to the size of a house comprises a good third of the total transport. Although this might sound high, reducing total transport rates by the alleged boulder transport would be barely noticeable in the plotted log-log transport relationships of Figure 30a and Figure 31a. For Helley-Smith samples at Little Granite Creek, fractional transport rates were given in 17 size classes of 0.5 phi increments, starting at 2-2.8 mm and ending at 360-512 mm.

When bedload trap samples were used for the site calibration, fractional transport rates were given in 10-11 size classes of 1 phi, starting at 0.25-0.5 mm at Hayden and Halfmoon Creek, and ending at 128-256 mm or 1 unnamed size class coarser. At Little Granite Creek, there were 11 size classes of 0.5 phi, starting at 2-2.8 mm and ending at 64-90 mm.

The reasons for these vast differences are unknown. Bedmaterial and bedload-size distributions were entered in the same size classes for all three streams (1-phi increments for sand and 0.5 phi increments for gravel). The entries started at 0% finer for the 0.125-0.25 mm size class for transport predictions based on Helley-Smith samples and at 0% finer for the size class 4-5.6 mm for those based on bedload trap samples. The size distributions extended to either 180-256 or 256-360 mm for bedmaterial, but varied of course for bedload samples. Whether the differences in the reported number and width of size classes for fractional transport rates were comparatively inconsequential quirks of the BAGS program or had some meaning and effect could not be determined, but they did not increase confidence in computed results.

3.4.3.4 Threshold flows for framework gravel based on 2% criterion

For Hayden and Halfmoon Creek that had framework gravels of 45 mm, fractional transport rates in the 1-phi class of 32-64 mm represented framework gravels. For Little Granite Creek, the framework gravel of 32 mm was represented by the fractional transport rates of the 0.5-phi size class 32-45 mm[37]. Thus, the width of the size class that was evaluated for exceeding a threshold transport rate differed among the three streams.

The site-calibration procedure takes as the channel maintenance flow the flow in which the transport rate of the framework gravel-size class comprises at least 2% of the total bedload transport rate. This is intended to indicate a small but measurable transport rate for the framework gravel size class. The 2% criterion was arbitrarily set in the Klamath Fall study. The predicted fractional transport rate representing the framework gravel size class was compared to 2% of the total transport rate for the study streams, except for cases in which the site-calibrated approach had provided completely unreasonable transport relationships that overpredicted measured transport rates by orders of magnitude.

The 2% criterion turned out to be unsuitable for this study. For transport relationships from Helley-Smith samples, the 2% criterion indicated threshold flows for framework gravel in a few cases. At Hayden Creek, a threshold flow was indicated at 32% Q_{bkf} when computations were based on a reach-averaged stream gradient, and at 26% Q_{bkf} when based on a local gradient. However, this was the case only for the original selection of calibration samples (Table 26). No threshold flows were obtained for the final selection of calibration samples although the transport relationships predicted from them provided a better fit with measured data. Similarly, computations based on the original selection of calibration samples and a reach-averaged slope indicated a threshold flow at 40% Q_{bkf} for Little Granite Creek, but none for the final selection.

When transport was predicted from bedload trap samples, fractional transport of the 32-64 mm or the 32-45 mm size class amounted to **more** than 2% of the total transport rates at **all** flows and thus failed to produce threshold flows for framework gravels (Table 26).

---

[37] *Future versions of the BAGS program should predict fractional transport rates in the same size classes as the bedmaterial and bedload entries. A 1-phi resolution for channel maintenance flows seems overly wide because flows required for moving particles larger than 32 and just below 64 mm are quite different.*

The 2% criterion did also not indicate threshold flows for Halfmoon Creek, regardless of how transport rates were computed.

Table 26: Threshold flows indicated from the site-calibrated approach for the size class 32-64 mm for the three study streams.

Stream	Sample selection	Reach-averaged water surface slope				Local water surface slope			
		Q_{crit} (m^3/s)		Q_{crit} (% Q_{bkf})		Q_{crit} (m^3/s)		Q_{crit} (% Q_{bkf})	
		HS	Traps	HS	Traps	HS	Traps	HS	Traps
Hayden Creek	Orig. selection	0.61	-	32	-	0.49	-	26	-
	Final selection	-	-	-	-	-	-	-	-
Little Granite Creek	Orig. selection	2.29	-	40	-	-	-	-	-
	Final Selection	-	-	-	-	4.79	-	85	-
Halfmoon Creek	Orig. selection	-	-	-	-	-	-	-	-
	Final or dismissed selection	-	-	-	-	-	-	-	-

None of these three threshold flows is within a reasonable range. For one thing, they were only obtained from original selections of calibration data (that had poorer fits), while none were obtained from final selections of calibration data. Furthermore, Helley-Smith samples collected in the study streams showed that flows between 26 and 40% Q_{bkf} are not competent to transport framework gravels that require flows of about 94 and 85% Q_{bkf} at Hayden and Little Granite Creek, and at 66% at Halfmoon Creek[38] for transport (Section 3.5)

The only threshold flow for framework gravels indicated from the site-calibrated approach in this study that was within the expected range occurred at 85% Q_{bkf} for the final selection of Helley-Smith samples at Little Granite Creek and when transport rates were computed using the local slope. A value of 85% Q_{bkf} corresponds to the commonly held belief that channel forming gravels start to move at approximately 80% of bankfull flow (Whiting 2002).

The question arises why the Klamath Falls channel maintenance procedure fails to indicate threshold flows for framework gravel in almost all cases (Table 26). The reasonable result for Little Granite Creek (but only for the special case that calibration samples were from the Helley-Smith sampler and that a local water surface slope was used) appears to be a random occurrence among the otherwise absent or poorly

[38] *An exception is the occasional involuntary pick-up of medium or large gravel particles in the Helley-Smith sampler at low flows. Such samples are easily identified because several size classes below the pick-up particle contain no sediment.*

explainable results for the other two streams. It may be the case that the Klamath Falls channel maintenance procedure is not applicable to streams other than those used at the Klamath Falls study. It is more likely, however, that the Klamath Falls channel maintenance procedure was not properly implemented in the BAGS program.

3.4.3.5 Attempts to explain the poor success of site-calibrated approach to indicate threshold flows

An attempt was made to find out why the site-calibrated approach did not produce threshold flows. The first steps were to examine if and how the few indicated threshold flows were tied to factors within the study, such as (1) the degree to which transport rates from the site-calibrated approach fitted measured transport rates, (2) the values obtained for *exp* and τ^*_{r50} from the site-calibrated approach, and (3) the use of different sampling devices. Other factors, such as (4) the physical characteristics of the streams in this and the Klamath Falls study, were considered as well.

Degree of fit with measured transport rates

One might assume that threshold flows become better discernable when transport relationships computed from the site-calibrated approach fit well with measured bedload transport rates. Comparison of Table 24 with Table 26 shows that this is not always the case. Hayden and Halfmoon Creek had acceptable fits of predicted with measured transport rates, but this did not lead to discernable threshold flows. Threshold flows indicated for Hayden and Little Granite Creek occurred when transport rates from the site-calibrated approach underpredicted measured data at low flows and overpredicted them at high flow. However, not all cases with this kind of a relationship lead to an indicated threshold flow. Thus, the degree of fit between measured and predicted transport rates did not affect computed threshold flows.

Values of exponents and τ^*_{50}

Comparison of Table 25 with Table 26 shows that threshold flows for framework gravels only occurred when values for the exponent were relatively high (i.e., 0.030 to 0.035). Those values were only obtained from original selections of Helley-Smith samples, while exponents obtained for the final selection of Helley-Smith and bedload trap samples averaged 0.024 and 0.012, respectively. The occurrence of threshold flows for framework gravel was not tied to particular values of τ^*_{50}.

Different bedload sampling devices

The absence of threshold flows for bedload trap samples is perplexing, particularly considering that transport rates predicted from the site-calibrated approach corresponded better to transport rates measured with bedload traps than with a Helley-Smith sampler. Which factor, if not a good fit with measured data, serves as a prerequisite for an indication of threshold flows? One could speculate that the absence of threshold flows for bedload trap samples might be due to the lower exponents (see above) or that the fact

that sediment collected in bedload traps is larger than 4 mm and required the subarmor-size distribution to be truncated at 4 mm had something to do with it.

Streams in this study too different from the Klamath Falls study

Because none of the above factors clearly explained the poor success of the site-calibrated approach to provide threshold flows (for a 2% threshold transport rate), the possibility remains that the streams in this study are too different from those in the Klamath Falls study. Streams in this study are steeper and coarser than those studied in Oregon, and one has a different lithology.

Steeper gradients

The streams in this study were not only generally steeper than those in the Klamath Falls study but reach-averaged water surface gradients that were twice as steep as the local gradients. By contrast, Dawdy (1995) had specified that the sampling site should be located within a reach without changes in stream gradient, however, an even stream gradient along the study reach had not been a selection criterion for streams in this study.

Coarser beds

All streams in this study have relatively coarse beds and contain small boulders in the armor and the subarmor layer. None of the streams met the conditions specified by Dawdy (1995) for the site-calibrated approach: that (1) bedmaterial at the sampling sites should not contain particles larger than those moveable at bankfull flow, and that (2) streams in which the largest particles had a diameter of half the bankfull water depth were unsuited for the site-calibration approach. Hayden Creek in particular has a rough streambed dominated by either low-gradient step-pool morphology or reaches in which flow shoots through rough and laterally confined channels, while wide and low gradient stream section are relatively scarce.

Higher supply of fines

Halfmoon Creek, for which no threshold flows were indicated, transported a large amount of fines at low and moderate flows that were collected in the Helley-Smith sampler. The Klamath Falls streams likely did not have high supplies of fines because those streams have mainly volcanic watersheds.

Did something go wrong with the computations?

Questions, uncertainties and inconsistencies that cast doubt on the accuracy of the computed results have been reported throughout this study. There is a possibility that something went wrong with the computations and caused the poor success of the site-calibrated approach to indicate threshold flows (for the 2% criterion). However, rechecking computations did not uncover reasons for inconsistencies in reported results[39].

---

[39] *It would be quite helpful if the BAGS guidelines contained a few sample data sets that explain why exponents and τ^*_{r50} have particular values and how these are affected by different stream characteristics and selections of different calibration samples.*

3.4.3.6 Site-specific threshold transport rates and resulting threshold flows

The site-calibrated approach did not indicate threshold flows because transport of the framework gravel size class exceeded 2% of the total transport rates for all flows. This raised the possibility that threshold flows could be identified if the transport threshold criterion was set higher. Taking the idea of site-calibration a step further, threshold transport rates were increased in 1% increments from the original 2% to 10%. Threshold flows were then re-evaluated for all streams, the two sampling devices, original and final selection of calibration samples, as well as reach-averaged and local stream gradients.

Threshold transport rates between 6 and 8% of the total transport rate yielded threshold flows for bedload trap samples at Hayden and Little Granite Creek (Figure 32 a and b). At Halfmoon Creek, the range was 5 to 7% (Figure 32c). These threshold flows generally increased with increasing threshold transport rates. Because the threshold transport rate is to be small but measurable, threshold flows that resulted from the smallest identifiable threshold transport rate were selected as representative in this study. Considering only the final selections of calibration samples, and averaging the results for the reach-averaged and the local slope (that did not differ much from each other), threshold flows were indicated at 120 and 111% Q_{bkf} for bedload trap samples at Hayden and Little Granite Creek, respectively, and at 50% Q_{bkf} at Halfmoon Creek (see circled values in Figure 32).

For final sets of Helley-Smith calibration samples, threshold flows could be identified when threshold transport rates were set to 2, 3 or 4% of the total transport rate. Again, considering only the final selection of calibration samples and the threshold flows resulting from the smallest identifiable threshold transport rate, threshold flows for Hayden and Little Granite Creek were 70 and 85% of bankfull flow, and 23% for Halfmoon Creek. These values for bedload traps and the Helley-Smith sampler are similar to those obtained from the breakpoint analysis (Section 3.2.4.5). However, the question remains whether the site-specific selection of threshold transport criteria is permissible in the site-calibrated approach.

3.4.4 Summary and Conclusion

3.4.4.1 Overview of the study outcome

This study computed bedload transport relationships using the site-calibrated approach for three mountain gravel-bed streams for which good data sets of bedload transport rates and bedmaterial-size distributions were available. Between 10 and 20 bedload samples were selected for the site-calibration from the total 55 to 179 samples collected with bedload traps and the Helley-Smith sampler per site. The bedmaterial was characterized from several large samples of the armor and subarmor layers.

Transport relationships computed from the site-calibrated approach fit measured transport rates better than those predicted from the uncalibrated bedload equations by Parker and Klingeman (1982) and Parker et al. (1982). Site-calibrated transport relationships correspond better to the relatively steep transport relationships measured with bedload

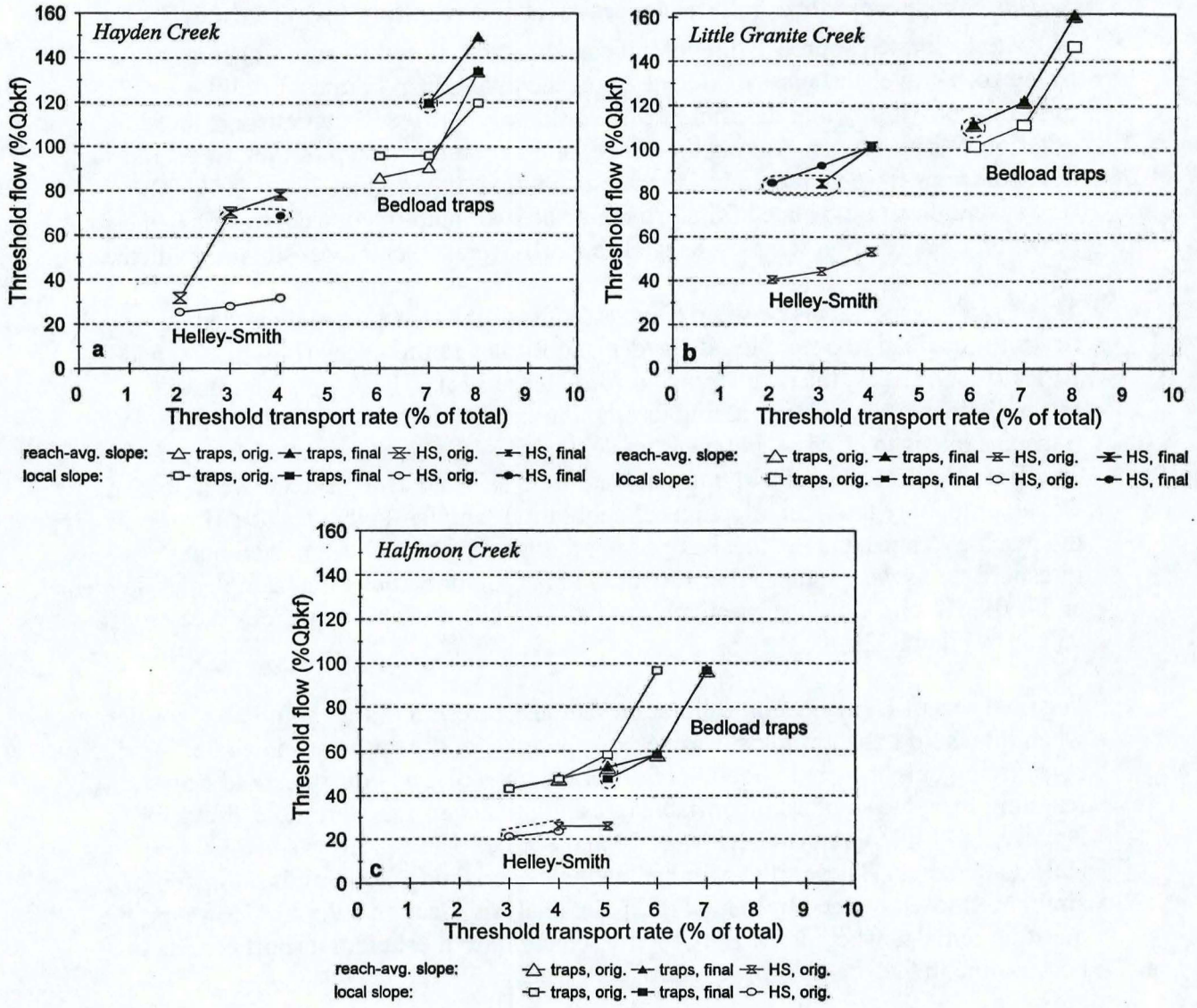

Figure 32: Threshold flows in percent of bankfull computed for threshold transport rates between 2 and 10% for bedload trap and Helley-Smith samples at the three study streams. The threshold flow resulting from the smallest threshold transport rate is circled by a stippled line in each plot.

traps than the flatter ones obtained from Helley-Smith samples. Whereas the degree of fit was not significantly affected by whether the site-calibrated approach used the relatively gentle local or a steeper reach-averaged stream gradient, the fit to measured transport rates was generally improved when the selected calibration samples emphasized samples collected at high flows. However, if the bedload D_{50} particle size of the calibration samples does not increase with increasing flow, a fit with measured transport rates is not obtained. The site-calibrated approach is not suited for streams in which the transport of fines dominates the bedload particle-size distribution—a phenomenon common in streams with granitic or disturbed watersheds.

By using calibration samples, the site-calibrated approach tunes the values of the exponent (Eq. 6) and τ^*_{r50} (Eq. 5) to each site. Values obtained for τ^*_{r50} in this study ranged between 0.04 and 0.13. They were thus higher than the P-K value of 0.0374 and indicated less erodible beds. Values for the exponent generally fell between (-)0.01 and (-)0.04 in this study and were far removed from the value of (-)0.972 assumed in the P-K equations. Values as low as -0.4 have been reported in the literature, but none as low as (-)0.1 or less. Whether the extremely low values in this study indicate the complete absence of equal mobility transport in the study streams or some hidden error in the computations could not be identified.

Bakke et al. (1999) defined the channel maintenance flow as the flow at which the framework gravel size-class comprises 2% of the total transport rate. This threshold criterion was not suitable for this study because transport within the framework gravel size class commonly exceeded 2% of the total transport for all flows. No threshold flows were predicted when bedload trap samples were used for the site-calibrations, none for Halfmoon Creek, and for only a few of the Helley-Smith samples. Of those indicated for Helley-Smith samples, only the one at 85% Q_{bkf} obtained at Little Granite Creek can be considered a reasonable result. The site-calibrated approach thus failed to provide threshold flows in a reliable way for this study.

When threshold transport rates for framework gravel were increased by a few percent, threshold flows could be identified for each site and both sampling devices. Considering only the threshold flow resulting from the smallest threshold transport rate at a given site and only results obtained from the final selection of calibration samples, threshold flows occurred at 120 and 111% Q_{bkf} for bedload trap samples at Hayden and Little Granite Creek, and at 50% Q_{bkf} at Halfmoon Creek. Threshold flows were significantly lower for Helley-Smith samples: 70 and 85% Q_{bkf} at Hayden and Little Granite Creek, and 23% Q_{bkf} at Halfmoon Creek. Threshold flows for both samplers are similar to breakpoint flows obtained from the various versions of the breakpoint analysis (Section 3.2.4.5).

3.4.4.2 Why not plot fractional transport and flow competence curves directly from measured bedload samples?

The large number of problems and inconsistencies leads one to wonder how accurate transport relationships and threshold flows predicted from the site-calibrated approach as implemented in the BAGS program are. Considering that a large number of calibration bedload samples or a careful selection of samples from a large data pool improves the calibration result, collecting more than the absolutely necessary 10 to 20 samples over a wide range of flows is advisable. If, however, a study has collected 30-50 bedload samples over a wide range of flows (e.g., between 30 and 120% of Q_{bkf}), the samples themselves should suffice to plot fractional rating curves and the flow competence curve. Both relationships can be employed to compute the critical flow for framework gravel directly. The detour of modeling transport relationships, even when applying site-calibration, is not likely to add accuracy to the computed result. For one thing, the modeled, curved transport relationships (in log-log scale) cannot describe straight transport relationships that are typically measured in mountain gravel-bed streams.

Furthermore, the site-calibration approach within the BAGS program is time-consuming and sometimes produces unexplained results that cast doubt on the accuracy of the obtained results. Given all this, time might be spent more advantageously in the field collecting more bedload samples than by attempting to tweak the predictions of transport relations from the site-calibration approach and decipher the meaning of the often strange results.

3.5 Measured mobility of coarse gravel bedload

Annual or biennial mobility of large gravels in gravel- or cobble-bed streams is considered necessary for maintaining the channel form. It is therefore the aim of channel maintenance flow procedures to determine the flows at which channel forming or stabilizing particles start to move. Unfortunately, science has not determined the exact particle size that needs to be moved for channel maintenance, and that size likely differs between streams. Whiting and King (2003) proposed that the particle size to be moved is the threshold size between supply and hydraulically controlled bedload transport as determined from the collapse size analysis. Bakke et al. (1999) proposed that the threshold between framework and matrix gravel was the particle size that needed to be moved for channel maintenance. Other possible candidates are the surface or the subarmor D_{50} particle sizes, or the surface D_{16} to D_{25} size as suggested by Ryan et al. (2005). This study has high-quality data sets of measured bedload transport rates and its particle sizes sampled at various flows using a Helley-Smith sampler and bedload traps at the three study streams. These data offer a good opportunity of comparing the flows at which the various proposed critical particle sizes for channel maintenance start to move.

3.5.1 Introduction

Mobility of a specific gravel particle size can be computed in two different ways. One approach is based on the flow at which some small mass of gravel in the i^{th} size class is transported, and it requires computing fractional bedload transport rating curves from measured field data. The other approach is based on a relationship of the largest transported particle size and the flow at which the sample was collected and requires setting up a flow competence curve.

Fractional bedload transport rating curve

Fractional transport rating curves are obtained from plots of transport rates in the i^{th} size class (Q_{Bi}) versus flow (Q). Fitted power function rating curves specify the Q_{Bi} *vs.* Q relationships and separate relationships are required for each size class. The flow at which a preset transport rate for a specified size class necessary for channel maintenance (e.g., framework gravels or subarmor D_{50} size) is exceeded is then considered the channel maintenance flow. The problem with this approach is the definition of a threshold transport rate in terms of a specific number or mass of particles collected in the i^{th} size class within a given sampling time. For one thing, the exact amount of a small but measurable transport rate in terms of number or mass of particles per time is still debated[40], thus any chosen value could be considered arbitrary. Furthermore, what constitutes a "reasonable" time unit for threshold transport rates is sampler-specific and tightly connected to the sampler deployment time. For Helley-Smith samples that are usually collected over 30 to 120 seconds, a likely threshold transport rate might be one or a few particles of the i^{th} size class collected within a 30 to 120 second interval. For bedload traps that are typically deployed for about 1 hour, a likely threshold transport rate would be 1 or a few particles collected within 1 hour. Both threshold transport rates are

[40] *Bakke et al. (1999) suggested the 2% criterion (Section 3.4.3.4); Parker and Klingeman (1982) used the criterion of W* = 0.002.*

quite different, and they remain different even when expressed in the same unit of time (Bunte et al. 2004).

Flow competence curves

Flow competence curves are obtained from plots of the largest bedload particle size class collected in a sample (D_{max}) and the flow (Q) at which the sample was collected. A fitted power function rating curve specifies the D_{max} *vs.* Q relationship where D_{max} is the dependent and Q the independent variable. Flow competence curves, like fractional rating curves, are affected by the sampling device. Samplers with large openings and long deployment times provide a better chance for collecting large and infrequently moving bedload particles than those with small openings and short deployment times. Other sampler characteristics have effects as well. A sampler that is set directly on a bed picks up particles involuntary, while a plate between the sampler and the bed prevents this from happening (Bunte et al. 2005). However, in highly erodible, fine-gravel beds, scour at the plate can also disturb the interaction between bedload transport and the sampler entrance (Bunte and Swingle 2006).

Wilcock (1988) suggested that the measured flow at which some small rate of transport for gravel of the i^{th} size class occurs (fractional transport rate) and the flow at which gravel particles of the i^{th} size class starts to be collected (flow competence curve) differ, and that the difference between the two threshold flows is due to imperfections in the way bedload is typically collected. Bunte et al. (2004) showed for two mountain gravel-bed streams that both methods of incipient motion computations yield similar results when samples were collected with bedload traps. However, bedload traps are not used in every study concerned with channel maintenance flows, and equality between the two incipient motion methods cannot be assumed.

This study selected measured flow competence curves as the method with the best potential for accurate estimates of the flows at which particles of a specified size class start to move in different streams. Both, fractional transport rates and the flow competence curves are affected by the sampling device and the sampling scheme, but the flow competence curve is the easier analysis because it requires only one relationship (D_{max} *vs.* Q) from which the flow that transports a specific particle size can be read whereas a number of separate relationships would have to be established for the fractional rating curve approach.

3.5.2 Methods

Two methods are available to evaluate the flow that entrains the largest mobile particle-size class: the flow competence curve and the curve of critical flow. Both methods use the same data, but while the flow competence curve plots D_{max} (y) versus the flow (Q) at the time of sampling (x), the critical flow curve makes the flow at the time of sampling the dependent variable (y), calls it Q_{crit} and plots it versus D_{max} (x). Exchanging the independent for the dependent variable is a questionable practice because it swaps cause and effect, but it allows the user a mathematically somewhat easier evaluation of the flow

that transports a specified particle-size class. In the absence of scatter in the relationship between D_{max} and Q, both methods would yield identical results, but as the relationship of D_{max} *vs.* Q is typically quite scattered, results from both methods differ, a fact that is generally not acknowledged in the literature. In order not to complicate matters of this study with a computational issue, this study uses only the flow competence approach[41].

3.5.2.1 Flow competence curve

The relationships between the largest bedload particle sizes (D_{max}) transportable by a given flow (Q) were evaluated using large data sets of bedload samples collected with the Helley-Smith sampler and bedload traps in the three study streams. Power function regressions in the form

$$D_{max} = a \cdot Q^{b} \quad (= \text{flow competence curve}) \qquad \text{(Eq. 6)}$$

were fitted to the data from the three streams and yielded flow competence curves where a is the coefficient and b the exponent. Solving the flow competence relationship for flow (Q_{mob}) provides the D_{max} particle size that can be mobilized by Q_{mob}. To do so, equation 6 needs to be rearranged and becomes:

$$Q_{mob} = \left(\frac{D_{max}}{a}\right)^{1/b} \quad (= \text{flow competence curve solved for } Q_{mob}) \qquad \text{(Eq. 7)}$$

3.5.2.2 Bias correction factor

To adjust for the inherent underestimation in the prediction of the y-estimate from a value of x in a power function relationship, the y-estimate needs to be multiplied by a bias correction factor (CF). Several factors are available (e.g., Ferguson 1986, 1987; Duan 1983; Koch and Smilie 1986). This study used the one by Ferguson (1987) that is defined as

$$CF_{Ferg} = \exp^{(2.651 \cdot Sy\text{^}2)} \qquad \text{(Eq. 8)}$$

where s_y is the standard error of the y-estimate and typically provided in a spreadsheet regression table. To predict the mobilizing flow for a D_{max} particle size, Eq. 7 needs to be appended to include the bias correction factor and becomes

$$Q_{mob} = \left(\frac{D_{max}}{a \cdot CF_{Ferg}}\right)^{1/b} \quad (= \text{flow competence curve solved for } Q_{mob}) \qquad \text{(Eq. 9)}$$

Note that when solving the flow competence curve for Q_{mob}, the bias correction factor decreases the predicted flow value.

---

[41] *Results from an analysis of critical flow curves ($Q_{crit} = f(D_{max})$) are available from the author upon request.*

3.5.3 Results

3.5.3.1 D_{max} *vs.* Q and fitted flow competence curves

The largest measured bedload particle sizes and the discharge at the time of sampling for the three study streams as well as the fitted flow competence curves are shown in Figure 33. The flow competence curves are considerably steeper and have larger exponents for bedload traps than for samples collected with the Helley-Smith sampler[42] (Figure 33 a and b; Table 27 and Table 28), and the flow competence curves from both samplers intersect. This means that according to bedload trap samples, the size of transported bedload particles increases at a faster rate with increasing flows than for Helley-Smith samples. The difference in mobilizing flows can be attributed to differences between the sampling devices. Helley-Smith samplers that are set directly onto the streambed tend to pick up small- and medium-sized gravel at flows that generally do not move those particles, while at high flows, the small Helley-Smith sampler opening, and the short sampling time provide less chance of collecting large and infrequently moving particles. By contrast, bedload traps that are installed on ground plates avoid involuntary particle pick up. The sampler openings are large enough to allow large gravel and small cobbles to enter, while the long sampling time gives infrequently moving particles a chance to be collected. Thus, flow competence curves from both samplers intersect, and curves the bedload traps suggest a lower mobility of small and medium gravel, but a higher mobility of large gravel compared to samples collected using a Helley-Smith sampler.

Table 27: Coefficients, exponents, and bias correction factors **for flow competence relationships fitted to Helley-Smith** samples collected at the three study streams.

Stream	Coefficients and exponents	r^2	Bias correction Factor
Hayden Creek	$D_{max} = 16.03 \cdot Q\text{^}0.716$	0.60	1.07
Little Granite Creek	$D_{max} = 4.87 \cdot Q\text{^}0.889$	0.46	1.23
Halfmoon Creek	$D_{max} = 6.86 \cdot Q\text{^}1.026$	0.59	1.08

Table 28: Coefficients, exponents, and bias correction factors **for flow competence relationships fitted to bedload trap** samples collected at the three study streams.

Stream	Coefficients and exponents	r^2	Bias correction factor
Hayden Creek	$D_{max} = 9.70 \cdot Q\text{^}1.74$	0.73	1.11
Little Granite Creek	$D_{max} = 0.11 \cdot Q\text{^}3.49$	0.67	1.11
Halfmoon Creek	$D_{max} = 3.88 \cdot Q\text{^}1.40$	0.57	1.09

[42] *Exponents of the flow competence curves for the Helley-Smith sampler in this study are similar to those determined by Whiting et al. (1999) for 6 streams in Idaho.*

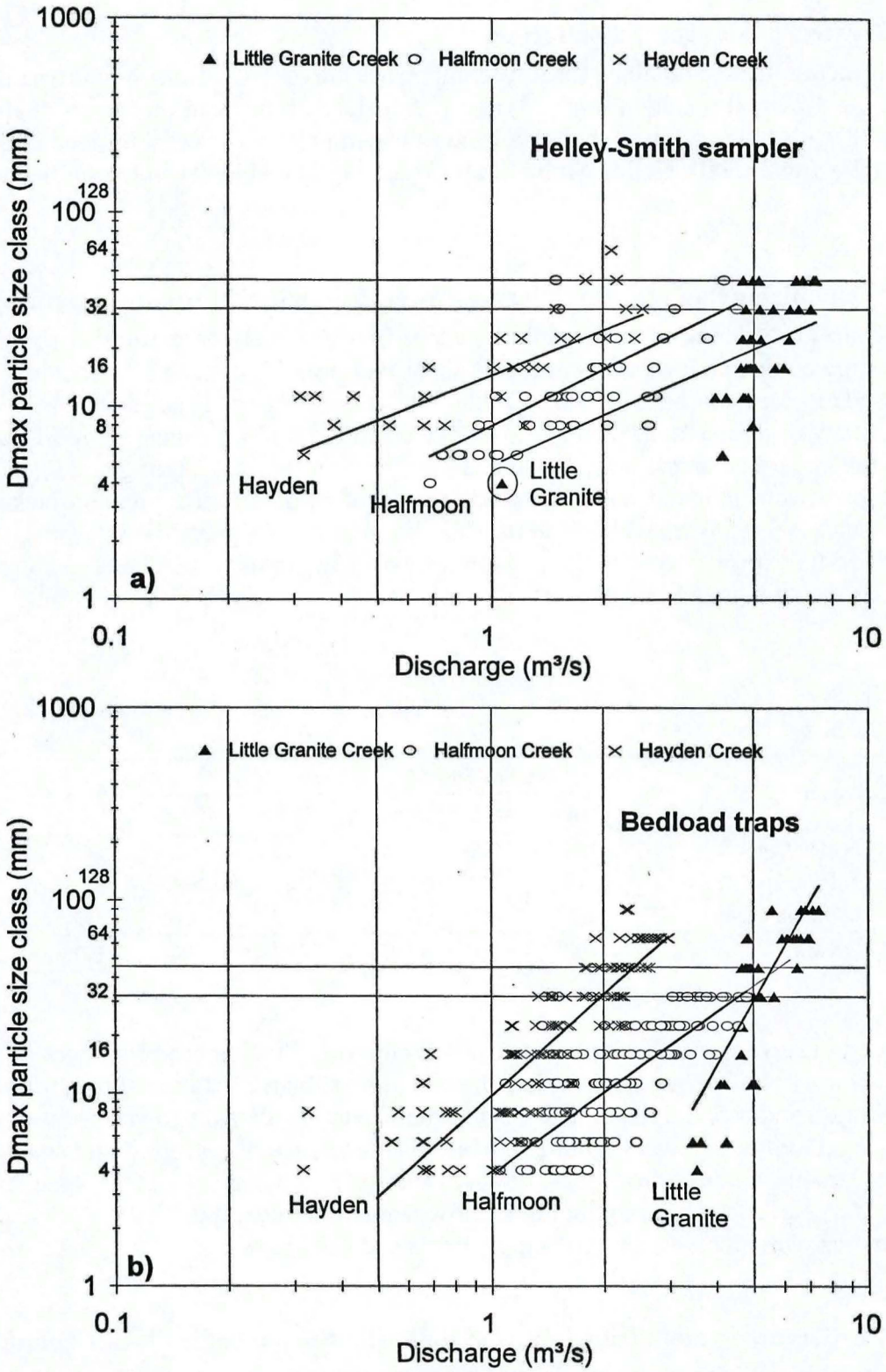

Figure 33: Flow competence curves: largest sampled bedload particle sizes (D_{max}) versus the flow at which the sample was collected from (a) the Helley-Smith sampler and (b) bedload traps at the three study streams. The fitted function for Helley-Smith samples at Little Granite Creek includes the large data set by Ryan and Emmett (2002) that has many data points between 1 and 4 m^3/s into which the apparent outlier data point near 1 m^3/s fits well.

3.5.3.2 Effect of bias correction factors

Bias correction factors obtained for flow competence curves from Helley-Smith samples are 1.07 to 1.23 in this study (Table 27) and 1.09 to 1.11 for bedload trap samples are (Table 28). Mobilizing flows predicted from flow competence curves thus need to be reduced by 7 to 23% for Helley-Smith samples (see Eq. 9) and by 9 to 11% for bedload traps.

3.5.3.4 Mobilizing flows for three coarse gravel sizes in the three study streams

To evaluate how measured gravel mobility varies between the three streams, mobilizing (Q_{mob}) were computed for three gravel particle-size classes 32, 45, and 64 mm and expressed as percent of bankfull flow (Table 29). The three particle sizes were selected because they cover the range of framework gravels in the study streams (Table 21), are within the range as collapse sizes (Section 3.3.3.1) determined by Whiting and King (2003) for streams in Idaho, and represent the range of particle sizes typical of the surface and subsurface (or subarmor) bedmaterial D_{50} size in mountain gravel-bed streams, i.e., these sizes are expected to be within the range of sizes important for channel maintenance flows in mountain gravel-bed streams.

Table 29: Mobilizing flows (in percent of bankfull flow) for three gravel particle-sizes (mm) in the study streams.

Stream	Helley-Smith			Bedload traps		
	32 mm	45 mm	64 mm	32 mm	45 mm	64 mm
Hayden Creek	124	200	326	97	118	145
Little Granite Creek	117	171	254	87	96	106
Halfmoon Creek	67	93	131	68	87	112
Average	102	154	237	84	100	121

Compared to Hayden and Little Granite Creek, Halfmoon Creek transports larger D_{max} particles for a specified % Q_{bkf} flow than the other two streams, both for samples from the Helley-Smith and bedload traps. Thus, Halfmoon Creek requires the lowest flows for mobilizing 32-64 mm gravel (Table 29), while Hayden Creek, the steepest and coarsest of the three streams requires the highest flows, again, for both samplers. It thus appears that steeper and coarser streams require higher flows for entraining a specified gravel size than streams with relatively low stream gradients and finer beds.

3.5.3.5 Difference in mobilizing flows for Helley-Smith and bedload trap samples

Results in Table 29 also show the effects of the two samplers on measured gravel mobility. Because the D_{max} particle size increases at a steeper rate with flow for samples from bedload traps than the Helley-Smith sampler (Table 27 and Table 28), bedload trap samples indicate lower entraining flows for coarse gravel than Helley-Smith samples. To better show the difference between the two samplers, the ratio of entraining flows

between the two samplers is plotted in Figure 34. At Hayden and Little Granite Creek, mobilizing flows for 64 mm particles indicated from bedload trap samples are less than half as large as those from Helley-Smith samples. The difference in results between the two samplers becomes less pronounced for gravels of 22 mm, and for smaller gravels, bedload traps indicate higher mobilizing flows than the Helley-Smith sampler. At Halfmoon Creek (where the low highflow and rather slow increase of the bedload D_{max} size with flow caused more scatter in the D_{max} *vs.* Q relationship), both Helley-Smith and bedload traps samples suggest similar mobilizing flows.

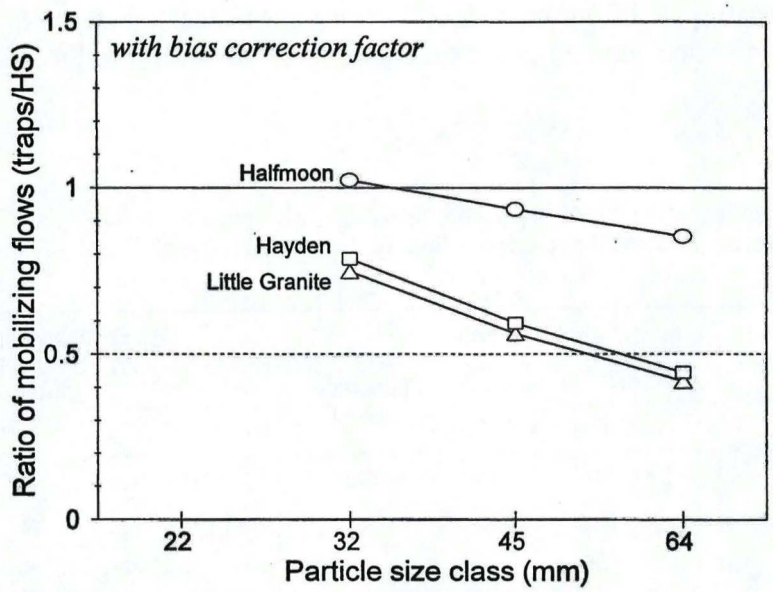

Figure 34: Ratio of mobilizing flows between bedload traps and the Helley-Smith sampler.

3.5.3.6 Mobilizing flows for surface and subarmor sizes as well as framework gravel

Channel maintenance flows do not necessarily refer to the same gravel sizes at different streams. More likely, channel maintenance flows are tied to the entrainment of some site-characteristic bedmaterial size, although there is little agreement yet as to what that size might be. Ryan et al. (2002) had suggested that the onset of Phase 2 transport was associated with the mobility of the subarmor D_{50} size. Ryan et al. (2005) suggested that Phase 2 transport falls together with the onset of motion of particles in the range of 16 to 32 mm which in the streams of that study constituted the surface D_{16} to D_{25} size. Whiting and King (2003) proposed that the threshold particle size between supply and hydraulically controlled bedload transport as determined from the collapse size analysis needs to be moved for channel maintenance (Section 3.3), whereas the Klamath Falls procedure (Bakke et al. 1999) proposed that the threshold between framework and matrix gravel was the particle size that needed to be moved for channel maintenance (Section 3.4).

Because site-specific particle sizes vary between streams, entraining flows for those bedmaterial sizes likely differ between streams as well and may be related to some stream

characteristic such as stream gradient, bankfull flow, sediment supply, or the degree of bed armoring. Such relatedness would help in the prediction of channel maintenance flows for different stream channels.

Mobilizing flows for various percentiles of the surface particle sizes[43], the D_{50} subarmor bedmaterial sizes, and framework gravel sizes (see Table 21 for the mm sizes of these sediments) were computed for both samplers for the three study streams (Table 30) and expressed in percent of bankfull flow. Collapse sizes are not included in this comparison because the analysis of collapse sizes did not appear suitable for the three study streams. Entraining flows computed from both samplers for the surface, subarmor D_{50} sizes varied between streams and between samplers, following patterns similar to those outlined above:

Table 30: Mobilizing flows (in percent of bankfull flow) for various percentiles of the surface and the D_{50} of the subarmor bedmaterial, as well as the lower limit of the framework gravel sizes in the three study streams.

Stream	Helley-Smith					Bedload traps				
	Surface			Subarmor	Framework	Surface			Subarmor	Framework
	D_{16}	D_{25}	D_{50}	D_{50}	gravel	D_{16}	D_{25}	D_{50}	D_{50}	gravel
Hayden Creek	28	56	206	146	200	53	70	120	104	118
Little Granite Creek	68	104	206	180	117	76	85	101	97	87
Halfmoon Creek	30	48	101	48	93	38	54	92	54	87
Mean, all streams	42	69	171	125	137	56	70	104	85	97
CV (%)	54	44	35	55	41	34	22	14	32	18

Comparison of entraining flows between different sediment sizes

Flows required for mobilization of the surface D_{16} and D_{25} sizes (Ryan et al. 2005) average 42 and 69% Q_{bkf} for the Helley Smith sampler and 56 to 70% Q_{bkf} for bedload traps. These flows would indicate that the channel maintenance flows needed to start at 40 to 70% Q_{bkf} which is relatively low, compared to the notion that channel maintenance flows should be in the neighborhood of 80 to 90% Q_{bkf}. A percentile in the neighborhood of the surface D_{40} might be more suitable.

Flows required for entraining surface D_{50} particles range between 101 and 206% Q_{bkf} for the Helley-Smith sampler and between 92 and 120% Q_{bkf} for bedload traps. If particles of the surface D_{50} size need to be entrained, channel maintenance flows set in (way) past bankfull flow which appears high. Flows required to entrain the subarmor D_{50} and framework gravel sizes take an intermediate position, averaging 125 and 137% Q_{bkf} for the Helley-Smith sampler and 85 to 97% Q_{bkf} for bedload traps.

[43] *The surface D_{50} sizes here refer to the vicinity of the sampling sites, not to the reach-averaged size.*

Flows required to entrain the surface D_{50} and framework gravels are more similar among the three streams than those for the subarmor D_{50} and surface D_{16} sizes. The relatively low variability of entraining flows for the surface D_{50} and framework sizes among sites perhaps suggests that these two site-specific gravel sizes need to be entrained for channel maintenance, but a much larger number of streams would have to be evaluated to confirm this possibility.

Comparison of entraining flows between the three study streams
Entraining flows for almost all sediment sizes described in Table 30 are higher for Hayden and Little Granite Creek than those for Halfmoon Creek. This hints at higher entrainment flows being required for steeper and coarser streams both for absolute as well as site-characteristic gravel sizes.

Comparison of entraining flows among the two samplers
Entraining flows vary strongly between the two samplers and are typically lower when measured using bedload traps than those based on Helley-Smith samples, except for the D_{16} and D_{25} percentiles of the surface sediment. The difference in entraining flows among the two samplers is most pronounced for Hayden and Little Granite Creek where the D_{max} *vs.* Q relationships are well defined and steep. For Halfmoon Creek with its higher but flatter and less well defined D_{max} *vs.* Q relationship, both samplers indicate similar entraining flows.

3.5.4 Summary and Conclusion

Flow competence curves were fitted to samples from bedload traps and the Helley-Smith sampler at the three study streams. The D_{max} *vs.* Q relationships were better developed (steeper, with higher r^2) for bedload trap than for Helley-Smith samples. This difference can be attributed to the sampler characteristics: bedload traps with large openings and long sampling times provide a better chance for collecting large and infrequently moving gravels, while setting bedload traps onto ground plates avoids unwanted particle pick-up from the bed. The result is a better defined and steeper flow competence curve.

Mobilizing flows were computed for fixed gravel sizes of 32, 45, and 64 mm, as well as for framework gravels and characteristic bedmaterial particle sizes such as three percentiles of the surface and the subarmor D_{50} particle size for the three study streams. The main patterns and effects observed from the flow competence analyses can be summarized as follows:

Channel maintenance flows for different streams
Analyses showed that entraining flows required for fixed as well as well as site-characteristic particle sizes (e.g., surface and subarmor D_{50} sizes) increased with the steepness of the stream gradient and the coarseness of the reach-averaged surface D_{50}

size. Three streams are admittedly not sufficient to determine a relationship between incipient motion conditions and stream characteristics; however, the repeated result for all particle sizes suggests that the analyses should be repeated with a larger data set to confirm or reject the observed trend.

Channel maintenance flows for different samplers

Samples collected with a Helley-Smith sampler generally indicate higher entraining flows for coarse gravel than bedload traps. Averaged over the three study streams, entrainment flows for Helley-Smith samples ranged from 102 to 237% Q_{bkf} for gravel sizes of 32, 45 and 64 mm, but were 84 to 121% Q_{bkf} for the bedload trap sampler. A similar trend was indicated for site-characteristic gravel sizes. For framework gravels as well as the surface and subsurface D_{50} sizes, Helley-Smith samples indicate mobilizing flows of 117 - 206% Q_{bkf} (mean of 176) for Hayden and Little Granite Creek, while bedload traps indicated flows of 87 to 120% Q_{bkf}.

The high flows required for the Helley-Smith sampler may be attributed to the small opening size of a Helley-Smith sampler that makes it difficult (and thus a relatively rare event) for large gravels to enter the sample. This causes a relatively flat and not very well defined flow competence curve. Bedload trap samples, by contrast, provide not only a better fit in the D_{max} *vs.* Q relationship, but flows indicated for entrainment of the framework as well as the surface and subsurface D_{50} sizes are thus within the broad vicinity of bankfull flow (where channel maintenance flows are expected to be). Flows 120 to 200% Q_{bkf} as indicated by the Helley-Smith have recurrence intervals of approximately 2 to 12 years[44] which appears to be on the infrequent side for channel maintenance.

[44] *These values were determined from the record of instantaneous peak flows at Halfmoon Creek (Bunte and Swingle 2005). Similar values should hold for many coarse-bedded Rocky Mountain streams with snowmelt discharge regimes in general because those streams have similar flood frequency distributions.*

4. Comparison of channel maintenance flows obtained from different procedures

In this report, channel maintenance flows were computed from the five main procedures as well as for several alternative sub-procedures. The procedures were:

1. Bedload explosion (Section 3.1)
2. Breakpoint flows (Section 3.2) from
   - Piecewise regression procedure in SAS
   - Visual estimate
   - Visual estimate for data sets truncated stepwise between Q_{max} and Q_{bkf}
3. Entraining flows from the collapse-size analysis (Section 3.3)
4. Threshold flows computed from the site-calibrated approach (Section 3.4)
5. Entraining flows (Section 3.5) computed from flow competence curves for
   - gravels of 32, 45, and 64 mm
   - framework gravels
   - surface D_{16}, D_{25}, and D_{50} particle sizes
   - subarmor D_{50} particle size

For all procedures, channel maintenance flows were analyzed for samples collected with the Helley-Smith sampler and bedload traps at three study streams. Computed results are summarized in Table 31. Channel maintenance flows for all procedures, all streams and the two samplers extend over a wide range, reaching from as low as 16% to as high as 326% Q_{bkf}.

Table 31: **Channel maintenance flows (in % Q_{bkf}) computed from the various procedures discussed in this study.**

Stream	Bedload Explosion		Breakpoint flows						Site-calibrated approach		Collapse- size analysis	
			SAS		Visual		Vis., truncated (in % Q_{max})					
	HS	Traps	HS	Traps	HS	Traps	HS	Traps	HS	Traps	HS	Traps
Hayden	109	130	73	112	194	115	75	79	70	120	16	38
Little Granite	87	107	85	102	85	107	75	85	85	111	46	70
Halfmoon	46	50	48	64 (49)	40	50	-	-	23	50	67	72

Table 34, continued.

Stream	Flow competence curve															
	32 mm		45 mm		64 mm		Framework gravel		Surface D_{16}		Surface D_{25}		Surface D_{50}		Subarmor D_{50}	
	HS	Traps	HS	Traps	HS	Traps	HS	Traps	HS	Traps	HS	Traps	HS	Traps	HS	Traps
Hayden	124	97	200	118	326	145	200	118	28	53	56	70	206	120	146	104
Little Granite	117	87	171	96	254	106	117	87	68	76	104	85	206	101	188	97
Halfmoon	67	68	93	87	131	112	93	87	30	38	48	54	101	92	48	54

Values in parentheses refer to a secondary breakpoint flow

This section of the study compares channel maintenance flows between samplers, among procedures, and among the three study streams and discusses their differences or commonalities. Specifically, computed channel maintenance flows are analyzed with respect to the following questions:

- How do channel maintenance flows vary between the two bedload samplers?
- How do channel maintenance flows vary among the different procedures?
- Are channel maintenance flows consistently higher or lower for any of the streams?

Of the numerous procedures and sub-procedures from which channel maintenance flows were computed (Table 31), the following eight procedures are selected for comparison:

1. Bedload explosion
2. Breakpoint flow computed using the piecewise regression analysis (SAS routine)
3. Breakpoint flow from the visual analysis
4. Site-calibrated approach
5. Collapse-size analysis
6. Flow competence for the surface D_{50} particle size
7. Flow competence for the subarmor D_{50} particle size
8. Flow competence for the framework gravel size

Channel maintenance flows computed from these eight procedures for the three study streams using the Helley-Smith sampler and bedload traps are combined in Table 32.

Table 32: Channel maintenance flows (in % Q_{bkf}) computed for Helley-Smith and bedload trap samples from the eight procedures selected for comparison.

Stream	Bedload Explosion		Breakpoint flows				Site-calibrated approach		Collapse-size analysis		Flow competence curve					
			Visual		SAS						Surface D_{50}		Subarmor D_{50}		Framework gravel	
	HS	traps	HS	traps	HS	traps	HS	Traps	HS	traps	HS	traps	HS	traps	HS	traps
Hayden	109	130	107	115	73	112	70	120	16	38	206	120	146	104	200	118
Litl. Granite	87	107	85	107	85	102	85	111	46	70	206	101	180	97	117	87
Halfmoon	46	50	40	50	48	64(49)	23	50	67	72	101	92	48	54	93	87
Mean	81	96	77	91	69	93(88)	59	94	43	60	171	104	125	85	137	97
CV%	40	43	34	38	28	27(39)	54	41	60	32	35	14	55	32	41	18
Rank HS	4		5		6		7		8		1		3		2	
Rank traps		3		6		5		4		8		1		7		2

Values in parentheses refer to a secondary breakpoint flow and its derived computed values.

4.1 Differences in channel maintenance flows between samplers

One question of this study was whether channel maintenance flows differ depending on the sampling device used for collecting bedload samples. Analyses in previous sections

of this study yielded different channel maintenance flows depending on whether samples were collected using a Helley-Smith sampler or bedload traps. To better compare channel maintenance flows between the two samplers, among procedures, and among streams, results obtained for the eight procedures are listed separately for Helley-Smith samples in Table 33 and for bedload trap samples in Table 34.

Table 33: Channel maintenance flows (in % Q_{bkf}) computed for the eight main procedures based on **Helley-Smith** samples.

Stream	Bedload Expl.	Breakp.flows		Site-calibr. Appr.	Collps. sizes	Flow competence curve			All proc.		Excl. coll. size	
		SAS	Visual			Surface D_{50}	Subarmor D_{50}	Framewrk. gravel	Mean	CV (%)	Mean	CV (%)
Hayden	109	73	94	70	16	206	146	200	114	58	128	44
Litl. Granite	87	85	85	85	46	206	188	117	112	50	122	43
Halfmoon	46	48	40	23	67	101	48	93	58	46	57	50
Mean	81	69	73	59	43	171	127	137	95	51	102	46
CV %	40	27	40	55	60	36	56	41				
Rank (means)	4	6	5	7	8	1	3	2				

Table 34: Channel maintenance flows (in % Q_{bkf}) computed for the eight main procedures based on **bedload trap** samples.

Stream	Bedload Expl.	Breakp. flows		Site-calibr. Appr.	Collps. Sizes	Flow competence curve			All proc.		Excl. Coll. size	
		SAS	Visual			Surface D_{50}	Subarmor D_{50}	Framewrk. gravel	Mean	CV (%)	Mean	CV (%)
Hayden	130	112	115	120	38	120	104	118	107	27	117	7
Litl. Granite	107	102	107	111	70	101	97	87	98	14	102	8
Halfmoon	50	64 (49)	50	50	72	92	54	87	65	26	64	29
Mean	96	93 (88)	91	94	60	104	85	97	90	22	94	14
CV %	43	27 (39)	39	41	32	14	32	18				
Rank (means)	3	5	6	4	8	1	7	2				

* Values in parenthesis refer to a secondary breakpoint identified from the SAS procedure.

Mean channel maintenance flows for the two samplers

A pattern that jumps out from Table 33 and Table 34 is that for five of the eight procedures (bedload explosion, breakpoints flows (SAS and visual), the site-calibrated approach, and the collapse-size analysis), channel maintenance flows were higher when computed from bedload trap samples than from Helley-Smith samples. Averaged over the three study streams, mean channel maintenance flows for these five procedures were 65% Q_{bkf} for Helley-Smith samples and 87% Q_{bkf} for bedload traps. By contrast, the mean channel maintenance flow for the flow competence for framework gravel, surface

and subarmor D_{50} particle sizes was 154% Q_{bkf} for Helley-Smith samples and 101% Q_{bkf} for bedload traps. Although absolute channel maintenance flows differed among the three streams, the pattern of relatively low and high channel maintenance flows for Helley-Smith samples compared to intermediate channel maintenance flows for bedload traps was consistent for all three study streams.

4.2 Comparison among procedures

4.2.1 Variability and ranking

An important question of this study was to determine by how much channel maintenance flows differed among procedures and whether that difference would vary between the two samplers. Averaged over the three study streams, channel maintenance flows covered a wide range among the eight procedures, spanning 46 to 177% Q_{bkf} (a factor of 3.8) for bedload samples collected with a Helley-Smith sampler. The large difference in channel maintenance flows between procedures amounts to coefficients of variation (CV) of 46 to 58% among the three streams (Table 33). Excluding the collapse size analysis decreases the variability of channel maintenance flows slightly to CVs of 43 to 50% (Table 33).

For bedload samples collected using bedload traps, channel maintenance flows obtained by the eight procedures were less different from each other than those computed from Helley-Smith samples. Averaged over the three streams, channel maintenance flows ranged from 60 to 104% Q_{bkf}, a ratio of 1.7. This resulted in coefficients of variation among procedures of 14 to 27% for the three study streams. These results suggest that use of bedload traps for sample collection reduces the variability among procedures to less than half compared to a Helley-Smith sampler. Excluding the collapse size analysis from the inter-method comparison reduces the variability to an average CV of 14%, which is third of the variability among methods obtained from sampling with a Helley-Smith sampler (46%) (Table 34).

Figure 35 shows the ranking of the procedures from lowest to highest channel maintenance flow as obtained for Helley-Smith samples. Averaged over the three streams, the collapse size yielded the lowest channel maintenance flows and the flow competence for the surface D_{50} size the highest. The site calibration approach, breakpoint flows, and bedload explosion formed a slightly increasing mid-range, while the flow competence approaches produced the highest channel maintenance flows. For bedload samples collected with bedload traps, the collapse size analysis continued to yield the lowest average channel maintenance flows for all streams. However, almost all of the other procedures yielded quite similar average channel maintenance flows within 85 to 97% Q_{bkf} whereas the flow competence for the surface D_{50} size still yielded the highest value (104% Q_{bkf}) (Figure 35).

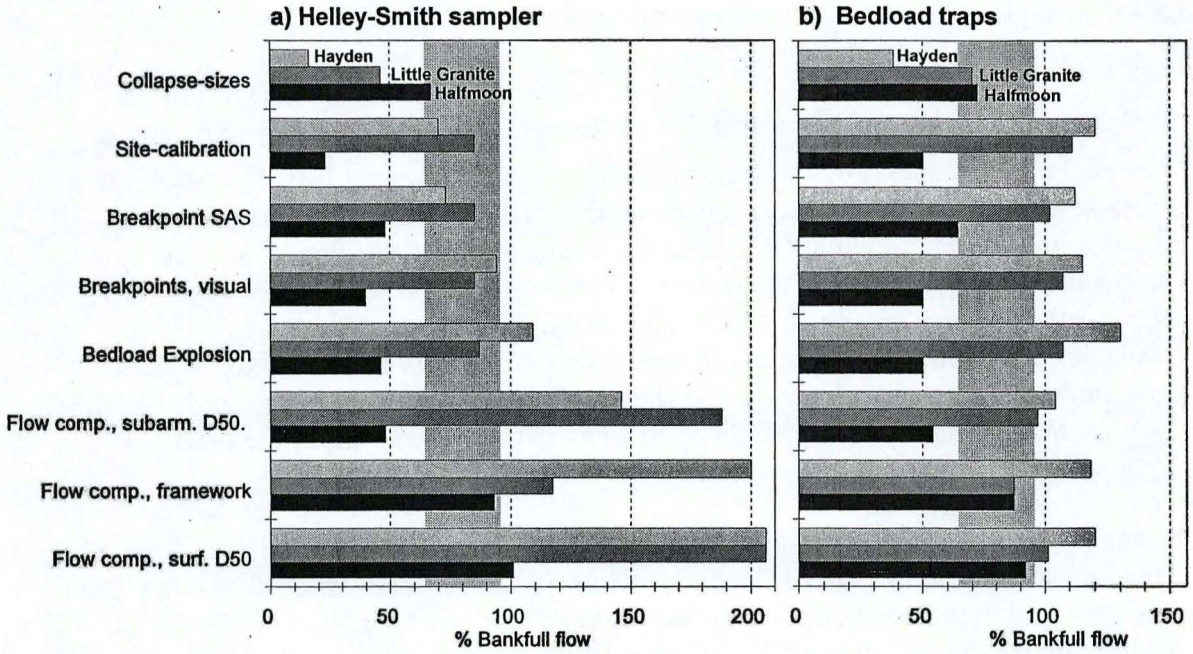

Figure 35: Channel maintenance flows computed for the eight selected procedures from Helley-Smith samples (a) and bedload trap samples (b) for the three study streams. Procedures are plotted from lowest to highest ranking for Helley-Smith samples. The gray background band indicates the range of 65-95% Q_{bkf} into which most of the breakpoint flows computed by Ryan et al. (2005) fell.

4.2.2 Similarity among procedures

Although channel maintenance flows varied—sometimes widely—among procedures, several of the procedures had similar results. When samples were collected using the Helley-Smith sampler, the group of procedures with similar results included the conceptually similar bedload explosion and breakpoint flows (SAS and visual), plus either the site calibration or the competent flow for the subarmor D_{50} size. Channel maintenance flows were most similar among the three streams when computed using the SAS breakpoint procedure (CV of 27%) (Table 33). Thus, if one followed the idea that channel maintenance flows ought to be relatively similar among mountain gravel-bed streams, breakpoint flows determined using SAS are most likely to produce similar channel maintenance flows for different streams based on Helley-Smith samples.

When samples were collected using bedload traps, most of the channel maintenance flow procedures yielded similar results: breakpoint flows (SAS and visual), bedload explosions, site calibrations, and at least one or two of the flow competence approaches. Thus, when using bedload traps for sample collection, the procedure selected for channel maintenance flow computation is of much less importance compared to when using the Helley-Smith sampler. Using bedload traps, the procedures that provided the most similar channel maintenance flow among the three streams was the flow competence for

the surface D_{50} or the framework gravel size (CV of 14 and 18%), then followed by the SAS breakpoint procedure (CV = 27%) (Table 34).

4.2.3 Channel maintenance flows less variable for bedload traps

Channel maintenance flows were more variable when computed from Helley-Smith than from bedload trap samples. Averaged over the three study streams, mean channel maintenance flows for Helley Smith samples for the three flow competence approaches were quite high (154% Q_{bkf}), but quite low (65% Q_{bkf}) for the other five procedures (bedload explosion, breakpoint flows, site-calibrated approach and collapse size analysis). By contrast, mean channel maintenance flows for bedload trap samples generally remained in the neighborhood of bankfull flow, yielding an average of 101% Q_{bkf} for flow competence approaches and an average of 87% Q_{bkf} for the other five approaches.

There were similarities among several procedures. The conceptually similar breakpoint flows (visual and SAS) and bedload explosions yielded similar results for Helley-Smith samples, and the SAS breakpoint flows produced the least variability among streams. For bedload trap samples, almost all of the procedures (except for the collapse sizes) produced similar channel maintenance flows, and the flow competence for the surface D_{50} size produced the most similar result among the three streams.

Producing channel maintenance flows that are less variable among computational methods, samples from bedload traps seem better suited for computing channel maintenance flows than Helley-Smith samples, because for bedload trap samples, the method used for determining channel maintenance flows is of less importance than for Helley-Smith samples.

4.3 Differences in channel maintenance flows between streams

Another question for this study was whether there was a consistent difference in channel maintenance flows between the three study streams and whether computed channel maintenance flows are predictable from easily measurable stream characteristics. Of the three study streams, Hayden Creek with a mixed step-pool/plane-bed morphology has the steepest gradient and the coarsest reach-averaged surface D_{50} size (Table 3). Halfmoon Creek has the lowest gradient, the finest surface D_{50} size and a mixed plane-bed/pool-riffle morphology. Again, this analysis is done for each sampler separately.

4.3.1 Streams with consistently higher or lower channel maintenance flows

Mean channel maintenance flows averaged over all procedures were 114 and 112% Q_{bkf} for Hayden and Little Granite, but only 58% Q_{bkf} for Halfmoon Creek when bedload was collected using a Helley-Smith sampler. Halfmoon Creek had the lowest channel maintenance flows for all procedures except the collapse sizes procedure. The position

between Hayden and Little Granite Creek was mixed (Figure 35a). Out of the 8 procedures, Little Granite Creek had the highest channel maintenance flows for 4 procedures and Hayden for 3, while one procedure gave equally high channel maintenance flows for both streams.

Based on bedload trap samples, mean channel maintenance flows were 107 and 98% Q_{bkf} for Hayden and Little Granite, and 65% Q_{bkf} for Halfmoon Creek. Hayden Creek has generally the highest and Halfmoon Creek the lowest channel maintenance flows (section 4.1.2.1). The sequence Hayden – Little Granite – Halfmoon was maintained for all procedures except the collapse size analysis (Figure 35b).

Channel maintenance flows somewhere below bankfull flow are assumed typical for mountain gravel-bed streams. Requiring channel maintenance flows that start as low as 50-70% Q_{bkf} (as computed for Halfmoon Creek) appears quite low. The question whether Halfmoon Creek truly requires flows starting at 50-70% Q_{bkf} for channel maintenance, or whether this flow requirement might be affected by the way the channel maintenances procedures are computed is not easy to answer. At Halfmoon Creek, the granitic watershed supplies a large amount of subsurface fines which cause a high degree of armoring. This armoring causes the relatively slow increases of bedload transport rates with flow (i.e., flat bedload rating curves), both for bedload trap and Helley-Smith samples. By contrast, Halfmoon Creek transports the largest D_{max} particle sizes for a given flows of the three streams. Flat bedload rating curves definitely cause low breakpoint flows (Section 3.2.4.3), while transporting large particles at relatively low flows causes low entraining flows in a flow competence analysis, particularly when a high amount of subsurface fines cases the subarmor D_{50} size to be small. It thus appears that the low channel maintenance flows obtained for Halfmoon Creek are explainable as consequences of the procedures to the bedmaterial and bedload transport characteristics at Halfmoon Creek.

Although the three streams differ in their absolute channel maintenance flows, they are similar regarding the range of variability produced by the various procedures. Excluding channel maintenance flows from the collapse size analysis, the three streams have similar CVs of 43, 44 and 50% for Helley-Smith samples and 7, 8 to 29% for bedload traps. The difference in channel maintenance flows obtained from various mountain gravel-bed streams is larger than the difference obtained between samplers!

4.3.2 Prediction of channel maintenance flows?

Ryan et al. (2002, 2005) and Whiting (2002) suggested that channel maintenance flows should generally set at about 80 or 90% Q_{bkf}. However, Ryan et al. (2005) found a wide range of breakpoint flows computed from Helley-Smith samples between 40 and 110% Q_{bkf}, of which most (79%) breakpoint flows occurred between 65 and 95% Q_{bkf}. Whiting and King (2003) reported a similarly wide range of channel maintenance flows from 53 to 115% Q_{bkf} for 12 streams in Idaho with a mean of 88% Q_{bkf}. A value of 80-90% Q_{bkf} might constitute an average for a large number of streams, but may not be a precise estimate for a specific stream. Ryan et al. (2005) did not find any relationships between

breakpoint flows and characteristics of the channel, streambed or watershed. However, their data suggest a slight negative relationship with the bankfull bedload transport rate (Figure 15). Similarly, Whiting and King (2003) did not report any relationships between channel maintenance flows from the collapse-size analysis and stream characteristics. However, their data suggest a slightly increasing trend for channel maintenance flows with stream gradient.

Simply assigning an average value of 80-90% Q_{bkf} as channel maintenance flows for a specified stream from may not be adequate for a given stream. When based on bedload trap samples, channel maintenance flows increased with the steepness and coarseness of the stream for the three streams in this study. The consistently low channel maintenance flows for Halfmoon Creek with its high amount of subsurface fines could likewise suggest a relationship between channel maintenance flows and bed armoring. Such relationships could serve to predict channel maintenance requirements for different streams. However, channel maintenance flow analyses need to done for a larger number of streams with different channel, streambed and watershed characteristics in order to confirm these relationships.

4.4 Evaluation of different channel maintenance procedures

Channel maintenance flows computed from the different procedures varied widely, being as low as 23% and as high as 206% Q_{bkf}. It is not possible to compare results obtained in this study to truth because the true percentage of flow needed for channel maintenance is not known and whether that percentage might vary depending on stream characteristics has not been convincingly proven in the literature. The assertion that channel maintenance flows should encompass flows higher than about 80% of bankfull flow is the result of gross arithmetic averaging over a wide range of computed channel maintenance flows (40 to 130% Q_{bkf}) reported in several studies that examined up to about 20 different streams (Emmett 1999; Ryan et al. 2002, 2005; Whiting and King 2003).

4.4.1 Effort involved in the computations

Quantitative evaluations of the various channel maintenance procedures were undertaken in earlier sections of this study. Here, channel maintenance procedures are compared and evaluated with respect to their computational effort as well as the accuracy obtained from the computations. To facilitate a ranking among the procedures, the evaluation encompassed several categories: data requirements, effort of field work, restriction to streams with particular characteristics, effort of computations, potential for operator variability (i.e., certainty of the result), and the effect that an individual bedload sample can have on the computed result (i.e., the potential for computing different channel maintenance flows for different data sets from the same stream). Scoring high (or favorably) in any of the categories yielded 2 points, moderate or neutral scores yielded 1 point and low (or unfavorable) scores 0 points. Points were then summed over the different categories. Results of this evaluation and ranking are combined in Table 35.

Table 35: Evaluation of various channel maintenance procedures with respect to data requirements, effort in data collection and computations, the potential for operator error and variability due to effects of individual data points as well as the resulting scores and ranks. This evaluation does not include scientific merit. Low effort is indicated by **bold** print, high effort by print in ***italics***.

	Data collection				Effort of data collection (est. weeks of fieldwork)	Restriction to streams with part. characteristics	Computational effort for hydrologist/ geomorphologist with average computing skills	Between operator error-potential of computed result	Pot. effect of indiv. bedload sample	Score, (rank)
	Bed-load transp. rates	Bed-load D_{max} sizes	Surface D_{50}	Sub-armor D_{50}						
Flow competence, $D_{50\ surface}$	-	Full range of flows	Near-site pebble count		***>4 weeks at high flow, +few hrs. at low flow***	**No**	**Common spreadsheet skills, not difficult**	**No variability and precise**	**Small**	7, (1a)
Flow competence, $D_{50\ subs}$, *framewrk.*	-	Full range of flows	Near-site pebble count	Near-site sub-armor samples	***>4 weeks at high flow, + 0.5 weeks at low flow***	***Not suitable for step-pool streams***	**Common spreadsheet skills, not difficult**	**No variability and precise**	**Small**	6, (1b)
Visual break-points	Full range of flows	-	-	-	***>4 weeks at high flow***	**No**	**Basic spreadsheet plotting skill, quick and easy**	Some variability, but not erroneous	Mode-rate	5, (2a)
SAS break-points	Full range of flows	-	-	-	***>4 weeks at high flow***	**No**	***Need access to and familiarity with SAS, but then easy to apply to large number of streams***	**No variability and precise**	**Small**	5, (2b)
Site-calibrated approach	Some samples	-	Near-site pebble count	Near-site sub-armor samples	**>1 weeks at high flow, 0.5 weeks at low flow**	***To streams with low roughness and few subsurface fines***	***Mostly a user-friendly program but problems with data entry and user guidance***	No variability but potentially erroneous	***High***	3, Low
Collapse-size analysis	-	Full range of flows	Reach-avgd. pebble count	Near-site sub-armor samples	***>4 weeks at high flow, + 0.5 weeks at low flow***	***To streams with granitic lithology***	**Common spreadsheet skills, extended computations, not difficult**	Some variability, but not erroneous	-	3, Low
Bedload explosion	Full range of flows	-	-	-	***>4 weeks at high flow***	**No**	**Basic spreadsheet plotting skill, quick and easy**	***Variability, potentially erroneous***	***High***	3, Low

The procedure with the highest score is the flow competence approach. The procedure is not restricted to any stream type when based a percentile of the surface size distribution. However, the method is difficult to apply to step-pool streams when based on the mobility of a subsurface percentile size or framework gravel. Computation is not difficult using a spreadsheet and there is little potential for operator subjectivity. The potential for variability when using different data sets from the same streams is small (provided there is no general change in the D_{max} *vs.* Q relationship). The second place is shared between breakpoint flows obtained from visual estimates and computed with the piecewise regression analysis using the SAS procedure. Comparing the combined time and effort expenditures among the channel maintenance procedures, the visual breakpoint analysis is the easiest and fastest method. Visually estimated breakpoint flows yield unbiased estimates of breakpoint flows computed with the SAS analysis, although the estimate may differ from the SAS result by as much as 30% for about one third of the streams. The SAS procedure largely eliminates operator subjectivity, but is difficult to compute unless one has access to and is familiar with the SAS program. Visual estimates have some potential for operator subjectivity as well as potential for individual data point to influence the result.

A problem with all procedures is that science has not clearly determined sediment sizes and amounts to be mobilized for channel maintenance, and different procedures follow different hypotheses. The flow competence procedure has the disadvantage that it is not clear-cut, i.e., flow competence could be computed for any particle size, be that a percentile of the surface or subsurface sediment size or a combination thereof (framework gravel). This might, however, also be considered as an asset of the method. Disadvantages of the piecewise regression procedure using the SAS routine are that it requires access to and familiarity with SAS and that it is based on a hypothesis of bedload transport dynamics (i.e., that a significant, abrupt increase of transport rates occurs at the onset of Phase 2 transport). Another problem with breakpoint flows is the scale-dependent nature of the computed channel maintenance flow. To avoid scale-dependency, the range of measured flows must be fixed, either to bankfull or some other agreed upon flow. Visual breakpoint estimates are likewise based on the Phase 2 concept, are also dependent on scale, and require a fixed range of flows. Furthermore, visual estimates can easily be affected by operator variability and a single data point.

Scores did not differ much among the low ranking procedures. The bedload explosion procedure that uses fractional transport rates not only requires more computation than visual breakpoint analyses, but also has an increased potential for an individual data point to influence the result and thus a potential for high operator subjectivity. The collapse-size analysis is time consuming and seems to be applicable only to streams in granitic watersheds that receive cobbles and boulders from hillslopes and exhumed beds as well as high amounts of fines from the weathering products of granite. The site-calibrated approach is likewise time-consuming, not applicable to streams with high roughness and subsurface fines, and leaves a lot of questions open for the user to decide. Being a black-box model and allowing the user to select calibration data and threshold values adds to subjectivity.

4.4.2 Computations of channel maintenance flows: a big task

The task of computing channel maintenance flows using various procedures evolved into a much bigger task than anticipated. The computations not only took a lot of time because they were repeated for three streams and two samplers each, but some of the procedures were not easy to compute or poorly described, while sub-procedures were explored for others, all of which resulted in numerous extra computations and analyses.

Finally getting an output from a procedure

Use of the channel maintenance flows programs was not without problems. Running the Piecewise Regression analysis program within the SAS application required establishing access to and getting familiar with SAS. The BAGS program for the site-calibrated approach (Excel macro) provided different outputs depending on the selection of calibration samples and offered endless possibilities of tweaking the outcome. The verbal description of the collapse-size analysis (Whiting and King 2003) left a lot of questions open when using data sets from the study streams that may not have occurred to the authors with their particular data sets. Thus, most of the procedures required several tries to figure out how channel maintenance flows were actually computed.

Alternative sub-procedures were explored

For two of the procedures, this study explored related alternative approaches. Several spreadsheet approaches were explored for breakpoint flows, while critical flows were investigated as an alternative to the flow competence curves and channel maintenance flows were computed for framework gravels, as well as surface and subarmor D_{50} sizes. Exploring these alternative procedures increased the total number of procedures from the original 5 to 18. Results of these attempts are not discussed in this report to keep matters simple, but are available from the author upon request.

New insights were gained

The numerous computations and re-computations made the analyses of the various channel maintenance procedures in this study quite thorough. The results hopefully shed light onto previously unknown complications and restrictions of the various channel maintenance procedures. They showed, for example, that both the collapse-size analysis and the site-calibrated approach are restricted to the type of streams in which the methodology was developed: the collapse-size analysis approach only provides "reasonable" results in granitic stream beds with coarse surface and fine subarmor sediment, whereas the site-calibrated approach provides reasonable results only in streams that are not granitic, do not have a large amount of subarmor fines, and do not have particularly coarse beds. They showed that breakpoint flows are scale-dependent and require setting a fixed rage of flows for the analyses to eliminate the effects of scale dependency. And they showed that for the computation of entraining flows, science needs to evaluate which characteristic bedmaterial size needs to be entrained and whether to compute entraining flows from flow competence or critical flow curves.

More field research is needed for understanding bedload transport processes

Science has barely begun to illuminate processes of bedload transport in coarse-bedded mountain streams, while procedures have already been developed and are used to

compute channel maintenance flows. With many questions still open in the understanding of bedload transport processes and interaction between different particle sizes, there is also little understanding which bedmaterial particle sizes need to be moved for channel maintenance, or what magnitude of transport rates are needed, how often the channel maintenance flows are needed and for how long, and how channel maintenance requirements vary among different types of streams. Further advancements in the general understanding of bedload transport processes in mountain gravel- and cobble-bed streams may help to better determine the magnitude (and duration) of channel maintenance flows and illuminate the processes that need to happen in the stream in order to maintain the channel.

Acknowledgements
Laurie Porth (statistician, USDA Forest Service, Rocky Mountain Research Station) patiently explained the Piecewise Regression procedure to me, ran the procedure for some of the streams, and guided me to run the program by myself. Sandra Ryan (research hydrologist, USDA Forest Service, Rocky Mountain Research Station) kindly provided the data sets of bedload transport rates collected with a 3-inch Helley-Smith during her studies and loaned us equipment for use during field and lab work.

A big thank you goes to my husband Kurt Swingle who spent many weeks with me in the field each year to collect bedload transport and bedmaterial data and who set up the experimental Excel spreadsheet that was to provide an easier means of computation for breakpoint flows in this study.

I thank John Potyondy and Steve Abt for support and encouragement and John Potyondy for a thorough review of an earlier version of this document. This study was funded by the Stream Systems Technology Center, USDA Forest Service, Rocky Mountain Research Station who I thank for the exciting opportunity to investigate how mountain gravel-bed streams work.

5. References

Andrews, E.D., 1983. Entrainment of gravel from naturally sorted riverbed material. *Geological Society of America Bulletin* 94: 1225-1231.

Andrews, E.D., 1984. Bed-material entrainment and hydraulic geometry of gravel-bed rivers in Colorado. *Geological Society of America Bulletin* 95: 371-378.

Andrews, E.D., 1994. Marginal bed load transport in a gravel bed stream, Sagehen Creek, California. *Water Resources Research* 30 (7): 2241-2250.

Andrews, E.D. and D.C. Erman, 1986. Persistence in the size distribution of surficial bed material during an extreme snowmelt flood. *Water Resources Research* 22 (2): 191-197.

Andrews, E.D. and J.M. Nankervis, 1995. Effective discharge and the design of channel maintenance flows for gravel-bed rivers. In: *Natural and Anthropogenic Influences in Fluvial Geomorphology*. J.E. Costa, A.J. Miller, K.W. Potter, and P.R. Wilcock, (eds.), Geophysical Monograph 89: 151-164.

Andrews, E.D. and G. Parker, 1987. Formation of a coarse surface layer as the response to gravel mobility. In: *Sediment Transport in Gravel-Bed Rivers.* C.R. Thorne, J.C. Bathurst and R.D. Hey (eds.). John Wiley and Sons, New York, p. 269-325.

Andrews, E.D. and J.D. Smith, 1992. A theoretical model for calculating marginal bedload transport rates of gravel. In: *Dynamics of Gravel-Bed Rivers*. P. Billi, R.D. Hey, C.R. Thorne, and P. Tacconi (eds.), John Wiley and Sons, Chichester, p. 41-52.

Ashiq, M. and J.C. Bathurst, 1999. Comparison of bed load sampler and tracer data on initiation of motion. *Journal of Hydraulic Engineering* 125 (5): 661-664.

Ashworth, P.J. and R.I. Ferguson, 1989. Size-selective entrainment of bed load in gravel bed streams. *Water Resources Research* 25(4): 627-634.

Bagnold, R.A., 1973. The nature of saltation and of 'bed-load' transport in water. *Proceedings of the Royal Society of London*, Series A, 332: 473-504.

Bagnold, R.A., 1980. An empirical correlation of bedload transport rates in flumes and natural rivers. *Proceedings of the Royal Society of London,* Series A, 372: 453-473.

BAGS (2006). Bedload Assessment in Gravel-Bedded Streams program. Beta version (f1) of a Microsoft Excel program package created by Pitlick, J., P. Wilcock, G. Parker, J. Potyondy, P. Bakke, and Y. Cui for computation of 6 bedload equations. Stream Systems Technology Center, USDA Forest Service, Rocky Mountain Research Station, Fort Collins, CO.

Bakke, P.D., P.O. Basdekas, D.R. Dawdy, and P.C. Klingeman, 1999. Calibrated Parker-Klingeman model for gravel transport. *Journal of Hydraulic Engineering* 125 (6): 657-660.

Barry, J. J., J. M. Buffington, and J. G. King, 2004. A general power equation for predicting bed load transport rates in gravel bed rivers. *Water Resources Research,* 40, W10401, doi:10.1029/2004WR003190.

Bathurst, J.C., 1987a. Measuring and modelling bedload transport in channels with coarse bed material. In: *River Channels. Environment and Process*. K.S. Richards (ed.), The Institute of British Geographer Special Publication Series, Basil Blackwell, Oxford, p. 272-294.

Bathurst, J.C., 1987b. Critical conditions for bed material movement in steep, boulder-bed streams. In: *Erosion and Sedimentation in the Pacific Rim.* IAHS Publ. no. 165: 309-318.

Bathurst, J.C.,W.H. Graf and H.H. Cao, 1987. Bed load discharge equations for steep mountain rivers. In: *Sediment Transport in Gravel-Bed Rivers.* C.R. Thorne, J.C. Bathurst and R.D. Hey (eds.), John Wiley and Sons, Chichester, p. 453-491.

Beschta, R.L., 1987. Conceptual models of sediment transport in streams. In: *Sediment Transport in Gravel-Bed Rivers.* C.R. Thorne, J.C. Bathurst, and R.D. Hey (eds.), John Wiley, Chichester, p. 387-419.

Boise Adjudication Team (BAT) Web site. (Spreadsheet information on sediment transport, bedmaterial, channel geometry and discharge for 31 Idaho streams; short reports on data analysis.) [Online] Available: http://www.fs.fed.us/rm/boise/research/watershed/BAT/index.shtml

Bunte, K., 1992a. Particle number grain-size composition of bedload in a mountain stream. In: *Dynamics of Gravel Bed Rivers.* P. Billi, R.D. Hey, C.R. Thorne and P. Tacconi (eds.), John Wiley, Chichester, p. 55-72.

Bunte, K. 1992b. Discussion of Komar and Shih (1992): Equal grain mobility versus changing grain sizes in gravel-bed streams. In: *Dynamics of Gravel Bed Rivers.* P. Billi, R.D. Hey, C.R. Thorne and P. Tacconi (eds.), John Wiley, Chichester, p. 93-96.

Bunte, K., 1996. Analyses of the temporal variation of coarse bedload transport and its grain size distribution (Squaw Creek, Montana, USA). *U.S.D.A., Forest Service, Rocky Mountain Forest and Range Experiment Station, General Technical Report* RM-GTR-288, 123 pp.

Bunte, K., 1999a. Field testing of bedload traps for measuring entrainment of pebbles and cobbles at Little Granite Creek, WY. Report prepared for the Stream Systems Technology Center, USDA Forest Service, Rocky Mountain Research Station, Fort Collins, CO, 78 pp.

Bunte, K., 1999b. Field testing of bedload traps for measuring entrainment of pebbles and cobbles at Cherry Creek, OR. Report prepared for the Water Resources Team, Winema National Forest, USDA Forest Service, Klamath Falls, OR, and the Stream Systems Technology Center, USDA Forest Service, Rocky Mountain Research Station, Fort Collins, CO, 75 pp.

Bunte, K. and S.R. Abt, 2001a. Sampling Surface and Subsurface Particle-Size Distributions in Wadable Gravel- and Cobble-Bed Streams for Analysis in Sediment Transport, Hydraulics, and Streambed Monitoring. USDA Forest Service, Rocky Mountain Research Station, Fort Collins, CO, *General Technical Report* RMRS-GTR-74, 428 pp. [Online] Available: http://www.fs.fed.us/rm/pubs/rmrs/gtr_74.html

Bunte, K. and S.R. Abt, 2001b. Sampling frame for improving pebble count accuracy in coarse gravel-bed streams. *Journal of the American Water Resources Association* 37(4): 1001-1014.

Bunte, K. and S. R. Abt, 2005. Effect of sampling time on measured gravel bed load transport rates in a coarse-bedded stream. *Water Resources Research, 41,* W11405, doi:10.1029/2004WR003880.

Bunte, K., S.R. Abt, J.P. Potyondy, and S.E. Ryan, 2004. Measurement of coarse gravel and cobble transport using a portable bedload trap. *Journal of Hydraulic Engineering,* 130(9): 879-893.

Bunte, K., S.R. Abt, J.P. Potyondy and K.W. Swingle, 2007. A comparison of coarse bedload transport measured with bedload traps and Helley-Smith samplers. *Geodinamica Acta* (Supplement to the Gravel-Bed Rivers VI Meeting), in press.

Bunte, K., S.R. Abt, and K.W. Swingle, 2005. Ground Plates may Improve Accuracy of Helley-Smith Bedload Samples. *Eos Trans. AGU, 86*(52), Fall Meeting Supplement, Abstract H53B-0471.

Bunte, K., S.R. Abt, and K.W. Swingle, 2006b. Predictability of bedload rating and flow competence curves from bed armoring, stream width and basin area. Proceedings of the Eighth Federal Interagency Sedimentation Conference, April 2-6, 2006 in Reno, NV., Session 4A-2, 9 pp. [Online] Available: http://www.jfic.org/confInfo.pdf.

Bunte, K. and K.W. Swingle 2005. Using bedload traps at Halfmoon Creek, 2004: Transport rates, spatial variability of gravel transport, and long nets. Report submitted to the Stream Systems Technology Center, USDA Forest Service, Rocky Mountain Research Station, Fort Collins, CO, 116 pp.

Bunte, K. and K.W. Swingle, 2006. Continued development and testing of bedload trap technology through flume experiments at the National Center for Earth-Surface Dynamics (NCED) in the St. Anthony Falls Laboratory. Report in preparation to be submitted to the Stream Systems Technology Center, USDA Forest Service, Rocky Mountain Research Station, Fort Collins, CO, ca. 50 pp.

Bunte, K., K. Swingle, and S.R. Abt, 2006c. Guidelines for using bedload traps in coarse-bedded mountain streams: Construction, installation, operation and sample processing. Manuscript submitted to USDA Forest Service, Rocky Mountain Research Station, for publication as a General Technical Report, 93 pp. [Online] Available: http://www.fs.fed.us/rm/pubs/rmrs_gtr191.pdf

Carling, P.A., 1987. Bed stability in gravel streams, with reference to stream regulation and Ecology. In: *River Channels*. K.S. Richards (ed.), Special Publications of the Transactions of the Institute of British Geographers, p. 321-347.

Carling, P.A., 1988. The concept of dominant discharge applied to two gravel-bed streams in relation to channel stability thresholds. *Earth Surface Processes and Landforms* 13:355-367.

Church, M., D.G. McLean and J.F. Walcott, 1987. River bed gravels: sampling and analysis. In: *Sediment Transport in Gravel-Bed Rivers*, C.R. Thorne, J.C. Bathurst and R.D. Hey (eds.), John Wiley and Sons, Chichester, p. 43-87.

Dawdy, D.R., 1995 (est.). A sediment computation program using the P-K method. (Instructions and code of a Fortran program.) Prepared for the Winema National Forest, Klamath Falls, OR, 21 pp.

Dietrich, W.E., J.W. Kirchner, H. Ikeda, and F. Iseya, 1989. Sediment supply and the development of the coarse surface layer in gravel-bedload rivers. *Nature* 340: 215-217.

Dixon, M. and S.E Ryan, 2001. Using an underwater video camera for observing bedload transport in mountain streams. *Proceedings of the Seventh Federal Interagency Sedimentation Conference, March 25-29, Reno, Nevada*, Vol. 1, Poster 70 - Poster 73.

Duan, N., 1983. Smearing estimate: a nonparametric retransformation method. *Journal of the American Statistical Association* 87: 605-610.

Einstein, H.A., 1950. The bed-load function for sediment transportation in open channel flows. In: *U.S. Dept. of Agriculture, Soil Conservation Service*, Technical Bulletin 1026, 71 pp.

Emmett, W.W., 1976. Bedload transport in two large, gravel-bed rivers, Idaho and Washington. In: *Proceedings of the Third Federal Inter-Agency Sedimentation Conference,* Denver, Colorado, Sedimentation Committee of the Water Resources Council, p. 4.191-4.114.

Emmett, W.W., 1999. Quantification of channel maintenance flows for gravel-bed rivers. In: *Wildland Hydrology.* D.S. Olsen and J.P. Potyondy (eds.), American Water Resources Association, Herndon VA, TPS-99-3, p. 77-84.

Emmett, W.W. and M.G. Wolman, 2001. Effective discharge and gravel-bed rivers. *Earth Surface Processes and Landforms* 26: 1369-1380.

Ferguson, R.I., 1986. River loads underestimated by rating curves. *Water Resources Research* 22(1): 74-76.

Ferguson, R.I., 1987. Accuracy and precision of methods for estimating river loads. *Earth Surface Processes and Landforms* 12: 95-104.

Ferguson, R.I., 1994. Critical discharge for entrainment of poorly sorted gravel. *Earth Surface Processes and Landforms* 19: 179-186.

Haschenburger, J.K. and P.R. Wilcock, 2003. Partial transport in a natural gravel bed channel. Warer Resources Research 39(1), 1020, doi:10.1029/2002WR001532, 2003.

Hassan, M.A. and M. Church, 2001. Sensitivity of bedload transport in Harris Creek: Seasonal and spatial variation over a cobble-gravel bar. *Water Resources Research* 37 (3): 813-825.

Hill, M.T., W.S. Platts and R.L. Beschta, 1991. Ecological and geomorphological concepts for instream and out-of-channel flow requirements. *Rivers* 2 (3): 198-210.

Jackson, W.L. and R.L. Beschta, 1982. A Model of Two-Phase Bedload Transport in an Oregon Coast Range Stream. *Earth Surface Processes and Landforms* 7: 517-527.

King, J.G., W.W. Emmett, P.J. Whiting, R.P. Kenworthy and J.J. Barry, 2004. *Sediment transport data and related Information for Selected Coarse-Bed Streams and Rivers in Idaho.* USDA Forest Service, Rocky Mountain Research Station, General Technical Report RMRS-GTR 131, 26 pp. [Online] Available: http://www.fs.fed.us/rm/pubs/rmrs_gtr131.html

Klingeman, P.C. and Emmett, W.W., 1982. Gravel bedload transport processes. In: *Gravel-bed Rivers. Fluvial Processes, Engineering and Management.* R.D. Hey; J.C. Bathurst and C.R. Thorne (eds.), John Wiley and Sons, Chichester, p. 141-179.

Koch, R.W. and G.M. Smillie, 1986. Bias in hydrologic prediction using log-transformed prediction models. *Water Resources Bulletin* 22(5): 717-723.

Komar, P.D., 1996. Entrainment of sediments from deposits of mixed grain sizes and densities. In: *Advances in Fluvial Dynamics and Stratigraphy,* P.A. Carling and M.R. Dawson (eds.), John Wiley and Sons, Chichester, p. 127-181.

Komar, P.D. and S.-M. Shih, 1992. Equal mobility versus changing bedload grain size in gravel-bed streams. In: *Dynamics of Gravel Bed Rivers.* P. Billi, R.D. Hey, C.R. Thorne and P. Tacconi (eds.), John Wiley, Chichester, p.73-106.

Kuhnle, R.A., 1992. Fractional transport rates of bedload on Goodwin Creek. In: *Dynamics of Gravel Bed Rivers.* P. Billi, R.D. Hey, C.R. Thorne and P. Tacconi (eds.), John Wiley, Chichester, p.141-155.

Kuhnle, R.A., 1993. Incipient motion of sand-gravel sediment mixtures. *Journal of Hydraulic Engineering* 119 (12): 1400-1415.

Laronne, J.B. and I. Reid, 1993. Very high rates of bedload sediment transport by ephemeral desert rivers. *Nature* 366: 148-150.

Leaf, C.F., 1998. An analytical framework for evaluating channel maintenance flows in Colorado. *Journal of the American Water Resources Association* 34 (4): 865-876.

Lenzi, M.A., 2004. Displacement and transport of marked pebbles, cobbles and boulders during floods in a steep mountain stream. *Hydrological Processes* 18: 1899-1914. DIO:10.1002/hyd.1456.

Lenzi, M.A., 2005. Experience from sediment transport monitoring and investigations in the Rio Cordon. *Geophysical Research Abstracts*, 7, SRef-ID: 1607-7962/gra/ EGU05-A-06419.

Lenzi, M. A., L. Mao, and F. Comiti, 2004. Magnitude-frequency analysis of bed load data in an Alpine boulder bed stream, Water Resour. Res., 40, W07201, doi:10.1029/2003WR002961.

Leopold, L.B. and W.W. Emmett, 1976. Bedload measurements, East Fork River, Wyoming. *Proceedings of the National Academy of Sciences, USA* 73(4): 1000-1004.

Ligon, F.K., W.E. Dietrich, and W.J. Trush, 1995. Downstream ecological effects of dams. *BioScience* 45 (3): 183-192.

Lisle, T.E., 1989. Sediment transport and resulting deposition in spawning gravels, north coastal California. *Water Resources Research* 25(6): 1303-1319.

Lisle, T.E., 1995. Particle size variations between bed load and bed material in natural gravel bed channels. *Water Resources Research* 31 (4): 1107-1118.

Lisle, T.E., submitted. The evolution of sediment waves influenced by varying transport capacity in heterogeneous rivers. Manuscript submitted to the Gravel-Bed Rivers 6 Symposium, held in Lienz, Austria, Sept. 2005.

Lisle, T.E. and M. Church, 2002. Sediment transport-storage relations for degrading, gravel bed channels. *Water Resources Research* 38 (11),1219, doi:10,1029/2001WR0001086, 2002.

McBain, S. and W.J. Trush, 1997. Thresholds for managing regulated river ecosystems. In: *Proceedings of the Sixth Biennial Watershed Management Conference*. S. Sommarstrom (ed.), Water Resources Center Report No. 92, University of Davis, California, p.11-13.

McNamara, M.L., P.C. Klingeman, P.D. Bakke and R.J. Sullivan, 2000. Channel Maintenance flows in the upper Klamath Basin, Oregon. In: *Riparian Ecology and Management in Multi-Land Use Watersheds*. P.J. Wigington and R.L. Beschta (eds.), American Water Resources Association, Middleburg, Virginia, TPS-00-2, 616 pp.

Milhous, R., 1973. Sediment transport in a gravel-bottomed stream. Ph.D. thesis, Oregon State University, Corvallis, USA.

Montgomery, D.R. and J.M. Buffington, 1997. Channel-reach morphology in mountain drainage basins. *Geological Society of America Bulletin* 109 (5): 596-611.

Mueller, E.R., J. Pitlick, and J.M. Nelson, 2005. Variation in the reference Shields stress for bed load transport in gravel-bed streams and rivers. *Water Resources Research* 41, W04006, doi:10.1029/2004WR003692.

O'Leary, S.J. and R.L. Beschta, 1981. Bed load transport in an Oregon Coast Range stream. *Water Resources Bulletin* 17(5): 886-894.

Paintal, A.S., 1971. A stochastic model of bedload transport. *Journal of Hydraulic Research* 9(4): 527-553.

Parker, G., 1990. Surface based bedload transport relation for gravel rivers. *Journal of Hydraulic Research* 28(4): 417-436.

Parker, G. and P.C. Klingeman, 1982. On why gravel bed streams are paved. *Water Resources Research* 18(5): 1409-1423.

Parker, G., P.C. Klingeman and D.G. McLean, 1982. Bedload and the size distribution of paved gravel-bed streams. *Journal of the Hydraulics Division*, ASCE, 108 (HY4): 544-571.

Petit, F. 1994. Dimensionless critical shear stress evaluation from flume experiments using different gravel beds. *Earth Surface Processes and Landforms* 19: 565-576.

Pitlick, J., Y. Cui and P. Wilcock, 2006. Manual for computing bedload transport in gravel-bed streams. Part II: Instructions in software operations. Report submitted to the Stream Systems Technology Center, USDA Forest Service, Rocky Mountain Research Center, Fort Collins, CO, 56 pp.

Porth, L.S., 2004. 1_ BRKPTREG.SAS. (Code of a SAS program in 5 steps to compute the breakpoint flow for the discharge/bedload transport relationship using a piecewise regression analysis), unpublished manuscript, 10 pp.

Reid, I. and J.B. Laronne, 1995. Bed load sediment transport in an ephemeral stream and a comparison with seasonal and perennial counterparts. *Water Resources Research* 31(3): 773-781.

Reid, I., L.E. Frostick, J.T. Layman, 1985. The incidence and nature of bedload transport during flood flows in coarse-grained alluvial channels. *Earth Surface Processes and Landforms* 10: 33-44.

Rickenmann, D., 1994. Bedload transport and discharge in the Erlenbach stream. In: *Dynamics and Geomorphology of Mountain Rivers*. P. Ergenzinger and K.-H. Schmidt (eds.). Lecture Notes in Earth Sciences 52: 53-66, Springer Verlag, Berlin.

Rosgen, D., 2006. FLOWSED/POWERSED – Prediction models for suspended and bedlod transport. *Proceedings of the Eighth Federal Interagency Sedimentation Conference*, April 2-6, 2006, Reno, Nevada, Session 10B-4, 9 pp, [Online] Available: http://www.jfic.org/confInfo.pdf.

Rosgen, D.L., H.L. Silvey and J.P. Potyondy, 1986. The use of channel maintenance flow concepts in the Forest Service. *Hydrological Science and Technology: Short Papers* 2 (1): 19-26.

Ryan, S.E. and M. Dixon, 2002. Bedload movement in a mountain gravel-bed stream. A video. Technology Transfer, Stream Systems Technology Center, Fort Collins, CO., www.stream.fs.us.

Ryan, S.E. and W.W. Emmett, 2002. The nature of flow and sediment movement in Little Granite Creek near Bondurant, WY. USDA Forest Service, Rocky Mountain Research Station, General Technical Report 90. [Online] Available: http://www.fs.fed.us/rm/pubs/rmrs_gtr090.pdf

Ryan, S.E. and L.S. Porth, 1999. A field comparison of three pressure-difference bedload samplers. *Geomorphology* 30: 307-322.

Ryan, S.E. and L.S. Porth 2007. A tutorial on the piecewise regression approach applied to bedload transport data. General Technical Report, RMRS-GTR-189. Fort Collins,

CO, U.S. Department of Agriculture, Forest Service, Rocky Mountain Research Station, 41 p. [Online] http://www.fs.fed.us/rm/pubs/rmrs_gtr189.pdf

Ryan, S.E., L.S. Porth and C.A. Troendle, 2002. Defining phases of bedload transport using piecewise regression. *Earth Surface Processes and Landforms*, 27(9): 971-990.

Ryan S.E., Porth, L.S. and Troendle, C.A., 2005. Coarse sediment transport in mountain streams in Colorado and Wyoming, USA. *Earth Surface Processes and Landforms* 30: 269-288. DOI: 10.1002/esp.1128.

Schmidt, L.J. and J.P. Potyondy, 2001. Flow regimes needed to maintain channels in gravel-bed rivers. *Proceedings of the Seventh Federal Interagency Sedimentation Conference, March 25-29, Reno, Nevada*, Vol. 1, Poster 66 - Poster 69.

Schmidt, L.J. and J.P. Potyondy, 2004. Quantifying Channel Maintenance Instream Flows: An Approach for Gravel-Bed Streams in the Western United States. General Technical Report RMRS-GTR128. USDA, Forest Service, Rocky Mountain Research Station, Fort Collins, 33pp.

Sterling, S.M. and M. Church, 2002. Sediment trapping characteristics of a pit trap and the Helley-Smith sampler in a cobble gravel-bed river. *Water Resources Research* 38(6), 10.1029/2000WR000052, 2002.

Toms, J.D. and M.L. Lesperance, 2003. Piecewise regression: a tool for identifying ecological thresholds. *Ecology* 84 (8): 2034–2041.

Thorne, C.R., 1992. Discussion of Komar, P.D. and S.-M. Shih, (1992) "Equal mobility versus changing bedload grain size in gravel-bed streams". In: *Dynamics of Gravel Bed Rivers*. P. Billi, R.D. Hey, C.R. Thorne and P. Tacconi (eds.), John Wiley, Chichester, p. 112.

Troendle, C.A., 1993. Sediment transport for instream flow/channel maintenance. Proceedings of the Technical Workshop on Sediments, Feb. 3-7, 1992, Corvallis, Oregon. Terrene Institute, Washington DC, p. 31-34.

Troendle, C.A. and W.K. Olsen, 1994. Potential effects of timber harvest and water management on streamflow dynamics and sediment transport. In: *Sustainable Ecological Systems: Implementing an Ecological Approach to Land Management.* USDA, Forest Service, Rocky Mountain Forest and Range Experiment Station, Fort Collins, CO, General Technical Report RM-247: 34-4

Troendle, C.A., D.L Rosgen, S.E. Ryan, L.S. Porth, and J.M. Nankervis 2001. Developing a "reference" sediment transport relationship. *Proceedings of the Seventh Federal Interagency Sedimentation Conference, March 25-29, Reno, Nevada*, Vol. 1: II 73-II 80.

Trush, W.J., S.M. McBain and L.B. Leopold, 2000. Attributes of an alluvial river and their relation to water policy and management. *Proceedings of the National Academy of Sciences of the United States of America*, 97 (22): 11858-11863.

Warburton, J., 1990. An alpine proglacial fluvial sediment budget. *Geografiska Annaler* 72 A (3/4): 261-272.

Warburton, J., 1992. Observations of bedload transport and channel bed changes in a proglacial mountain streams. *Arctic and Alpine Research* 24(3): 195-203.

Whitaker, A.C., 1997. *The initiation of coarse bed load transport in gravel bed streams.* Ph.D. Dissertation, University of Montana, Missoula, 148 pp.

Whitaker, A.C. and D.F. Potts, 1996. Validation of two threshold models for bedload initiation in an upland gravel-bed stream. In: *Watershed Restoration Management -*

Physical, Chemical, and Biological Considerations. J. J. McDonnell, D.J. Leopold, J.B. Stribling, and L.R. Neville, (eds.), Proceedings of the Annual Symposium of the American Water Resources Association, 1996, p. 85-94. New York City Water Supply Studies, Syracuse, New York.

Whiting, P. J., 2002. Streamflow necessary for environmental maintenance. *Annual Review of Earth and Planetary Sciences* 30:181-206. DOI: 10.1146/annurev.earth.30.083001.161748

Whiting, P.J. and J.G. King, 2003. Surface particle sizes on armoured gravel stream-beds: effects of supply and hydraulics. *Earth Surface Processes and Landforms* 28, 1459-1471, DOI: 10.1002/esp.1049.

Whiting, P.J., J.F. Stamm, D.B. Moog and R.L. Ornsdorff, 1999. Sediment transporting flows in headwater streams. *Geological Society of America Bulletin*, 111(3): 450-466.

Wilcock, P.R., 1988. Methods for estimating the critical shear stress of individual fractions in mixed-sized sediment. *Water Resources Research* 24 (7): 1127-1135.

Wilcock, P.R., 1997. The components of fractional transport rate. *Water Resources Research* 33 (1): 247-258.

Wilcock, P.R., 1998. Sediment maintenance flows: feasibility and basis for prescription. *Gravel-Bed Rivers in the Environment.* P.C. Klingeman, R.L. Beschta, P.D. Komar, and J.B. Bradley, eds., 609-636, Water Resources Publications LLC, Highlands Ranch, Colorado.

Wilcock, P.R. and J.C. Crow, 2003. Surface-based transport model for mixed-size sediment. *Journal of Hydraulic Engineering* 129(2): 120-128.

Wilcock, P.R. and B.W. McArdell, 1993. Surface-based fractional transport rates: mobilization thresholds and partial transport of a sand-gravel sediment. *Water Resources Research* 29 (4): 1297-1312.

Wilcock, P.R. and B.W. McArdell, 1997. Partial transport of a sand/gravel sediment. *Water Resources Research* 33 (1): 235-245.

Wilcox, M.S., C.A. Troendle and J.M. Nankervis, 1996. Bedload transported in gravelbed streams in Wyoming. Proceedings of the Sixth Federal Interagency Sedimentation Conference, March 10-14, Las Vegas, Nevada. Interagency Advisory on Water Data, Subcommittee on Sedimentation, Vol. 2: VI.28-VI.33.

Wolman, M.G., 1954. A method of sampling coarse river-bed material. *Transactions, American Geophysical Union* 35(6): 951-956.